JPRS L/10364

4 March 1982

Translation

ROTOR VIBRATION GYROSCOPES IN NAVIGATION SYSTEMS

By

Yu.B. Vlasov and O.M. Filonov

FBIS FOREIGN BROADCAST INFORMATION SERVICE

NOTE

JPRS publications contain information primarily from foreign newspapers, periodicals and books, but also from news agency transmissions and broadcasts. Materials from foreign-language sources are translated; those from English-language sources are transcribed or reprinted, with the original phrasing and other characteristics retained.

Headlines, editorial reports, and material enclosed in brackets [] are supplied by JPRS. Processing indicators such as [Text] or [Excerpt] in the first line of each item, or following the last line of a brief, indicate how the original information was processed. Where no processing indicator is given, the information was summarized or extracted.

Unfamiliar names rendered phonetically or transliterated are enclosed in parentheses. Words or names preceded by a question mark and enclosed in parentheses were not clear in the original but have been supplied as appropriate in context. Other unattributed parenthetical notes within the body of an item originate with the source. Times within items are as given by source.

The contents of this publication in no way represent the policies, views or attitudes of the U.S. Government.

APPROVED FOR RELEASE: 2007/02/09: CIA-RDP82-00850R000500040010-1

JPRS L/10364

4 March 1982

ROTOR VIBRATION GYROSCOPES IN NAVIGATION SYSTEMS

Leningrad ROTORNYYE VIBRATSIONNYYE GIROSKOPY V SISTEMAKH NAVIGATSII in Russian 1980 (signed to press 22 Aug 80) pp 1-221

[Book "Rotor Vibration Gyroscopes in Navigation Systems", by Yuriy Borisovich Vlasov and Oleg Mikhaylovich Filonov, Izdatel'stvo "Sudostroyeniye", 1,200 copies, 221 pages]

CONTENTS

[Text] ANNOTATION

The authors present materials concerning the investigation of the characteristics of rotor vibration gyroscopes and methods for balancing them, in addition to formulating requirements for information extraction and processing devices. They also present techniques for synthesizing a regulator for stabilization and correction circuits for the purpose of obtaining the required characteristics.

FOREWORD

In recent years, rotor vibration gyroscopes (RVG) have been used more and more frequently in navigation systems. Since they are small in size and low in weight, they make it possible to miniaturize the sensitive elements of navigation systems and obtain characteristics with a level of accuracy that is no worse than that of gyroscopic devices constructed according to the classical method.

In order to obtain the best characteristics of such systems, it is important to describe correctly not only the static, but also the dynamic characteristics of RVG's as components of an automatic control system. In turn, when planning RVG's it is necessary to take the special features of their operation into consideration in the composition of the specific control system. All of this requires a detailed investigation of the theory of RVG's and gyroscopic systems in which they are used.

This book consists of five chapters. In the first two we discuss the generalized model on which most existing RVG systems are based. The analysis of the equations of motion is carried out with the utilization of well-developed operator methods. The special features of RVG's as two-dimensional measuring units make it possible to use a special apparatus that was developed for two-dimensional automatic control systems [16,17]. Such an approach to the analysis of the operation of RVG's makes it possible to perform operations directly with their transfer functions. For the simplest RVG systems, the transfer functions--as approximated in the area of the essential frequencies--are described by simple analytical expressions. For complex

systems, the analogous frequency characteristics can be constructed quite easily with the help of a computer. A knowledge of the frequency characteristics makes it possible to select the instrument's basic parameters in such a manner as to provide it with the required dynamic characteristics. This is especially important for RVG's operating in automatic regulation and control systems. For the analysis of RVG's having rotors with different angular velocities, we propose to use the spectral methods of (Khil's) generalized theory of equations [10,16,27,34].

In the second chapter we discuss the most common errors in RVG's with a single drive motor. The basic attention is devoted to errors related to angular vibrations of the motor's shaft at a frequency equal to twice its frequency of rotation and to static disbalance of the rotors.

In the third chapter we present one of the most promising (from the authors' viewpoint) layouts for composite RVG's. In an example of this layout we investigate the basic errors in this type of instrument, as well as methods of reducing them.

The fourth and fifth chapters are devoted to an investigation of the special features of the operation of gyroscopically stabilized platforms (GSP) based on RVG's. The investigation is based on the frequency methods of analyzing and synthesizing automatic control systems that are widely used in engineering calculations. Here there is a detailed discussion of the technique for selecting the stabilization channels' basic parameters. There is an analysis of the effect of the non-steady-state component of an RVG's output signal on the operation of a GSP. Multi-dimensional stabilization systems are discussed from the viewpoint of the effect on their operation of the specific cross-couplings between the stabilization channels.

This book lays no claims to being a complete explication of the theory of RVG's and systems that utilize them. In it we do not discuss questions of the optimum synthesis of systems with RVG's, the effect of basic nonlinearities on the operation of such systems, the theory of systems using composite RVG's that are self-orienting in the plane of the horizon and the meridian, and others. The investigation of these questions is necessary for the creation of RVG-based gyroscopic systems operating effectively in various navigation complexes.

The book is intended for engineers and scientific workers specializing in the field of the development and use of new gyroscopic instruments.

The authors are deeply grateful to Professor Ye.L. Smirnov, doctor of technical sciences, for his valuable advice and the comments he made during the preparation of the manuscript for publication.

INTRODUCTION

Modern navigation systems are constructed on the basis of the most recent achievements of computer technology and, for all practical purposes, carry out completely those operations that were previously performed by man.

Despite the presence of modern information processing facilities, the accuracy of navigation systems is determined primarily by the accuracy of the instruments that they utilize as sources of primary information. A special group among these instruments is composed of gyroscopic instruments and systems. They are used as the basis

for the construction of inertial navigation (ISN) and orientation (ISO) systems that insure the independent determination of an object's location and its spatial orientation, regardless of the presence of external reference points.

In order to create an ISN, it is necessary to have on board information about the object's orientation relative to a reference system of coordinates and the instantaneous absolute velocities or accelerations displacing its center of mass. When designing platformless inertial systems (BIS), the sources of such information are gyroscopic sensors of absolute angular velocities and accelerometers or gyroscopic linear acceleration integrators (GILU). In other ISN design variants, the reference system of coordinates is created directly on board the object with the help of GSP's. In this case the accelerometers or GILU's are installed either on the GSP or in the object itself.

Most of the gyroscopic instruments now in use are designed according to the classic method of a precession gyroscope in a cardan suspension. The basic element of these instruments is a massive, rapidly spinning rotor, in which an additional one or two degrees of freedom is provided because of the suspension's framework. An improvement in the accuracy of such gyroscopes is achieved by increasing the rotor's kinetic moment and reducing the disturbing moments. Judging by voluminous data that are available, the possibilities for improving gyroscopes built according to the classic method have been exhausted to a considerable degree, and further progress in this direction would require significant expenditures.

The high degree of saturation of modern transportation facilities with on-board instrument-type equipment makes a matter of concern the question of the miniaturization of separate elements of this equipment, with particular emphasis on electromechanical devices, among which are included gyroscopic instruments and systems. At the same time, a reduction in the size and weight of gyroscopic instruments designed according to the classical method entails considerable design and technological difficulties, as well as a reduction in the kinetic moment, which leads to a lowering of their accuracy. All of this has forced the developers of ISO's and ISN's to look for new ways to create gyroscopic instruments that, along with high accuracy, would be small in size and cost comparatively little.

At the present time we have seen several fundamentally new trends in the creation of gyroscopic instruments capable of competing successfully with gyroscopes constructed according to the classic method [19]. One of the most highly developed directions is the construction of rotor vibration gyroscopes. The term "vibration gyroscope" (VG) is understood to mean a device containing special elements that, given absolute angular velocities of the gyroscope's base, perform induced oscillations. It can be said that any vibration gyroscope can modulate a constant input angular velocity by transforming it into an amplitude-modulated gyroscopic moment. If the frequency of the change in the gyroscopic moment coincides with the natural frequency of the mechanical system transforming this moment into angular deflections of the sensitive elements, resonance occurs in the instrument that makes it possible to increase its transmission factor by several orders of magnitude. In connection with this the value of the kinetic moment still does not play an eseential role, which means that high sensitivity can be achieved along with miniaturization of the instrument.

The suspension of a VG's sensitive elements is usually made of elastic elements, which eliminates such an important source of errors as the "dry" friction that

occurs in the ball-bearing supports of gyroscopes constructed according to the classic method. The presence of an amplitude-modulated output signal makes it possible, with the help of well-developed radio engineering methods, to avoid the effects of a number of sources of random interference in the information extraction and processing system.

The first serious attempts to create vibration gyroscopes resulted in the realization of designs of so-called oscillator VG's, among which the tuning-fork gyrosopce [3,4] is included. Oscillator VG's lack rotating masses, and in order to create Coriolis acceleration in the presence of absolute angular velocities of the base, forced vibrations of special elastic elements (tuning fork blads, strings, rods and so forth) are used. The Coriolis forces' amplitude-modulated moment acts on an elastic suspension that is tuned to resonance on a carrier frequency in order to increase the instrument's transmission factor.

Oscillator VG's have a whole series of advantages: small size and low energy consumption, high reliability with a fundamentally achievable high sensitivity to absolute angular velocities of the base, and so on. However, the transmission factor of oscillator VG's is very sensitive to even insignificant changes in the instrument's parameters. The high sensitivity of oscillator VG's is achieved by tuning the elastic system's natural oscillations into resonance, with the minimum possible damping factor. Keeping this performance stable requires that the frequency of the elastic system's natural oscillations and the frequency of the forced vibrations be kept constant during operation, which is hardly achievable at the present time without the use of complicated and cumbersome special equipment. The result of the effect of these facts is that instruments built according to the plan of oscillator VG's are in extremely limited practical use.

Dynamically tuned RVG's are, to a considerable degree, free of the basic flaw inherent in oscillator VG's. In them, the amplitude-modulated gyroscopic moment is created because of one or several rotating bodies. In connection with this, the positional moments, which try to bring the system into a position of equilibrium, are determined not only by static rigidity, but also by dynamic rigidity (or the so-called centrifugal-pendulum rigidity). An RVG's parameters are usually selected so that in the resonance operating mode, the static rigidity is much less than the dynamic. In connection with this, a change in the elastic system's characteristics changes only the static rigidity and has an insignificant effect on the system's total rigidity. However, a change in the drive motor's frequency of rotation, which causes a change in the frequency of the gyroscopic moment acting on the elastic system, results in a corresponding change in the dynamic rigidity, which means a change in the elastic system's total rigidity. Detuning from resoance obviously has a considerably smaller effect in this case than under analogous conditions for oscillator VG's, the rigidity of the elastic suspension of which does not depend on the frequency of the inducing force. Therefore, the most recent developments and successes in the field of the creation of VG's are basically related to the realization of various plans for dynamically tuned RVG's [15].

The theoretical principles of the operation of RVG's have been created primarily through the efforts of Soviet and American scientists. Among the numerous investigations, the basic ones are the works of Ye.L. Smirnov and L.I. Brozgul' [3,4] and A.I. Sukov, (Dzh. N'yuton), E. Howe, R. Craig and P. Savet [20,33,42,46]. These works (with the exception of [42]) are devoted to the theory of single- and

double-rotor RVG's, which are the easiest to realize. However, the systems discussed in them do not give a complete picture of the potential capabilities of RVG's.

The existence of basic RVG defects, which are related to angular vibrations in the supports of the drive motor's shaft at a frequency twice that of the frequency of rotation, as well as static disbalance of the rotors under conditions of linear acceleration of the base, forces us to look for ways of reducing these defects. Tightening of the tolerances in the production process for the separate elements and assemblies of an instrument leads to the same problems encountered by the developers of gyroscopes built according to the traditional method. Therefore, some investigators are looking into the possibility of improving RVG accuracy by creating multirotor VG's [42] and VG's having different angular velocities of the rotors. A great deal of interest is being shown in systems of composite RVG's, which make it possible to combine a two-component measurer of absolute angular velocities and linear accelerations of the base in a single instrument [43,48]. The theory of multirotor VG's, allowing for the possibility of imparting different angular velocities to the rotors, as well as composite RVG's, is not yet sufficiently developed.

Previously, the development and use of RVG's was held back by technological problems that were difficult to solve. The present state of the technology is such that we can speak as boldly about RVG's as about today's gyroscopes. Their widespread use will make it possible to create a new generation of gyroscopic instruments and systems distinguished by high accuracy, small size and relatively low cost.

CHAPTER 1. CLASSIFICATION AND MATHEMATICAL MODEL OF ROTOR VIBRATION GYROSCOPES

1.1. Equations of Motion of a Generalized Rotor Vibration Gyroscope Model

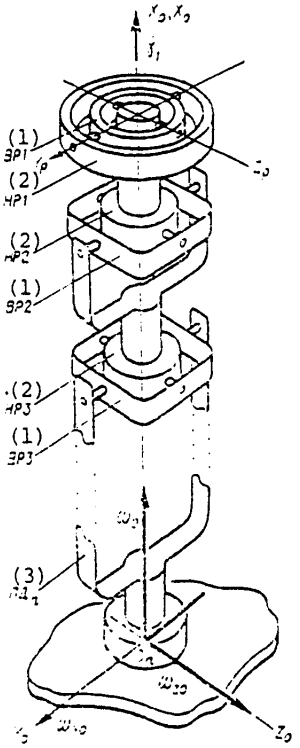

Figure 1. Layout of generalized RVG model.

Key: 1. VR.
2. NR.
3. PD.

In accordance with the data in the introduction, in the general case we will understand an RVG to be a system consisting of n material bodies that are connected to each other sequentially and have different moments of inertia relative to their main axes, which are rotating around a common axis at different rates of speed. Relative to each other, these bodies must have degrees of freedom of angular displacement around axes lying in a plane that is perpendicular to the axis of rotation. The system must also contain units that measure the bodies' angular rotations relative to each other or to the housing. A functional diagram of such a generalized RVG model is depicted in Figure 1, while the system of coordinates is shown in Figure 2.

Let us derive the equations of motion of the generalized RVG model, and introduce the concept of a stage of the generalized model. We will understand a stage of the generalized model to mean the drive motor's rotor PD_i, which has axial moment of inertia $J^{(i)}$ and equatorial moment of inertia $J_e^{(i)}$ and rotates at a relative velocity of ϕ_i; inner rotor VR_i, which is attached to it, has moments of inertia $J_{XV}^{(i)}$, $J_{YV}^{(i)}$ and $J_{ZN}^{(i)}$ [sic] and rotates at an angle ψ_i relative to an axis that is perpendicular to the axis of rotation of rotor PD_i; outer rotor NR_i, which is attached to inner rotor VR_i, has moments of inertia $J_{XN}^{(i)}$, $J_{YN}^{(i)}$ and $J_{ZN}^{(i)}$ and rotates at an angle θ_i relative to an axis that is perpendicular to the plane in which the axis of rotation of rotor PD_i and the axis of rotation of VR_i

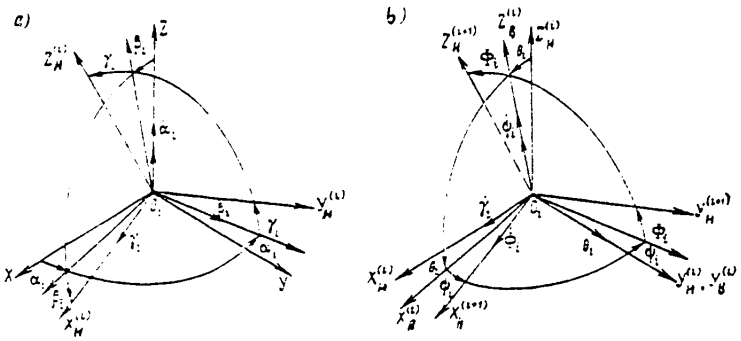

Figure 2. Systems of coordinates.

relative to rotor PD_i are located. Subscript "i" indicates that the structural elements and their parameters belong to the i-th stage. Thus, the proposed generalized RVG model can be regarded as a set of elementary stages in which the stator (PD) of the preceding stage is coupled rigidly with the NR of the following one. We will stipulate that the numbering of the stages begins with the stage that is farthest from the base.

In formulating the equations of motion, let us introduce the following basic assumption: we will assume the angles of rotation of NR_i and VR_i relative to the base to be quite small. This, naturally, means that the relative angles ψ_i and θ_i are also required to be small. Considering the diversity of methods for taking readings from an RVG, wel will formulate the generalized model's equations of motion in the inertial system of coordinates O_iXYZ. In order to do this in accordance with Figure 2, we will introduce angles α_i, β_i, γ_i of rotation of NR_i in the inertial system of reference, having related system of coordinates $O^{(i)}X_H^{(i)}Y_H^{(i)}Z_H^{(i)}$ to NR_i and system $O^{(i)}X_B^{(i)}Y_B^{(i)}Z_B^{(i)}$ to VR_i. In order to determine the characteristic features of motion of motion of the RVG elements and obtain visible results, we will limit ourselves to a discussion of linearized equations of motion only and take into consideration only terms of the first order of smallness when the PD is in a steady-state operating mode.

The equations of motion of the generalized model's first stage were derived in [8]. Using these equations, and allowing for the presence of the gyroscopic moments generated by rotor PD in the subsequent stages' equations of motion, we write the equations of motion of the generalized RVG model in the following form:

$$
\begin{aligned}
&[I_C^{(1)} - I_{Cn}^{(1)}\cos 2\gamma_1]\ddot{\alpha}_1 - I_{Cn}^{(1)}\sin 2\gamma_1\ddot{\beta}_1 = \\
&= 2R_1^{(1)}\psi_1\cos\gamma_1(\dot{\gamma}_2 - \dot{\Phi}_1)^2 - R_2^{(1)}\dot{\beta}_1(\dot{\gamma}_2 - \dot{\Phi}_1) + \\
&+ 2I_{Cn}^{(1)}(\dot{\alpha}_1\sin 2\gamma_1 - \dot{\beta}_1\cos 2\gamma_1)(\dot{\gamma}_2 - \dot{\Phi}_1) + \mu_C^{(1)}\dot{\psi}\cos\gamma_1 + \\
&+ \mu_B^{(1)}\dot{\theta}_1\sin\gamma_1 + M_C^{(1)}\cos\gamma_1 + M_B^{(1)}\sin\gamma_1 + M_x^{(1)} + \\
&+ R_1^{(1)}\dot{\gamma}_1\beta_2 - R_1^{(1)}\dot{\gamma}_1(\beta_2\cos 2\gamma_1 - \alpha_2\sin 2\gamma_1); \\
&[I_C^{(1)} - I_{Cn}^{(1)}\cos 2\gamma_1]\ddot{\beta}_1 - I_{Cn}^{(1)}\sin 2\gamma_1\ddot{\alpha}_1 = \\
&= -2R_1^{(1)}\psi_1\sin\gamma_1(\dot{\gamma}_2 - \dot{\Phi}_1)^2 + R_2^{(1)}\dot{\alpha}_1(\dot{\gamma}_2 - \dot{\Phi}_1) - \\
&\cdots\cdots\cdots
\end{aligned}
$$

$$
\begin{aligned}
&+ 2I_{Cn}^{(1)}(\dot{\alpha}_1\cos 2\gamma_1 - \dot{\beta}_1\sin 2\gamma_1)(\dot{\gamma}_2 - \dot{\Phi}_1) - \mu_C^{(1)}\dot{\psi}_1\sin\gamma_1 + \\
&+ \mu_B^{(1)}\dot{\theta}_1\cos\gamma_1 - M_C^{(1)}\sin\gamma_1 + M_B^{(1)}\cos\gamma_1 + \\
&+ M_\beta^{(1)} - R_1^{(1)}\dot{\gamma}_1\dot{\alpha}_2 - R_1^{(1)}\dot{\gamma}_1(\dot{\beta}_2\sin 2\gamma_1 - \dot{\alpha}_2\cos 2\gamma_1);
\end{aligned}
$$

$$
\dot{\Phi}_1 + \dot{\gamma}_1 = \dot{\gamma}_2;
$$

$$
\begin{aligned}
\dot{\theta}_1 &= -\dot{\alpha}_1\sin\gamma_1 - \dot{\beta}_1\cos\gamma_1 + (\dot{\gamma}_2 - \dot{\Phi}_1)\psi_1 + \\
&+ \dot{\beta}_2\cos(\gamma_2 - \Phi_1) + \dot{\alpha}_2\sin(\gamma_2 - \Phi_1);
\end{aligned}
$$

$$
\begin{aligned}
\dot{\psi}_1 &= -\dot{\alpha}_1\cos\gamma_1 + \dot{\beta}_1\sin\gamma_1 - (\gamma_2 - \dot{\Phi}_1)\theta_1 - \\
&- \dot{\beta}_2\sin(\gamma_2 - \Phi_1) + \dot{\alpha}_2\cos(\gamma_2 - \Phi_1);
\end{aligned}
\qquad (1.1)
$$

. . . . . .

$$
\begin{aligned}
&[I_C^{(n)} + I_{Cn}^{(n)}\cos 2\gamma_n]\ddot{\alpha}_n - I_{Cn}^{(n)}\sin 2\gamma_n\ddot{\beta}_n - H_{n-1}\dot{\beta}_n = \\
&= 2R_1^{(n)}\psi_n\cos\gamma_n\omega_0^2 - R_2^{(n)}\dot{\beta}_n\omega_0 - \\
&- 2I_{Cn}^{(n)}(\dot{\alpha}_n\sin 2\gamma_n + \dot{\beta}_n\cos 2\gamma_n)\omega_0 - \mu_C^{(n)}\dot{\psi}_n\cos\gamma_n + \\
&+ \mu_B^{(n)}\dot{\theta}_n\sin\gamma_n - M_C^{(n)}\cos\gamma_n + M_B^{(n)}\sin\gamma_n + \\
&+ M_\alpha^{(n)} - R_1^{(n)}\dot{\gamma}_n\dot{\beta}_{n-1} + R_1^{(n)}\dot{\gamma}_n(\omega_{Y0}\cos 2\gamma_n + \omega_{Z0}\sin 2\gamma_n);
\end{aligned}
$$

$$
\begin{aligned}
&[I_C^{(n)} - I_{Cn}^{(n)}\cos 2\gamma_n]\ddot{\beta}_n - I_{Cn}^{(n)}\sin 2\gamma_n\ddot{\alpha}_n + H_{n-1}\dot{\alpha}_n = \\
&= -2R_1^{(n)}\psi_n\sin\gamma_n\omega_0^2 + R_2^{(n)}\dot{\alpha}_n\omega_0 - \\
&- 2I_{Cn}^{(n)}(\dot{\alpha}_n\cos 2\gamma_n - \dot{\beta}_n\sin 2\gamma_n)\omega_0 - \mu_C^{(n)}\dot{\psi}_n\sin\gamma_n + \\
&+ \mu_B^{(n)}\dot{\theta}_n\cos\gamma_n - M_C^{(n)}\sin\gamma_n + M_B^{(n)}\cos\gamma_n - \\
&- M_\beta^{(n)} - R_1^{(n)}\dot{\gamma}_n\dot{\alpha}_{n-1} - R_1^{(n)}\dot{\gamma}_n(\omega_{Y0}\sin 2\gamma_n - \omega_{Z0}\cos 2\gamma_n);
\end{aligned}
$$

$$
\dot{\gamma}_n = -\omega_0;
$$

$$
\begin{aligned}
\dot{\theta}_n &= -\dot{\alpha}_n\sin\gamma_n - \dot{\beta}_n\cos\gamma_n - \omega_0\psi_n + \\
&+ \omega_{Y_0}\cos\omega_0 t - \omega_{Z_0}\sin\omega_0 t;
\end{aligned}
$$

$$
\begin{aligned}
\dot{\psi}_n &= -\dot{\alpha}_n\cos\gamma_n + \dot{\beta}_n\sin\gamma_n + \omega_0\theta_n + \\
&+ \omega_{Y_0}\sin\omega_0 t + \omega_{Z_0}\cos\omega_0 t,
\end{aligned}
$$

where

$$
I_C^{(n)} = \frac{1}{2}(I_{ZB}^{(n)} + I_{Yn}^{(n)} + I_{Zn}^{(n)} + I_e^{(n-1)});
$$

$$
I_{Cn}^{(n)} = \frac{1}{2}(I_{Zn}^{(n)} - I_{Yn}^{(n)} + I_{Zn}^{(n)});
$$

$$
R_1^{(n)} = \frac{1}{2}(I_{Xn}^{(n)} - I_{Yn}^{(n)} - I_{Zn}^{(n)});
$$

$$
R_2^{(n)} = I_{Xn}^{(n)} + I_{Zn}^{(n)};
$$

$J_e^{(n-1)}$ = equatorial moment of inertia of rotor PD of the (n - 1)-th stage; $H_{n-1} = J^{(n-1)}\dot{\gamma}_{n-1}$ = kinetic moment of rotor PD of the (n - 1)-th stage; $\mu_C^{(n)}$, $\mu_B^{(n)}$ = moments of viscous friction along the axes of suspension of the n-th stage; $M_\alpha^{(n)}$, $M_\beta^{(n)}$ = moments acting on NR_n in the inertial system of coordinates, $M_C^{(n)}$, $M_B^{(n)}$ = moments acting on the axes of suspension of the n-th stage.

It is obvious that in the first part of equations (1.1) there must be terms allowing for the disturbing moments, the elastic moments in the suspension axes and the reaction moments superimposed from the (n - 1)-th stage onto the n-th stage. In the simplest case, the moments of the elastic forces are described by the expressions

$$M_C^{(n)} = -C_C^{(n)}\psi_n; \quad M_B^{(n)} = -C_B^{(n)}\theta_n, \tag{1.2}$$

where $C_C^{(n)}$, $C_B^{(n)}$ = torsional rigidity of the elastic moments along the axes of suspension of the n-th stage.

The reaction moments on the n-th stage are composed of the inertial and gyroscopic moments generated by the (n - 1)-th stage's VR, as well as the moments of the elastic forces and forces of viscous friction along the suspension axes of the (n - 1)-th stage. Using Euler's method, let us derive the expressions for the reaction moments, which have the following form when the equations are written in the inertial system of coordinates:

$$\begin{aligned}
2M_\beta^{(n)} = &-I_{Y_B}^{(n-1)}\ddot{\beta}_{n-1} - \left(I_{X_B}^{(n-1)} + I_{Y_B}^{(n-1)} - I_{Z_B}^{(n-1)}\right)\dot{\gamma}_{n-1}\dot{\alpha}_{n-1} - \\
&- I_{Y_B}^{(n-1)}\left(\ddot{\alpha}_{n-1}\sin 2\gamma_{n-1} + \ddot{\beta}_{n-1}\cos 2\gamma_{n-1}\right) - \\
&- \left(I_{X_B}^{(n-1)} + I_{Y_B}^{(n-1)} - I_{Z_B}^{(n-1)}\right)\dot{\gamma}_{n-1}\left(\dot{\alpha}_{n-1}\cos 2\gamma_{n-1} - \dot{\beta}_{n-1}\sin 2\gamma_{n-1}\right) - \\
&- 2I_{Y_B}^{(n-1)}\dot{\theta}_{n-1}\cos\gamma_{n-1} - 2\mu_B^{(n-1)}\dot{\theta}_{n-1}\cos\gamma_{n-1} + \\
&+ 2\mu_C^{(n-1)}\dot{\psi}_{n-1}\sin\gamma_{n-1} - 2C_B^{(n-1)}\theta_{n-1}\cos\gamma_{n-1} + \\
&+ 2C_C^{(n-1)}\psi_{n-1}\sin\gamma_{n-1} - 2\left(I_{X_B}^{(n-1)} - I_{Z_B}^{(n-1)}\right)\dot{\gamma}_{n-1}^2\theta_{n-1}\cos\gamma_{n-1}; \\
2M_\alpha^{(n)} = &-I_{Y_B}^{(n-1)}\ddot{\alpha}_{n-1} + \left(I_{X_B}^{(n-1)} + I_{Y_B}^{(n-1)} - I_{Z_B}^{(n-1)}\right)\dot{\gamma}_{n-1}\dot{\beta}_{n-1} + \\
&+ I_{Y_B}^{(n-1)}\left(\ddot{\alpha}_{n-1}\cos 2\gamma_{n-1} - \dot{\beta}_{n-1}\sin 2\gamma_{n-1}\right) - \\
&- \left(I_{X_B}^{(n-1)} + I_{Y_B}^{(n-1)} - I_{Z_B}^{(n-1)}\right)\dot{\gamma}_{n-1}\left(\dot{\alpha}_{n-1}\sin 2\gamma_{n-1} + \right. \\
&\left. + \dot{\beta}_{n-1}\cos 2\gamma_{n-1}\right) - 2I_{Y_B}^{(n-1)}\dot{\theta}_{n-1}\sin\gamma_{n-1} - \\
&- 2\mu_B^{(n-1)}\dot{\theta}_{n-1}\sin\gamma_{n-1} - 2\mu_C^{(n-1)}\dot{\psi}_{n-1}\cos\gamma_{n-1} - \\
&- 2C_B^{(n-1)}\theta_{n-1}\sin\gamma_{n-1} - 2C_C^{(n-1)}\psi_{n-1}\cos\gamma_{n-1} - \\
&- 2\left(I_{X_B}^{(n-1)} - I_{Z_B}^{(n-1)}\right)\dot{\gamma}_{n-1}^2\theta_{n-1}\sin\gamma_{n-1}.
\end{aligned} \tag{1.3}$$

Thus, when expressions (1.2) and (1.3) are taken into consideration, equations (1.1) are a linearized, generalized mathematical model of the RVG represented by the functional diagram in Figure 1.

Equations (1.1) contain the absolute coordinates of rotation of the rotors in inertial space and the relative coordinates of their rotation in the suspension axes. Let us eliminate the relative coordinates from the equations of motion. In order to do this, we will determine the solution of the three kinematic equations for each stage. The first equation has the obvious solution

$$\theta_{n-1} + \gamma_{n-1} = \int \dot{\gamma}_n\,dt = \gamma_n + \varphi_n, \tag{1.4}$$

where φ_n = initial phase of rotation of the NR.

In order to solve the two remaining equations, let us write them in complex form:

$$\dot{\bar{\lambda}}_{n-1} + i\dot{\gamma}_{n-1}\bar{\lambda}_{n-1} = -\dot{\bar{\chi}}_{n-1}e^{-i\dot{\gamma}_{n-1}t} + \dot{\bar{\chi}}_n e^{-i\dot{\gamma}_{n-1}t}, \tag{1.5}$$

where $\bar{\lambda}_{n-1} = \theta_{n-1} + i\psi_{n-1}$; $\bar{\chi}_{n-1} = \beta_{n-1} + i\alpha_{n-1}$, while angle ϕ_n is assumed to be zero. It is obvious that the solution of equation (1.5) has the form

$$\bar{\lambda}_{n-1} = \bar{\lambda}^0_{n-1} e^{-i\dot{\gamma}_{n-1}t} - \bar{\chi}_{n-1} e^{-i\dot{\gamma}_{n-1}t} + \bar{\chi}_n e^{-i\dot{\gamma}_{n-1}t}, \tag{1.6}$$

where $\lambda^0_{n-1} = \theta^0_{n-1} + i\psi^0_{n-1}$ = vector of the initial angles of rotation in the suspension of the (n - 1)-th stage.

Henceforth, in order to shorten and simplify the computations we will make use of the complex coordinates we have introduced in order to write the equations of motion of the generalized RVG model. First, let us write in complex form the expressions for the moments of the elastic forces acting along the suspension axes and the reaction moments of the (n - 1)-th stage on the n-th stage. Considering (1.2) and (1.6), the vector of the moment of the elastic forces is determined by the expression

$$\begin{aligned} -\bar{M}^{(n)} = &- C_n\bar{\lambda}^0_n + C_n\bar{\chi}_n + \bar{\lambda}^{0*}_n \Delta C_n e^{i2\dot{\gamma}_n t} - \bar{\chi}^*_n \Delta C_n e^{i2\dot{\gamma}_n t} - \\ &- C_n\bar{\chi}_{n+1} + \Delta C_n \bar{\chi}^*_{n+1} e^{-i2\dot{\gamma}_n t}, \end{aligned} \tag{1.7}$$

where

$$\bar{M}^{(n)} = M^{(n)}_\beta + iM^{(n)}_\alpha; \quad C_n = \frac{C^{(n)}_C + C^{(n)}_B}{2}, \quad \Delta C_n = \frac{C^{(n)}_C - C^{(n)}_B}{2},$$

while the vector of the reactive moment is

$$\begin{aligned} \bar{M}^{(n)} = &- \tfrac{1}{2} I^{(n-1)}_{Y_B} \ddot{\bar{\chi}}_n + (iI^{(n-1)}_{Y_B}\dot{\gamma}_{n-1} - \mu_{n-1})\dot{\bar{\chi}}_n - \\ &- (R^{(n-1)}_1 \dot{\gamma}^2_{n-1} - i\dot{\gamma}_{n-1}\mu_{n-1} + C_{n-1})\bar{\chi}_n + \\ &+ \left[- \tfrac{1}{2} I^{(n-1)}_{Y_B} \ddot{\bar{\chi}}^*_n - (iI^{(n-1)}_{Y_B}\dot{\gamma}_{n-1} - \Delta\mu_{n-1})\dot{\bar{\chi}}^*_n - \right. \\ &\left. - (R^{(n-1)}_1 \dot{\gamma}^2_{n-1} - i\dot{\gamma}_{n-1}\Delta\mu_{n-1} - \Delta C_{n-1})\bar{\chi}^*_n \right] e^{i2\dot{\gamma}_{n-1}t} + \\ &+ (iR^{(n-1)}_1 \dot{\gamma}_{n-1} + \mu_{n-1})\dot{\bar{\chi}}_{n-1} + \\ &+ (R^{n-1}_1 \dot{\gamma}^2_{n-1} - i\dot{\gamma}_{n-1}\mu_{n-1} + C_{n-1})\bar{\chi}_{n-1} + \\ &+ [-(iR^{(n-1)}_1 \dot{\gamma}_{n-1} + \Delta\mu_{n-1})\dot{\bar{\chi}}^*_{n-1} + \\ &+ (R^{(n-1)}_1 \dot{\gamma}^2_{n-1} - i\dot{\gamma}_{n-1}\Delta\mu_{n-1} - \Delta C_{n-1})\bar{\chi}^*_{n-1}] e^{i2\dot{\gamma}_{n-1}t} - \\ &- \tfrac{1}{2} I^{(n-1)}_{Y_B} \ddot{\bar{\lambda}}^0_{n-1} + (iI^{(n-1)}_{Y_B}\dot{\gamma}^{n-1} - \mu_{n-1})\dot{\bar{\lambda}}^0_{n-1} - \\ &- (R^{(n-1)}_1 \dot{\gamma}^2_{n-1} - i\dot{\gamma}_{n-1}\mu_{n-1} + C_{n-1})\bar{\lambda}^0_{n-1} - \\ &- \left[\tfrac{1}{2} I^{(n-1)}_{Y_B} \ddot{\bar{\lambda}}^{0*}_{n-1} + (iI^{(n-1)}_{Y_B}\dot{\gamma}_{n-1} - \Delta\mu_{n-1})\dot{\bar{\lambda}}^{0*}_{n-1} + \right. \\ &\left. + (R^{(n-1)}_1 \dot{\gamma}^2_{n-1} - i\dot{\gamma}_{n-1}\Delta\mu_{n-1} - \Delta C_{n-1})\bar{\lambda}^{0*}_{n-1} \right] e^{i2\dot{\gamma}_{n-1}t}. \end{aligned} \tag{1.8}$$

Let us write, in system (1.1), the equations of motion of each stage in complex form and, considering expressions (1.7) and (1.8), in operator form we will obtain

$$\frac{1}{W_1(p)}\,\bar{\chi}_1 - \frac{1}{\Delta W_1^*(p-i2\dot{\gamma}_1)}\,\bar{\chi}_1^* e^{i2\dot{\gamma}_1 t} = A_1\bar{\lambda}_1^0 - \tilde{A}_1\bar{\lambda}_1^{0*}e^{i2\dot{\gamma}_1 t} +$$
$$+ W_1^+(p)\,\bar{\chi}_2 + \tilde{W}_1^+(p-i2\dot{\gamma}_1)\,\bar{\chi}_2^* e^{i2\dot{\gamma}_1 t} + \bar{M}^{(1)} + \bar{M}_{\text{ш}}^{(1)} e^{i\dot{\gamma}_1 t};$$
$$\cdots\cdots\cdots\cdots\cdots\cdots\cdots\cdots$$
$$\frac{1}{W_n(p)}\,\bar{\chi}_n - \frac{1}{\Delta W_n^*(p-i2\dot{\gamma}_n)}\,\bar{\chi}_n^* e^{i2\dot{\gamma}_n t} -$$
$$- \frac{1}{\Delta\tilde{W}_{n-1}^*(p-i2\dot{\gamma}_{n-1})}\,\bar{\chi}_n^* e^{i2\dot{\gamma}_{n-1}t} = A_n\bar{\lambda}_n^0 - \tilde{A}_n\bar{\lambda}_n^{0*}e^{i2\dot{\gamma}_n t} +$$
$$+ W_n^+(p)\,\bar{\chi}_{n+1} + \tilde{W}_n^+(p-i2\dot{\gamma}_n)\,\bar{\chi}_{n+1}^* e^{i2\dot{\gamma}_n t} + B_{n-1}\bar{\lambda}_{n-1}^0 +$$
$$+ \tilde{B}_{n-1}\bar{\lambda}_{n-1}^0 e^{i2\dot{\gamma}_{n-1}t} + W_n^-(p)\,\bar{\chi}_{n-1} +$$
$$+ \tilde{W}_n^-(p-i2\dot{\gamma}_{n-1})\,\bar{\chi}_{n-1}^* e^{i2\dot{\gamma}_{n-1}t} + \bar{M}^{(n)} + \bar{M}_{\text{ш}}^{(n)} e^{i\dot{\gamma}_n t},$$

$$\frac{1}{W_{\text{ш}}(p)} = \left(I_C^{(n)} + \frac{1}{2}\,I_{Y\text{ш}}^{(n-1)}\right)p^2 +$$
$$+ \left[i\left(-R_2^{(n)}\dot{\gamma}_n - I_{Y\text{ш}}^{(n-1)}\dot{\gamma}_{n-1} + H_{n-1}\right) + \mu_n + \mu_{n-1}\right]p +$$
$$+ \left[R_1^{(n)}\dot{\gamma}_n^2 + R_1^{(n-1)}\dot{\gamma}_{n-1}^2 -\right.$$
$$\left. - i\left(\mu_n\dot{\gamma}_n + \mu_{n-1}\dot{\gamma}_{n-1}\right) + C_n + C_{n-1}\right];$$
$$\frac{1}{\Delta W_n(p)} = I_{Cn}^{(n)}p^2 + \left(-i2I_{C\text{ш}}^{(n)}\dot{\gamma}_n + \Delta\mu_n\right)p +$$
$$+ \left(R_1^{(n)}\dot{\gamma}_n^2 - i\Delta\mu_n\dot{\gamma}_n + \Delta C_n\right);$$
$$\frac{1}{\Delta\tilde{W}_{n-1}(p)} = -\frac{1}{2}\,I_{Y\text{ш}}^{(n-1)}p^2 + \left(iI_{Y\text{ш}}^{(n-1)}\dot{\gamma}_{n-1} + \Delta\mu_{n-1}\right)p -$$
$$- \left(R_1^{(n-1)}\dot{\gamma}_{n-1}^2 + i\Delta\mu_{n-1}\dot{\gamma}_{n-1} - \Delta C_{n-1}\right);$$
$$W_n^-(p) = iR_1^{(n-1)}\dot{\gamma}_{n-1} + \mu_{n-1} +$$
$$+ \frac{1}{p}\left(R_1^{(n-1)}\dot{\gamma}_{n-1}^2 - i\mu_{n-1}\dot{\gamma}_{n-1} + C_{n-1}\right);$$
$$\tilde{W}_n^-(p) = -\left(iR_1^{(n-1)}\dot{\gamma}_{n-1} + \Delta\mu_{n-1}\right) +$$
$$+ \frac{1}{p}\left(R_1^{(n-1)}\dot{\gamma}_{n-1}^2 - i\dot{\gamma}_{n-1}\Delta\mu_{n-1} - \Delta C_{n-1}\right);$$
$$W_n^+(p) = iR_1^{(n)}\dot{\gamma}_n + \mu_n + \frac{1}{p}\left(R_1^{(n)}\dot{\gamma}_n^2 - i\mu_n\dot{\gamma}_n + C_n\right);$$
$$\tilde{W}_n^+(p) = iR_1^{(n)}\dot{\gamma}_n - \Delta\mu_n - \frac{1}{p}\left(R_1^{(n)}\dot{\gamma}_n^2 + i\Delta\mu_n\dot{\gamma}_n + \Delta C_n\right);$$
$$A_n = R_1^{(n)}\dot{\gamma}_n^2 - i\mu_n\dot{\gamma}_n + C_n;$$
$$\tilde{A}_n = R_1^{(n)}\dot{\gamma}_n^2 - i\Delta\mu_n\dot{\gamma}_n + \Delta C_n;$$
$$B_{n-1} = -\frac{1}{2}\,I_{Y\text{ш}}^{(n-1)}p^2 + \left(iI_{Y\text{ш}}^{(n-1)}\dot{\gamma}_{n-1} - \mu_{n-1}\right)p -$$
$$- R_1^{(n-1)}\dot{\gamma}_{n-1}^2 + i\mu_{n-1}\dot{\gamma}_{n-1} - C_{n-1};$$
$$\tilde{B}_{n-1} = -\frac{1}{2}\,I_{Y\text{ш}}^{(n-1)}p^2 + \Delta\mu_{n-1}p -$$
$$- R_1^{(n-1)}\dot{\gamma}_{n-1}^2 - i\dot{\gamma}_{n-1}\mu_{n-1} + \Delta C_{n-1}.$$

(1.9)

In the first approximation the absolute angular velocity $\dot{\gamma}_n$ for each stage is, obviously, expressed easily from the kinematic equations in terms of the PD's relative angular velocities with the help of the following equality:

$$\dot{\gamma}_{n-k} = -\sum_{l=1}^{k} \dot{\Phi}_{n-l} - \omega_0, \tag{1.10}$$

where ω_0 = angular velocity of the PD mounted on the nonrotating base.

Equations (1.9) are quite convenient for investigating the motion of the RVG's elements in inertial space. However, they do not reflect all of the characteristics of the RVG as a measuring instrument, since readings are usually made in the system of coordinates that is linked with the base. Therefore, it is necessary to have the possibility of writing the equations of motion in a measuring system of coordinates. Depending on the type and structural features of the RVG, the measurement can be made in a system of coordinates that is rotating and immobile relative to the base. In connection with this, it is possible to measure the angles of rotation of the instrument's elements relative to the base and to each other. In the case of measurement of the angles of rotation relative to the base, with due consideration for the assumptions we have made, the transition to the measuring system of coordinates can be made with the help of the expression

$$\bar{\lambda}_n^{\text{II}} = \bar{\lambda}_n^{\text{II}} e^{i\dot{\gamma}_n t} = -\bar{\chi}_n + \int \bar{\omega}\, dt, \tag{1.11}$$

where $\vec{\lambda}_n^{\text{N}}$ = vector of the angle of rotation of the n-th stage's NR relative to the base in the nonrotating measuring system; $\vec{\lambda}_n^{\text{V}}$ = the same, in the system rotating along with the rotor.

When measuring the relative angles of rotation of the rotors of the ℓ-th and k-th stages, it is possible to use a system of coordinates that is immobile relative to the base, as well as one that is rotating together with the rotor of either the ℓ-th or k-th stage. In the first case, in order to convert to the measuring system of coordinates it is possible to use the relationship

$$\bar{\lambda}_{lk}^{0} = -\bar{\chi}_l + \bar{\chi}_k. \tag{1.12}$$

In the second and third cases the conversion formulas take on the following forms, respectively:

$$\bar{\lambda}_{lk}^{l} = (-\bar{\chi}_l + \bar{\chi}_k)\, e^{-i\dot{\gamma}_l t}; \tag{1.13}$$

$$\bar{\lambda}_{lk}^{k} = (-\bar{\chi}_l + \bar{\chi}_k)\, e^{-i\dot{\gamma}_k t}. \tag{1.14}$$

Within the framework of the assumptions we have made, the derived equations of motion of the generalized RVG model describe the operation of all types of gyroscopes with kinematics corresponding to the system depicted in Figure 1. From them, we derive the equations of motion of practically all mechanical gyroscopes constructed according to the classic method as a special case.

1.2. Classification of Layouts of Rotor Vibration Gyroscopes

In any branch of science and technology, the problem of classification and development of a unified terminology is one of the most important ones. Its solution makes it possible to review completed investigations, generalize their results, and plan the path of further development work.

The term "rotor vibration gyroscopes" limits substantially the class of gyroscopic instruments under discussion by indicating their structural features and the features of their component elements' motion. At the present time, however, a generally accepted classification of RVG's themselves does not exist, for all practical purposes. An attempt to create one was made in [4]. There, the basis used for the classification of RVG's was the nature of the rotor's motion in a nonrotating system of coordinates. In that work, however, the authors do not allow for several structural features of possible RVG layouts, such as the number of rotors and drive motors, as well as methods for reading the signal from an RVG's rotor. Using the model described in Section 1.1, we will attempt to create a classification that will reflect, as completely as possible, all the characteristic features of instruments constructed according to RVG principles.

The broadest concept in this classification should obviously be that of "rotor gyroscopes" (RG), which we will take to mean any mechanical gyroscopes containing a rotating rotor. RG's can be divided into two large groups: rotor vibration gyroscopes and precession rotor gyroscopes (PRG), which include practically all the possible types of gyroscopes constructed according to the traditional plan for a gyroscope in a cardan suspension. The gradation of RVG's should be done on different levels, each of which defines the characteristic features of the plan of the instrument's structure.

On the first level we will differentiate RVG's according to the number of PD's or--using radio engineering terminology--modulation frequency "generators" they have. When an RVG has a single PD, the useful signal can have a modulation frequency that equals the PD's angular velocity or a multiple of it. We will call these RVG's modulation rotor gyroscopes (MRG), understanding the word "modulation" to mean the presence of only a single modulation of the useful signal. RVG's having two or more PD's will be called heterodyne rotor gyroscopes (GRG). The presence of several PD's results in a situation where a GRG's useful signal follows not only on the PD's rotation frequencies and multiples of them, but also on composite frequencies. Since in this case there is a direct analogy with the basic elements of heterodyne instruments, the use of the corresponding terminology is logical.

On the second level we will divide RVG's according to the number of separate, rotating rotor bodies, excluding the rotor of the PD, which is mounted directly on the base. Correspondingly, let us introduce the following terms: single-rotor modulation gyroscope (OMG), two-rotor modulation gyroscopes (DMG) and so on and, analogously, two-rotor heterodyne gyroscope (DGG), three-rotor heterodyne gyroscope (TGG) and so on. The concept of a single-rotor heterodyne gyroscope obviously does not make physical sense. Given an equal number of rotors, multirotor GRG's can be differentiated structurally by the number of rotors in each of the stages that is coupled with a specific PD.

Following [4], on the third level we classify RVG's according to the position of their suspension axes relative to the base. Here there are three possible cases. In the first case, the suspension axes rotate relative to the base jointly with the PD's shaft. Such RVG's we will call RVG's with rotating suspension (VP), assuming that each rotor has three degrees of freedom. In the second case, the suspension axes remain immobile relative to the base. This is an RVG with nonrotating suspension (NP). Finally, it is possible to have a situation where part of the suspension axes remain immobile and part of them rotate relative to the base along with the

PD's shaft. Such suspension we will call composite, and the instruments belong to the group of RVG's with composite suspension (KP). In the general case, an NP can have three degrees of freedom, while a KP GRG can have a different number of degrees of freedom for each of the stages.

On the fourth (and last) level, we will classify RVG's according to the systems for taking readings that are used in them. As has already been said, for multirotor RVG's readings can be taken by several methods: in different coordinate systems, between different bodies and so forth. We will use a frequency feature, which makes it possible to generalize signal reading methods to some degree. It follows directly from the equations of motion that it is possible to read a useful signal on a zero carrier frequency (permanent deviation of the rotor in the measuring system of coordinates), on the PD's frequencies of rotation and multiples of them for MRG's, and on composite frequencies for GRG's. It is also possible to have composite signal reading when readings are taken for a single instrument by several methods at the same time. Thus, when determining the affiliation of an RVG with a certain group, we should give the characteristics of its system for taking readings with respect to the frequency on which further discrimination of the useful signal takes place.

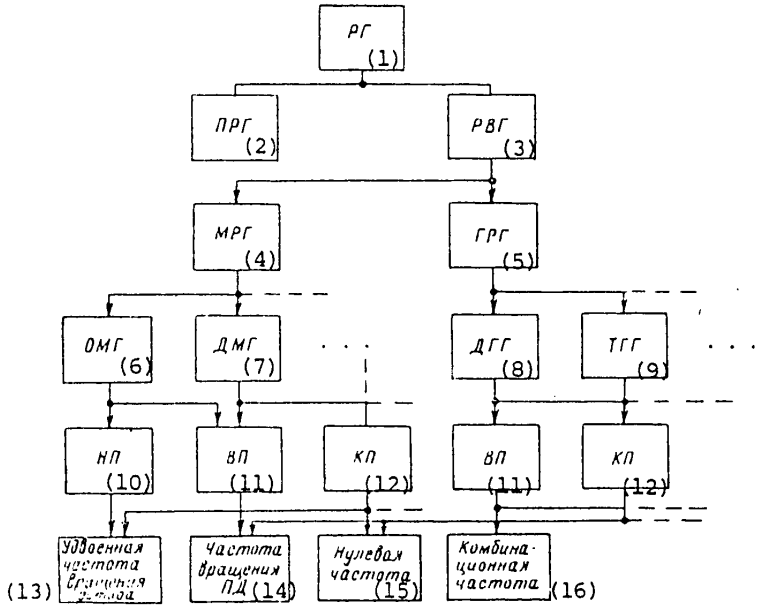

Figure 3. Classification diagram for rotor vibration gyroscopes.

Key:

1. RG
2. PRG
3. RVG
4. MRG
5. GRG
6. OMG
7. DMG
8. DGG
9. TGG
10. NP
11. VP
12. KP
13. Doubled frequency of rotation of rotor
14. Frequency of rotation of PD
15. Zero frequency
16. Composite frequency

Figure 3 is a diagram that illustrates the proposed classification. It should be mentioned here that all types of RVG's coming under this classification are described by equations of motion (1.9), and that their layouts can be derived from the layout of the generalized RVG model presented in Figure 1.

As an example, let us examine several types of MRG's. Widely known layouts of OMG's with VP are obtained from an examination on only the first stage of the generalized model, which corresponds to the layout of a DMG with orthogonal positioning of the rotors' suspension axes. If, in connection with this, the VR's moments of inertia equal zero, we obtain the plan of an OMG, the suspension of which to the shaft of the PD has two degrees of freedom. In order to obtain an OMG with one degree of freedom of the rotor's suspension from the shaft, in the preceding plan it is necessary to change the rigidity along one of the suspension axes to infinity. Two stages of the generalized model make it possible to obtain the plan of a four-rotor modulated gyroscope (ChMG) with VP and with KP, in which the suspension of each rotor has only one degree of freedom. In the first case, the frequency of rotation of PD1 should be set equal to zero ($\dot{\Phi}_1 = 0$). In connection with this, any angle between the axes of the suspension of the second and third (reading from the PD's shaft) rotors can be given. In the second case it is necessary to set the frequency of rotation of PD2 equal to zero ($\omega_0 = 0$). Layouts of TMG's with VP and with KP are derived from the corresponding ChMG plans. In connection with this, depending on which rotor is eliminated from the discussion, the suspension of the next (reading from the base) rotor will have two degrees of freedom with respect to the preceding one. Assuming that the rigidity along one of this rotor's suspension axes equals infinity, we obtain a TMG with one-stage suspension of the rotors. Finally, by eliminating yet another rotor from the discussion, we can obtain a DMG in which the suspension of each rotor has two degrees of freedom. The special features of the operation of some of these systems will be investigated in the following sections.

1.3. Equations of Motion of Rotor Vibration Gyroscopes

From the discussion of the generalized RVG model it follows that it can be used as a basis for constructing various (multistage) RVG layouts. At the present time, however, multistage RVG's are of theoretical interest only, since their realization entails the solution of an entire complex of problems. Therefore, from now on we will limit ourselves to the investigation of only those of them that are obtained on the basis of two stages of the generalized model.

As derived from equations (1.9) with due consideration for equality (1.10), the equations of motion of the two stages take on the following form:

$$\left.\begin{aligned}
&\frac{1}{W_1(p)}\bar{\chi}_1 - \frac{1}{\Delta W_1^*(p+i2(\dot{\Phi}_1+\omega_0))}\bar{\chi}_1^* e^{-i2(\dot{\Phi}_1+\omega_0)t} = \\
&\quad - A_1\bar{\lambda}_1 - \tilde{A}\bar{\lambda}_1^* e^{-i2(\dot{\Phi}_1+\omega_0)t} + W_1^+(p)\bar{\chi}_2 + \\
&\quad + \tilde{W}_1^+(p+i2(\dot{\Phi}_1+\omega_0))\bar{\chi}_2^* e^{-i2(\dot{\Phi}_1+\omega_0)t} + \\
&\quad + \bar{M}^{(1)} + \bar{M}_0^{(1)} e^{-i(\dot{\Phi}_1+\omega_0)t}; \\
&\frac{1}{W_2(p)}\bar{\chi}_2 - \frac{1}{\Delta W_2^*(p+i2\omega_0)}\bar{\chi}_2^* e^{-i2\omega_0 t} - \\
&\quad - \frac{1}{\Delta\tilde{W}_1^*(p+i2(\dot{\Phi}_1+\omega_0))}\bar{\chi}_2^* e^{-i2(\dot{\Phi}_1+\omega_0)t} =
\end{aligned}\right| \qquad (1.15)$$

$$
\left.
\begin{aligned}
&\cdots\cdots\cdots\\
&= A_2\bar{\lambda}_2^0 - \tilde{A}_2\bar{\lambda}_2^{0*}e^{-i2\omega_0 t} + W_2^+(p)\,\bar{\omega} +\\
&+ \tilde{W}_2(p+i2\omega_0)\,\bar{\omega}^* e^{-i2\omega_0 t} + B_1\bar{\lambda}_1^0 +\\
&+ B_1\bar{\lambda}_1^{0*}e^{-i2(\dot{\Phi}_1+\omega_0)t} + W_2^-(p)\,\bar{\chi} +\\
&+ \tilde{W}_2^-(p+i2(\dot{\Phi}_1+\omega_0))\times\\
&\bar{\chi}_1^* e^{-i2(\dot{\Phi}+\omega_0)t} + \bar{M}^{(2)} + M_n^{(2)}e^{-i\omega_0 t},
\end{aligned}
\right|
$$

where

$$
\frac{1}{W_1(p)} = I_C^{(1)}p^2 + [iR_2^{(1)}(\dot{\Phi}_1+\omega_0)+\mu_1]\,p + R_1^{(1)}(\dot{\Phi}_1+\omega_0)^2 +
$$
$$
+ i\mu_1(\dot{\Phi}_1+\omega_0) + C_1;
$$
$$
\frac{1}{W_2(p)} = \left(I_C^{(2)} + \frac{1}{2}I_{Y_B}^{(1)}\right)p^2 + \left[i\left(R_2^{(2)}\omega_0 + \frac{1}{2}I_{Y_B}^{(1)}(\dot{\Phi}_1+\omega_0) -\right.\right.
$$
$$
\left.\left. - I^{(2)}(\dot{\Phi}_1+\omega_0)\right) + \mu_2 + \mu_1\right]p + \left[R_1^{(2)}\omega_0^2 + R_1^{(1)}(\dot{\Phi}+\omega_0)^2 +\right.
$$
$$
\left. + i(\mu_2\omega_0 + \mu_1(\dot{\Phi}_1+\omega_0)\right) + C_1 + C_2\Big];
$$

$$
\frac{1}{\Delta W_1(p)} = I_{Cn}^{(1)}p^2 + [i2I_{Cn}^{(1)}(\dot{\Phi}_1+\omega_0) + \Delta\mu_1]\,p + R_1^{(1)}(\dot{\Phi}_1+\omega_0)^2 +
$$
$$
+ i\Delta\mu_1(\dot{\Phi}+\omega_0) + \Delta C_1;
$$
$$
\frac{1}{\Delta W_2(p)} = I_{Cn}^{(2)}p^2 + (i2I_{Cn}^{(2)}\omega_0 + \Delta\mu_2)\,p + R_1^{(2)}\omega_0^2 +
$$
$$
+ i\Delta\mu_2\omega_0 + \Delta C_2;
$$
$$
\frac{1}{\Delta\tilde{W}_1(p)} = -\frac{1}{2}I_{Y_B}^{(1)}p^2 + [-iI_{Y_B}^{(1)}(\dot{\Phi}_1+\omega_0) + \Delta\mu_1]p -
$$
$$
- R_1^{(1)}(\dot{\Phi}_1+\omega_0)^2 + i\Delta\mu_1(\dot{\Phi}_1+\omega_0) + \Delta C_1;
$$
$$
A_1 = R_1^{(1)}(\dot{\Phi}_1+\omega_0)^2 + i\mu_1(\dot{\Phi}_1+\omega_0) + C_1;
$$
$$
A_2 = R_1^{(2)}\omega_0^2 + i\mu_2\omega_0 + C_2;
$$
$$
\tilde{A}_1 = R_1^{(1)}(\dot{\Phi}_1+\omega_0)^2 + i\Delta\mu_1(\dot{\Phi}_1+\omega_0) + \Delta C_1;
$$
$$
\tilde{A}_2 = R_1^{(2)}\omega_0^2 + i\Delta\mu_2\omega_0 + \Delta C_2;
$$
$$
W_1^+(p) = -iR_1^{(1)}(\dot{\Phi}_1+\omega_0) + \mu_1 +
$$
$$
+ \frac{1}{p}[R_1^{(1)}(\dot{\Phi}_1+\omega_0)^2 + i\mu_1(\dot{\Phi}_1+\omega_0) + C_1];
$$

$$
W_2^+(p) = -iR_1^{(2)}\omega_0 + \mu_2 + \frac{1}{p}(R_1^{(2)}\omega_0^2 + i\mu_2\omega_0 + C_2);
$$

$$
\tilde{W}_1^+(p) = -iR_1^{(1)}(\dot{\Phi}_1+\omega_0) - \Delta\mu_1 -
$$
$$
- \frac{1}{p}[R_1^{(1)}(\dot{\Phi}_1+\omega_0)^2 - i\Delta\mu_1(\dot{\Phi}_1+\omega_0) + \Delta C_1];
$$

$$
\tilde{W}_2^+(p) = -iR_1^{(2)}\omega_0 - \Delta\mu_2 - \frac{1}{p}[R_1^{(2)}\omega_0^2 - i\Delta\mu_2\omega_0 + \Delta C_2];
$$

$\cdots\cdots\cdots$

$$B_1 = -\frac{1}{2} I_{Ys}^{(1)} \rho^2 - [i I_{Ys}^{(1)} (\dot{\Phi}_1 + \omega_0) - \mu_1]\, p -$$
$$- R_1^{(1)} (\dot{\Phi}_1 + \omega_0)^2 - i\mu_1 (\dot{\Phi}_1 + \omega_0) - C_1;$$
$$\tilde{B}_1 = -\frac{1}{2} I_{Ys}^{(1)} \rho^2 + \Delta\mu_1 p - R_1^{(1)} (\dot{\Phi}_1 + \omega_0)^2 + i\Delta\mu_1 (\dot{\Phi}_1 + \omega_0) + \Delta C_1;$$
$$W_2^- (p) = -iR_1^{(1)} (\dot{\Phi} + \omega_0) + \mu_1 +$$
$$+ \frac{1}{p} [R_1^{(1)} (\dot{\Phi}_1 + \omega_0)^2 + i\mu_1 (\dot{\Phi} + \omega_0) + C_1];$$
$$\tilde{W}_2^- (p) = iR_1^{(1)} (\dot{\Phi}_1 + \omega_0) - \Delta\mu_1 +$$
$$+ \frac{1}{p} [R_1^{(1)} (\dot{\Phi}_1 + \omega_0)^2 + i\Delta\mu_1 (\dot{\Phi}_1 + \omega_0) - \Delta C_1].$$

Let us first turn to the equations of motion of layouts with single modulation of the signal. There are two varieties of such layouts, namely when the modulation is provided by the second stage's drive motor PD2 and when it is provided by the first stage's drive motor PD1. Let us examine these two cases in sequence.

In the first case, in equations (1.15) it is necessary to set $\dot{\Phi}_1 = 0$, $I^{(2)} = I_e^{(2)} = 0$. In connection with this, the first and second stages' suspension axes are arbitrarily oriented relative to each other in the plane of rotation. In order to allow for this orientation, we will introduce angle ϕ_{12}, which characterizes the rotation of the first stage's suspension axis relative to the second, from an initial position where the suspension axes of the corresponding rotors in each stage coincide, in the direction of rotation at velocity ω_0. In equations (1.15), it is then necessary to set, additionally, $\dot{\Phi}_1 t = \phi_{12}$. Thus, the equations of motion of a four-rotor VG with single modulation realized by the rotation of PD2 have the form:

$$\left.\begin{aligned}
&\frac{1}{W_1(p)}\bar{\chi}_1 - \frac{1}{\Delta W_1^*(p+i2\omega_0)}\bar{\chi}_1^* e^{-i2\varphi_{12}} e^{-i2\omega_0 t} = \\
&= A_1\bar{\lambda}_1^0 - \tilde{A}_1\bar{\lambda}_1^{0*} e^{-i2\varphi_{12}} e^{-i2\omega_0 t} + W_1^+(p)\bar{\chi}_2 + \\
&+ \tilde{W}_1^+(p+i2\omega_0)\bar{\chi}_2^* e^{-i2\varphi_{12}} e^{-i2\omega_0 t} + \bar{M}^{(1)} + M_{11}^{(1)} e^{-i\varphi_{12}} e^{-i\omega_0 t}; \\
&\frac{1}{W_2(p)}\bar{\chi}_2 - \frac{1}{\Delta W_2^*(p+i2\omega_0)}\bar{\chi}_2^* e^{-i2\omega_0 t} - \\
&- \frac{1}{\Delta\tilde{W}_1^*(p+i2\omega_0)}\bar{\chi}_2^* e^{-i2\varphi_{12}} e^{-i2\omega_0 t} = \\
&= A_2\bar{\lambda}_2^0 - \tilde{A}_2\bar{\lambda}_2^{0*} e^{-i2\omega_0 t} + W_2^+(p)\bar{\omega} + \\
&+ \tilde{W}_2^+(p+i2\omega_0)\bar{\omega}^* e^{-i2\omega_0 t} + B_1\bar{\lambda}_1^0 + \tilde{B}_1\bar{\lambda}_1^{0*} e^{-i2\varphi_{12}} e^{-i2\omega_0 t} + \\
&+ W_2^-(p)\bar{\chi} + \tilde{W}_2^-(p+i2\omega_0)\bar{\chi}_1^* e^{-i2\varphi_{12}} \times \\
&\times e^{-i2\omega_0 t} + \bar{M}^{(2)} + M_{11}^{(2)} e^{-i\omega_0 t}.
\end{aligned}\right\} \qquad (1.16)$$

Three-, two- and single-rotor MRG's are special cases of this layout. In order to obtain the equations of motion for a three-rotor MRG in which each subsequent rotor has only one degree of freedom relative to the preceding one, it is sufficient to set $I_{XB}^{(2)} = I_{YB}^{(2)} = I_{ZB}^{(2)} = 0$ and $C_B^{(2)} \to \infty$ in equations (1.16). If the suspension of the third (counting from the instrument's base) rotor has two degrees of freedom in the plane of rotation relative to the second rotor, in equations (1.16) we should set $I_{XB}^{(1)} = I_{YB}^{(1)} = I_{ZB}^{(1)} = 0$. If the second rotor has two degrees of freedom relative

to the first, we should set $I_{XB}^{(2)} = I_{YB}^{(2)} = I_{ZB}^{(2)} = 0$, and if the first rotor has two degrees of freedom relative to the PD's shaft, we should set $I_{XB}^{(2)} = I_{YB}^{(2)} = I_{ZB}^{(2)} = 0$.

A two-rotor MRG with one degree of freedom of the suspension of each rotor is well known [3] and is a setup that has already been realized in practice. Its equation corresponds to the first equation in (1.16), for $\dot{\chi}_2 = \bar{\omega}$ and $\phi_{12} = 0$:

$$\frac{1}{W_1(p)}\bar{\chi}_1 - \frac{1}{\Delta W_1^*(p+i2\omega_0)}\dot{\chi}_1^* e^{-i2\omega_0 t} = A_1\bar{\lambda}_1^0 - \tilde{A}_1\bar{\lambda}_1^{0*}e^{-i2\omega_0 t} + \\ + W_1^+(p)\bar{\omega} + \tilde{W}_1^+(p+i2\omega_0)\bar{\omega}^* e^{-i2\omega_0 t} + \overline{M}^{(1)}\overline{M}_n^{(1)}e^{-i\omega_0 t}, \tag{1.17}$$

where

$$\frac{1}{W_1(p)} = I_C^{(1)}p^2 + (iR_2^{(1)}\omega_0 + \mu_1)p + R_1^{(1)}\omega_0^2 + i\mu_1\omega_0 + C_1;$$

$$\frac{1}{\Delta W_1(p)} = I_{Cn}^{(1)}p^2 + (i2I_{Cn}\omega_0 + \Delta\mu_1)p + R_1^{(1)}\omega_0^2 + i\Delta\mu_1\omega_0 + \Delta C_1;$$

$$A_1 = R_1^{(1)}\omega_0^2 + i\mu_1\omega_0 + C_1;$$

$$\tilde{A}_1 = R_1^{(1)}\omega_0^2 + i\Delta\mu_1\omega_0 + \Delta C_1;$$

$$W_1^+(p) = -iR_1^{(1)}\omega_0 + \mu_1 + \frac{1}{p}(R_1^{(1)}\omega_0^2 + i\mu_1\omega_0 + C_1);$$

$$\tilde{W}_1^+(p) = -iR_1^{(1)}\omega_0 - \Delta\mu_1 - \frac{1}{p}(R_1^{(1)}\omega_0^2 - i\Delta\mu_1\omega_0 + \Delta C_1).$$

The equation of motion of the most widely used type of two-rotor MRG--the so-called (Khaui) gyroscope--is obtained by substituting into formula (1.17) the equalities $I_{ZB}^{(1)} = I_{JB}^{(1)}$, $I_{ZH}^{(1)} = I_{JH}^{(1)}$, $C_B = C_C$, $\mu_B = \mu_C$.

Finally, the equation of motion of a single-rotor VG, which is sometimes called a (Seyvet) gyroscope, allowing for the flexural as well as the torsional rigidity of the torsion bars, is obtained by substituting the equality $I_{ZB}^{(1)} = I_{XB}^{(1)} = I_{YB}^{(1)} = 0$ into (1.17).

The equations of motion of a four-rotor VG with single modulation realized with PDl are obtained from (1.15) by substituting the equalities $\omega_0 = 0$, $\phi_{21} = 0$, and has the form

$$\left.\begin{aligned}
&\frac{1}{W_1(p)}\bar{\chi}_1 - \frac{1}{\Delta W_1^*(p+i2\dot{\Phi}_1)}\dot{\bar{\chi}}_1^* e^{-i2\dot{\Phi}_1 t} = A_1\bar{\lambda}_1^0 - \\
&- \tilde{A}_1\bar{\lambda}_1^{0*}e^{-i2\dot{\Phi}_1 t} + W_1^+(p)\bar{\chi}_2 + \tilde{W}_1^+(p+i2\dot{\Phi}_1)\dot{\bar{\chi}}_2^* e^{-i2\dot{\Phi}_1 t} + \\
&+ \overline{M}^{(1)} + \overline{M}_n^{(1)}e^{-i\dot{\Phi}_1 t}; \\
&\frac{1}{W_2(p)}\bar{\chi}_2 - \frac{1}{\Delta W_2^*(p)}\dot{\bar{\chi}}_2^* - \frac{1}{\Delta\tilde{W}_1^*(p+i2\Phi_1)}\dot{\bar{\chi}}_2^* e^{-i2\dot{\Phi}_1 t} = \\
&= A_2\bar{\lambda}_2^0 - \tilde{A}_2\bar{\lambda}_2^{0*} + W_2^+(p)\bar{\omega} + \tilde{W}_2^+(p)\bar{\omega}^* + B_1\bar{\lambda}_1^0 + \\
&+ \tilde{B}_1\bar{\lambda}_1^{0*}e^{-i2\dot{\Phi}_1 t} + W_2^-(p)\bar{\chi}_1 + \tilde{W}_2^-(p+i2\dot{\Phi}_1)\dot{\bar{\chi}}_1^* e^{-i2\dot{\Phi}_1 t} + \\
&+ \overline{M}^{(2)} + \overline{M}_n^{(2)}.
\end{aligned}\right\} \tag{1.18}$$

If the first stage has a single rotor, in equations (1.18) it is necessary to set $I^{(1)}_{XB} = I^{(1)}_{YB} = I^{(1)}_{ZB} = 0$. If, in connection with this, $C^{(2)}_{B} = C^{(2)}_{C} = 0$, from (1.18) we will obtain the equations of motion of an OMG with NP, or a so-called precession-vibration astatic gyroscope (PVAG) [16], allowing for the finite rigidity of the shaft of the gyroscope's rotor. The equations of motion of a gyrotachometer with a rotor having unequal equatorial moments of inertia also follow from equations (1.18) [45]. In order to derive these equations it is sufficient to set $I^{(2)}_{XH} = I^{(2)}_{YH} = I^{(2)}_{ZH} = I^{(1)}_{XB} = I^{(1)}_{YB} = I^{(1)}_{ZB} = I^{(1)} = I^{(2)}_{e} = 0$.

It is interesting to note that equations (1.18) also describe the motion of a biaxial gyrostabilized platform when its suspension axes are in a position that is close to orthogonal and the sensitive elements are two- or one-rotor ($I^{(1)}_{XB} = I^{(1)}_{YB} = I^{(1)}_{ZB} = 0$) RVG's with single modulation. In connection with this, the relationship $C^{(2)}_{B} = C^{(2)}_{C} = 0$ must be fulfilled.

The equations of motion of an RVG with single modulation realized by PD2 are nonstationary and have periodically changing coefficients. The nonstationary nature of the equations for this type of gyroscope is caused by the choice of the inertial reading system when describing their motion, and can be eliminated with the help of the method proposed in [16]. Actually, let us examine equations (1.16). They contain four unknowns: $\bar{\chi}_1$, $\bar{\chi}_2$, $\bar{\chi}_1^* e^{-2i\omega_0 t}$, $\bar{\chi}_2^* e^{-2i\omega_0 t}$. To each of these equations we will apply operator $e^{-i2\omega_0 t}$, and then the operation of complex conjugation to the left and right sides of the ensuing equations. As a result, we obtain two equations:

$$\left.\begin{aligned}
&\frac{1}{W_1^*(p+i2\omega_0)}\,\bar{\dot{\chi}}_1^* e^{-i2\omega_0 t} - \frac{e^{+i2\varphi_{12}}}{\Delta W_1(p)}\,\bar{\chi}_1 = A_1^* \bar{\lambda}_1^0 e^{-i2\omega_0 t} - \\
&\tilde{A}_1^* \bar{\lambda}_1^0 e^{i2\varphi_{12}} + W_1^{+*}(p+i2\omega_0)\,\bar{\dot{\chi}}_2^* e^{-i2\omega_0 t} + \\
&+ \tilde{W}_1^{+*}(p)\,\bar{\dot{\chi}}_2 e^{i2\varphi_{12}} + \bar{M}^{(1)*} e^{-i2\omega_0 t} + \bar{M}_n^{(1)*} e^{i\varphi_{12}} e^{-i\omega_0 t}; \\
&\frac{1}{W_2^*(p+i2\omega_0)}\,\bar{\dot{\chi}}_2^* e^{-i2\omega_0 t} - \frac{1}{\Delta W_2(p)}\,\bar{\chi}_2 - \frac{e^{i2\varphi_{12}}}{\Delta \tilde{W}_1(p)}\,\bar{\chi}_2 = \\
&= A_2^* \bar{\lambda}_2^{0*} e^{-i2\omega_0 t} - \tilde{A}_2^* \bar{\lambda}_2^0 + W_2^{+*}(p+i2\omega_0)\,\bar{\omega}^* e^{-i2\omega_0 t} + \\
&+ \tilde{W}_2^{+*}(p)\,\bar{\omega} + \tilde{B}_1^* \bar{\lambda}_1^0 e^{i2\varphi_{12}} + \\
&+ W_2^{-*}(p+i2\omega_0)\,\bar{\dot{\chi}}_1^* e^{-i2\omega_0 t} + B_1^* \bar{\lambda}_1^{0*} e^{-i2\omega_0 t} + \\
&+ \tilde{W}_2^{-*}(p)\,\bar{\dot{\chi}}_1 e^{i2\varphi_{12}} + \bar{M}^{(2)*} e^{-i2\omega_0 t} + \bar{M}_n^{(2)*} e^{-i\omega_0 t},
\end{aligned}\right\} \qquad (1.19)$$

which, together with equations (1.16), form a system of four algebraic equations relative to the four indicated unknowns. Having solved system of equations (1.16) and (1.19) for χ_1 and χ_2, we obtain stationary equations of motion for a four-rotor VG with single modulation from PD2, in the form

$$\begin{aligned}
\bar{\dot{\chi}}_1 = \frac{1}{W(p)}\{&[A_1 W_{11}(p) - \tilde{A}_1^* e^{i2\varphi_{12}} W_{13}(p) + B_1 W_{12}(p) + \\
&+ \tilde{B}_1^* e^{i2\varphi_{12}} W_{14}(p)]\,\bar{\lambda}_1^0 + [A_2 W_{12}(p) - \\
&- \tilde{A}_2^* W_{14}(p)]\,\bar{\lambda}_2^{0*} + [-\tilde{A}_1 e^{-i2\varphi_{12}} W_{11}(p) + \\
&+ A_1^* W_{13}(p) + \tilde{B}_1 e^{-i2\varphi_{12}} W_{12}(p) + B_1^* W_{14}(p)]\,\bar{\lambda}_1^{0*} e^{-i2\omega_0 t} + \\
&\cdots\cdots\cdots
\end{aligned}$$

$$+[-\tilde{A}_2W_{12}(p)+A_2^*W_{14}(p)]\,\bar{\lambda}_2^{0*}e^{-i2\omega_0 t}+[W_2^+(p)W_{12}(p)+$$

$$+\tilde{W}_2^{+*}(p)W_{14}(p)]\,\bar{\omega}+[\tilde{W}_2^+(p+i2\omega_0)W_{12}(p)+$$

$$+W_2^{+*}(p+i2\omega_0)W_{14}(p)]\,\bar{\omega}^*e^{-i2\omega_0 t}+W_{11}(p)\,\overline{M}^{(1)}+$$

$$+W_{13}(p)\,\overline{M}^{(1)*}e^{-i2\omega_0 t}+W_{11}(p)\,e^{-i\varphi_{12}}\overline{M}_n^{(1)}e^{-i\omega_0 t}+$$

$$+W_{13}(p)\,e^{i\varphi_{12}}\overline{M}_n^{(1)*}e^{-i\omega_0 t}+W_{12}(p)\,\overline{M}^{(2)}+W_{14}(p)\,\overline{M}^{(2)*}e^{-i2\omega_0 t}+$$

$$+W_{12}(p)\,\overline{M}_n^{(2)}e^{-i\omega_0 t}+W_{14}(p)\,\overline{M}_n^{(2)*}e^{-i\omega_0 t}\Big\}; \qquad (1.20)$$

$$\bar{\chi}_2=\frac{1}{W(p)}\Big\{[A_1W_{21}(p)-\tilde{A}_1^*e^{i2\varphi_{12}}W_{23}(p)+B_1W_{22}(p)+$$

$$+\tilde{B}_1^*e^{i2\varphi_{12}}W_{24}(p)]\,\bar{\lambda}_1^0+[A_2W_{22}(p)-\tilde{A}_2^*W_{24}(p)]\,\bar{\lambda}_2^0+$$

$$+[-\tilde{A}_1e^{-i2\varphi_{12}}W_{21}(p)+A_1^*W_{23}(p)+\tilde{B}_1e^{-2\varphi_{12}}\times$$

$$\times W_{22}(p)+B_1^*W_{24}(p)]\,\bar{\lambda}_1^{0*}e^{-i2\omega_0 t}+[-\tilde{A}_2W_{22}(p)+$$

$$+A_2^*W_{24}(p)]\,\bar{\lambda}_2^{0*}e^{-i2\omega_0 t}+[W_2^+(p)W_{22}(p)+\tilde{W}_2^{+*}(p)W_{24}(p)]\,\bar{\omega}+$$

$$+[W_2^+(p+i2\omega_0)+W_{22}(p)+W_2^{+*}(p+i2\omega_0)W_{24}(p)]\,\bar{\omega}^*e^{-i2\omega_0 t}+$$

$$+W_{21}(p)\,\overline{M}^{(1)}+W_{23}(p)\,M^{(1)*}e^{-i2\omega_0 t}+W_{21}(p)\,e^{-i\varphi_{12}}\overline{M}_n^{(1)}e^{-i\omega_0 t}+$$

$$+W_{23}(p)\,e^{i\varphi_{12}}\overline{M}_n^{(1)*}e^{-i\omega_0 t}+W_{22}(p)\,\overline{M}^{(2)}+W_{24}(p)\,\overline{M}^{(2)*}e^{-i2\omega_0 t}+$$

$$+W_{22}(p)\,\overline{M}_n^{(2)}e^{-i\omega_0 t}+W_{24}(p)\,\overline{M}_n^{(2)*}e^{-i\omega_0 t}\Big\},$$

where

$$W(p)=\frac{1}{W_1(p)}W_{11}(p)-pW_2^-(p)W_{12}(p)-\frac{e^{i2\varphi_{12}}}{\Delta W_1(p)}W_{13}(p)-$$

$$-p\tilde{W}_2^{-*}(p)\,e^{i2\varphi_{12}}W_{14}(p);$$

$$W_{11}(p)=\frac{1}{(p+i2\omega_0)^2}\frac{1}{W_2(p)}\frac{1}{W_1^*(p+i2\omega_0)}\frac{1}{W_2^*(p+i2\omega_0)}-$$

$$-\frac{pe^{i2\varphi_{12}}}{p+i2\omega_0}\tilde{W}_1^{+*}(p)W_2^{-*}(p+i2\omega_0)\times\left[\frac{1}{\Delta W_2^*(p+i2\omega_0)}+\right.$$

$$\left.+\frac{e^{-i2\varphi_{12}}}{\Delta\tilde{W}_1^*(p+i2\omega_0)}\right]-\left[\frac{1}{\Delta\tilde{W}_1(p)}+\frac{e^{-i2\varphi_{12}}}{\Delta W_1(p)}\right]\times$$

$$\times\tilde{W}_2^-(p+i2\omega_0)W_1^{+*}(p+i2\omega_0)-\frac{1}{(p+i2\omega_0)^2}\left[\frac{e^{i2\varphi_{12}}}{\Delta\tilde{W}_1(p)}+\frac{1}{\Delta W_2(p)}\right]\times$$

$$\times\left[\frac{1}{\Delta W_2^*(p+i2\omega_0)}+\frac{e^{-i2\varphi_{12}}}{\Delta\tilde{W}_1^*(p+i2\omega_0)}\right]\frac{1}{W_2^*(p+i2\omega_0)}-$$

$$-\frac{p}{p+i2\omega_0}\frac{\tilde{W}_1^{+*}(p)\tilde{W}_2^-(p+i2\omega_0)}{W_2^*(p+i2\omega_0)}-$$

$$\cdots\cdots\cdots$$

$$-\frac{1}{W_2(p)}\,W_1^{+\bullet}(p+i2\omega_0)\,W_2^{-\bullet}(p+i2\omega_0),$$

$$W_{12}(p)=\frac{p}{(p+i2\omega_0)^2}\,\frac{W_1^{+}(p)}{W_1^{\bullet}(p+i2\omega_0)\,W_2^{\bullet}(p+i2\omega_0)}+$$

$$+\,p\tilde{W}_1^{+\bullet}(p)\,W_2^{-\bullet}(p+i2\omega_0)\,\tilde{W}_1^{+}(p+i2\omega_0)+$$

$$+\left[\frac{1}{\Delta\tilde{W}_1(p)}+\frac{e^{-i2\varphi_{12}}}{\Delta W_2(p)}\right]\frac{W_1^{+\bullet}(p+i2\omega_0)}{\Delta W_1^{\bullet}(p+i2\omega_0)}\,\frac{1}{p+i2\omega_0}+$$

$$+\left[\frac{1}{\Delta\tilde{W}_1(p)}+\frac{e^{-i2\varphi_{12}}}{\Delta W_2(p)}\right]\frac{\tilde{W}_1^{+}(p+i2\omega_0)}{W_1^{\bullet}(p+i2\omega_0)}\,\frac{1}{p+i2\omega_0}+$$

$$+\frac{p}{(p+i2\omega_0)^2}\,\frac{\tilde{W}_1^{+\bullet}(p)}{W_2^{\bullet}(p+i2\omega_0)\,\Delta W_1^{\bullet}(p+i2\omega_0)}-$$

$$-\,pW_1^{+}(p)\,W_1^{+\bullet}(p+i2\omega_0)\,W_2^{-\bullet}(p+i2\omega_0);$$

$$W_{13}(p)=\frac{pe^{i2\varphi_{12}}}{p+i2\omega_0}\,\frac{W_1^{+}(p)\,\tilde{W}_2^{-}(p+i2\omega_0)}{W_2^{\bullet}(p+i2\omega_0)}-\left[\frac{1}{\Delta\tilde{W}_1(p)}+\frac{e^{-i2\varphi_{12}}}{\Delta W_2(p)}\right]\times$$

$$\times\left[\frac{1}{\Delta W_2^{\bullet}(p+i2\omega_0)}+\frac{e^{-i2\varphi_{12}}}{\Delta\tilde{W}_1^{\bullet}(p+i2\omega_0)}\right]\frac{1}{(p+i2\omega_0)^2}\,\frac{1}{\Delta W_1^{\bullet}(p+i2\omega_0)}+$$

$$+\frac{e^{-i2\varphi_{12}}}{W_2(p)}\,W_2^{-\bullet}(p+i2\omega_0)\,\tilde{W}_1^{+}(p+i2\omega_0)+$$

$$+\left[\frac{e^{i2\varphi_{12}}}{\Delta\tilde{W}_1(p)}+\frac{1}{\Delta W_2(p)}\right]e^{-i4\varphi_{12}}\,\tilde{W}_2^{-}(p+i2\omega_0)\,\tilde{W}_1^{+}(p+i2\omega_0)+$$

$$+\frac{e^{-i2\varphi_{12}}}{(p+i2\omega_0)^2}\,\frac{1}{W_2(p)}\,\frac{1}{\Delta W_1^{\bullet}(p+i2\omega_0)}\,\frac{1}{W_2^{\bullet}(p+i2\omega_0)}+$$

$$+\frac{p}{p+i2\omega_0}\,W_1^{+}(p)\,W_2^{-\bullet}(p+i2\omega_0)\left[\frac{1}{\Delta W_2^{\bullet}(p+i2\omega_0)}+\frac{e^{-i2\varphi_{12}}}{\Delta\tilde{W}_1^{\bullet}(p+i2\omega_0)}\right];$$

$$W_{14}(p)=pW_1^{+}(p)\,W_1^{+\bullet}(p+i2\omega_0)\,\tilde{W}_2^{-}(p+i2\omega_0)\,e^{-i2\varphi_{12}}+$$

$$+\frac{p}{(p+i2\omega_0)^2}\left[\frac{1}{\Delta W_2^{\bullet}(p+i2\omega_0)}+\frac{e^{-i2\varphi_{12}}}{\Delta\tilde{W}_1^{\bullet}(p+i2\omega_0)}\right]\frac{\tilde{W}_1^{+\bullet}(p)}{\Delta W_1^{\bullet}(p+i2\omega_0)}+$$

$$+\frac{e^{-i2\varphi_{12}}}{p+i2\omega_0}\,\frac{1}{W_2(p)}\,\frac{\tilde{W}_1^{+}(p+i2\omega_0)}{W_1^{\bullet}(p+i2\omega_0)}-e^{-i2\varphi_{12}}p\tilde{W}_1^{+\bullet}(p)\,\tilde{W}_1^{+}(p+i2\omega_0)\times$$

$$\times\,\tilde{W}_2^{-}(p+i2\omega_0)+\frac{p}{(p+i2\omega_0)^2}\left[\frac{1}{\Delta W_2^{\bullet}(p+i2\omega_0)}+\frac{e^{-i2\varphi_{12}}}{\Delta\tilde{W}_1^{\bullet}(p+i2\omega_0)}\right]\times$$

$$\times\,\frac{W_1^{+}(p)}{W_1^{\bullet}(p+i2\omega_0)}+\frac{e^{-i2\varphi_{12}}}{p+i2\omega_0}\cdot\frac{1}{W_2(p)}\,\frac{W_1^{+\bullet}(p+i2\omega_0)}{\Delta W_1^{\bullet}(p+i2\omega_0)};$$

$$W_{21}(p)=\frac{p}{(p+i2\omega_0)^2}\,\frac{W_2^{-}(p)}{W_1^{\bullet}(p+i2\omega_0)}\,\frac{1}{W_2^{\bullet}(p+i2\omega_0)}+$$

$$+\frac{e^{i2\varphi_{12}}}{p+i2\omega_0}\,\frac{W_2^{-\bullet}(p+i2\omega_0)}{\Delta W_1(p)}\left[\frac{1}{\Delta W_2^{\bullet}(p+i2\omega_0)}+\frac{e^{-i2\varphi_{12}}}{\Delta\tilde{W}_1^{\bullet}(p+i2\omega_0)}\right]+$$

$$\cdots\cdots\cdots$$

$$\cdots\cdots\cdots$$

$$+ p\tilde{W}_2^{-*}(p)\,\tilde{W}_2^{-}(p+i2\omega_0)\,W_1^{+*}(p+i2\omega_0) +$$

$$+ \frac{pe^{i2\varphi_{12}}}{(p+i2\omega_0)^2}\,\frac{\tilde{W}_2^{-*}(p)}{W_1^{*}(p+i2\omega_0)}\left[\frac{1}{\Delta W_2^{*}(p+i2\omega_0)} + \frac{e^{-i2\varphi_{12}}}{\Delta\tilde{W}_1^{*}(p+i2\omega_0)}\right] +$$

$$+ \frac{1}{p+i2\omega_0}\,\frac{\tilde{W}_2^{-}(p+i2\omega_0)}{\Delta W_1(p)}\,\frac{1}{W_2^{*}(p+i2\omega_0)} =$$

$$- pW_2^{-}(p)\,W_2^{-*}(p+i2\omega_0)\,W_1^{+*}(p+i2\omega_0);$$

$$W_{22}(p) = \frac{1}{(p+i2\omega_0)^2}\,\frac{1}{W_1(p)}\,\frac{1}{W_1^{*}(p+i2\omega_0)}\,\frac{1}{W_2^{*}(p+i2\omega_0)} -$$

$$- \frac{p}{p+i2\omega_0}\,\frac{\tilde{W}_2^{-*}(p)\,W_1^{+*}(p+i2\omega_0)}{\Delta W_1^{*}(p+i2\omega_0)} - W_2^{-*}(p+i2\omega_0)\times$$

$$\times\,\frac{\tilde{W}_1^{+}(p+i2\omega_0)}{\Delta W_1(p)} - \frac{p}{p+i2\omega_0}\,\frac{\tilde{W}_2^{-*}(p)\,\tilde{W}_1^{+}(p+i2\omega_0)}{W_1^{*}(p+i2\omega_0)} -$$

$$- \frac{W_2^{-*}(p+i2\omega_0)\,W_1^{+*}(p+i2\omega_0)}{W_1(p)} - \frac{1}{(p+i2\omega_0)^2}\,\frac{1}{\Delta W_1(p)}\times$$

$$\times\,\frac{1}{\Delta W_1^{*}(p+i2\omega_0)}\,\frac{1}{W_2^{*}(p+i2\omega_0)};$$

$$W_{23}(p) = \frac{e^{-i2\varphi_{12}}}{p+i2\omega_0}\,\frac{1}{W_1(p)}\,\frac{\tilde{W}_2^{-}(p+i2\omega_0)}{W_2^{*}(p+i2\omega_0)} + \frac{p}{(p+i2\omega_0)^2}\times$$

$$\times\,\frac{\tilde{W}_2^{-*}(p)}{\Delta W_1^{*}(p+i2\omega_0)}\left[\frac{1}{\Delta W_2^{*}(p+i2\omega_0)} + \frac{e^{-i2\varphi_{12}}}{\Delta\tilde{W}_1^{*}(p+i2\omega_0)}\right] +$$

$$+ pe^{-i2\varphi_{12}}\,W_2^{-}(p)\,\tilde{W}_1^{+}(p+i2\omega_0)\,W_2^{-*}(p+i2\omega_0) -$$

$$- pe^{-i2\varphi_{12}}\,\tilde{W}_2^{-*}(p)\,\tilde{W}_2^{-}(p+i2\omega_0)\,\tilde{W}_1^{+}(p+i2\omega_0) +$$

$$+ \frac{pe^{-i2\varphi_{12}}}{(p+i2\omega_0)^2}\,\frac{1}{W_2^{*}(p+i2\omega_0)}\,\frac{W_2^{-}(p)}{\Delta W_1^{*}(p+i2\omega_0)} +$$

$$+ \frac{1}{p+i2\omega_0}\,\frac{W_2^{-*}(p+i2\omega_0)}{W_1(p)}\left[\frac{1}{\Delta W_2^{*}(p+i2\omega_0)} + \frac{e^{-i2\varphi_{12}}}{\Delta\tilde{W}_1^{*}(p+i2\omega_0)}\right];$$

$$W_{24}(p) = \frac{e^{-i2\varphi_{12}}}{W_1(p)}\,\tilde{W}_2^{-}(p+i2\omega_0)\,W_1^{+*}(p+i2\omega_0) -$$

$$- \frac{1}{(p+i2\omega_0)^2}\,\frac{1}{\Delta W_1(p)}\,\frac{1}{\Delta W_1^{*}(p+i2\omega_0)}\left[\frac{1}{\Delta W_2^{*}(p+i2\omega_0)} +\right.$$

$$\left. + \frac{e^{-i2\varphi_{12}}}{\Delta\tilde{W}_1^{*}(p+i2\omega_0)}\right] + \frac{pe^{-i2\varphi_{12}}}{p+i2\omega_0}\,\frac{W_2^{-}(p)\tilde{W}_1^{+}(p+i2\omega_0)}{W_2^{*}(p+i2\omega_0)} +$$

$$+ \frac{e^{-i2\varphi_{12}}}{\Delta W_1(p)}\,\tilde{W}_2^{-}(p+i2\omega_0)\,\tilde{W}_1^{+}(p+i2\omega_0) +$$

$$+ \frac{1}{(p+i2\omega_0)^2}\left[\frac{1}{\Delta W_2^{*}(p+i2\omega_0)} +\right.$$

$$\cdots\cdots\cdots$$

$$+\frac{e^{-i2\varphi_{11}}}{\Delta\tilde{W}_1^*(p+i2\omega_0)}\Big]\frac{1}{W_1(p)}\cdot\frac{1}{W_1^*(p+i2\omega_0)}+$$

$$+\frac{pe^{-i2\varphi_{11}}}{p+i2\omega_0}\cdot\frac{W_2^-(p)\,W_2^{+*}(p+i2\omega_0)}{\Delta W_1^*(p+i2\omega_0)}.$$

The stationary equation of motion of a two-rotor MRG can be derived either directly from (1.20) or by applying an analogous method to equation (1.17). It has the form

$$\vec{\chi}_1=\frac{1}{W(p)}\Big\{W_\lambda(p)\,\vec{\lambda}_1^0+\tilde{W}_\lambda(p)\,\vec{\lambda}_1^{0*}e^{-i2\omega_0 t}+\frac{W_\omega(p)}{p}\bar{\omega}+$$

$$+\frac{\tilde{W}_\omega(p)}{p+i2\omega_0}\,\bar{\omega}^*e^{-i2\omega_0 t}+\frac{1}{W_1^*(p+2i\omega_0)}\,\overline{M}^{(1)}+$$

$$+\frac{1}{\Delta W_1^*(p+i2\omega_0)}\,\overline{M}^{(1)*}e^{-i2\omega_0 t}+\frac{1}{W_1^*(p+i2\omega_0)}\,\overline{M}_{11}e^{-i\omega_0 t}+ \tag{1.21}$$

$$+\frac{1}{\Delta W_1^*(p+i2\omega_0)}\,\overline{M}_{11}^*e^{-i\omega_0 t}\Big\},$$

where

$$W(p)=\frac{1}{W_1(p)\,W_1^*(p+i2\omega_0)}-\frac{1}{\Delta W_1(p)\,\Delta W_1^*(p+i2\omega_0)};$$

$$W_\lambda(p)=R_1^{(1)}\omega_0^2\Big[\frac{1}{W_1^*(p+i2\omega_0)}-\frac{1}{\Delta W_1^*(p+i2\omega_0)}\Big]+$$

$$+i\omega_0\Big[\frac{\mu_1}{W_1^*(p+i2\omega_0)}+\frac{\Delta\mu_1}{\Delta W_1^*(p+i2\omega_0)}\Big]+$$

$$+\frac{C_1}{W_1^*(p+i2\omega_0)}-\frac{\Delta C_1}{\Delta W_1^*(p+i2\omega_0)};$$

$$\tilde{W}_\lambda(p)=-R_1^{(1)}\omega_0^2\Big[\frac{1}{W_1^*(p+i2\omega_0)}-\frac{1}{\Delta W_1^*(p+i2\omega_0)}\Big]+$$

$$+i\omega_0\Big[\frac{\Delta\mu_1}{W_1^*(p+i2\omega_0)}+\frac{\mu_1}{\Delta W_1^*(p+i2\omega_0)}\Big)-$$

$$-\frac{\Delta C_1}{W_1^*(p+i2\omega_0)}+\frac{C_1}{\Delta W_1^*(p+i2\omega_0)};$$

$$W_\omega(p)=p\Big\{\Big[-iR_1^{(1)}\omega_0^2\Big(\frac{1}{W_1^*(p+i2\omega_0)}-\frac{1}{\Delta W_1^*(p+i2\omega_0)}\Big)+$$

$$+\frac{\mu_1}{W_1^*(p+i2\omega_0)}-\frac{\Delta\mu_1}{\Delta W_1^*(p+i2\omega_0)}\Big]\omega_0 W_c(p)+$$

$$+\frac{C_1}{p}\,\frac{1}{W_1^*(p+i2\omega_0)}-\frac{\Delta C_1}{p}\,\frac{1}{\Delta W_1^*(p+i2\omega_0)}\Big\},$$

$$\tilde{W}_\omega(p)=(p+i2\omega_0)\Big\{\Big[-iR_1^{(1)}\omega_0\Big(\frac{1}{W_1^*(p+i2\omega_0)}-\frac{1}{\Delta W_1^*(p+i2\omega_0)}\Big)-$$

$$-\frac{\Delta\mu_1}{W_1^*(p+i2\omega_0)}+\frac{\mu_1}{\Delta W_1^*(p+i2\omega_0)}\Big]\omega_0 W_c^*(p+i2\omega_0)-$$

$$-\frac{\Delta C_1}{p+i2\omega_0}\,\frac{1}{W_1^*(p+i2\omega_0)}+\frac{C_1}{p+i2\omega_0}\,\frac{1}{\Delta W_1^*(p+i2\omega_0)}\Big\};$$

. . . . . .

$$W_C(p) = \frac{1}{p}\left(\frac{1}{\omega_0}p + i\right).$$

With the help of this method, the equations of motion of an RVG with single modulation realized by PD1 can be reduced to a stationary form only if the following condition is fulfilled:

$$\frac{1}{\Delta W_2^*(p)} = 0. \tag{1.22}$$

From (1.15) it follows that condition (1.22) takes place only when the following relationships between the MRG's parameters are fulfilled:

$$\Delta C_2 = 0; \quad \Delta\mu_2 = 0; \quad J_{C\text{н}}^{(2)} = \frac{1}{2}\left(J_{Z\text{в}}^{(2)} - J_{Y\text{н}}^{(2)} + J_{Z\text{н}}^{(2)}\right) = 0.$$

The first two of these require that the second stage's suspension be uniformly rigid and have identical damping coefficients along both axes. The third condition can be fulfilled either if there is an inverted cardan suspension or if the suspension has an inner framework with $J_{ZB}^{(2)} = 0$.

Thus, when condition (1.22) is fulfilled, the equations of motion of an RVG with single modulation by PD1 take on the following form:

$$\left.\begin{aligned}
&\tilde{\chi}_1 = \frac{1}{W(p)}\{[A_1 W_{11}(p) - \tilde{A}_1^* W_{13}(p) + B_1 W_{12}(p) + \tilde{B}_1^* W_{14}(p)]\,\tilde{\lambda}_1^0 + \\
&+ [-\tilde{A}_1 W_{11}(p) + A_1^* W_{13}(p) + \tilde{B}_1 W_{12}(p) + B_1^* W_{14}(p)]\,\tilde{\lambda}_1^{0*} e^{-i2\dot{\Phi}_1 t} + \\
&+ C_2 W_{12}(p)\,\tilde{\lambda}_2^0 + C_2 W_{14}(p)\,\tilde{\lambda}_2^{0*} e^{-i2\dot{\Phi}_1 t} + W_2^+(p)\,W_{12}(p)\,\tilde{\omega} + \\
&+ W_2^{+*}(p + i2\dot{\Phi}_1)\,W_{14}(p)\,\tilde{\omega}^* e^{-i2\dot{\Phi}_1 t} + W_{11}(p)\,\overline{M}^{(1)} + \\
&+ W_{13}(p)\,\overline{M}^{(1)*} e^{-i2\dot{\Phi}_1 t} + W_{12}(p)\,\overline{M}^{(2)} + W_{14}(p)\,\overline{M}^{(2)*} e^{-i2\dot{\Phi}_1 t} + \\
&+ W_{11}(p)\,\overline{M}_{\text{п}}^{(1)} e^{-i\dot{\Phi}_1 t} + W_{13}(p)\,\overline{M}_{\text{п}}^{(1)*} e^{-i\dot{\Phi}_1 t} + W_{12}(p)\,\overline{M}_{\text{п}}^{(2)} + \\
&+ W_{14}(p)\,\overline{M}_{\text{п}}^{(2)*} e^{-i2\dot{\Phi}_1 t}; \\
&\tilde{\chi}_2 = \frac{1}{W(p)}\{[A_1 W_{21}(p) - \tilde{A}_1^* W_{23}(p) + B_1 W_{22}(p) + \\
&+ \tilde{B}_1^* W_{24}(p)]\,\tilde{\lambda}_1^0 + [-\tilde{A}_1 W_{21}(p) + A_1^* W_{23}(p) + \tilde{B}_1 W_{22}(p) + \\
&+ B_1^* W_{24}(p)]\,\tilde{\lambda}_1^{0*} e^{-i2\dot{\Phi}_1 t} + C_2 W_{22}(p)\,\tilde{\lambda}_2^0 + C_2 W_{24}(p)\,\tilde{\lambda}_2^{0*} e^{-i2\dot{\Phi}_1 t} + \\
&+ W_2^+(p)\,W_{22}(p)\,\tilde{\omega} + W_2^{+*}(p + i2\dot{\Phi}_1)\,W_{24}(p)\,\tilde{\omega}^* e^{-i2\dot{\Phi}_1 t} + \\
&+ W_{21}(p)\,\overline{M}^{(1)} + W_{22}(p)\,\overline{M}^{(2)} + W_{23}(p)\,\overline{M}^{(1)*} e^{-i2\dot{\Phi}_1 t} + \\
&+ W_{21}(p)\,\overline{M}^{(2)*} e^{-i2\dot{\Phi}_1 t} + W_{22}(p)\,\overline{M}_{\text{п}}^{(2)} + W_{24}(p)\,\overline{M}_{\text{п}}^{(2)*} e^{-i2\dot{\Phi}_1 t} + \\
&+ W_{21}(p)\,\overline{M}_{\text{п}}^{(1)} e^{-i\dot{\Phi}_1 t} + W_{23}(p)\,\overline{M}_{\text{п}}^{(1)*} e^{-i\dot{\Phi}_1 t}\},
\end{aligned}\right\} \tag{1.23}$$

where the expressions for operators $W_{k\ell}(p)$ coincide with the analogous expressions presented in equations (1.20) when the equalities $\omega_0 = \dot{\Phi}_1$ and $\phi_{12} = 0$ are substituted into the latter.

RVG systems with double modulation can be differentiated by the number of rotors in the first and second stages. In addition to a four-rotor setup, it is possible to have setups with one first-stage rotor, one second-stage rotor and one first- and

second-stage rotor. The operation of all these systems is described by equations (1.15) when the appropriate values of the instrument's parameters are substituted into them.

Equations (1.15) are nonstationary, with harmonically changing coefficients. In connection with this, there are two coefficient-changing frequencies: frequency $2\omega_0$, which is the PD2's doubled frequency of rotation, and frequency $2(\dot{\Phi}_1 + \omega_0)$, which is the doubled total frequency of rotation of PD1 and PD2. The periodic coefficients that change with frequency $2\omega_0$ can obviously be eliminated by selecting the appropriate system of coordinates for writing the equations of motion. Making use of this fact, let us transform equations (1.15) so that in them we have periodic coefficients that change with only one frequency. With this purpose in mind, by using the previously applied method we first eliminate the periodic coefficients in front of the unknown χ_1 in the first equation (1.15). As a result, we obtain

$$\chi_1 = \frac{1}{W_3(p)}\left\{W_5(p)\,\tilde{\lambda}_1^0 + \tilde{W}_5(p)\,\tilde{\lambda}_1^{0*}e^{-i2(\dot{\Phi}_1+\omega_0)} + W_4(p)\bar{\chi}_2 + \right.$$
$$+ \tilde{W}_4(p)\,\bar{\chi}_2^* e^{-i2(\dot{\Phi}_1+\omega_0)t} + \frac{1}{W_1^*(p+i2(\dot{\Phi}_1+\omega_0))}\left(\overline{M}^{(1)} + \right.$$
$$\left. + \overline{M}_n^{(1)}e^{-i(\dot{\Phi}_1+\omega_0)t}\right) + \frac{1}{\Delta W_1^*(p+i2(\dot{\Phi}_1+\omega_0))}\left(\overline{M}^{(1)*}e^{-i2(\dot{\Phi}_1+\omega_0)t} + \right. \tag{1.24}$$
$$\left.\left. + \overline{M}_n^{(1)*}e^{-i(\dot{\Phi}_1+\omega_0)t}\right)\right\},$$

where

$$W_3(p) = \frac{1}{W_1(p)\,W_1^*(p+i2(\dot{\Phi}+\omega_0))} - \frac{1}{\Delta W_1(p)\,\Delta W_1^*(p+i2(\dot{\Phi}_1+\omega_0))};$$

$$W_5(p) = \frac{A_1}{W_1^*(p+i2(\dot{\Phi}_1+\omega_0))} - \frac{\tilde{A}_1^*}{\Delta W_1^*(p+i2(\dot{\Phi}_1+\omega_0))};$$

$$\tilde{W}_5(p) = -\frac{\tilde{A}_1}{W_1^*(p+i2(\dot{\Phi}_1+\omega_0))} + \frac{A_1^*}{\Delta W_1^*(p+i2(\Phi_1+\omega_0))};$$

$$W_4(p) = \frac{W_1^\dagger(p)}{W_1^*(p+i2(\dot{\Phi}_1+\omega_0))} + \frac{\tilde{W}_1^{\dagger*}(p)}{\Delta W_1^*(p+i2(\dot{\Phi}_1+\omega_0))};$$

$$\tilde{W}_4(p) = \frac{\tilde{W}_1^\dagger(p+i2(\dot{\Phi}_1+\omega_0))}{W_1^*(p+i2(\dot{\Phi}+\omega_0))} + \frac{W_1^{\dagger*}(p+i2(\dot{\Phi}_1+\omega_0))}{\Delta W_1^*(p+i2(\dot{\Phi}_1+\omega_0))}.$$

Let us substitute expression (1.24) that was derived for χ_1 into the second equation of system (1.15):

$$N(p)\,\chi_2 - \frac{1}{\Delta W_2^*(p+i2\omega_0)}\,\dot{\bar{\chi}}_2^* e^{-i2\omega_0} - \tilde{N}(p)\,\bar{\chi}_2^* e^{-i2(\dot{\Phi}_1+\omega_0)t} =$$
$$= A_2\tilde{\lambda}_2^0 - \tilde{A}_2\tilde{\lambda}_2^{0*}e^{-i2\omega_0 t} + L(p)\,\tilde{\lambda}_1^0 + \tilde{L}(p)\,\tilde{\lambda}_1^{0*}e^{-i2(\dot{\Phi}_1+\omega_0)t} +$$
$$+ W_2^\dagger(p)\,\tilde{\omega} + \tilde{W}_2^\dagger(p+i2\omega_0)\,\tilde{\omega}^* e^{-i2\omega_0 t} + \overline{M}^{(2)} + \overline{M}_n^{(2)}e^{-i\omega_0 t} + \tag{1.25}$$
$$+ M(p)\left(\overline{M}^{(1)} + M_n^{(1)}e^{-i(\dot{\Phi}_1+\omega_0)t}\right) + \tilde{M}(p)\left(\overline{M}^{(1)*}e^{-i2(\dot{\Phi}_1+\omega_0)t} + \right.$$
$$\left. + M_n^{(1)*}e^{-i(\Phi_1+\omega_0)t}\right),$$

where

$$N(p) = \frac{1}{W_2(p)} - p^2 W_4(p) \frac{W_2^-(p)}{W_3(p)} - p\{p + i2(\dot{\Phi}_1 + \omega_0)\} \frac{\tilde{W}_2^-(p + i2(\dot{\Phi}_1 + \omega_0))}{W_3(p)} \tilde{W}_4^*(p + i2(\dot{\Phi}_1 + \omega_0));$$

$$\tilde{N}(p) = \frac{1}{\Delta \tilde{W}_1^*(p + i2(\dot{\Phi}_1 + \omega_0))} + p\{p + i2(\dot{\Phi}_1 + \omega_0)\} \frac{\tilde{W}_4(p)}{W_3(p)} W_2^-(p) + \{p + i2(\dot{\Phi}_1 + \omega_0)\}^2 \frac{W_4^*(p + i2(\dot{\Phi}_1 + \omega_0))}{W_3(p)} \tilde{W}_2^-(p + i2(\dot{\Phi}_1 + \omega_0));$$

$$L(p) = B_1 + p \frac{W_5(p)}{W_3(p)} W_2^-(p) + \{p + i2(\dot{\Phi}_1 + \omega_0)\} \frac{\tilde{W}_5^*(p + i2(\dot{\Phi}_1 + \omega_0))}{W_3(p)} \tilde{W}_2^-(p + i2(\dot{\Phi}_1 + \omega_0));$$

$$\tilde{L}(p) = \tilde{B}_1 + p \frac{\tilde{W}_5(p)}{W_3(p)} W_2^-(p) + \{p + i2(\dot{\Phi}_1 + \omega_0)\} \frac{W_5^*(p + i2(\dot{\Phi}_1 + \omega_0))}{W_3(p)} \tilde{W}_2^-(p + i2(\dot{\Phi}_1 + \omega_0));$$

$$M(p) = p \frac{W_2^-(p)}{W_3(p) W_1^*(p + i2(\dot{\Phi}_1 + \omega_0))} + \{p + i2(\dot{\Phi}_1 + \omega_0)\} \frac{\tilde{W}_2^-(p + i2(\dot{\Phi}_1 + \omega_0))}{W_3(p) \Delta W_1(p)};$$

$$\tilde{M}(p) = p \frac{W_2^-(p)}{W_3(p) \Delta W_1^*(p + i2(\dot{\Phi}_1 + \omega_0))} + \{p + i2(\dot{\Phi}_1 + \omega_0)\} \frac{\tilde{W}_2^-(p + i2(\dot{\Phi}_1 + \omega_0))}{W_3(p) W_1(p)}.$$

In order to eliminate from (1.25) the periodic coefficients that change with frequencies $2\dot{\Phi}_0$ and $2(\dot{\Phi}_1 + \omega_0)$, we will derive two additional equations. In order to do this, we will apply to both parts of equation (1.25) the operators $e^{i2\omega_0 t}$ and $e^{i2(\dot{\Phi}_1 + \omega_0)t}$ and then perform the operation of complex conjugation on the obtained equations. As a result of these operations, the additional equations will take on the following form:

$$-\frac{1}{\Delta W_3(p)} \tilde{\chi}_2 + N^*(p + i2\omega_0) \tilde{\chi}_2^* e^{-i2\omega_0 t} - \tilde{N}^*(p + i2\omega_0) \tilde{\chi}_2 e^{i2\dot{\Phi}_1 t} =$$

$$= A_2^* \tilde{\lambda}_2^{0*} e^{-i2\omega_0 t} - \tilde{A}_2^* \tilde{\lambda}_2^0 + L^*(p + i2\omega_0) \tilde{\lambda}_1^{0*} e^{-i2\omega_0 t} +$$

$$+ \tilde{L}^*(p + i2\omega_0) \tilde{\lambda}_1^0 e^{i2\dot{\Phi}_1 t} + W_2^{+*}(p + i2\omega_0) \tilde{\omega}^* e^{-i2\omega_0 t} +$$

. . . . . .

$$
\begin{aligned}
&\cdots\cdots\cdots\\
&+\tilde{W}_2^{+*}(p)\,\tilde{\omega}+\overline{M}^{(2)*}e^{-i2\omega_0 t}+\overline{M}_{\text{п}}^{(2)*}e^{-i\omega_0 t}+\\
&+M^{*}(p+i2\omega_0)\left(\overline{M}^{(1)*}e^{-i2\omega_0 t}+\overline{M}_{\text{п}}^{(1)*}e^{i(\dot{\Phi}_1-\omega_0)t}\right)+\\
&+\tilde{M}^{*}(p+j2\omega_0)\left(\overline{M}^{(1)}e^{i2\dot{\Phi}_1 t}+\overline{M}_{\text{п}}^{(1)}e^{i(\dot{\Phi}_1-\omega_0)t}\right);\\
&-\tilde{N}^{*}(p+i2(\Phi_1+\omega_0))\,\tilde{\chi}_2+\dot{N}^{*}(p+i2(\dot{\Phi}_1+\\
&+\omega_0))\,\tilde{\chi}_2^{*}e^{-i2(\dot{\Phi}_1+\omega_0)t}-\frac{1}{\Delta W_2(p+i2\dot{\Phi}_1)}\,\tilde{\chi}_2 e^{-i2\dot{\Phi}_1 t}=\\
&=A_2^{*}\tilde{\lambda}_2^{0*}e^{-i2(\dot{\Phi}_1+\omega_0)t}-\tilde{A}_2^{*}\tilde{\lambda}^{0}e^{-i2\dot{\Phi}_1 t}+L^{*}(p+i2(\dot{\Phi}_1+\\
&+\omega_0))\,\tilde{\lambda}_1^{0*}e^{-i2(\dot{\Phi}_1+\omega_0)t}+\tilde{L}^{*}(p+i2(\dot{\Phi}_1+\omega_0))\,\tilde{\lambda}_1^{0}+\\
&+W_2^{+*}(p+i2(\dot{\Phi}_1+\omega_0))\,\tilde{\omega}^{*}e^{-i2(\dot{\Phi}_1+\omega_0)t}+\tilde{W}_2^{+}(p+i2\dot{\Phi}_1)\,\tilde{\omega}e^{-i2\dot{\Phi}_1 t}+\\
&+\overline{M}^{(2)*}e^{-i2(\dot{\Phi}_1+\omega_0)t}+\overline{M}_{\text{п}}^{(2)*}e^{-i(2\dot{\Phi}_1+\omega_0)t}+M^{*}(p+i2(\dot{\Phi}_1+\\
&+\omega_0))\left(\overline{M}^{(1)*}e^{-i2(\dot{\Phi}_1+\omega_0)t}+\overline{M}_{\text{п}}^{(1)*}e^{-i(\dot{\Phi}_1+\omega_0)t}\right)+\\
&+\tilde{M}^{*}(p+i2(\dot{\Phi}_1+\omega_0))\left(\overline{M}^{(1)}+\overline{M}_{\text{п}}^{(1)}e^{-i(\dot{\Phi}_1+\omega_0)t}\right).
\end{aligned}
\tag{1.26}
$$

By determining $\overrightarrow{\chi}_{2}^{*}e^{-i2\omega_0 t}$ from the first equation in system (1.26) and $\overrightarrow{\chi}_{2}^{*}e^{-i2(\dot{\Phi}_1+\omega_0)t}$ from the second and substituting them into equation (1.25), we obtain

$$
\begin{aligned}
&\Phi_{12}(p)\,\tilde{\chi}_2-\Phi_{22}(p)\,\tilde{\chi}_2 e^{i2\dot{\Phi}_1 t}-\Phi_{32}(p)\,\tilde{\chi}_2 e^{-i2\dot{\Phi}_1 t}=\\
&=\left[A_2-\frac{1}{\Delta W_2^{*}(p+i2\omega_0)}\,\frac{\tilde{A}_2^{*}}{N^{*}(p+i2\omega_0)}\right]\tilde{\lambda}_2^{0}-\\
&-\left[\tilde{A}_2-\frac{1}{\Delta W_2^{*}(p+i2\omega_0)}\,\frac{A_2^{*}}{N^{*}(p+i2\omega_0)}\right]\tilde{\lambda}_2^{0*}e^{-i2\omega_0 t}-\\
&-\frac{\tilde{A}_2^{*}\tilde{N}(p)}{N^{*}(p+i2(\dot{\Phi}_1+\omega_0))}\,\tilde{\lambda}_2^{0}e^{-i2\dot{\Phi}_1 t}+\frac{A_2^{*}\tilde{N}(p)}{N^{*}(p+i2(\dot{\Phi}_1+\omega_0))}\,\tilde{\lambda}_2^{0*}e^{-i2(\dot{\Phi}_1+\omega_0)t}+\\
&+\left[L(p)+\tilde{N}(p)\frac{\tilde{L}^{*}(p+i2(\dot{\Phi}_1+\omega_0))}{N^{*}(p+i2(\dot{\Phi}_1+\omega_0))}\right]\tilde{\lambda}_1^{0}-\left[\tilde{L}(p)+\right.\\
&\left.+\tilde{N}(p)\,\frac{L^{*}(p+i2(\dot{\Phi}_1+\omega_0))}{N^{*}(p+i2(\dot{\Phi}_1+\omega_0))}\right]\tilde{\lambda}_1^{0*}e^{-i2(\dot{\Phi}_1+\omega_0)t}+\\
&+\frac{1}{\Delta W_2^{*}(p+i2\omega_0)}\,\frac{L^{*}(p+i2\omega_0)}{N^{*}(p+i2\omega_0)}\,\tilde{\lambda}_1^{0*}e^{-i2\omega_0 t}+\\
&+\frac{1}{\Delta W_2^{*}(p+i2\omega_0)}\,\frac{\tilde{L}^{*}(p+i2\omega_0)}{N^{*}(p+i2\omega_0)}\,\tilde{\lambda}_1^{0}e^{i2\dot{\Phi}_1 t}+\left[W_2^{+}(p)+\right.\\
&\left.+\frac{\tilde{W}_2^{+*}(p)}{\Delta W_2^{*}(p+i2\omega_0)\,N^{*}(p+i2\omega_0)}\right]\tilde{\omega}+\left[\tilde{W}_2^{+}(p+i2\omega_0)+\right.\\
&\left.+\frac{W_2^{+*}(p+i2\omega_0)}{\Delta W_2^{*}(p+i2\omega_0)\,N^{*}(p+i2\omega_0)}\right]\tilde{\omega}^{*}e^{-i2\omega_0 t}+\\
&\cdots\cdots\cdots
\end{aligned}
$$

$$
\begin{aligned}
&\cdots\cdots\cdots\\
&+\tilde{N}(p)\,\frac{\tilde{W}_2^{+}(p+i2\dot{\Phi}_1)}{N^*(p+i2(\dot{\Phi}_1+\omega_0))}\,\tilde{\omega}e^{-i2\dot{\Phi}_1 t}+\\
&+\tilde{N}(p)\,\frac{W_2^{+*}(p+i2(\dot{\Phi}_1+\omega_0))}{N^*(p+i2(\dot{\Phi}_1+\omega_0))}\,\tilde{\omega}^* e^{-i2(\dot{\Phi}_1+\omega_*)t}+\overline{M}^{(2)*}+\\
&+\frac{1}{\Delta W_2^*(p+i2\omega_0)}\,\frac{1}{N^*(p+i2\omega_0)}\,\overline{M}^{(2)*}e^{-i2\omega_* t}+\\
&+\frac{\tilde{N}(p)}{N^*(p+i2(\Phi_1+\omega_0))}\,\overline{M}^{(2)*}e^{-i2(\dot{\Phi}_1+\omega_*)t}+\overline{M}_{\text{п}}^{(2)}e^{-i\omega_* t}+\\
&+\frac{1}{\Delta W_2^*(p+i2\omega_0)}\,\frac{1}{N^*(p+i2\omega_0)}\,\overline{M}_{\text{п}}^{(2)*}e^{-i\omega_* t}+\\
&+\tilde{N}(p)\,\frac{1}{N^*(p+i2(\dot{\Phi}_1+\omega_0))}\,\overline{M}_{\text{п}}^{(2)*}e^{-i2(\dot{\Phi}_1+\omega_*)t}+\\
&+\left[M(p)+\tilde{N}(p)\,\frac{\tilde{M}^*(p+i2(\dot{\Phi}_1+\omega_0))}{N^*(p+i2(\dot{\Phi}_1+\omega_0))}\right]\overline{M}^{(1)}+\\
&+\left[\tilde{M}(p)+\tilde{N}(p)\,\frac{M^*(p+i2(\dot{\Phi}_1+\omega_0))}{N^*(p+i2(\dot{\Phi}_1+\omega_0))}\right]\overline{M}^{(1)}e^{-i2(\dot{\Phi}_1+\omega_*)t}+\frac{1}{\Delta W_2^*(p+i2\omega_0)}\,\frac{M^*(p+i2\omega_0)}{N^*(p+i2\omega_0)}\,\overline{M}^{(1)*}e^{-i2\omega_* t}+\\
&+\frac{1}{\Delta W_2^*(p+i2\omega_0)}\,\frac{\tilde{M}^*(p+i2\omega_0)}{N^*(p+i2\omega_0)}\,\overline{M}^{(1)}e^{i2\dot{\Phi}_1 t}+\left[M(p)+\tilde{N}(p)\,\frac{M^*(p+i2(\dot{\Phi}_1+\omega_0))}{N^*(p+i2(\dot{\Phi}_1+\omega_0))}\right]\overline{M}_{\text{п}}^{(1)}e^{-i(\dot{\Phi}_1+\omega_*)t}+\\
&+\left[\tilde{M}(p)+\tilde{N}(p)\,\frac{M^*(p+i2(\dot{\Phi}_1+\omega_0))}{N^*(p+i2(\dot{\Phi}_1+\omega_0))}\right]\overline{M}_{\text{п}}^{(1)*}e^{-i(\dot{\Phi}_1+\omega_*)t}+\\
&+\frac{1}{\Delta W_2^*(p+i2\omega_0)}\,\frac{M^*(p+i2\omega_0)}{N^*(p+i2\omega_0)}\,\overline{M}_{\text{п}}^{(1)*}e^{-i(\dot{\Phi}_1-\omega_*)t}+\frac{1}{\Delta W_2^*(p+i2\omega_0)}\,\frac{\tilde{M}^*(p+i2\omega_0)}{N^*(p+i2\omega_0)}\,\overline{M}_{\text{п}}^{(1)}e^{i(\dot{\Phi}_1-\omega_*)t},
\end{aligned}
\tag{1.27}
$$

where

$$
\Phi_{12}(p)=N(p)-\frac{1}{\Delta W_2(p)}\,\frac{1}{\Delta W_2^*(p+i2\omega_0)}\,\frac{1}{N^*(p+i2\omega_0)}-
$$

$$
-\tilde{N}(p)\,\frac{\tilde{N}^*(p+i2(\dot{\Phi}_1+\omega_0))}{N^*(p+i2(\dot{\Phi}_1+\omega_0))};
$$

$$
\Phi_{22}(p)=\frac{1}{\Delta W_2^*(p+i2\omega_0)}\,\frac{\tilde{N}^*(p+i2\omega_0)}{N^*(p+i2\omega_0)};
$$

$$
\Phi_{32}(p)=\frac{1}{\Delta W_2(p+i2\dot{\Phi}_1)}\,\frac{\tilde{N}(p)}{N^*(p+i2(\dot{\Phi}_1+\omega_0))}.
$$

Thus, in order to solve system (1.15) it is necessary to solve equation (1.27) with harmonic coefficients that change with frequency $2\dot{\Phi}_1$ and then substitute the solution that has been found with respect to χ_2 into equation (1.24) and integrate the derived stationary equation with respect to χ_1.

1.4. Signal Reading and Information Processing Systems

One of the most important components of an RVG, and one that has much to do with determining its accuracy and sensitivity, is the system for reading the angle of

rotation of the RVG's rotors relative to the base or each other and then processing the obtained information. Depending on the reading method that is used, the useful information about the angular velocities of the base's rotation relative to the instrument's axes of sensitivity consists either of constant angular deflections of the rotors in a system of coordinates that is coupled with the base or of amplitude-modulated oscillations of the rotors at frequencies that are equal to or multiples of the PD's frequencies of rotation or are composite frequencies. For any signal reading method, however, the range of working angles for the unit that measures a rotor's angle of rotation should range from approximately 0.01 to tens of angular seconds. The measurement of such small angular movements is a quite complicated technical problem. In principle it can be solved with the help of angle measurers of different types [38]. In connection with this, the general requirements for them are:

1) high static accuracy; that is, the absence at the angle measurer's output of a zero signal that is synchronous with the useful signal and exceeds a given level;
2) high dynamic accuracy, which means that signal formation must take place with minimum distortions within the limits of the instrument's band of operating frequencies;
3) high sensitivity and a low sensitivity threshold;
4) minimum reactive effect on the RVG's rotors;
5) sufficiently high output signal power;
6) high reliability and resistance to interference when operating under conditions determined by the tactical and technical requirements.

Angle measurers can be divided, according to their operating principle, into:

1) passive measurers, requiring an external power source;
2) active measurers, which generate a signal proportional to the value being measured.

Passive measurers include those of the capacitive and inductive types, while active ones include those of the induction and piezoelectric types. In order to eliminate the effect of linear oscillations of the rotors on the instrument's operation and provide the maximum possible sensitivity, all of these measurers are built with differential circuitry.

Let us examine several features of passive angle measurers. Their operating principle is based on the measurement of the change in the reactance of the gap between a sensitive element and the sensor's elements. In the case of a capacitive measurer, the sensitive element is one of the capacitor's plates. A second capacitor plate is mounted on the housing or rotating part of the instrument. When the rotor is deflected the size of the gap in the capacitor changes and, consequently, there is a change in its capacitance. For an inductive measurer, the rotor acts as an armature that completes the magnetic current of the sensitive coil.

A comparative analysis of capacitive and inductive measurers showed that, all other conditions being equal, the sharpness of a capacitive measurer's signal is 50-100 times higher than that of an inductive measurer. Some comparative characteristics of these sensors are given in Table 1. From the table it follows that with respect to all the basic parameters, a capacitive sensor is considerably better than an inductive one.

Figure 4 is a diagram of a capacitive measurer. Rotor P is located between four plates O, which--depending on the choice of the measuring system of coordinates--are

Table 1.

Характеристики (1)	Тип датчика угла (2)	
	емкостный (3)	индуктивный (4)
Крутизна, В/град (5)	1—10	10^{-2}—10^{-3}
Уровень шума, мВ (6)	0,5—4	5
Габарит, о. е. (7)	1	3
Масса, о. е. (8)	1	4

Key:
1. Characteristics
2. Type of angle sensor
3. Capacitive
4. Inductive
5. Transconductance, V/deg
6. Noise level, mV
7. Size, rel. units
8. Weight, rel. units

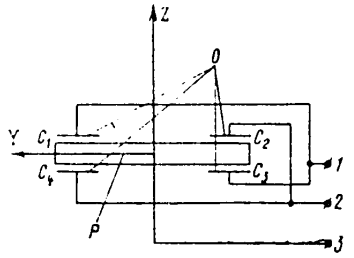

Figure 4. Diagram of capacitive angle sensor.

attached to the base, or rotate together with the PD's shaft, or are mounted on another of the RVG's rotors. The rotor, together with the plates, forms four capacitances C_1, C_2, C_3 and C_4. When the rotor turns through angle α, capacitances C_1 and C_3 will be reduced, while C_2 and C_4 will increase, and vice versa. Capacitances C_1, C_2, C_3 and C_4 are connected in parallel, in pairs, and can be connected to the arms of a bridge (Figure 5). If plates C_1-C_4 are mounted on the rotating part of an instrument, an inductive or capacitive commutator is used to transmit the signal to the base. The former consists of a transformer, one of the windings L_1, L_2 (which is mounted on the PD's shaft) and another winding L_3 that is on the instrument's housing (Figure 5b). A capacitive commutator consists of two pairs of concentric rings,

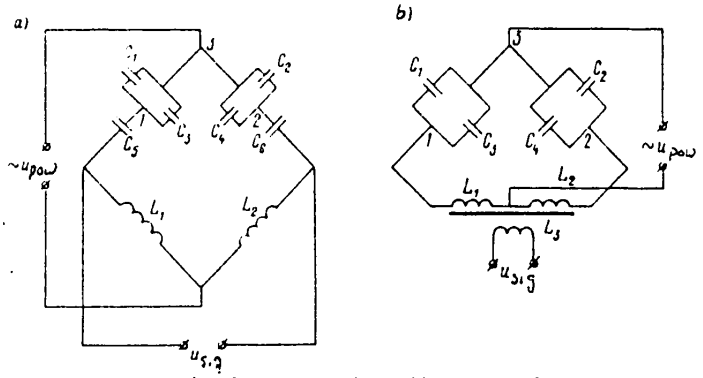

Figure 5. Electrical connection diagrams for capacitive angle sensors.

one of which in each pair is mounted on the rotating part, while the other is mounted on the housing. These rings form capacitances C_5 and C_6 (Figure 5a). Since the commutator's capacitances are connected in series with the capacitances that are

changing with angle α, in order to obtain high reading system sensitivity it is necessary that $C_5 >> C_1 + C_3$ and $C_6 >> C_2 + C_4$. Variable power voltage u_{pow} is fed into one of the bridge's diagonals. In accordance with the recommendations for this type of measurer, the power frequency is chosen in the 0.1-1 MHz band. Signal voltage u_{sig} is read from the bridge's other diagonal. The signal voltage can be calculated with the formula

$$u_{sig} = \frac{2\delta r u_{pow}}{\Delta\delta^2 - \alpha^2 r^2}\alpha, \qquad (1.28)$$

$$\delta = 4\pi^2 L f^2 \varepsilon\varepsilon_0 S,$$

where L = inductance of the measuring bridge's choke coils ($L = L_1 = L_2$); f = frequency of the power voltage; $\varepsilon\varepsilon_0$ = absolute permittivity of the air gap; S = area of the capacitors' plates'

$$\Delta\delta = \delta - d_0, \quad d_0 = \frac{\varepsilon\varepsilon_0 S}{C_0},$$

d_0 = initial size of the gap between the capacitors' plates when the rotor is in the equilibrium position; C_0 = initial capacitance of the capacitors.

From formula (1.28) it follows that the dependence of u_{sig} on angle α is, in the general case, of a nonlinear nature. Therefore, it is extremely important to take into consideration the required range of measured frequencies and the allowable nonlinearity of the instrument's static characteristic when selecting the initial value of the gap between the sensitive element and the capacitors' plates.

In order to create an instrument with a linear static characteristic, it is possible to use a transformer-type bridge connection circuit. Such a circuit corresponds to the one depicted in Figure 5b if u_{pow} is fed into winding L_3 and the signal is read from the bridge's other diagonal. Disregarding the bridge's reactance, the output signal's dependence on angle α then has the form

$$u_{sig} = \frac{r u_{pow}}{2d_0}\alpha. \qquad (1.29)$$

However, such a circuit has a high noise level and a high sensitivity threshold.

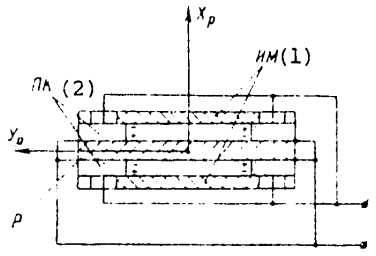

Figure 6. Connection diagram of piezoelectric sensor.
Key: 1. IM
2. PK

It is feasible to use a piezoelectric sensor [8] only when the amplitude of the RVG's sensitive elements' oscillations that is being measured is of a sufficiently high frequency. The connection diagram of such a sensor is shown in Figure 6. It provides for the measurement of angular vibrations, with self-compensation for linear vibrations, with accuracy up to that of the identity of the piezocrystals' (PK) parameters. The transconductance of a piezoelectric sensor is computed with the formula

$$u_{sig} = \frac{d_{33} m_N r}{C_K + C_0}\alpha, \qquad (1.30)$$

where d_{33} = piezomodule of the crystal; m_{IN} = inertial mass (IM); C_k = capacitance of the piezocrystal; C_0 = input capacitance of the signal processing unit.

The signal voltage's dependence on angular acceleration α is linear. Consequently, the dependence of u_{sig} on the base's angular veloity will also be linear.

The shortcomings of a piezoelectric sensor include the effect of the processing circuit's capacitance and the cable's capacitance on the output signal's value, as well as the necessity of deriving the signal from the rotating part of the RVG.

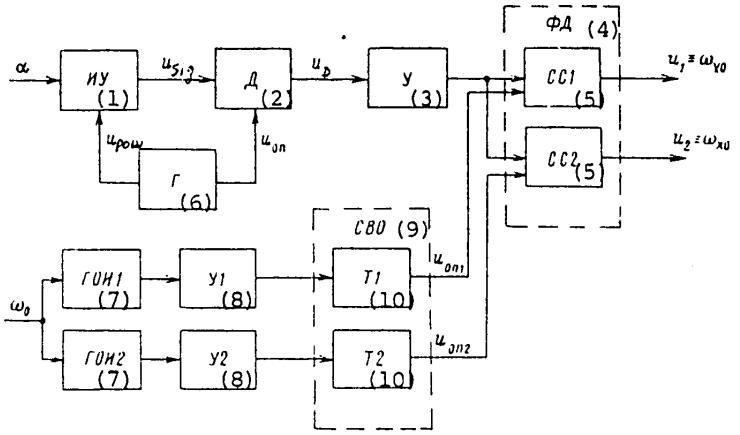

Figure 7. Functional diagram of information processing system.

Key:
1. IU
2. D
3. U
4. FD
5. SS.
6. G
7. GOI.
8. U.
9. SVO
10. T.

When the useful signal is read in the form of amplitude-modulated oscillations, the processing system solves the problem of obtaining two direct-current signals that are proportional to the angular velocities of the base's motion relative to the instrument's axes of sensitivity. Figure 7 is a functional diagram of such a system. The signal arriving from the bridge of the measurer of angular rotor displacements (IU) consists of oscillations with the frequency of the change in the power voltage and balance-modulated oscillations with the useful signal's frequency. The amplitude and phase of the latter contain the information about the base's angular velocities.

The first stage of the signal's processing is its demodulation on frequency f_{pow}. In order for this to take place, the signal u_{sig} from the bridge enters demodulator D, into which a signal from generator G (which generates the bridge's power voltage) is sent as a reference signal. Oscillations with an amplitude proportional to the RVG rotor's angle of rotation are obtained at D's output. This part of the circuit is absent in active measurers.

After preliminary amplification by amplifier U, the signal u_D from D's output is sent into phase-sensitive demodulator FD. The reference signal for FD is generated

with the help of reference pulse generators GOI. A GOI consists of a magnet that is press-fitted into the rotating part of the instrument and a coil mounted on the housing. When the magnet passes by the coil, an EDS [electromotive force] in the form of a short pulse is induced in it. The magnets in the rotating part are situated at an angle of 180° to each other, while the two coils in the housing are at an angle of 90° to each other. When reading on intermediate frequencies, the magnets and coils can be situated on the appropriate rotating parts. After amplification with the help of amplifiers U1 and U2, the pulses from the GOI's enter reference signal processing circuit SVO. When necessary, this circuit can contain a frequency conversion circuit. On receiving signals from GOI1 and GOI2, triggers T1 and T2, which are operating in a waiting mode, generate rectangular reference voltage pulses that are shifted 90° relative to each other.

The phase-sensitive demodulator is a comparison circuit (SS1 and SS2). The reference voltages from the triggers and the amplified signal from the demodulator enter it and constant voltages u_1 and u_2, which are proportional to the base's angular velocities, are obtained at its output.

The extremely simple circuits for reading and processing information from an RVG are not the only ones possible. Inductive angle sensors can be used successfully in instruments of this type. In order to increase their sensitivity, capacitive or inductive sensors can be built into the driving crystal oscillator's resonant circuit. Preliminary processing of the useful signal, by placing electronic units directly on the rotating part of an instrument, is used quite frequently. Conversion from amplitude modulation to frequency modulation or to amplitude modulation on some intermediate frequency is another practice that is used.

This brief analysis of RVG information reading and processing systems shows that, in contrast to gyroscopes constructed according to the traditional plan, RVG's are a symbiosis of mechanical and electrical parts, with the latter having a substantial effect on the design and basic characteristics of these instruments. This fact compels us to develop a new approach to the process of designing such gyroscopes that involves a more nearly complete consideration of the demands made on the mechanical part by the information reading and processing system.

1.5. Methods for Solving Differential Equations With Periodic Coefficients

As was shown in Section 1.3, in the general case RVG's are described by linear differential equations with harmonically changing coefficients. In connection with this--and regardless of the information reading and processing method--a characteristic of all RVG's is the presence in the output signal of a harmonic component that changes with the doubled frequency of rotation of the instrument's rotor, while for RVG's with multiple modulation it also changes with multiples of this frequency and composite frequencies. Therefore, when there is inadequate filtration of the output signal and a broad transmission band, systems containing RVG's will (in the general case) by described by differential equations with periodically changing coefficients.

According to Lyapunov's fundamental theorem [11], any differential equation with periodic coefficients can be reduced to an equivalent linear differential equation with constant coefficients. At the present time, however, no universal algorithm for this reduction has yet been found. Therefore, the analysis of the properties of

solutions of equations with periodic coefficient usually involves considerable difficulties.

The development in recent years of electronic computer technology makes it possible to use the methods of numerical integration of differential equations to analyze equations of motion. When these methods are used, however, the presence in an RVG's output signal of a slowly changing component and a harmonic component having a rather high frequency should be taken into consideration. The requirement that both components be allowed for means that the amount of machine time needed to integrate the equations of motions is increased sharply. At the same time, the necessity of solving the synthesis problems that are related to the numerous possible structures of systems and their parameters, as well as the parameters of the RVG's themselves, stipulates the use of analytical methods to investigate the properties of the differential equations with harmonic coefficients that describe the operation of RVG's and systems containing them.

For the investigation of periodically nonstationary systems, the most fruitful ideas proved to be those related to the use of a Laplace transform [14]. The complete theory of such linear systems, as presented in [28], makes it possible to derive the parametric transfer functions and the pulse-frequency characteristics of a nonstationary system. However, the use of these characteristics in engineering calculations is considerably more complicated than the use of normal transfer functions and the frequency characteristics corresponding to them. The spectral theory of differential equations with periodic coefficients is explained in the works of V.A. Taft [34,35] and modified in [16] for the case of two-dimensional systems with amplitude modulation. There the result of the solution is presented in the form of an infinite sequence of determinants, for the formation of which it is required to know the specific parameters of a system already, which narrows the possibilities of using this approach. For the purpose of developing the spectral theory, in [27] the author proposes an algorithm of a rather simple method that is free from the defects enumerated above and, in principle, makes it possible to obtain stationary transfer functions of two-dimensional linear systems with periodically changing parameters. Let us discuss the features of the use of this algorithm in the investigation of linear differential equations with periodic coefficients and the possibility of writing their solution analytically [10].

It is not difficult to demonstrate that any linear differential equation with monoharmonic coefficients can be represented, with the help of Euler's formula, in the form

$$x + \Phi_2(p)\, xe^{i\omega t} + \Phi_3(p)\, xe^{-i\omega t} = R(p)\, u, \tag{1.31}$$

where $\Phi_2(p)$, $\Phi_3(p)$, $R(p)$ = operators representing rational functions of differentiation operator p and having complex coefficients (in the general case); ω = frequency of change of the coefficients of the nonstationary part of equation (1.31).

As the first step in the solution (n = 1), let us perform the following operations. To the left and right sides of equation (1.31) we will first apply operator $e^{i\omega t}$ and then operator $e^{-i\omega t}$. As a result, we obtain two equations from which the values of $xe^{i\omega t}$ and $xe^{-i\omega t}$ can be found. Substituting these values into equation (1.31), we obtain the first-step equation

$$[1 - \Phi_2(p)\Phi_3(p - i\omega) - \Phi_3(p)\Phi_2(p + i\omega)]x -$$
$$- \Phi_2(p)\Phi_2(p - i\omega)xe^{+i2\omega t} - \Phi_3(p)\Phi_3(p + i\omega)xe^{-i2\omega t} = \quad (1.32)$$
$$= R(p)u - \Phi_2(p)R(p - i\omega)ue^{i\omega t} - \Phi_3(p)R(p + i\omega)ue^{-i\omega t},$$

which is equivalent to the original equation (1.31).

Let us redesignate the operators in equation (1.32):

$$\Phi_1^{(1)}(p) = 1 - \Phi_2(p)\Phi_3(p - i\omega) - \Phi_3(p)\Phi_2(p + i\omega);$$

$$\Phi_2^{(1)}(p) = \Phi_2(p)\Phi_2(p - i\omega);$$
$$\Phi_3^{(1)}(p) = \Phi_3\Phi_3(p + i\omega),$$

and as our second step (n = 2) apply--analogously to the first step--operators $e^{i2\omega t}$ and $e^{-i2\omega t}$ to equation (1.32). As a result of the substitution of the values of $xe^{i2\omega t}$ and $xe^{-i2\omega t}$ that we have found into equation (1.32), we obtain the second-step equation

$$\left[\Phi_1^{(1)}(p) - \frac{\Phi_2^{(1)}(p)\Phi_3^{(1)}(p - i2\omega)}{\Phi_1^{(1)}(p - i2\omega)} - \frac{\Phi_3^{(1)}(p)\Phi_2^{(1)}(p + i2\omega)}{\Phi_1^{(1)}(p + i2\omega)}\right]x -$$

$$- \Phi_2^{(1)}(p)\frac{\Phi_2^{(1)}(p - i2\omega)}{\Phi_1^{(1)}(p - i2\omega)}xe^{i4\omega t} - \Phi_3^{(1)}(p)\frac{\Phi_3^{(1)}(p + i2\omega)}{\Phi_1^{(1)}(p + i2\omega)}xe^{-i4\omega t} =$$

$$= R(p)u - R(p - i\omega)\left[\Phi_2(p) + \Phi_2^{(1)}(p)\frac{\Phi_3(p - i2\omega)}{\Phi_1^{(1)}(p - i2\omega)}\right]ue^{i\omega t} -$$

$$- R(p + i\omega)\left[\Phi_3(p) + \Phi_3^{(1)}(p)\frac{\Phi_2(p + i2\omega)}{\varphi_1^{(1)}(p + i2\omega)}\right]ue^{-i\omega t} + \quad (1.33)$$

$$+ R(p - i2\omega)\frac{\Phi_2^{(1)}(p)}{\Phi_1^{(1)}(p - i2\omega)}ue^{i2\omega t} + R(p + i\omega)\frac{\Phi_3^{(1)}(p)}{\Phi_1^{(1)}(p + i2\omega)}ue^{-i2\omega t} -$$

$$- R(p - i3\omega)\frac{\Phi_2^{(1)}(p)\Phi_2(p - i2\omega)}{\Phi_1^{(1)}(p - i2\omega)}ue^{i3\omega t} -$$

$$- R(p + i3\omega)\frac{\Phi_3^{(1)}(p)\Phi_3(p + i2\omega)}{\Phi_1^{(1)}(p + i2\omega)}ue^{-i3\omega t}.$$

If the harmonic coefficients change with frequency ω in the original equation, in the first-step equation they change only with frequency 2ω, and in the second-step equation with frequency 4ω. After n steps we obtain an equation, equivalent to the original one, in which the harmonic coefficients change with frequency $2^n\omega$. In connection with this, the recurrent relationships for determining the operators in the left side of the equation are determined by the following expressions:

$$\Phi_1^{(n)}(p) = \Phi_1^{(n-1)}(p) - \frac{\Phi_2^{(n-1)}(p)\Phi_3^{(n-1)}(p - i2^{n-1}\omega)}{\Phi_1^{(n-1)}(p - i2^{n-1}\omega)} - \frac{\Phi_3^{(n-1)}(p)\Phi_2^{(n-1)}(p + i2^{n-1}\omega)}{\Phi_1^{(n-1)}(p + i2^{n-1}\omega)}; \quad (1.34)$$

$$\Phi_2^{(n)}(p) = \Phi_2^{(n-1)}(p)\frac{\Phi_2^{(n-1)}(p - i2^{n-1}\omega)}{\Phi_1^{(n-1)}(p - i2^{n-1}\omega)} = \frac{\prod_{k=0}^{2^{n-1}-1}\Phi_2(p - 2k\omega)}{\prod_{l=1}^{n-1}\left[\prod_{k=0}^{2^{n-l-1}-1}\Phi_1^{(l)}(p - i2^l(1 + 2k)\omega)\right]}; \quad (1.35)$$

$$\Phi_3^{(n)}(p)=\Phi_3^{(n-1)}(p)\frac{\Phi_3^{(n-1)}\left(p+i2^{n-1}\omega\right)}{\Phi_1^{(n-1)}\left(p+i2^{n-1}\omega\right)}=\frac{\prod\limits_{k=0}^{2^{n-1}-1}\Phi_3\left(p+i2k\Phi\right)}{\prod\limits_{l=1}^{n-1}\left[\prod\limits_{k=0}^{2^{n-l-1}-1}\Phi_1^{(l)}\left(p+i2^l(1+2k)\omega\right)\right]}. \tag{1.36}$$

The right side of the n-th step's equation can be derived in the following manner. It is obvious that at the (n - 1)-th step, the right side of the equation has the form

$$\sum_{k=0}^{2^{n-1}-1}\left[A_k^{(n-1)}(p)\,ue^{ik\omega t}+B_k^{(n-1)}(p)\,ue^{-ik\omega t}\right]. \tag{1.37}$$

In the n-th step, the right side will then be found from the expression

$$\begin{aligned}
&\left[A_0(p)+B_0(p)\right]u+\sum_{k=1}^{2^{n-1}-1}\left\{\left[A_k^{(n-1)}(p)-\frac{\Phi_2^{(n-1)}(p)}{\Phi_1^{(n-1)}\left(p-i2^{n-1}\omega\right)}B_{2^{n-1}-k}^{(n-1)}(p-\right.\right.\\
&\left.-i2^{n-1}\omega)\right]ue^{ik\omega t}-\frac{\Phi_2^{(n-1)}(p)}{\Phi_1^{(n-1)}\left(p-i2^{n-1}\omega\right)}\left[A_0(p-i2^{n-1}\omega)+\right.\\
&+B_0(p-i2^{n-1}\omega)\left]ue^{i2^{n-1}\omega t}-\frac{\Phi_2^{(n-1)}(p)}{\Phi_1^{(n-1)}\left(p-i2^{n-1}\omega\right)}A_{2^{n-1}-k}^{(n-1)}(p-\right.\\
&-i2^{n-1}\omega)\,ue^{i(2^{n-1}+k)\omega t}+\left[B_k^{(n-1)}(p)-\frac{\Phi_3^{(n-1)}(p)}{\Phi_1^{(n-1)}\left(p+i2^{n-1}\omega\right)}A_k^{(n-1)}(p+\right.\\
&\left.+i2^{n-1}\omega)\right]ue^{-ik\omega t}-\frac{\Phi_3^{(n-1)}(p)}{\Phi_1^{(n-1)}\left(p+i2^{n-1}\omega\right)}B_k^{(n-1)}(p+\\
&+i2^{n-1}\omega)\,ue^{-i2^{n-1}\omega t}-\frac{\Phi_3^{(n-1)}(p)}{\Phi_1^{(n-1)}\left(p+i2^{n-1}\omega\right)}B_k^{(n-1)}(p+\\
&\left.+i2^{n-1}\omega)\,ue^{-i(2^{n-1}+k)\omega t}\right\}.
\end{aligned} \tag{1.38}$$

Using expressions (1.37) and (1.38), for any n it is possible to obtain the values of the operators standing before each disturbance harmonic in the right side of the equation. Let us present the expressions for the operators on the first three harmonics:

$$\left.\begin{aligned}
A_1^{(n)}(p)&=-\frac{R(p-i\omega)}{\Phi_1(p-i\omega)}\left\{\Phi_2(p)-\right.\\
&\left.-\sum_{k=1}^{n-1}\left[(-1)^k\prod_{l=1}^{k}\Phi_2^{(k)}(p)\frac{\Phi_3^{(l-1)}\left(p-i2^l\omega\right)}{\Phi_1^{(l)}\left(p-i2^l\omega\right)}\right]\right\};\\
B_1^{(n)}(p)&=-\frac{R(p+i\omega)}{\Phi_1(p+i\omega)}\left\{\Phi_3(p)-\right.\\
&\left.-\sum_{k=1}^{n-1}\left[(-1)^k\prod_{l=1}^{k}\Phi_3^{(k)}(p)\frac{\Phi_2^{(l-1)}\left(p+i2^l\omega\right)}{\Phi_1^{(l)}\left(p+i2^l\omega\right)}\right]\right\};
\end{aligned}\right| \tag{1.39}$$

$$\left.\begin{aligned} A_2^{(n)}(p) &= -\frac{R(p-i2\omega)}{\Phi_1(p-i2\omega)}\frac{1}{\Phi_1^{(1)}(p-i2\omega)}\left\{\Phi_2^{(1)}(p)-\right.\\ &\left.-\sum_{k=2}^{n-1}\left[(-1)^k\prod_{l=2}^{k}\Phi_2^{(k)}(p)\frac{\Phi_3^{(l-1)}(p-i2^l\omega)}{\Phi_1^{(l)}(p-i2^l\omega)}\right]\right\};\\ B_2^{(n)}(p) &= -\frac{R(p+i2\omega)}{\Phi_1(p+i2\omega)}\frac{1}{\Phi_1^{(1)}(p+i2\omega)}\left\{\Phi_3^{(1)}(p)-\right.\\ &\left.-\sum_{k=2}^{n-1}\left[(-1)^k\prod_{l=2}^{k}\Phi_3^{(k)}(p)\frac{\Phi_2^{(l-1)}(p+i2^l\omega)}{\Phi_1^{(l)}(p+i2^l\omega)}\right]\right\}; \end{aligned}\right\} \quad (1.40)$$

$$\left.\begin{aligned} A_3^{(n)}(p) &= \frac{R(p-i3\omega)}{\Phi_1(p-i3\omega)}\frac{\Phi_2(p-i2\omega)}{\Phi_1^{(1)}(p-i2\omega)}\left\{\Phi_2^{(1)}(p)-\right.\\ &-\left[-\Phi_3(p-i4\omega)\frac{\Phi_1^{(1)}(p-i2\omega)}{\Phi_2(p-i2\omega)}+\right.\\ &\left.\left.+\Phi_3^{(1)}(p-i4\omega)\right]\sum_{k=3}^{n}\left[(-1)^k\prod_{l=3}^{k}\frac{\Phi_2^{(k-1)}(p)\Phi_3^{(l-2)}(p-i2^{l-1}\omega)}{\Phi_1^{(l-1)}(p-i2^{l-1}\omega)}\right]\right\};\\ B_3^{(n)}(p) &= \frac{R(p+i3\omega)}{\Phi_1(p+i3\omega)}\frac{\Phi_3(p+i2\omega)}{\Phi_1^{(1)}(p+i2\omega)}\left\{\Phi_3^{(1)}(p)+\right.\\ &+\left[-\Phi_2(p+i4\omega)\frac{\Phi_1^{(1)}(p+i2\omega)}{\Phi_3(p+i2\omega)}+\right.\\ &\left.\left.+\Phi_2^{(1)}(p+i4\omega)\right]\sum_{k=3}^{n}\left[(-1)^k\prod_{l=3}^{k}\frac{\Phi_3^{(k-1)}(p)\Phi_2^{(l-2)}(p+i2^{l-1}\omega)}{\Phi_1^{(l-1)}(p+i2^{l-1}\omega)}\right]\right\}; \end{aligned}\right\} \quad (1.41)$$

If the functional sequences $\Phi_1^{(n)}(p)$, $A_k^{(n)}(p)$ and $B_k^{(n)}(p)$ converge outside the area of definition for all values of p, while the sequences $\Phi_2^{(n)}(p)$ and $\Phi_3^{(n)}(p)$ converge to zero, in the case of the limiting transition for $n \to \infty$ we obtain a differential equation with constant coefficients that is equivalent to the original differential equation (1.31) with periodic coefficients.

Let us examine some conditions under which the convergence of the indicated sequences is quite easy to prove. We will turn first to sequences (1.35) and (1.36). In order to determine their limit, let us examine sequences $|\Phi_2^{(n)}(p)|$ and $|\Phi_3^{(n)}(p)|$. We will select the number ν in such a fashion that

$$\nu = \max\{|\Phi_2(p)|, |\Phi_3(p)|\}, \quad (1.42)$$

and formulate a numerical sequence, the common term of which is described by the expression

$$a_n = \frac{\nu^{2n}}{(1-2\nu^2)\{(1-2\nu^2)^2-2\nu^4\}\ldots(\{\{(1-2\nu^2)^2-2\nu^4\}^2-2\nu^8\}^2-\ldots-2\nu^{2n-1})}. \quad (1.43)$$

It is not difficult to see that sequence (1.43) is a mazhoriruyushchaya [possibly majorizing] one with respect to the sequences formed from the moduli of the terms of sequences (1.35) and (1.36). Let us rewrite expression (1.43) in a more convenient form:

$$a_n = \frac{\nu^2}{\left(\frac{1}{\nu^2}-2\right)\left[\left(\frac{1}{\nu^2}-2\right)^2-2\right]\ldots\left(\left\{\left[\left(\frac{1}{\nu^2}-2\right)^2-2\right]^2-2\right\}^2-\ldots-2\right)}. \tag{1.44}$$

From expression (1.44) it follows that a sufficient condition for the existence of a limit that equals zero for sequence a_n is the condition

$$\nu \leqslant \frac{1}{2}. \tag{1.45}$$

Thus, according to (Veyyershtrass's) criterion [29], sequences (1.35) and (1.36) converge and have a limit equal to zero in that case where the following relationship is fulfilled for all p:

$$\max\{|\Phi_2(p)|, |\Phi_3(p)|\} \leqslant \frac{1}{2}. \tag{1.46}$$

Let us determine the conditions for convergence of sequences $\Phi_1^{(n)}(p)$, $A_k^{(n)}(p)$ and $B_k^{(n)}(p)$. For sequence $|\Phi_1^{(n)}(p)|$ the mazhoriruyushchaya numerical sequence will be

$$C_n = \frac{\{\{[(1-2\nu^2)^2-2\nu^4]^2-2\nu^8\}^2-\ldots-2\nu^{2^{n-1}}\}^2-2\nu^{2^n}}{(1-2\nu^2)[(1-2\nu^2)-2\nu^4]\ldots(\{\{[(1-2\nu^2)^2-2\nu^4]^2-2\nu^8\}^2-\ldots-2\nu^{2^{n-1}})}, \tag{1.47}$$

where $\nu \geqslant \max|\Phi_1(p)|$, which can put into correspondence the numerical series

$$\sum_{n=1}^{\infty} C_n = 1-2\nu^2-\frac{2\nu^4}{1-2\nu^2}-\frac{2\nu^8}{(1-2\nu^2)[(1-2\nu^2)^2-2\nu^4]}-\ldots$$
$$\ldots-\frac{2\nu^{2^n}}{(1-2\nu^2)[(1-2\nu^2)^2-2\nu^4]\ldots(\{[(1-2\nu^2)^2-2\nu^4]^2-2\nu^8\}^2-\ldots-2\nu^{2^{n-1}}}. \tag{1.48}$$

Let us make use of (Dalamber's) criterion for series convergence [40]. For series (1.48),

$$\rho_n = \frac{1}{\left\{\left[\left(\frac{1}{\nu^2}-2\right)^2-2\right]^2-2\right\}^2-\ldots-2} \tag{1.49}$$

and the condition $\lim_{n\to\infty}\rho_n < 1$ occurs for all $\nu \leqslant 1/2$, which means that the sequence $|\Phi_1^{(n)}(p)|$ is a converging one under these conditions.

The convergence of sequences $A_k^{(n)}(p)$ and $B_k^{(n)}(p)$ is proven analogously, providing that condition (1.46) is fulfilled.

Let us examine the case where the conditions

$$|\Phi_2(p)| \underset{p\to\pm\infty}{\to} 0, \qquad |\Phi_3(p)| \underset{p\to\pm\infty}{\to} 0 \tag{1.50}$$

are fulfilled and the area of definition of functions $\Phi_2(p)$ and $\Phi_3(p)$ is limited. Then, obviously, the limit of the n-th number of infinite products in the denominators of expressions (1.35) and (1.36) is unity and the given products converge; that is, they have a finite limit that is not zero. In view of condition (1.50), the numerator of these expressions converges to zero and, consequently, functions $\Phi_2^{(n)}(p)$ and $\Phi_3^{(n)}(p)$ also converge to zero. In connection with this, from expression (1.3) it follows that $|\Phi_1^{(n)}(p)| - |\Phi_1^{(n-1)}(p)| \to 0$ for $n \to \infty$, which means that the

functional sequence $\Phi_1^{(n)}(p)$ converges. It is not difficult to show that the functional sequences $A_k^{(n)}(p)$ and $B_k^{(n)}(p)$ also converge.

The two cases we have examined do not encompass the entire area of convergence of the method. However, it can be mentioned here that convergence must take place for any linear differential equations that describe real physical systems, since the existence in a system of oscillations with infinite frequency and finite amplitude requires unlimited power resources.

This method can also be used successfully in the more general case, when a linear differential equation contains coefficients described by a periodic time function. Then, by distributing the periodic function into a Fourier series, this equation can be written in the form

$$\Phi_1(p)\,x + \sum_{k=1}^{\infty} \Phi_{2k}(p)\,xe^{ik\omega t} + \sum_{k=1}^{\infty} \Phi_{3k}(p)\,xe^{-ik\omega t} = R(p)\,u. \tag{1.51}$$

As we did previously, let us apply the operators $e^{i\omega t}$ and $e^{-i\omega t}$ to both sides of equation (1.51). As a result, we obtain the following system of equations:

$$\begin{aligned}
&\Phi_1(p - i\omega)\,xe^{i\omega t} + \Phi_{32}(p - i\omega)\,xe^{-i\omega t} = -\Phi_{21}(p - i\omega)\,x - \\
&- \sum_{k=1}^{\infty} \Phi_{2k}(p - i\omega)\,x^{i(k+1)\omega t} - \sum_{k=3}^{\infty} \Phi_{3k}(p - i\omega)\,xe^{i(k-1)\omega t} + \\
&+ R(p - i\omega)\,ue^{i\omega t}, \\
&\Phi_{22}(p + i\omega)\,xe^{i\omega t} + \Phi_1(p + i\omega)\,xe^{-i\omega t} = -\Phi_{21}(p + i\omega)\,x - \\
&- \sum_{k=3}^{\infty} \Phi_{2k}(p + i\omega)\,xe^{i(k-1)\omega t} - \sum_{k=1}^{n} \Phi_{3k}(p + i\omega)\,xe^{-i(k+1)\omega t} + \\
&+ R(p + i\omega)\,ue^{-i\omega t}.
\end{aligned} \tag{1.52}$$

Solving system of algebraic equations (1.52) for unknowns $xe^{i\omega t}$ and $xe^{-i\omega t}$ and substituting these values into the original equation (1.51), we obtain the first-step equation, which--with the appropriate designations--will take on the form

$$\begin{aligned}
&\Phi_1^{(1)}(p)\,x + \sum_{k=2}^{\infty} \Phi_{2k}^{(1)}(p)\,xe^{-ik\omega t} - \sum_{k=2}^{\infty} \Phi_{3k}^{(1)}(p)\,xe^{-ik\omega t} = \\
&= [A_0^{(1)}(p) + B_0^{(1)}(p)]\,u + A_1^{(1)}(p)\,ue^{i\omega t} + B_1^{(1)}(p)\,ue^{-j\omega t}.
\end{aligned} \tag{1.53}$$

After n analogous steps, we obtain the following equation, which is equivalent to the original one:

$$\begin{aligned}
&\Phi_1^{(n)}(p)\,x + \sum_{k=2^n}^{\infty} \Phi_{2k}^{(n)}(p)\,xe^{k\omega t} + \sum_{k=2^n}^{\infty} \Phi_{3k}^{(n)}(p)\,xe^{-ik\omega t} = \\
&= \sum_{k=0}^{2^n-1} [A_k^{(n)}(p)\,ue^{ik\omega t} + B_k^{(n)}(p)\,ue^{-ik\omega t}].
\end{aligned} \tag{1.54}$$

If the functional sequences $\Phi_{2k}^{(n)}(p)$ and $\Phi_{3k}^{(n)}(p)$ converge to zero, while $\Phi_1^{(n)}(p)$, $A_k^{(n)}(p)$ and $B_k^{(n)}(p)$ converge, then for $n \to \infty$ we will obtain an equation with constant coefficients that is equivalent to the original one.

The realization of the mentioned limiting transition in practice is an extremely complicated problem. In most cases, however, this is unnecessary, since even the first steps provide a level of accuracy that is fully adequate for engineering calculations and the higher harmonics can be simply ignored when the filtering properties of real systems are taken into consideration. The accuracy of the approximations that have been made can be evaluated easily from the recurrent relationships that were derived.

The method we have been discussing is convenient for creating standard programs for digital computers, with the help of which investigations can be conducted of instruments and systems described by linear differential equations with periodic coefficients.

1.6. Dynamic Characteristics of Rotor Vibration Gyroscopes

It is a well-known fact that the basic properties of automatic systems, as well as the principles by which they are constructed, are determined essentially by their sensitive elements' dynamic characteristics. In engineering practice, dynamic characteristics are normally described by transfer functions, which are operators that convert a signal at an instrument's input into an output signal. For RVG's, the input signal can be assumed to be the vector $\bar{\omega}$ of the instantaneous angular velocity of rotation of the base in the instrument's sensitivity plane, while the output signal is the vector $\bar{u}$ of the signal at the output of the information reading and processing system. Let us examine the dynamic characteristics of different RVG systems.

An RVG with single modulation is described by equations (1.20). Before analyzing an instrument's dynamic characteristics, it is necessary to represent its equations of motion in a measuring system of coordinates. For an RVG with single modulation, such systems are a system of coordinates that is immobile relative to the base and a system that rotates relative to the base along with the PD's shaft. Using conversion formula (1.11), let us write the equation of motion in the nonrotating system of coordinates:

$$\bar{\lambda}_1'' = \frac{W(p) - [W_2^+(p) W_{12}(p) + \tilde{W}_2^{+*}(p) W_{11}(p)]}{pW(p)} p\bar{\omega} - \frac{\tilde{W}_2^+(p + i2\omega_0) W_{12}(p) + W_2^{+*}(p + i2\omega_0) W_{11}(p)}{W(p)} \bar{\omega}^* e^{-i2\omega_0 t}; \quad (1.55)$$

$$\bar{\lambda}_2'' = \frac{W(p) - [W_2^+(p) W_{22}(p) + \tilde{W}_2^{+*}(p) W_{21}(p)]}{pW(p)} p\bar{\omega} - \frac{\tilde{W}_2^+(p + i2\omega_0) W_{22}(p) + W_2^{+*}(p + i2\omega_0) W_{21}(p)}{W(p)} \bar{\omega}^* e^{-i2\omega_0 t}. \quad (1.56)$$

The signal is read from the first or second stage's outer rotor on the zero carrier frequency or a frequency equal to the doubled frequency of rotation. It is possible to measure the rotors' relative angle of rotation. Besides this, it is possible to read the signal by measuring the parameters of the motion relative to the base and to each other of the inner rotors in each stage.

Let us discuss an RVG's transfer functions for reading on the zero carrier frequency. Assuming the signal filtration provides us with reliable suppression of the

oscillations on frequency $2\omega_0$ and that the area of the essential frequencies is limited, we will discuss only the first components in the right sides of equations (1.55) and (1.56). Equation (1.55) should be analyzed when reading the signal from the first rotor. By replacing the operators with their values expressed in terms of the instrument's parameters, it is easy to see that the free term of the numerator of the rational expression being derived is identical with zero. The instrument's transfer function can then be written in the form

$$W_1^{\text{II}}(p) = \frac{\sum_{l=0}^{7} A_l p^l}{\sum_{n=0}^{8} B_n p^n}, \tag{1.57}$$

where A_i and B_n are complex numbers in the general case.

Thus, the instrument in a steady state is a two-dimensional angular velocity measurer with a transfer factor

$$K_{\text{э}} = \frac{A_0}{B_0}. \tag{1.58}$$

The transfer factor is increased by dynamic tuning of the instrument; that is, the realization in it of a resonance operating mode. Mathematically, this means minimization of the value of B_0 and, in the absence of damping, fulfillment of the equality

$$B_0 = 0. \tag{1.59}$$

Substituting the values of the instrument's parameters into equality (1.59), we obtain the following condition for dynamic tuning:

$$\begin{aligned}
&[(R_3^{(2)} + R_1^{(2)} + R_1^{(1)})\omega_0^2 + C_2 + C_1](R_1^{(2)}\omega_0^2 + C_2) \times \\
&\times \{[(R_3^{(1)} + R_1^{(1)})\omega_0^2 + C_1](R_1^{(1)}\omega_0^2 + C_1) - (R_1^{(1)}\omega_0^2 + \Delta C_1)^2\} + \\
&+ (R_1^{(2)}\omega_0^2 + C_2)(R_1^{(1)}\omega_0^2 - C_1)[(R_1^{(1)}\omega_0^2)^2 + C_1^2 - 2\Delta C_1^2] - \\
&- [(R_3^{(1)} + R_1^{(1)})\omega_0^2 + C_1][(R_1^{(1)}\omega_0^2 + C_1)(R_1^{(2)}\omega_0^2 + \Delta C_2)^2 + \\
&+ (R_1^{(1)}\omega_0^2 - \Delta C_1)^2(R_1^{(2)}\omega_0^2 + C_2)] + (R_1^{(2)}\omega_0^2 + \Delta C_2)^2 \times \\
&\times (R_1^{(1)}\omega_0^2 + \Delta C_1)^2 = 0.
\end{aligned} \tag{1.60}$$

Let us find the dynamic tuning conditions for RVG's constructed according to plans that are special cases of the one under discussion. For a three-rotor VG in which the NR is coupled with intermediate elastic elements possessing commensurate torsional rigidities relative to the orthogonal axes OY and OZ, in (1.60) we should set $R_1^{(1)} = 0$. The dynamic tuning condition will then be written in the form

$$\begin{aligned}
&(R_3^{(2)} + R_1^{(2)})\omega_0^2 + C_2 + C_1](R_1^{(2)}\omega_0^2 + C_2)[(R_3^{(1)}\omega_0^2 + C_1)C_1 - \Delta C_1^2] - \\
&- C_1(R_1^{(2)}\omega_0^2 + C_2)(C_1^2 - 2\Delta C_1^2) - (R_3^{(1)}\omega_0^2 + C_1) \times \\
&\times [C_1(R_1^{(2)}\omega_0^2 + \Delta C_2)^2 + \Delta C_1^2(R_1^{(2)}\omega_0^2 + C_2)] + \\
&+ \Delta C_1^2(R_1^{(2)}\omega_0^2 + \Delta C_2)^2 = 0.
\end{aligned} \tag{1.61a}$$

If the suspension of the first (counting from the base) rotor possesses rigidities that are commensurate with respect to the orthogonal axes in the plane of rotation, the dynamic tuning condition for a three-rotor MRG is derived from (1.60) by substituting $R_1^{(2)} = 0$:

$$\begin{aligned}&[(R_3^{(2)} + R_1^{(1)})\,\omega_0^2 + C_2 + C_1]\,C_2\,\{[(R_3^{(1)} + R_1^{(1)})\,\omega_0^2 + C_1] \times \\ &\times (R_1^{(1)}\omega_0^2 + C_1) - (R_1^{(1)}\omega_0^2 + \Delta C_1^2)\} + C_2\,(R_1^{(1)}\omega_0^2 - C_1) \times \\ &\times [(R_1^{(1)}\omega_0^2)^2 + C_1^2 - 2\Delta C_1^2] - [(R_3^{(1)} + R_1^{(1)})\,\omega_0^2 + C_1] \times \\ &\times [\Delta C_2^2\,(R_1^{(1)}\omega_0^2 + C_1) + C_2\,(R_1^{(1)}\omega_0^2 - \Delta C_1)^2] + \\ &+ \Delta C_2^2\,(R_1^{(1)}\omega_0^2 + \Delta C_1)^2 = 0.\end{aligned} \tag{1.61b}$$

The intermediate rotor of a three-rotor MRG can be suspended in the same manner. In this case the dynamic tuning condition is derived by substituting $R_3^{(2)} = 0$ into (1.60).

If a three-rotor MRG is made in such a fashion that the rigidity of the suspension of the first rotor to the PD's shaft and the subsequent rotors to the preceding ones is incommensurably greater along one of the orthogonal axes lying in the plane of rotation than along the other, the dynamic tuning condition can be derived (for example) from (1.61) by equating to zero the coefficient for the highest degree of rigidity, which is moving toward infinity. Assuming, for example, that $C_C^{(2)} \to \infty$, we obtain

$$\begin{aligned}&\{[(R_3^{(1)} + R_1^{(1)})\,\omega_0^2 + C_1]\,(R_1^{(1)}\omega_0^2 + C_1) - (R_1^{(1)}\omega_0 + \Delta C_1)^2\} \times \\ &\times [(R_3^{(2)} + R_1^{(1)})\,\omega_0^2 + C_1 + 2C_B^{(2)}] + C_B^{(1)}C_C^{(1)}\,(R_1^{(1)}\omega_1^2 - C_1) - \\ &- (R_1^{(1)}\omega_0^2 - \Delta C_1)\,[R_3^{(1)}\omega_0^2\,(R_1^{(1)}\omega_0^2 - \Delta C_1) + 2R_1^{(1)}\omega_0^2 C_B^{(1)}] = 0.\end{aligned} \tag{1.62}$$

Two-rotor MRG's can also be differentiated among themselves according to the method by which the elastic suspension of the rotors is realized. When the rigidity of each rotor's suspension is commensurate with respect to both axes, the tuning condition is derived from equation (1.61) if in it we set $R_1^{(2)} = 0$:

$$\begin{aligned}&C_2\,(R_3^{(2)}\omega_0^2 + C_2 + C_1)\,[(R_3^{(1)}\omega_0^2 + C_1)\,C_1 - \Delta C_1^2] - C_2 C_1\,(C_1^2 - 2\Delta C_1^2) - \\ &- (R_3^{(1)}\omega_0^2 + C_1)\,(C_1\Delta C_2^2 + C_2\Delta C_1^2) + \Delta C_1^2\Delta C_2^2 = 0.\end{aligned} \tag{1.63}$$

For two-rotor MRG's in which the NR has only one degree of freedom relative to the VR ($C_C^{(1)} \to \infty$), the dynamic tuning condition is derived thusly:

$$\begin{aligned}&\left(\tfrac{1}{2}\,R_3^{(1)}\omega_0^2 + C_B^{(1)}\right)[(R_3^{(2)}\omega_0^2 + C_2)\,C_2 - \Delta C_2^2] + \\ &+ C_2 C_B^{(1)} R_3^{(1)}\omega_0^2 = 0.\end{aligned} \tag{1.64}$$

If, however, the VR has one degree of freedom relative to the PD's shaft ($C_C^{(2)} \to \infty$), the resonance tuning condition for such an instrument (on the basis of (1.63)) will be written in the form

$$\begin{aligned}&(R_3^{(2)}\omega_0^2 + C_1 + 2C_B^{(2)})\,[(R_3^{(1)}\omega_0^2 + C_1)\,C_1 - \Delta C_1^2] - \\ &- [R_3^{(1)}\omega_0^2\Delta C_1^2 + C_1 C_C^{(1)} C_B^{(1)}] = 0.\end{aligned} \tag{1.65}$$

When designing the elastic suspension of a two-rotor MRG's rotors that provides the VR relative to the PD's shaft and the NR relative to the VR with only one degree of freedom, its motion is described by the equations of motion of the first stage of our generalized VRG model. In this case, the dynamic tuning condition is found from expression (1.60), if in it we set $R_1^{(2)} = R_3^{(2)} = 0$, $\Delta C_2 = 0$ and $C_2 \to \infty$. This condition was discussed in [3] and has the form

$$(R_3^{(1)}\omega_0^2 + C_1)(R_1^{(1)}\omega_1^2 + C^1) + R_1^{(1)}\omega_0^2 C_1 - \\ - \Delta C_1 (2R_1^{(1)}\omega_0^2 + \Delta C_1) = 0. \tag{1.66}$$

Finally, the resonance tuning condition for a single-rotor VG is obtained if in (1.66) we set equal to zero the VR's moments of inertia:

$$(R_3^{(1)}\omega_0^2 + C_1) C_1 - \Delta C_1^2 = 0. \tag{1.67}$$

In the case where the rigidity along one axis of the suspension is considerably greater than that along the other one ($C_B^{(1)} \to \infty$, for example), we obtain the well-known [3] resonance tuning condition

$$-\frac{1}{2} R_3^{(1)}\omega_0^2 = C_C^{(1)}. \tag{1.68}$$

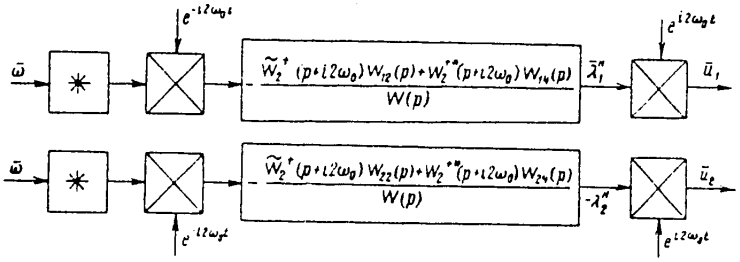

Figure 8. Structural diagram of MRG with signal reading on frequency ω_0.

When the signal is read on the frequency that equals the rotor's doubled frequency of rotation, in expressions (1.55) and (1.56) it is necessary to examine the second terms on the right sides. Then, when describing the instrument's dynamic characteristics it is necessary to take into consideration the system for splitting the signal with respect to the sensitivity axes, which is a normal phase demodulator in the simplest case. Figure 8 is a structural diagram of the conversion of the base's absolute angular velocity of rotation into a signal at the outputs of an RVG's demodulator. Here the fact is taken into consideration that the demodulator is constructed on the basis of measurers of the rotor's angles of rotation relative to the two coordinate axes that are coupled with the base. From expressions (1.55) and (1.56) it follows that, in general, complete information about the angular velocity vector is supplied by one angle measurer. However, the use of two such measurers makes it possible to realize a demodulating function of the $e^{i2\omega_0 t}$ type and thereby (as follows from the structural diagram) get rid of the quadrature component at the demodulator's outlet. In the case under discussion, the expressions for the signals at the instrument's outputs can be written in the following form:

$$\bar{u}_1 = -\frac{\tilde{W}_2^+(p)W_{12}(p-i2\omega_0) + W_2^{+*}(p)W_{11}(p-i2\omega_0)}{W(p-i2\omega_0)}\bar{\omega}^*; \tag{1.69}$$

$$\bar{u}_2 = -\frac{\tilde{W}_1^{+}(p)\,W_{12}(p-i2\omega_0) + W_2^{+*}(p)\,W_{24}(p-i2\omega_0)}{W(p-i2\omega_0)}\,\bar{\omega}^*. \tag{1.70}$$

As with the case of signal reading on the zero frequency, the transfer function of such an RVG is a rational expression that is analogous to (1.57). In connection with this, the dynamic tuning conditions do not depend on the signal reading method and are determined by expressions (1.60)-(1.68) that we have derived.

Let us derive the transfer functions of an instrument when the signal is read from the VR's of the first and second stages. We will call $\bar{\eta}_1$ and $\bar{\eta}_2$ the vectors of the angles of rotation, respectively, of the VR's of the first and second stages in inertial space. It is obvious that the following relationships occur for $\bar{\eta}_1$ and $\bar{\eta}_2$:

$$\left.\begin{aligned}\bar{\eta}_1 &= \bar{\chi}_1 + 0_1 e^{-i\omega_0 t};\\ \bar{\eta}_2 &= \bar{\chi}_2 + 0_2 e^{-i\omega_0 t}.\end{aligned}\right\} \tag{1.71}$$

Making use of relationship (1.6), let us express the VR's absolute angles of rotation in terms of the NR's absolute angles of rotation and the base's absolute angular velocity of rotation around the instrument's axes of sensitivity:

$$\left.\begin{aligned}\bar{\eta}_1 &= \frac{1}{2}\left(\bar{\chi}_1 + \bar{\chi}_2 - \bar{\chi}_1^{*} e^{-i2\omega_0 t} + \bar{\chi}_2^{*} e^{-i2\omega_0 t}\right);\\ \bar{\eta}_2 &= \frac{1}{2}\left(\bar{\chi}_2 + \int \bar{\omega}\,dt - \bar{\chi}_2^{*} e^{-i2\omega_0 t} + e^{-i2\omega_0 t}\int \bar{\omega}\,dt\right).\end{aligned}\right\} \tag{1.72}$$

Substituting the values of $\bar{\chi}_1$ and $\bar{\chi}_2$ from expressions (1.20) into (1.72), we determine the dependence of the VR's absolute angles of rotation on the angular velocities of rotation of the base:

$$\begin{aligned}\bar{\eta}_1 = \frac{1}{2}\{&[W_{u1}(p) + W_{u2}(p) - \tilde{W}_{u1}(p) + \tilde{W}_{u2}(p)]\,\bar{\omega} +\\ &+ [\tilde{W}_{u1}(p+i2\omega_0) + \tilde{W}_{u2}(p+i2\omega_0) - W_{u1}^{*}(p+i2\omega_0) +\\ &+ W_{u2}^{*}(p+i2\omega_0)]\,\bar{\omega}^* e^{-i2\omega_0 t}\};\end{aligned} \tag{1.73}$$

$$\begin{aligned}\bar{\eta}_2 = \frac{1}{2}\Big\{&\Big[W_{u2}(p) - \tilde{W}_{u2}^{*}(p) + \frac{1}{p}\Big]\,\bar{\omega} + [\tilde{W}_{u2}(p+i2\omega_0) -\\ &- W_{u2}^{*}(p+i2\omega_0) + \frac{1}{p+i2\omega_0}\Big]\,\bar{\omega}^* e^{-i2\omega_0 t}\Big\},\end{aligned} \tag{1.74}$$

where

$$W_{u1}(p) = \frac{W_1^{+}(p)\,W_{12}(p) + \tilde{W}_2^{+*}(p)\,W_{14}(p)}{W(p)};$$

$$W_{u2}(p) = \frac{W_2^{+}(p)\,W_{22}(p) + \tilde{W}_2^{+*}(p)\,W_{24}(p)}{W(p)};$$

$$\tilde{W}_{u1}(p) = \frac{\tilde{W}_2^{+}(p)\,W_{12}(p-i2\omega_0) + W_2^{+*}(p)\,W_{14}(p-i2\omega_0)}{W(p-i2\omega_0)};$$

$$\tilde{W}_{u2}(p) = \frac{\tilde{W}_2^{+}(p)\,W_{22}(p-i2\omega_0) + W_2^{+*}(p)\,W_{24}(p-i2\omega_0)}{W(p-i2\omega_0)}.$$

The relative angles of rotation of the VR in the nonrotating system that is coupled with the instrument's base are determined by the expressions

$$\bar{\lambda}^{u}_{1B} = \frac{1}{2}\left\{\left[\frac{2}{p} - W_{u1}(p) - W_{u2}(p) + \tilde{W}^{*}_{u1}(p) - \tilde{W}^{*}_{u2}(p)\right]\bar{\omega} - \right.$$
$$- [\tilde{W}_{u1}(p + i2\omega_0) + \tilde{W}_{u2}(p + i2\omega_0) + W^{*}_{u2}(p + i2\omega_0) -$$
$$\left. - W^{*}_{u1}(p + i2\omega_0)]\,\bar{\omega}^{*}e^{-i2\omega_0 t}\right\}; \tag{1.75}$$

$$\bar{\lambda}^{u}_{2B} = \frac{1}{2}\left\{\left[\frac{1}{p} - W_{u2}(p) + \tilde{W}^{*}_{u2}(p)\right]\bar{\omega} - \right.$$
$$\left. - \left[\tilde{W}_{u2}(p + i2\omega_0) - W^{*}_{u2}(p + i2\omega_0) + \frac{1}{p + i2\omega_0}\right]\bar{\omega}^{*}e^{-i2\omega_0 t}\right\}. \tag{1.76}$$

From expressions (1.75) and (1.76) it follows that when the signal is read from the VR in the nonrotating system of coordinates that is linked to the base, the reading can be done on the zero frequency or on a carrier frequency that is the doubled frequency of rotation of the PD's shaft. In connection with this, it is easy to derive the instrument's transfer functions from expressions (1.75) and (1.76) in a manner analogous to the derivation of the transfer functions of an instrument when the signal is read from the NR, while the dynamic tuning conditions coincide with the tuning conditions (1.60)-(1.68) derived above. From expressions (1.73)-(1.76) it is also easy to derive an RVG's transfer functions if the signal is ready by measuring the rotors' motion relative to each other in the nonrotating system of coordinates.

Let us examine an RVG with single modulation and reading of the useful signal in a coordinate system that is rotating together with the PD's shaft. Considering transfer formula (1.11) and an MRG's equations of motion (1.20), the dependence of the rotors' NR's relative angles of rotation on the base's angular velocity has the form

$$\bar{\lambda}^{u}_{1} = \frac{W(p - i\omega_0) - (p - i\omega_0)\left[W^{+}_{2}(p - i\omega_0)W_{12}(p - i\omega_0) + \right.}{(p - i\omega_0)W(p - i\omega_0)}$$
$$\left. + \tilde{W}^{+*}_{2}(p - i\omega_0)W_{14}(p - i\omega_0)\right]$$
$$\bar{\omega}e^{i\omega_0 t} -$$
$$- \frac{\tilde{W}^{+}_{2}(p + i\omega_0)W_{12}(p - i\omega_0) + W^{+*}_{2}(p + i\omega_0)W_{14}(p - i\omega_0)}{W(p - i\omega_0)}\bar{\omega}^{*}e^{-i\omega_0 t}; \tag{1.77}$$

$$\bar{\lambda}^{u}_{2} = \frac{W(p - i\omega_0) - (p - i\omega_0)\left[W^{+}_{2}(p - i\omega_0)W_{22}(p - i\omega_0) + \right.}{(p - i\omega_0)W(p - i\omega_0)}$$
$$\left. + \tilde{W}^{+*}_{2}(p - i\omega_0)W_{24}(p - i\omega_0)\right]$$
$$\bar{\omega}e^{i\omega_0 t} -$$
$$- \frac{\tilde{W}^{+}_{2}(p + i\omega_0)W_{22}(p - i\omega_0) + W^{+*}_{2}(p + i\omega_0)W_{24}(p - i\omega_0)}{W(p - i\omega_0)}\bar{\omega}^{*}e^{-i\omega_0 t}, \tag{1.78}$$

while its dependence on the VR's angles of rotation is

$$\bar{\lambda}^{u}_{1B} = \frac{1}{2}\left\{\left[\frac{2}{p - i\omega_0} - W_{u1}(p - i\omega_0) - W_{u2}(p - i\omega_0) + \right.\right.$$
$$\left. + \tilde{W}^{*}_{u1}(p - i\omega_0) - \tilde{W}^{*}_{u2}(p - i\omega_0)\right]\bar{\omega}e^{i\omega_0 t} - [\tilde{W}_{u1}(p - i\omega_0) +$$
$$\left. + \tilde{W}_{u2}(p + i\omega_0) - W^{*}_{u1}(p + i\omega_0) + W^{*}_{u2}(p + i\omega_0)]\,\bar{\omega}^{*}e^{-i\omega_0 t}\right\}; \tag{1.79}$$

$$\bar{\lambda}^{B}_{2B} = \frac{1}{2}\int\left\{\left[\frac{1}{p-i\omega_0} - W_{n2}(p-i\omega_0) + \tilde{W}^{*}_{n2}(p-i\omega_0)\right]\bar{\omega}e^{i\omega_0 t} - \right.$$
$$\left. - \left[\tilde{W}_{n2}(p+i\omega_0) - W^{*}_{n2}(p+i\omega_0) + \frac{1}{p+i\omega_0}\right]\bar{\omega}^{*}e^{-i\omega_0 t}\right. . \qquad (1.80)$$

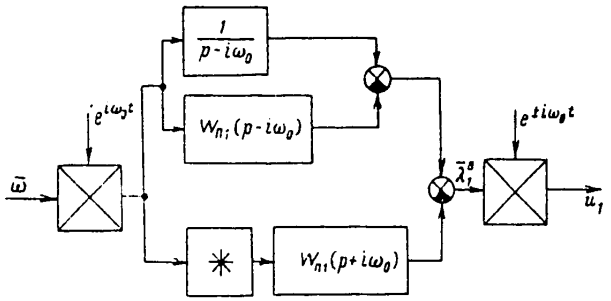

Figure 9. Structural diagram of MRG with signal reading on frequency ω_0.

In the rotating system it is possible to take readings only on a carrier frequency that equals the PD's frequency of rotation. Figure 9 is a structural diagram describing the operation of an instrument when the signal is read from the first stage's NR and the presence of a phase demodulator at the output is allowed for. When the signal is read from other rotors, the instrument's structural diagram takes on an analogous form. Depending on the methods used to construct the demodulator's circuitry, two reference functions can be realized in it: $e^{-i\omega_0 t}$ and $e^{i\omega_0 t}$. It should be mentioned here that the realization of such reference functions is possible only in the presence of two rotor rotation angle measurers located on mutually orthogonal axes in the instrument's plane of sensitivity. In the first case, when the demodulator uses reference function $e^{-i\omega_0 t}$, the instrument's transfer function coincides with the analogous one derived for signal reading on the zero frequency in the nonrotating system of coordinates, and is described by the first terms on the right sides of expressions (1.55) and (1.56). If the reference function used is $e^{i\omega_0 t}$, the instrument's transfer function is identical to the one derived for signal reading in the nonrotating system on the carrier frequency that is double the frequency of rotation of the PD's shaft.

Signal reading in the rotating system of coordinates is also possible with the use of only one measurer of the rotor's angle of rotation relative to one of the measuring axes lying in the instrument's plane of sensitivity. The structural diagram of an RVG corresponding to this case is shown in Figure 10. Depending on which suspension axis the measurer is attached to, the signal entering the demodulator is proportional to either $\mathrm{Re}\overline{\lambda^B}$ or $\mathrm{Im}\overline{\lambda^B}$. The first case corresponds to the upper signs in the operators of the linear part of the structural diagram, while the second corresponds to the lower ones. In turn, either $e^{i\omega_0 t}$ or $e^{-i\omega_0 t}$ can be used as the reference function. The instrument's transfer functions for each of these cases can be derived easily on the basis of this structural diagram. The structural diagram of an instrument where the signal is read from the RVG's other rotors has an analogous form.

Making use of the conclusions that have been reached, let us examine the dynamic and static characteristics of several types of RVG's with single modulation. The

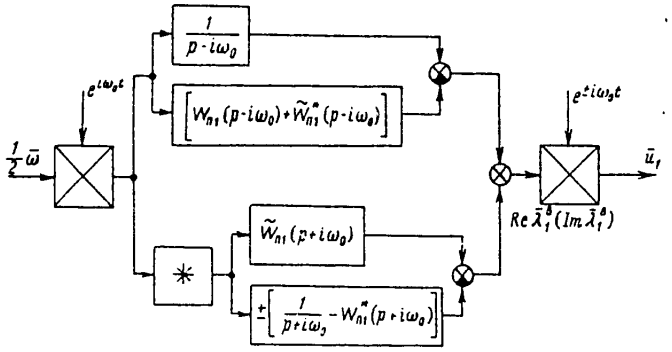

Figure 10. Structural diagram of MRG with signal reading from a single measuring axis.

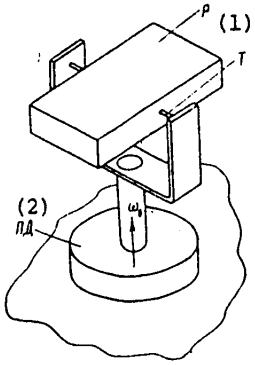

Figure 11. Diagram of OMG with rotating suspension.
Key: 1. R
2. PD

simplest of them is a single-rotor MRG with VP, a diagram of which is shown in Figure 11. The elastic suspension of rotor R is fashioned in such a manner that the flexural rigidity of torsion bars T is significantly greater than their torsional rigidity, which in the first approximation can be assumed to be infinite. We determine the transfer function of such an instrument from the general equations, equating to zero the moments of inertia of the second stage's VR and NR and the first stage's VR and directing toward infinity the suspension's rigidity along the second stage's axes and the rigidity of the first stage's suspension along one of the axes, such as $C_C^{(1)}$. As a result, by omitting the indices we obtain the transfer function for an OMG when the signal is read in the nonrotating system of coordinates:

$$W(p) = \frac{1}{2}\,\frac{I_{Y_H}p + \frac{1}{2}iR_3\omega_0 + I_{Y_H}2\omega_0}{I_{Y_H}p^2 + (iI_{Y_H}2\omega_0 + \mu_H)p + i\mu_H\omega_0 + \frac{1}{2}R_3\omega_0^2 + C_B}. \qquad (1.81)$$

It should be mentioned here that when the signal is read on the zero frequency and when it is read on the doubled frequency of rotation of the PD, the instrument's transfer functions prove to be identical to within the accuracy of the sign. In the rotating system, signal reading is possible only on frequency ω_0 with the help of an angle sensor that measures the rotor's rotation relative to the torsion bars' axis. In connection with this, the instrument's transfer function differs from expression (1.81) only in that its transfer factor is twice as large.

One of the most important characteristics of an RVG is its transfer factor K_g with respect to the base's angular velocity at a stable speed. For instruments of the type under discussion, K_g is determined from (1.81):

$$K_g = \frac{i}{2\omega_0}\,\frac{1 + \varkappa_Y}{i2\xi_B - (1 - \varkappa_Y - \nu_B^2)}, \qquad (1.82)$$

where $\varkappa_Y = (I_{XH} - I_{ZH})/I_{YH}$ = a structural parameter defining the geometry of the rotor; $\nu_B = (1/\omega_0)\sqrt{C_B/I_{YH}}$ = ratio of a nonrotating rotor's natural oscillation frequency to the PD shaft's frequency of rotation; $\xi_B = \mu_B/(2I_{YH}\omega_0)$ = relative damping factor of the RVG's rotor.

Considering the dimensionless parameters that have been introduced, dynamic tuning condition (1.68) will be written as

$$1 - \varkappa_Y - \nu_B^2 = 0, \tag{1.83}$$

while the instrument's transfer factor in the dynamic tuning mode will become

$$K_g = \frac{1 + \varkappa_Y}{4\xi_B\omega_0}. \tag{1.84}$$

Substituting condition (1.83) into expression (1.84), we find the transfer function of the type of MRG under discussion when it is operating in the dynamic tuning mode:

$$W(p) = \frac{1 + \varkappa_Y}{4\xi_B\omega_0} \frac{\frac{1}{(1 + \varkappa_Y)\omega_0}p + i}{\left(\frac{1}{\xi_B\omega_0}p + 1\right)\left(\frac{1}{2\omega_0}p + i + \frac{\xi_B}{2}\right)}. \tag{1.85}$$

In the area of essential frequencies ($\omega << \omega_0$), the RVG's transfer function is approximated by an even simpler expression:

$$W(p) = \frac{1 + \varkappa_Y}{4} T_g \frac{1}{T_g p + 1}, \tag{1.86}$$

where $T_g = 1/\xi_B\omega_0$.

Thus, this MRG is described by an aperiodic component element with a time constant T_g. In highly sensitive instruments, time constant T_g reaches quite high values (tens of seconds). Therefore, in the initial period of the transient process this instrument is completely identical to an integrating gyroscope with an integration factor

$$K_и = \frac{K_g}{T_g} \approx \frac{1}{2}. \tag{1.87}$$

Let us change over to a single-rotor MRG having commensurate rigidities of the rotor's suspension with respect to two orthogonal axes in the plane perpendicular to the PD's shaft. When the signal is read in the nonrotating system of coordinates, its transfer function with respect to the base's angular velocity has the form

$$W(p) = \frac{A(p)}{B(p)}, \tag{1.88}$$

where

$$A(p) = p^3 + (1i + \xi_C + \xi_B)\omega_0 p^2 + \left[\frac{1}{2}(\nu_C^2 + \nu_B^2) + i(\xi_C + \xi_B) - \right.$$

$$- 2(1 - \varkappa_Z)\left(\frac{1}{2}\frac{I_{ZH} + I_{YH}}{I_{YH}} + \frac{I_{XH}}{I_{YH}}\right) + (\xi_C(1 + \varkappa_Y) + \xi_B(1 + \varkappa_Z))i -$$

$$\left. - (1 + \varkappa_Y)(1 - \varkappa_Z)\right]\omega_0^2 p + \frac{1}{2} i\omega_0^3[(i2\xi_C + \nu_C^2)(1 + \varkappa_Y) + (i2\xi_B + \nu_B^2)(1 + \varkappa_Z) + 2R_3\frac{I_{XH}}{I_{ZH}I_{YH}}];$$

. . . . . .

. . . . . .

$$B(p) = p^4 + [4i + 2(\xi_C + \xi_B)]\omega_0 p^3 + [i6(\xi_C + \xi_B) + 4\xi_C\xi_B +$$

$$+ \nu_C^2 + \nu_B^2 - (1 + \varkappa_Z)(1 + \varkappa_Y) - (1 - \varkappa_Z)\left(1 + \frac{I_Z}{I_Y} + 2\frac{I_X}{I_Y}\right)]\omega_0^2 p^2 +$$

$$+ [-4(\xi_C + \xi_B) - 2(\xi_C(1 - \varkappa_Y) + \xi_B(1 - \varkappa_Z)) + 2(\xi_B\nu_C^2 + \xi_C\nu_B^2) +$$

$$+ i8\xi_C\xi_B + i2(\nu_C^2 + \nu_B^2) - i2\frac{I_X}{I_Y}(1 - \varkappa_Z)]\omega_0^3 p + [-i2\xi_C \times$$

$$\times (1 - \varkappa_Y - \nu_B^2) - i2\xi_B(1 - \varkappa_Z - \nu_C^2) + \nu_C^2\nu_B^2 - \nu_C^2(1 - \varkappa_Y) -$$

$$- \nu_B^2(1 - \varkappa_Z) - 4\xi_B\xi_C]\omega_0^4.$$

The relationship $\xi << \nu < 1$ occurs for a highly sensitive instrument. The dynamic tuning condition (1.67) of such an instrument, expressed in terms of its parameters, is written in the form

$$\nu_C^2\nu_B^2 - \nu_C^2(1 - \varkappa_Y) - \nu_B^2(1 - \varkappa_Z) = 0. \tag{1.89}$$

It is obvious that this condition can be fulfilled by preserving the following relationships of the instrument's parameters relative to each of the suspension axes:

$$\nu_B^2 = 2(1 - \varkappa_Y); \qquad \nu_C^2 = 2(1 - \varkappa_Z). \tag{1.90}$$

The instrument's transfer factor is then found, with sufficient accuracy, from the expression

$$K_g = \frac{i}{2\omega_0}\frac{\xi_C(1 + \varkappa_Y) + \xi_B(1 + \varkappa_Z)}{\xi_C(1 - \varkappa_Y) + \xi_B(1 - \varkappa_Z)}, \tag{1.91}$$

which, when the parameters with respect to both axes of the rotor's suspension are equal, changes into

$$K_g = \frac{i}{2\omega_0}\frac{1 + \varkappa}{1 - \varkappa}. \tag{1.92}$$

Thus, in this case the instrument's transfer factor is considerably less than that of an OMG having only a single degree of freedom in the plane of rotation. There are also significant differences in the instruments' dynamics. In the case of dynamic tuning, the numerator and denominator of the transfer function of an OMG with two degrees of rotor suspension freedom are the expressions

$$A(\bar{p}) \approx \omega_0^3\left\{\bar{p}^3 + i4\bar{p}^2 + \left[\frac{1}{2}(\nu_C^2 + \nu_B^2) - 2(1 - \varkappa_Z) \times\right.\right.$$

$$\left.\left. \times \left(\frac{1}{2}\frac{I_{Z\text{н}} + I_{Y\text{н}}}{I_{Y\text{н}}} + \frac{I_{Z\text{н}}}{I_{Y\text{н}}}\right) - (1 + \varkappa_Y)(1 + \varkappa_Z)\right]\bar{p} - \right. \tag{1.93}$$

$$\left. - \xi_C(1 + \varkappa_Y) - \xi_B(1 + \varkappa_Z);\right.$$

$$B(\bar{p}) \approx \omega_0^4\left\{\bar{p}^4 + i4\bar{p}^3 + \left[2(1 - \varkappa_Y) + \left(1 - \frac{I_Z}{I_Y} - 2\frac{I_X}{I_Y}\right)(1 - \varkappa_Z) -\right.\right.$$

$$\left. - (1 + \varkappa_Z)(1 + \varkappa_Y)\right]\bar{p}^2 + \left[i\left(4(1 - \varkappa_Y) + \left(4 - 2\frac{I_X}{I_Y}\right)(1 - \varkappa_Z)\right) -\right.$$

$$\left.\left. - \xi_C 2(1 + \varkappa_Y) - \xi_B 2(1 + \varkappa_Z)\right]\bar{p} + i2[\xi_C(1 - \varkappa_Y) + \xi_B(1 - \varkappa_Z)]\right|, \tag{1.94}$$

where $\bar{p} = p/\omega_0$ = a dimensionless operator.

For the sake of simplicity, we will analyze in detail only the case where the rotor has the same parameters with respect to both suspension axes; that is, $\nu_B = \nu_C$, $\xi_B = \xi_C$, $\varkappa_Y = \varkappa_Z$. In connection with this, we will allow for the fact that for rotors in which the height (the linear dimension along the axis of rotation) is substantially less than the length and width (the linear dimensions perpendicular to the axis of rotation in the plane of rotation), the value of $\varkappa$ is close to unity ($1 - \varkappa << 1$). In this case the instrument's transfer function takes on the form

$$W(\bar{p}) = \frac{1}{\omega_0} \frac{\bar{p}^3 + i4\bar{p}^2 - (1+\varkappa)^2\bar{p} - 2\xi(1+\varkappa)}{\bar{p}^4 + i4\bar{p}^3 + \left[2\left(1 - \frac{I_X}{I_Y}\right)(1-\varkappa) - (1+\varkappa)^2\right]\bar{p}^2 + \left[i\left(4 - \frac{I_X}{I_Y}\right)(1-\varkappa) - 2\xi(1+\varkappa)\right]2\bar{p} + i4\xi(1-\varkappa)}. \quad (1.95)$$

Examining transfer function (1.95) only in the area of essential frequencies ($\omega << \omega_0$) and approximating it by the product of the transfer functions of typical inertial components and components that have had a derivative introduced, we obtain

$$W(\bar{p}) = -\frac{1}{2\omega_0(1+\varkappa)} \frac{(1+\varkappa)\bar{p} + 2\xi}{\bar{p} - i\frac{12\xi^2}{1-\varkappa}\frac{\left(6-\varkappa-2\frac{I_X}{I_Y}\right)^2}{4-\frac{I_X}{I_Y}} + \frac{2\xi}{4-\frac{I_X}{I_Y}}} \times \frac{1}{\bar{p} - i\frac{(1-\varkappa)}{(1+\varkappa)^2}\left(4-\frac{I_X}{I_Y}\right) + 2\xi\frac{7-\varkappa-2\frac{I_X}{I_Y}}{(1+\varkappa)^2}}. \quad (1.96)$$

This approximation is correct when the following relationship among the instrument's parameters is fulfilled:

$$16\xi^2\left(\frac{1+\varkappa}{1-\varkappa}\right)^2\left(\frac{6-\varkappa-2\frac{I_X}{I_Y}}{4-\frac{I_X}{I_Y}}\right)^2 \ll 1.$$

From (1.96) it follows that when the base's motion develops spasmodically, the motion of an MRG's rotor consists of a slow (precessional) motion toward a steady-state position and nutational oscillations that are superimposed on it. The precessional motion is caused by the presence of viscous friction along the suspension axes. In connection with this, the projection of the rotor's pole moves along an attenuating spiral in the pictorial plane. The precessional motion's angular frequency, as referred to the PD's angular velocity, is

$$\nu_\pi = 12\xi^2\frac{\left(6-\varkappa-2\frac{I_X}{I_Y}\right)^2}{(1-\varkappa)\left(4-\frac{I_X}{I_Y}\right)}, \quad (1.97)$$

while the relative damping factor is

$$\xi_\pi = \frac{1}{6\xi}\frac{1-\varkappa}{\left(6-\varkappa-2\frac{I_X}{I_Y}\right)^2}. \quad (1.98)$$

the case where $\xi_\pi >> 1$, the dynamics of the precessional motion are described te accurately by the transfer function of a normal aperiodic component:

$$W_{\text{п}}(p) = i\,\frac{1}{T_g p + 1}\,\frac{1}{2\omega_0}\,\frac{1+\varkappa}{1-\varkappa}, \tag{1.99}$$

where $T_g = (4 - I_X/I_Y)/(2\xi\omega_0)$.

Thus, the precessional motion of the rotor of an OMG with two degrees of freedom of the suspension in the plane of rotation proves to be analogous to the motion of an OMG rotor with one degree of freedom. The only difference is the absence of nutational oscillations in the latter. The relative frequency of the nutational oscillations is determined from the expression

$$\nu_{\text{н}} = \frac{1-\varkappa}{(1+\varkappa)^2}\left(4 - \frac{I_X}{I_Y}\right), \tag{1.100}$$

while the relative damping factor is

$$\xi_{\text{н}} = \xi\,\frac{7 - \varkappa - 2\frac{I_X}{I_Y}}{1-\varkappa}\,\frac{1}{8 - 2\frac{I_X}{I_Y}}. \tag{1.101}$$

When such an instrument is used in automatic control systems, nutational oscillations in the system's band of essential frequencies can have unfavorable consequences. Therefore, it is desirable to select the instrument's parameters in such a manner that $\nu_{\text{н}}$ be as large as possible.

A component in the numerator of transfer function (1.96) defines the OMG's reaction to angular accelerations in the base's motion. The ratio of the instrument's transfer factor with respect to acceleration $K_{\text{п}}$ to the transfer factor with respect to velocity is

$$\frac{K_{\text{п}}}{K_g} = \frac{1}{2\xi\omega_0}(1+\varkappa). \tag{1.102}$$

The dynamic characteristics of a single-rotor MRG with nonidentical suspension parameters are qualitatively the same as those discussed above. The quantitative relationships for them can be derived in an analogous manner from expressions (1.93) and (1.94).

When the signal is read in the nonrotating system of coordinates on frequency $2\omega_0$, the following polynomials correspond to the numerator and denominator of the instrument's transfer function:

$$\begin{aligned} A(p) &= (\xi_C - \xi_B)\,\omega_0 p^2 + [-i(\xi_C - \xi_B) - i2\xi_C(1+\varkappa_Y) + \\ &+ i2\xi_B(1+\varkappa_Z) + (\nu_C^2 - \nu_B^2)]\,\omega_0^2 p - [(1+\varkappa_Y)(2\xi_C + i\nu_C^2) - \\ &- (1+\varkappa_Z)(2\xi_B + i\nu_B^2)]\,\omega_0^3; \\ B(p) &= p^4\left[-i4 - i(1-\varkappa_Y) + i\frac{I_Z}{I_Y}(1-\varkappa_Z) + 2(\xi_C + \xi_B)\right]\omega_0 p^3 + \\ &+ [-i6(\xi_C + \xi_B) + 4\xi_C\xi_B + (1+\varkappa_Z)(1+\varkappa_Y) + \nu_C^2 + \nu_B^2 - 2 - \\ &- (1-\varkappa_Z)\left(1 + \frac{I_X}{I_Y}\right) - 6(1-\varkappa_Y)]\,\omega_0^2 p^2 + [-i8\xi_C\xi_B - \\ &\cdots\cdots\cdots \end{aligned} \tag{1.103}$$

$$\cdots\cdots\cdots$$

$$-i2(\nu_C^2+\nu_B^2)-2\xi_C(\nu_B^2-3+\varkappa_Y)+2\xi_B(\nu_C^2-3+\varkappa_Z)- \tag{1.104}$$

$$-i2(1-\varkappa_Z)\left(4+\frac{I_X}{I_Y}\right)+i4(2-3\varkappa_Z-3\varkappa_Y)+$$

$$+i4(1+\varkappa_Z)(1+\varkappa_Y)]\omega_0^3 p+[i2\xi_C(1-\varkappa_Y-\nu_B^2)+$$

$$+i2\xi_B(1-\varkappa_Z-\nu_C^2)-4\xi_B\xi_C+\nu_C^2\nu_B^2-\nu_C^2(1-\varkappa_Y)-\nu_B^2(1-\varkappa_Z)].$$

From expression (1.103) it follows that, given identical instrument parameters relative to the suspension axes, it is invariant with respect to the base's angular motion. The larger the transfer factors K_g are, the greater this nonidentity. In connection with this, according to its characteristics the instrument is obviously close to the OMG discussed above that has a single degree of freedom in the plane of sensitivity.

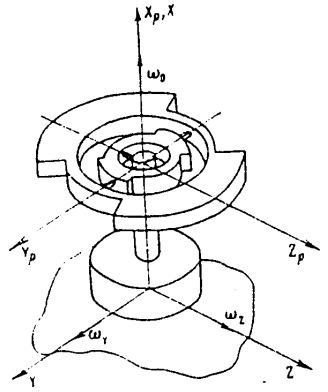

Figure 12. Diagram of DMG with rotating suspension.

When the signal is read on frequency ω_0 in the rotating system of coordinates, the instrument's transfer functions are the same as when it is read on the zero frequency in the nonrotating system.

Let us discuss the dynamic characteristics of a two-rotor modulation gyroscope. The simplest DMG layout is the one where the VR is suspended from the PD's shaft and the NR is suspended from the VR with the help of torsion bars with one degree of freedom (for all practical purposes). This layout is depicted in Figure 12. When the signal is read from the NR relative to the base in the nonrotating system of coordinates, the instrument's transfer function is analogous to (1.57), while the numerator and denominator are described by the following expressions:

$$B(p)=p^4+2(i2+\xi_C+\xi_B)\omega_0 p^3+\left[2\frac{R_1}{I_{Zn}}+\nu_C^2+\nu_B^2-(1+\varkappa_Y)\times\right.$$

$$\left.\times(1+\varkappa_{Zn})+i6(\xi_C+\xi_B)+4\xi_B\xi_C+R_3\frac{I_C+R_2}{I_{YH}I_{Zn}}\right]\omega_0^2 p^2+$$

$$+\left[2\frac{R_1}{I_{Zn}}(i(1+\varkappa_Y)+2\xi_B)+iR_3\frac{R_2-R_1}{I_{YH}I_{Zn}}+i2(\nu_C^2+\nu_B^2)+\nu_C^2 2\xi_B+\right. \tag{1.105}$$

$$\left.+\nu_B^2 2\xi_C+i8\xi_B\xi_C-4(\xi_B+\xi_C)-2\xi_C(1-\varkappa_Y)-2\xi_B(1-\varkappa_{Zn})\right]\times$$

$$\times\omega_0^3 p+\omega_0^4\left[\frac{R_1}{I_{Zn}}\left(2\nu_B^2+\frac{R^3}{I_{YH}}+i4\xi_B\right)+\nu_C^2\nu_B^2-\nu_C^2(1-\varkappa_Y)-\right.$$

$$\left.-\nu_B^2(1-\varkappa_{Zn})+i2(\xi_B\nu_C^2+\xi_C\nu_B^2)-i2\xi_C(1-\varkappa_Y)-i2\xi_B(1-\varkappa_{Zn})-\right.$$

$$\left.-4\xi_B\xi_C\right];$$

$$A(p) = p^3 + \left[i\left(4 + \frac{R_1}{I_{Z\Pi}}\right) + \xi_B + \xi_C\right]\omega_0 p^2 + \left[\frac{1}{2}(\nu_C^2 + \nu_B^2) - (1 + \varkappa_Y)(1 + \varkappa_{Z\Pi}) + i3(\xi_C + \xi_B)\right.$$
$$- i\xi_C(1 - \varkappa_Y) - i\xi_B(1 - \varkappa_{Z\Pi}) - 2(1 - \varkappa_{Z\Pi})\frac{I_C + R_2}{I_{Y\Pi}} -$$
$$\left. - \frac{R_1}{I_{Z\Pi}}(2 - \varkappa_Y - i2\xi_B)\right]\omega_0^2 p + \omega_0^3\left[i(\nu_C^2 + \nu_B^2) - \right. \quad (1.106)$$
$$- i\frac{1}{2}\nu_C^2(1 - \varkappa_Y) - i\frac{1}{2}\nu_B^2(1 - \varkappa_{Z\Pi}) - \xi_C(1 - \varkappa_Y) -$$
$$- \xi_B(1 - \varkappa_{Z\Pi}) - 2(\xi_C\varkappa_Y + \xi_B\varkappa_{Z\Pi}) - 2\xi_B\frac{R_1}{I_{Z\Pi}} + i\nu_B^2\frac{R_1}{I_{Z\Pi}} +$$
$$\left. + i\frac{R_1}{I_{Z\Pi}}(5\varkappa_Y - 3) - i2(1 - \varkappa_{Z\Pi})\frac{R_2 - R_1}{I_{Y\Pi}}\right],$$

where $I_{Z\pi} = I_{ZH} + I_{ZB}$ = adduced moment of inertia relative to the VR's suspension; $\varkappa = (I_{XH} - I_{YH} + I_{ZB})/I_{Z\pi}$.

The resonance tuning condition, as defined in terms of the dimensionless parameters we have adopted, is:

$$\nu_B^2\nu_C^2 - \nu_C^2(1 - \varkappa_Y) - \nu_B^2(1 - \varkappa_{Z\Pi}) + 2\frac{R_1}{I_{Z\Pi}}(\nu_B^2 - 1 + \varkappa_Y) = 0. \quad (1.107)$$

When the resonance tuning condition is fulfilled, the instrument's transfer factor with respect to the base's angular velocity is determined, with a sufficient degree of accuracy, by the expression

$$K_{\xi} = \frac{1}{4}\frac{2(\nu_C^2 + \nu_B^2) - \nu_B^2\nu_C^2 - 4(1 - 2\varkappa_Y)\frac{R_1}{I_{Z\Pi}} - 4(1 - \varkappa_{Z\Pi})\frac{R_2 - R_1}{I_{Y\Pi}}}{\xi_B\left(2\frac{R_1}{I_{Z\Pi}} + \nu_C^2 - 1 + \varkappa_{Z\Pi}\right) + \xi_C(\nu_B^2 - 1 + \varkappa_Y)}. \quad (1.108)$$

According to its dynamic characteristics, the DMG under discussion is qualitatively analogous to an OMG with two degrees of freedom in the plane of sensitivity. In the area of essential frequencies, its transfer function is described by the expression

$$W(\bar{p}) \approx K_{\xi} i\xi_{\Pi}\frac{i\frac{K_{\Pi}}{K_{\xi}}\bar{p} + 1}{\left(\frac{1}{\nu_{\Pi}}\bar{p} + i + \xi_{\Pi}\right)\left(\frac{1}{\nu_{H}}\bar{p} - i + \xi_{H}\right)}. \quad (1.109)$$

At the same time, the values of the frequencies of the nutational and precessional oscillations and the other parameters that are part of (1.109) differ substantially from the analogous values for the OMG, and when $\xi_B = \xi_C$, for most real instrument parameter values they are approximated by the following expressions:

$$\nu_{\Pi} \approx \xi^2 b^2\frac{\nu_C^2 + \nu_B^2 - (1 - \varkappa_Y)\frac{R_2}{I_{Z\Pi}} + 2\frac{R_1}{I_{Z\Pi}}}{(1 + \varkappa_Y)(1 + \varkappa_{Z\Pi})}; \quad (1.110)$$

$$\xi_{\Pi} \approx \frac{1}{\xi b}\left(\frac{4}{b}\frac{-1}{\nu_C^2 + \nu_B^2 - (1 - \varkappa_Y)\frac{R_2}{I_{Z\Pi}} + 2\frac{R_1}{I_{Z\Pi}}} + 1\right); \quad (1.111)$$

$$\nu_{H} \approx 2\frac{\nu_C^2 + \nu_B^2 - (1 - \varkappa_Y)\frac{R_2}{I_{Z\Pi}} + 2\frac{R_1}{I_{Z\Pi}}}{(1 + \varkappa_Y)(1 + \varkappa_{Z\Pi})} = \frac{2\nu_{\Pi}}{\xi^2 b^2}; \quad (1.112)$$

$$\xi_{\text{н}} \approx \xi \left(\frac{-2}{\nu_C^2 + \nu_B^2 - (1 - \varkappa_Y)\frac{R_2}{I_{Zn}} + 2\frac{R_1}{I_{Zn}}} + \frac{1}{2} b \right), \tag{1.113}$$

where b = some structural parameter determined from the expression

$$b = \frac{\begin{array}{c}[(1+\varkappa_Y)(1+\varkappa_{Zn})-4]\left(\nu_C^2+\nu_B^2+2\frac{R_1}{I_{Zn}}\right)+ \\ +\left[4\frac{R_2}{I_{Zn}}-(1+\varkappa_Y)(1+\varkappa_{Zn})\right](1-\varkappa_Y)-(1+\varkappa_Y)(1-\varkappa_{Zn}^2)\end{array}}{\left[\nu_C^2+\nu_B^2-(1-\varkappa_Y)\frac{R_2}{I_{Zn}}+2\frac{R_1}{I_{Zn}}\right]^2}, \tag{1.114}$$

$$K_n = (1+\varkappa_Y)(1+\varkappa_{Zn}). \tag{1.115}$$

In the case of reading the signal from the NR on carrier frequency $2\omega_0$, the denominator of the instrument's transfer function with respect to the base's angular velocity ω remains the same as when the signal is read on the zero frequency. The expression for the numerator takes on the form

$$\begin{array}{c}A(\tilde{p}) = \omega_0^3\left\{-\left(i\frac{R_1}{I_{Zn}}+\xi_C-\xi_B\right)\tilde{p}^2+\left[-\frac{R_1}{I_{Zn}}(2+\varkappa_Y+i2\xi_B)+\right.\right. \\ +i(\xi_C(2+\varkappa_Y)-\xi_B(2+\varkappa_{Zn}))-\frac{1}{2}(\nu_C^2-\nu_B^2)\Big]\tilde{p}- \\ -\frac{R_1}{I_{Zn}}[i(\nu_B^2-1-\varkappa_Y)+2\xi_B]+[\xi_C(1+\varkappa_Y)-\xi_B(1+\varkappa_{Zn})]+ \\ \left.+i\frac{1}{2}[\nu_C^2(1+\varkappa_Y)-\nu_B^2(1+\varkappa_{Zn})]\right\}.\end{array} \tag{1.116}$$

When operating in the dynamic tuning mode, the instrument's transfer factor with respect to the angular velocity is determined by the expression

$$K_{\xi} = \frac{1}{4}\frac{\begin{array}{c}\left(\nu_C^2+2\frac{R_1}{I_{Zn}}\right)(1+\varkappa_Y)-\nu_B^2\left(1+\varkappa_{Zn}+2\frac{R_1}{I_{Zn}}\right)- \\ -i2\left[\xi_C(1+\varkappa_Y)-\xi_B\left(1+\varkappa_{Zn}+2\frac{R_1}{I_{Zn}}\right)\right]\end{array}}{\xi_B\left(2\frac{R_1}{I_{Zn}}+\nu_C^2-1+\varkappa_{Zn}\right)+\xi_C\left(\nu_B^2-1+\varkappa_Y\right)}. \tag{1.117}$$

It is obvious that the larger K_{ξ} is, the greater the nonidentity between the DMG's parameters with respect to its suspension axes.

For reading in the nonrotating system of coordinates, the transfer factor of a DMG in which the NR has two degrees of freedom can be represented in the form of (1.58), where

$$\begin{array}{c}k_0 = \frac{1}{2}i\omega_0\{(1-e^{-i2\varphi_{12}})[(I_{Zн}-I_{Yн})C_B^{(1)}+I_{Zн}I_{Zв}(1-\varkappa_{Zн})\times \\ \times(1+\varkappa_{Zв})\omega_0^2]C_C^{(1)}+(1-\cos 2\varphi_{12})2I_{Xн}I_{Yн}(1-\varkappa_{Yн})\omega_0^2(C_C^{(1)}-C_B^{(1)})+ \\ +C_C^{(1)}C_B^{(1)}[I_{Zв}(1+\varkappa_{Zв})+I_{Zн}(1+\varkappa_{Zн})]+C_C^{(2)}[C_C^{(1)}I_{Yн}(1+\varkappa_{Zн})+ \\ +C_B^{(1)}I_{Zн}(1+\varkappa_{Yн})]-4I_{Xн}I_{Yн}\omega_0^2(1-\varkappa_{Yн})(2R_1\omega_0^2+C_C^{(2)})+ \\ +2C_C^{(1)}\omega_0^2[R_1I_{Yн}(1+\varkappa_{Yн})+R_3(R_1+R_2)]+ \\ +C_B^{(1)}\omega_0^2[2R_1I_{Zн}(1+\varkappa_{Zн})-R_3(I_{Yв}-I_{Zв})]\};\end{array} \tag{1.118}$$

$$B_0 = \Delta + i\omega_0 \left\{ \mu_C^{(1)} \left[R_3\omega_0^2 \frac{1}{2} \left(2R_1\omega_0^2 + C_C^{(2)} + C_B^{(1)}\right) + 2R_1\omega_0^2 C_B^{(1)} + \right.\right.$$
$$+ C_C^{(2)} C_B^{(1)} \Big] + \mu_B^{(1)} \left[\frac{1}{2} R_3\omega_0^2 \left(2R_1\omega_0^2 + C_C^{(2)} + C_C^{(1)}\right) + \right.$$
$$\left.\left. + 2R_1\omega_0^2 C_C^{(1)} + C_C^{(2)} C_C^{(1)} \right] + \mu_C^{(2)} \left(R_3\omega_0^2 C_1 + C_C^{(1)} C_B^{(1)}\right) \right\}, \tag{1.119}$$

while the value of Δ is determined by the left side of (1.65), and equals zero in the dynamic tuning mode. As is the case with other types of MRG's, in the case of resonance tuning and a low degree of damping, when there is a discontinuity in the angular velocity the transfer process will be extremely protracted. When operating in the initial section of the transfer process, with respect to the base's angular rotation the DMG can be regarded as an integrating gyroscope with integration factor

$$K_{\text{н}} = \frac{A_0}{B_1}, \tag{1.120}$$

where

$$B_1 = i\omega_0 \left\{ C_C^{(1)} C_B^{(1)} \left[(I_{Z\text{н}} - I_{Y\text{н}}) \cos 2\varphi_{12} + 2I_{Z\text{в}} + I_{Z\text{н}} + I_{Y\text{н}} \right] + \right.$$
$$+ C_C^{(2)} \left[I_{X\text{н}} R_3\omega_0^2 + 2C_C^{(1)} I_{Y\text{н}} + 2C_B^{(1)} I_{Z\text{н}} \right] +$$
$$+ C_C^{(1)}\omega_0^2 \left[2R_1 I_{Y\text{н}} (1 + \varkappa_Y) + R_3 (R_2 - R_1) + \frac{1}{2} I_{X\text{н}} R_3 (\cos 2\varphi_{12} - 1) \right] +$$
$$+ C_B^{(1)} \left[-\frac{1}{2} I_{X\text{н}} R_3\omega_0^2 (\cos 2\varphi_{12} - 1) - 2R_1 R_3\omega_0^2 + \right.$$
$$\left.\left. + \frac{1}{2} I_{Z\text{в}} (1 + \varkappa_{Z\text{в}}) R_3\omega_0^2 + 2I_{Z\text{н}} (1 + \varkappa_{Z\text{н}}) R_1\omega_0^2 \right] + 2I_{X\text{н}} R_3\omega_0^2 R_1\omega_0^2 \right\}.$$

If the VR's suspension has two degrees of freedom and the NR's suspension only one, the numerator and denominator of the instrument's transfer factor with respect to the base's angular velocity are determined by the following relationships, respectively:

$$A_0 = \left[C_B^{(1)} \frac{1}{2} \left\{ C_C^{(2)} \left[I_{Y\text{н}} (1 + \varkappa_{Y\text{н}}) + I_{Y\text{в}} (1 + \varkappa_{Y\text{в}}) + \right.\right.\right.$$
$$+ (I_{Z\text{н}} - I_{Y\text{н}}) (1 - e^{i2\varphi_{12}}) \Big] + C_B^{(2)} \left[I_{Z\text{н}} (1 + \varkappa_{Z\text{н}}) + I_{Z\text{в}} (1 + \varkappa_{Z\text{в}}) - \right.$$
$$\left.\left. - (I_{Z\text{н}} - I_{Y\text{н}}) (1 - e^{i2\varphi_{12}}) \right] + 2 (I_{X\text{в}} + I_{X\text{н}}) (R_3 + 4R_1)\omega_0^2 \right\} +$$
$$+ C_C^{(2)} C_B^{(2)} \frac{1}{2} I_{Y\text{н}} (1 + \varkappa_{Y\text{н}}) + \frac{1}{2} C_C^{(2)} \left\{ R_3\omega_0^2 \left[-I_{X\text{в}} + 2I_{Y\text{в}} (1 + \varkappa_{Y\text{в}}) + \right.\right.$$
$$+ I_{X\text{н}} (1 - \cos 2\varphi_{12}) - \frac{1}{2} I_{Y\text{в}} (1 + \varkappa_{Y\text{в}}) ((1 - e^{-i2\varphi_{12}}) \Big] + \tag{1.121}$$
$$\left.\left. + 2R_1\omega_0^2 I_{Y\text{н}} (1 + \varkappa_{Y\text{н}}) \right\} + \frac{1}{2} C_B^{(2)} \left\{ R_3\omega_0^2 \left[2I_{X\text{н}} + I_{Z\text{в}} (1 + \varkappa_{Z\text{в}}) - \right.\right.\right.$$
$$\left.\left. - I_{X\text{н}} (1 - \cos 2\varphi_{12}) - \frac{1}{2} I_{Z\text{в}} (1 + \varkappa_{Z\text{в}}) (1 - e^{-i2\varphi_{12}}) \right] + \right.$$
$$\left.\left. + 2R_1\omega_0^2 I_{Y\text{н}} (1 + \varkappa_{Y\text{н}}) \right\} + 2 (I_{X\text{в}} + I_{X\text{н}}) R_3\omega_0^2 R_1\omega_0^2 \right] i\omega_0;$$

$$B_0 = \Delta + i\omega_0 \Big\{ \mu_C^{(2)} \Big[R_1\omega_0^2 R_3\omega_0^2 + \frac{1}{2} R_3\omega_0^2 C_B^2 + \frac{1}{2} C_B^{(1)} (R_3 + 4R_1) + \\ + C_B^{(1)} C_B^{(2)} \Big] + \mu_B^{(2)} \Big[R_1\omega_0^2 R_3\omega_0^2 + \frac{1}{2} R_3\omega_0^2 C_C^{(2)} + \\ + \frac{1}{2} C_B^{(1)} (R_3 + 4R_1)\,\omega_0^2 + C_C^{(2)} C_B^{(1)} \Big] + \mu_B^{(1)} [C_2 (R_3 + 4R_1)\,\omega_0^2 + C_C^{(2)} C_B^{(2)}] \Big\}, \tag{1.122}$$

where Δ = the left side of expression (1.64).

The numerator of the integration factor of such a gyroscope coincides with expression (1.121), while the denominator has the form

$$B_1 \approx i\omega_0 \Big[C_B^{(1)} \{ (I_{X_B} + I_{X_H}) (R_3 + 4R_1)\,\omega_0^2 + C_C^{(2)} [2 (I_{Y_H} + I_{Y_B}) + \\ + (I_{Z_H} - I_{Y_H}) (1 - \cos 2\varphi_{12})] + C_B^{(2)} [2 (I_{Z_H} + I_{Z_B}) - \\ - (I_{Z_H} - I_{Y_H}) (1 - \cos 2\varphi_{12})] \} + C_C^{(2)} C_B^{(2)} 2I_{Y_H} + \\ + \frac{1}{2} C_C^{(2)} [R_3\omega_0^2 (-2R_1 + 2I_{Y_B} + I_{X_H} (1 - \cos 2\varphi_{12})) + \\ + 4R_1\omega_0^2 I_{Y_H} (1 + \varkappa_{Y_H})] + \frac{1}{2} C_B^{(2)} [R_3\omega_0^2 (-2R_1 + 2I_{Z_B} + \\ + 2I_{X_H} - I_{X_H} (1 - \cos 2\varphi_{12})) + 4R_1\omega_0^2 I_{Y_H} (1 + \varkappa_{Y_H})] + \\ + 2 (I_{X_B} + I_{X_H}) R_3\omega_0^2 R_1\omega_0^2 \Big]. \tag{1.123}$$

In the general case, when the suspension of each of the DMG's rings has two degrees of freedom, transfer factor K_g can be determined from the expression

$$A_0 = \Big[C_C^{(1)} C_B^{(1)} \Big\{ \frac{1}{2} C_C^{(2)} [I_{Y_H} (1 + \varkappa_{Y_H}) + I_{Y_B} (1 + \varkappa_{Y_B})] + \\ + \frac{1}{2} C_B^{(2)} [I_{Z_H} (1 + \varkappa_{Z_H}) + I_{Z_B} (1 + \varkappa_{Z_B})] + (I_{X_B} + I_{X_H}) (R_3 + 4R_1)\,\omega_0^2 \Big\} + \\ + 4C_1 (I_{X_B} + I_{X_H}) R_3\omega_0^2 R_1\omega_0^2 + C_C^{(1)} \Big\{ \frac{1}{2} C_C^{(2)} C_B^{(2)} I_{Y_H} (1 + \varkappa_{Y_H}) + \\ + C_C^{(2)} I_{Y_H} (1 + \varkappa_{Y_H}) R_1\omega_0^2 + C_B^{(2)}\omega_0^2 \Big[R_3 (I_{Z_B} - I_{X_H}) + \\ + 2R_1 \Big(2I_{X_H} - 2I_{Z_H} - \frac{1}{2} I_{Y_H} (1 + \varkappa_{Y_H}) \Big) \Big] \Big\} + \\ + C_B^{(1)} \Big\{ \frac{1}{2} C_C^{(2)} C_B^{(2)} I_{Z_H} (1 + \varkappa_{Z_H}) + C_C^{(2)}\omega_0^2 \Big[R_3 (I_{X_H} + I_{Y_H}) + \\ + 2R_1 \Big(2I_{X_H} - 2I_{Y_H} - \frac{1}{2} I_{Z_H} (1 + \varkappa_{Z_H}) \Big) \Big] + C_B^{(2)} I_{Z_H} (1 + \varkappa_{Z_H}) R_1\omega_0^2 \Big\} + \\ + I_{X_H} R_3\omega_0^2 (4R_1\omega_0^2 C_2 + C_C^{(2)} C_B^{(2)}) \Big] i\omega_0; \tag{1.124}$$

$$B_0 = \Delta + i\omega_0 \{ \mu_1 R_3\omega_0^2 (C_2 4R_1\omega_0^2 + C_C^{(2)} C_B^{(2)}) + \\ + \mu_C^{(1)} C_B^{(1)} [C_2 (R_3 + 4R_1)\,\omega_0^2 + C_C^{(2)} C_B^{(2)}] + \\ + \mu_B^{(1)} C_C^{(1)} [C_2 (R_3 + 4R_1)\,\omega_0^2 + C_C^{(2)} C_B^{(2)}] + \\ + \mu_2\omega_0^2 [C_1 4R_1 R_3\omega_0^2 + C_C^{(1)} C_B^{(1)} (R_3 + 4R_1)] + \\ + (\mu_C^{(2)} C_B^{(2)} + \mu_B^{(2)} C_C^{(2)}) (C_1 R_3\omega_0^2 + C_C^{(1)} C_B^{(1)}) \}, \tag{1.125}$$

where, for the sake of simplification, $\phi_{12} = 0$, while Δ = the left side of dynamic tuning condition (1.63).

If condition (1.63) is fulfilled in the instrument, its important characteristic is the integration factor, the numerator of which is A_0, while the denominator is B_1. For the DMG layout under discussion, the expression for B_1 has the following form when $\phi_{12} = 0$:

$$\begin{aligned}B_1 = {} & C_C^{(1)}C_B^{(1)}\{(I_{X_н}+I_{X_в})(R_3+4R_1)\omega_0^2+2C_C^{(2)}(I_{Y_н}+I_{Y_в})+\\ & +2C_B^{(2)}(I_{Z_н}+I_{Z_в})\}+C_C^{(1)}\{C_C^{(2)}C_B^{(2)}2I_{Y_н}+(I_{Y_в}R_3+I_{Y_н}4R_1)\omega_0^2C_C^{(2)}+\\ & +\{(I_{X_н}+I_{Z_в})R_3+I_{Y_н}4R_1\}\omega_0^2C_B^{(2)}+2(I_{X_в}+I_{X_н})R_3\omega_0^2R_1\omega_0^2\}+\\ & +C_B^{(1)}\{C_C^{(2)}C_B^{(2)}2I_{Z_н}+C_C^{(2)}\{(I_{X_н}+I_{Y_в})R_3+I_{Z_н}4R_1\}\omega_0^2+\\ & +C_B^{(2)}(I_{Z_в}R_3+I_{Z_н}4R_1)\omega_0^2+2(I_{X_в}+I_{X_н})R_3\omega_0^2R_1\omega_0^2\}+\\ & +I_{X_н}R_3\omega_0^2(4R_1\omega_0^2C_2+C_C^{(2)}C_B^{(2)}).\end{aligned} \tag{1.126}$$

In conclusion, let us examine the layout of a TMG [three-rotor modulation gyroscope] with the outer rotor on the zero frequency, for which the suspension of each rotor has only one degree of freedom on the zero frequency. We will limit ourselves to the case where the suspension of the second stage's inner and intermediate rotors is orthogonal. Assuming the absence of a first-stage VR in the generalized model, so that $C_B^{(1)} \to \infty$, we obtain the following expressions for the numerator and denominator of the instrument's transfer factor K_g with respect to angular velocity:

$$\begin{aligned}A_0 = {} & \Big|C_C^{(1)}\Big\{\frac{1}{2}C_C^{(2)}[I_{Y_н}^{(1)}(1+\varkappa_{Y_н}^{(1)})+I_{Y_н}^{(2)}(1+\varkappa_{Y_н}^{(2)})]+\\ & +\frac{1}{2}C_B^{(2)}[I_{Z_н}^{(1)}(1+\varkappa_{Z_н}^{(1)})+I_{Z_н}^{(2)}(1+\varkappa_{Z_н}^{(2)})]+\\ & +(I_{X_н}^{(1)}+I_{X_н}^{(2)})(R_3^{(1)}+R_3^{(2)})\omega_0^2+[4(I_{Y_н}^{(1)}+I_{Y_н}^{(2)})-I_{X_н}^{(1)}+2R_3^{(1)}+\\ & +R_3^{(2)}-R_2^{(2)}+2(I_{C_н}^{(2)}-I_{C_н}^{(1)})]R_2^{(1)}\omega_0^2+R_2^{(1)}(R_3^{(2)}\omega_0^2+C_B^{(2)})\Big\}+\\ & +\frac{1}{2}C_C^{(2)}C_B^{(2)}I_{Z_н}^{(1)}(1+\varkappa_{Z_н}^{(1)})+C_C^{(2)}\Big[R_3^{(1)}(I_{X_н}^{(1)}+I_{Y_н}^{(1)})+\\ & +\frac{1}{2}R_3^{(2)}\Big(2I_{X_н}^{(1)}-2I_{Y_н}^{(1)}-\frac{1}{2}I_{Z_н}^{(1)}(1+\varkappa_{Z_н}^{(1)})\Big)\Big]\omega_0^2+\\ & +C_B^{(2)}\Big[\frac{1}{4}R_3^{(2)}I_{Z_н}^{(1)}(1+\varkappa_{Z_н}^{(1)})+R_1^{(2)}(4I_{Z_н}^{(1)}+R_3^{(1)})\Big]\omega_0^2+\\ & +\frac{1}{2}R_3^{(1)}\omega_0^2R_3^{(2)}\omega_0^2(I_{X_н}^{(1)}+I_{X_н}^{(2)})+R_1^{(2)}\omega_0^2R_3^{(2)}\omega_0^2\Big(2I_{Z_н}^{(1)}-\frac{1}{2}I_{X_н}^{(1)}+\\ & +R_3^{(1)}-I_{C_н}^{(1)}\Big)+R_1^{(2)}\omega_0^2R_3^{(1)}\omega_0^2\Big(2I_{Y_н}^{(2)}+\frac{1}{2}R_3^{(2)}\Big)\Big]i\omega_0;\end{aligned} \tag{1.127}$$

$$\begin{aligned}B_0 = {} & \Delta+i\omega_0\Big\{\mu_C^{(1)}[C_2(R_3^{(1)}+R_3^{(2)})\omega_0^2+C_C^{(2)}C_B^{(2)}+\\ & +R_1^{(2)}\omega_0^2(R_3^{(1)}+R_3^{(2)})\omega_0^2+R_1^{(2)}\omega_0^2\cdot 2C_B^{(2)}]+\mu_2\omega_0^2\Big[\frac{1}{2}R_3^{(1)}R_3^{(2)}\omega_0^2+\\ & +C_C^{(1)}(R_3^{(1)}+R_3^{(2)})\Big]+\mu_C^{(2)}C_B^{(2)}\Big(\frac{1}{2}R_3^{(1)}\omega_0^2+C_C^{(1)}\Big)+\\ & +\mu_B^{(2)}\Big[C_C^{(2)}\Big(\frac{1}{2}R_3^{(1)}\omega_0^2+C_C^{(1)}\Big)+R_1^{(2)}\omega_0^2(R_3^{(1)}\omega_0^2+2C_C^{(1)})\Big]\Big\}.\end{aligned} \tag{1.128}$$

The TMG's dynamic tuning condition $\Delta = 0$ is derived from (1.62), with the appropriate renotation. Let us spend some time on one special case of the fulfillment of

the dynamic tuning conditions. The expression for A can be presented in the form

$$\Delta = R_3^{(1)}\omega_0^2\left\{\frac{1}{2}\left[4R_1^{(2)}\omega_0^2 + 2C_C^{(2)}\left(\frac{1}{2}R_3^{(2)}\omega_0^2 + C_B^{(2)}\right) + \frac{1}{2}R_3^{(2)}\omega_0^2 C_B^{(2)}\right] + \right.$$
$$\left. + \left[\left(\frac{1}{4}R_3^{(2)}\omega_0^2 + C_C^{(1)}\right)C_B^{(2)} + \left(2R_1^{(2)}\omega_0^2 + C_C^{(2)}\right)C_C^{(1)}\right]\right\} + \quad (1.129)$$
$$+ C_C^{(1)}\left[\left(4R_1^{(2)}\omega_0^2 + 2C_C^{(2)}\right)\left(\frac{1}{2}R_3^{(2)}\omega_0^2 + C_B^{(2)}\right) + \frac{1}{2}R_3^{(2)}\omega_0^2 C_B^{(2)}\right].$$

It is obvious that the dynamic tuning condition is fulfilled for the following relationships among the instrument's parameters:

$$\left.\begin{aligned}\frac{1}{2}R_3^{(1)}\omega_0^2 + C_C^{(1)} = 0;\\ \left(\frac{1}{4}R_3^{(2)}\omega_0^2 + C_C^{(1)}\right)C_B^{(2)} + \left(2R_1^{(2)}\omega_0^2 + C_C^{(2)}\right)C_C^{(1)} = 0.\end{aligned}\right\} \quad (1.130)$$

Expressions (1.30) make it possible to select the TMG's parameters quite easily. For example, if the rigidity of the third (counting from the base) rotor's suspension from the second and the second's from the first equal each other ($C_C^{(1)} = C_B^{(2)}$), the rotor's resonance frequency of rotation depends on the suspension's rigidities and the intermediate rotors' moments of inertia:

$$\omega_0^2 = -\frac{C_C^{(1)} + C_C^{(2)}}{\frac{1}{4}R_3^{(2)} + 2R_1^{(2)}}. \quad (1.131)$$

The ratio of the rigidities of the first and subsequent rotors' suspensions is determined by the relationship of their moments of inertia:

$$\frac{C_C^{(2)}}{C_C^{(1)}} = \frac{\frac{1}{2}R_3^{(2)} + 4R_1^{(2)}}{R_3^{(1)}} - 1. \quad (1.132)$$

If all the suspension rigidities equal each other, then in addition to the fulfillment of condition (1.131) it is required that the rotors' moments of inertia satisfy the equality

$$\frac{1}{2}R_3^{(2)} - 4R_1^{(2)} - 2R_3^{(1)} = 0. \quad (1.133)$$

The denominator of the integration factor of the TMG layout under discussion is determined by the expression

$$B_1 \approx C_C^{(1)}\left\{\left(I_{X_H}^{(1)} + I_{X_H}^{(2)}\right)\left(R_{(3)}^{(1)} + R_3^{(2)}\right)\omega_0^2 + 4R_1^{(2)}\left(I_{Y_H}^{(1)} + I_{Y_H}^{(2)}\right)\omega_0^2 + \right.$$
$$+ 2C_C^{(2)}\left(I_{Y_H}^{(1)} + I_{Y_H}^{(2)}\right) + 2C_B^{(2)}\left(I_{Z_H}^{(1)} + I_{Z_H}^{(2)}\right)\Big\} + C_C^{(2)}C_B^{(2)}2I_{Z_H}^{(1)} +$$
$$+ C_C^{(2)}\left[\left(I_{X_H}^{(1)} + I_{Y_H}^{(2)}\right)R_3^{(1)} + I_{Z_H}^{(1)}R_3^{(2)}\right]\omega_0^2 + C_B^{(2)}\left[I_{Z_H}^{(2)}R_3^{(1)} + I_{Z_H}^{(1)}R_3^{(2)} + \right. \quad (1.134)$$
$$\left. + 4R_1^{(2)}I_{Z_H}^{(1)}\right]\omega_0^2 + \frac{1}{2}\left(I_{X_H}^{(1)} + I_{X_H}^{(2)}\right)R_3^{(1)}\omega_0^2 R_3^{(2)}\omega_0^2 + I_{Z_H}^{(1)}2R_1^{(2)}\omega_0^2 R_3^{(2)}\omega_0^2 +$$
$$+ I_{Y_H}^{(2)}2R_1^{(2)}\omega_0^2 R_3^{(1)}\omega_0^2.$$

Analogous expressions for other TMG layouts can be derived quite simply from the generalized RVG model. The expressions for the transfer factor K_q and integration factor K_i, as well as for the frequency of the nutational (ν_H) and precessional (ν_π) oscillations are the original ones for the synthesis of the basic parameters of such instruments.

CHAPTER 2. DEFECTS IN ROTOR VIBRATION GYROSCOPES

2.1. Reaction of Rotor Vibration Gyroscopes to Harmonic Vibrations of the Base at a Frequency Equal to the Doubled Frequency of Rotation of a Rotor

Accuracy of measurement and threshold of sensitivity of gyroscopic instruments are extremely important characteristics, on which the possibility of using them to solve certain navigational problems basically depends. The accuracy of an RVG depends on the errors engendered in the mechanical part and the errors in the information reading and processing system. The sensitivity threshold is determined by the zero noise level at the instrument's output; that is, by the signal that is available at the output and is completely identical to the useful signal in the absence of a measured angular velocity of the base, as well as the possibility of distinguishing the useful signal against the background of this noise. Errors in the sensor of the angular rotation of an RVG's sensitive element and the information processing system are the subject of research in special branches of technology, so in this chapter we will limit ourselves to a discussion of the errors that arise only in the mechanical part of an instrument, assuming that its information reading and processing system is functioning ideally.

RVG errors can be methodological, operational, or technological. The first type is related to special features of their operation on an arbitrarily moving base that is subjected to angular and linear vibrations and overloads; the second, to a change during the operating process of the values of their basic parameters; the third, to the effect on an instrument's sensitive elements of disturbing moments caused by inaccuracy during production and tuning. In general form, let us discuss several of these errors--those typical of most RVG setups--using an RVG with single modulation as an example.

From the generalized mathematical model of an RVG with single modulation and a rotating suspension (1.20), it follows that angular vibrations of the base on a frequency equal to the doubled frequency of rotation of the PD's shaft lead to angular deflections of the sensitive elements, which means the appearance at the instrument's output of a signal that is identical to the signal caused by some constant angular velocity $\bar{\omega}_e$ of the base.

Let us discuss how to determine the value of $\bar{\omega}_e$ for different layouts of MRG's with VP. We will assume that the instrument's base is performing angular oscillations in its sensitivity plane, the velocity vector of which is determined by the expression

$$\bar{\omega} = \omega_A e^{-i2\omega_A t}. \qquad (2.1)$$

From (1.56) it follows that when the signal is read on the zero frequency of the nonrotating system of coordinates, the angle of rotation of NR1 relative to the base is determined by the expression

$$\tilde{\lambda}_1^{\text{н}} = \tilde{\chi}_1 = \frac{\tilde{W}_{\Sigma}^{+}(p+i2\omega_0)\,W_{12}(p) + W_{\Sigma}^{+*}(p+i2\omega_0)\,W_{14}(p)}{W(p)}\,\tilde{\omega}_A^{\bullet}. \tag{2.2}$$

The constant angular velocity of the base in the instrument's plane of sensitivity, which can be found from (1.56), also leads to rotation of NR1 at some angle $\lambda_1^{\text{п}}$, so that angular vibrations of the instrument's base at frequency $2\omega_0$ will lead to the appearance at its output of a signal that is identical (equivalent) to the signal from the base's constant angular velocity $\bar{\omega}_e$:

$$\bar{\omega}_e = \frac{\tilde{W}_{\Sigma}^{+}(p+i2\omega_0)\,W_{12}(p) + W_{\Sigma}^{+*}(p+i2\omega_0)\,W_{14}(p)}{W(p) - [W_{\Sigma}^{+}(p)\,W_{12}(p) + \tilde{W}_{\Sigma}^{+*}(p)\,W_{14}(p)]\,p}\,p\tilde{\omega}_A^{\bullet} \quad \text{for } p \to 0. \tag{2.3}$$

We will assume that the amplitude of the vibrations is constant and ignore damping with respect to the suspension axes. For an OMG, the equivalent angular velocity then equals

$$\tilde{\omega}_e = \frac{1}{2}\,\frac{(1-\varkappa_Y)\,\nu_C^2 - (1-\varkappa_Z)\,\nu_B^2}{4\,\frac{I_x}{I_Y}(1-\varkappa_Z) - (1+\varkappa_Z)\,\nu_B^2 - (1+\varkappa_Y)\,\nu_C^2}\,\tilde{\omega}_A^{\bullet}. \tag{2.4}$$

If the rotor has a uniformly rigid suspension ($C_C = C_B$), the equivalent angular velocity equals zero; that is, with a level of accuracy up to that of the assumptions that have been made the instrument has no error related to angular vibrations of the base on frequency $2\omega_0$. For an OMG with a single degree of freedom of the rotor's suspension from the PD's shaft, the dependence on the amplitude of the rate of vibration acquires the form

$$\tilde{\omega}_e = \pm\frac{1}{2}\,\frac{1-\varkappa}{1+\varkappa}\,\tilde{\omega}_A^{\bullet}. \tag{2.5}$$

In this case, a reduction in instrument error can be achieved only be reducing the value of $1 - \varkappa$ by the appropriate choice of the rotor's geometric configuration that also results in a reduction in the rigidity C of the torsion bars.

For a DMG having two degrees of freedom in the sensitivity plane, the equivalent angular velocity for base vibrations at frequency $2\omega_0$ is determined by the expression

$$\bar{\omega}_e = \frac{(1-\varkappa_{Zn})\,\nu_B^2 + (1-\varkappa_Y)\left(2\frac{R_1}{I_{Zn}} - \nu_C^2 e^{-i2\varphi_{12}}\right) - 2\,\frac{R_1}{I_{YH}}\,\nu_B^2}{2(\nu_C^2+\nu_B^2) - \nu_B^2\nu_C^2 - 4(1-2\varkappa_Y)\,\frac{R_1}{I_{Zn}} - 4(1-\varkappa_{Zn})\,\frac{R_2-R_1}{I_{YH}}}\,\tilde{\omega}_A^{\bullet}. \tag{2.6}$$

The smaller the values of $1 - \varkappa_Z$, $1 - \varkappa_Y$ and R_1, which are determined by the geometrical dimensions of the NR and VR, the smaller the error in a DMG. Instrument error also depends on the angle ϕ_{12} between the NR's and VR's suspension axes in the rotors' plane of rotation.

Let us examine the possibility of achieving a substantial reduction in this error by choosing the DMG's structural parameters appropriately. In order to do this it is necessary to have such relationships between the instrument's parameters that the numerator of expression (2.6) changes to zero, while the denominator is represented by some finite number. Such physically real conditions can be obtained only for the

cases $\phi_{12} = 0$ and $\phi_{12} = \pi/2$, the first of which corresponds to an orthogonal positioning of the axes, as was shown in Figure 12, while the second corresponds to a coaxial positioning of the torsion bars connecting the PD with the VR and the VR with the NR. Analysis shows that for a DMG of the Khaui type, with identical rigidities of the inner and outer suspensions' torsion bars ($\Delta C = 0$), the requirement that the numerator of expression (2.6) change to zero is incompatible with resonance tuning condition (1.66). Therefore, for instruments of this type operating in the dynamic tuning mode, the error caused by angular vibrations of the base at frequency $2\omega_0$ cannot, in principle, be eliminated by the proper selection of their parameters.

In the case of a coaxial positioning of the torsion bars' axes and resonance tuning, the numerator of expression (2.6) becomes zero when the following relationships of the instrument's parameters are observed:

$$\nu_C^2 = 0, \quad \nu_B^2 = \frac{2R_1(1-\varkappa_Y)}{2R_1 - I_{Zn}(1-\varkappa_Y)}; \tag{2.7}$$

$$\nu_C^2 = -2\frac{R_1}{I_{Zn}}, \quad \nu_B^2 = 0. \tag{2.8}$$

From (2.7) and (2.8) it follows that the degree of rigidity with respect to one of the suspension axes must be zero. This means that on one of the DMG's suspension axes it is necessary to install supports that do not impose any elastic moments on the rotors. However, all known types of mechanical supports that have a sufficiently high load-bearing capacity also have "dry" friction, and are practically unsuitable for a precision gyroscope of the RVG type.

When the suspension axes are arranged orthogonally, the conditions of equality to zero of the numerator of expression (2.6) for an instrument operating in the dynamic tuning mode have the following form in the presence of angular vibrations of the base (2.5):

$$\nu_C^2 = 0, \quad \nu_B^2 = \frac{2R_1(1-\varkappa_Y)}{2R_1 - I_{Zn}(1-\varkappa_Y)} \tag{2.9}$$

or

$$\nu_C^2 = 2\left(1 - \varkappa_{Zn} - \frac{R_1}{I_{Zn}}\right), \quad \nu_B^2 = 2(1-\varkappa_Y). \tag{2.10}$$

Conditions (2.9) coincide with conditions (2.7) and, as was stated above, are of no practical interest. Conditions (2.10) can be easily realized in practice. In connection with this, however, the denominator of expression (2.6) also becomes zero. In order to evaluate the indeterminacy that is being obtained, we should allow for damping with respect to the gyroscope's suspension axes. The instrument's transfer factor with respect to the base's angular velocity then takes on the form

$$K_{\vartheta} = \frac{\xi_B\left(1 + \varkappa_{Zn} + 2\frac{R_1}{I_{Zn}}\right) + \xi_C(1+\varkappa_Y)}{\xi_B(1-\varkappa_{Zn}) + \xi_C(1-\varkappa_Y)} \frac{i}{2\omega_0}, \tag{2.11}$$

while the equivalent angular velocity is determined by the expression

$$\tilde{\omega} = \frac{1}{2}\frac{-\xi_C(1-\varkappa_Y) + \xi_B\left(1 - \varkappa_{Zn} - 4\frac{R_1}{I_{Zn}}\right)}{\xi_C(1+\varkappa_Y) + \xi_B\left(1 + \varkappa_{Zn} + 2\frac{R_1}{I_{Zn}}\right)}\tilde{\omega}_A^*. \tag{2.12}$$

Thus, according to condition (2.10), during dynamic tuning an instrument does not acquire the characteristics that are typical of the resonance mode, primarily independence of K_g on the angular velocity of rotation ω_0 and an inversely proportional dependence of K_g on the coefficients of viscous friction along the suspension axes. Therefore, we will call this mode "pseudoresonance."

An analogous mode occurs for an OMG when conditions (1.90) are fulfilled and for a DMG with coaxial positioning of the torsion bars when conditions (2.8) are fulfilled. In the pseudoresonance mode an instrument's transfer factor can be increased noticeably by selecting the rotor's parameters appropriately so that $\varkappa_Y \to 1$ and $\varkappa_{Z\pi} \to 1$. However, it is necessary to reduce the suspension's rigidities in this case, which can have a negative effect on the instrument's strength properties.

It is also possible to reduce DMG errors caused by angular vibrations of the base when operating in the pseudoresonance mode by choosing the damping value and the rotor geometry properly. In connection with this, it is necessary to keep in mind the fact that the creation and preservation of a certain relationship between the extremely small coefficients of viscous friction along the suspension axes is hardly possible at the present time.

Let us discuss a DMG in which the NR's suspension from the VR or the VR's from the PD's shaft has two degrees of freedom. In the first case, the numerator of the operator in expression (2.3) takes on the following form for $p \to 0$:

$$-R_3\omega_0^2\left(C_C^{(1)}C_B^{(1)} + 2e^{-i2\varphi_{12}}\Delta C_1 C_C^{(2)}\right) - 4R_1\omega_0^2\left(R_3\omega_0^2 C_1 + C_B^{(1)}C_C^{(1)}\right), \tag{2.13}$$

while the denominator is determined by expression (1.118). If the NR's suspension from the VR is uniformly rigid ($\Delta C_1 = 0$), expression (2.13) becomes equal to zero for the following values of the first stage's suspension's rigidity:

$$C_1 = 0 \quad \text{и} \quad C_1 = -4\frac{R_3R_1}{R_3+4R_1}\omega_0^2. \tag{2.14}$$

Substituting (2.14) into the expression for dynamic tuning (1.65), we obtain the corresponding values for the rigidity of the VR's suspension from the PD:

$$C_C^{(2)} = -2R_1\omega_0^2 \quad \text{and} \quad C_C^{(2)} = 0. \tag{2.15}$$

From (2.14) and (2.15) it follows that when the NR's suspension from the VR is uniformly rigid, a substantial decrease in the error caused by angular vibrations of the base at frequency $2\omega_0$ can be achieved only by realizing a nonelastic suspension of the VR from the PD's shaft. When a nonelastic suspension of the NR from the VR is realized ($C_1 = 0$), the instrument will operate in a pseudoresonance mode.

In the case of inequality of rigidities $C_C^{(1)}$ and $C_B^{(1)}$, expressions (2.13) can become zero only when $\phi_{12} = 0$ and $\phi_{12} = \pi/2$.

In order to reduce the instrument's sensitivity to constant angular vibrations of the base at frequency $2\omega_0$, it is necessary that its parameters be linked by the relationship

$$C_B^{(2)} = -\frac{4R_1R_3\omega_0^2C_1 + (R_3+4R_1)C_CC_B}{2R_3\Delta C_1}, \tag{2.16}$$

where the indices related to the rigidities of the NR's suspension are omitted.

Substituting the value of $C_B^{(2)}$ from (2.16) into (1.65), we obtain two conditions, the fulfillment of each of which can insure a reduction in the instrument of the error being investigated the the instrument is functioning in the dynamic tuning mode:

$$C_B = -\frac{2R_1R_3\omega_0^2}{2R_1R_3\omega_0^2 + (R_3 + 4R_1)C_C} C_C; \tag{2.17}$$

$$C_C = -R_3\omega_0^2. \tag{2.18}$$

Let us determine the requirements for the rigidity of the VR's suspension. For the simultaneous fulfillment of equalities (2.16) and (2.17), it is necessary that $C_V^{(2)}$ equal zero. When relationship (2.18) is realized, the rigidity of the VR's suspension is determined by the expression

$$C_B^{(2)} = -\frac{C_B(R_3 + 2R_1) + 2R_1R_3\omega_0^2}{C_B + R_3\omega_0^2}\omega_0^2. \tag{2.19}$$

The simultaneous fulfillment of conditions (2.17) and $C_B^{(2)} = 0$ or (2.18) and (2.19) is necessary and sufficient for a substantial reduction of the error under discussion in the instrument. However, realization of a nonelastic VR suspension is required in the first case.

For a DMG in which the VR's suspension from the PD's shaft has two degrees of freedom ($C_C^{(1)} \to \infty$), the condition of low sensitivity to angular oscillations of the base at frequency $2\omega_0$ with a constant amplitude has the form

$$-R_3\omega_0^2\left(\Delta C_2 C_B^{(1)} + \frac{1}{2}e^{-i2\varphi_{12}}C_C^{(2)}C_B^{(2)}\right) - \\ - 4R_1\omega_0^2\Delta C_2\left(\frac{1}{2}R_3\omega_0^2 + C_B^{(1)}\right) = 0. \tag{2.20}$$

It is obvious that this condition is fulfillable only when the VR's suspension is not uniformly rigid and $\varphi_{12} = 0$ or $\varphi_{12} = \pi/2$. (We will not discuss the trivial case where the rigidity along one of the axes of the VR's suspension is zero.) From (2.20) let us determine the required relationship between the rigidities of the NR's and VR's suspensions:

$$C_B^{(1)} = -\frac{C_C C_B + 2R_1\omega_0^2(C_C - C_B)}{\left(1 + 4\frac{R_1}{R_3}\right)(C_C - C_B)}, \tag{2.21}$$

where the indices related to the rigidities of the VR's suspension are omitted.

Substituting expression (2.21) into the instrument's dynamic tuning condition, we obtain the relationship between the rigidities along the axes of the VR's suspension from the PD's shaft:

$$C_C = -\frac{(R_3 + 2R_1)\omega_0^2}{2R_1\omega_0^2 + C_B} C_B. \tag{2.22}$$

Using this relationship and expression (2.21), we find the relationship between the NR's suspension's rigidity and C_B:

$$C_B^{(1)} = -\frac{2R_1\omega_0^2 + C_B}{(R_3 + 4R_1)\omega_0^2 + C_B} R_3\omega_0^2. \tag{2.23}$$

Thus, when relationships (2.22) and (2.23) are realized in the resonance mode, the instrument error caused by angular vibrations of the base at frequency $2\omega_0$ will be extremely small. These conditions are not closed relative to the rigidity values. For certain relationships of the rings' moments of inertia, the rigidity along one of the suspension axes can be assigned arbitrarily on the basis of some additional considerations, although in this case conditions of realizability consisting of the simultaneous fulfillment of inequalities $C_B > 0$, $C_B^{(2)} > 0$ and $C_C > 0$ must be provided.

For a DMG in which the VR's and NR's suspensions have two degrees of freedom in the plane of rotation, the necessary condition for the equality to zero of the error caused by angular oscillations of the base at frequency $2\omega_0$, given the absence of moments of viscous friction, is written in the following form:

$$R_3\left(\Delta C_2 C_C^{(1)} C_B^{(1)} + e^{-i2\varphi_{12}}\Delta C_1 C_C^{(2)} C_B^{(2)}\right) + \\ + 4R_1\Delta C_2\left(R_3\omega_0^2 C_1 + C_B^{(1)} C_C^{(1)}\right) = 0. \tag{2.24}$$

The simplest way to fulfill this condition is the creation of elastic VR and NR suspensions that are uniformly rigid along both axes ($C_1 = C_2 = 0$). Dynamic tuning condition (1.63) then takes on the form

$$C_2 = -\frac{4R_1\omega_0^2 C_1 + R_3\omega_0^2(4R_1\omega_0^2 + C_1)}{R_3\omega_0^2 + C_1}. \tag{2.25}$$

If only the NR's suspension is uniformly rigid ($\Delta C_1 = 0$), a second condition for the fulfillment of equality (2.24) will be the absence of an elastic coupling along one of the VR's suspension axes. In the general case, when the NR and VR have a non-uniformly rigid suspension, the joint fulfillment of conditions (1.63) and (2.24) insures the absence in the instrument of errors caused by angular vibrations of the base during operation in the resonance tuning mode. This requirement, however, does not define an unambiguous relationship among the instrument's basic structural parameters, which can change within extremely broad limits.

In conclusion, let us examine a TMG in which the suspension of each succeeding rotor from the preceding one has only one degree of freedom ($R_1^{(2)} = 0$, $C_C^{(2)} \to \infty$). The condition of low sensitivity of such an instrument to angular oscillations of the base at frequency $2\omega_0$ will be written as

$$e^{-i2\varphi_{12}} 2C_B^{(2)}\left[R_1^{(1)}\left(R_3^{(1)}\omega_0^2 + 2C_B^{(1)}\right) - R_3^{(1)}\Delta C_1\right] - \\ - R_1^{(1)}\left(R_3^{(1)}\omega_0^2 + 2C_B^{(2)}\right)\left(R_3^{(2)}\omega_0^2 + 2C_C^{(1)}\right) - \\ - \left(R_3^{(1)} + R_3^{(2)}\right) C_C^{(1)} C_B^{(1)} - C_1 R_3^{(1)} R_3^{(2)}\omega_0^2 = 0. \tag{2.26}$$

Let us dwell on only two cases of the relative positioning of the axes of the suspensions of the first (counting from the PD's shaft) and second rotors: $\varphi_{12} = 0$ and $\varphi_{12} = \pi/2$. In the first case, on the basis of condition (2.26) the following relationship must be observed between the rigidity of the first rotor's suspension and the rigidities of the subsequent rotors' suspensions:

$$C_B^{(2)} = \frac{1}{2}\,\frac{R_1^{(1)}\left(R_3^{(1)}\omega_0^2 + 2C_B^{(1)}\right)\left(R_3^{(2)}\omega_0^2 + 2C_C^{(1)}\right) + \\ + \left(R_3^{(1)} + R_3^{(2)}\right) C_C^{(1)} C_B^{(1)} + C_1 R_3^{(1)} R_3^{(2)}\omega_0^2}{R_1^{(1)}\left(R_3^{(1)}\omega_0^2 + 2C_B^{(1)}\right) - R_3^{(1)}\Delta C_1}. \tag{2.27}$$

Substituting (2.27) into dynamic tuning condition (1.62), we obtain an expression that determines the required relationship between the rigidities of the second and

third rings' suspensions:

$$\begin{aligned}&\{2R_1^{(1)}[(R_3^{(2)}\omega_0^2+C_C^{(1)})(2(R_3^{(1)}+2R_1^{(1)})\omega_0^2+C_C^{(1)})+\\&+C_C^{(1)}(4R_1^{(1)}+2R_3^{(1)}+R_3^{(2)})\omega_0^2]+(R_3^{(1)}\omega_0^2+C_C^{(1)})[R_3^{(1)}R_3^{(2)}\omega_0^2+\\&+2C_C^{(1)}(R_3^{(1)}+R_3^{(2)})]\}C_B^{(1)2}+R_3^{(1)}\omega_0^2\{R_1^{(1)}[2(R_3^{(2)}\omega_0^2+C_C^{(1)})\times\\&\times((4R_1^{(1)}+R_3^{(1)})\omega_0^2+2C_C^{(1)})+C_C^{(1)}(2(R_3^{(1)}+4R_1^{(1)})\omega_0^2+\\&+R_3^{(2)}\omega_0^2-2C_C^{(1)})]+R_3^{(2)}(R_3^{(1)}\omega_0^2+C_C^{(1)})C_C^{(1)}\}C_B^{(1)}+\\&+R_1^{(1)}(R_3^{(1)}\omega_0^2)^2[2R_1^{(1)}R_3^{(2)}\omega_0^2+C_C^{(1)}(R_3^{(2)}+4R_1^{(1)})]\omega_0^2=0.\end{aligned}\tag{2.28}$$

The observance between the TMG's parameters of the relationships satisfying conditions (2.27) and (2.28) makes it possible, during operation in the resonance tuning mode, to practically eliminate the error caused by angular vibfation of the base. The analogous conditions for the case where $\phi_{12} = \pi/2$ have the form

$$C_B^{(2)}=-\frac{1}{2}\frac{R_1^{(1)}(R_3^{(1)}\omega_0^2+2C_B^{(1)})(R_3^{(2)}\omega_0^2+2C_C^{(1)})+(R_3^{(1)}+R_3^{(2)})C_C^{(1)}C_B^{(1)}+C_1R_3^{(1)}R_3^{(2)}\omega_0^2}{R_1^{(1)}(R_3^{(1)}\omega_0^2+2C_B^{(1)})-R_3^{(1)}\Delta C_1};\tag{2.29}$$

$$\begin{aligned}&\left\{2R_1^{(1)}(R_3^{(2)}\omega_0^2+2C_C^{(1)})+\left[\frac{1}{2}R_3^{(2)}R_3^{(1)}\omega_0^2+(R_3^{(1)}+R_3^{(2)})C_C^{(1)}\right]C_C^{(1)}\right\}C_B^{(2)2}+\\&+R_3^{(1)}\omega_0^2\left\{3R_1^{(1)}(R_3^{(2)}\omega_0^2+2C_C^{(1)})+\frac{1}{2}R_3^{(1)}R_3^{(2)}\omega_0^2+\right.\\&\left.+\left(R_3^{(1)}+\frac{3}{2}R_3^{(2)}\right)C_C^{(1)}\right\}C_B^{(1)}+(R_3^{(1)}\omega_0^2)^2\left[R_3^{(2)}R_1^{(1)}\omega_0^2+\right.\\&\left.+\left(2R_1^{(1)}+\frac{1}{2}R_3^{(2)}\right)C_C\right]=0.\end{aligned}\tag{2.30}$$

If the realization of the dynamic tuning mode is achieved by fulfillment of relationships (1.131) and (1.132) among the instrument's parameters, an additional condition that makes it possible to achieve a substantial reduction in the effect on its accuracy of angular vibrations at frequency $2\omega_0$ is

$$R_3^{(1)}=R_3^{(2)}.\tag{2.31}$$

Fulfillment of this condition entails some structural complications, but in principle it is possible.

Thus, for modulation RVG's having two or more rotors, when the signal is read in a nonrotating system of coordinates on the zero carrier frequency, it is possible to select the parameters such that in the resonance tuning mode, a significant reduction of the instrument's sensitivity to angular vibrations of the base with a frequency of $2\omega_0$ is insured.

For an MRG with signal reading on a frequency equal to the doubled frequency of rotation of the rotor $2\omega_0$, angular vibrations of the base in the instrument's plane of sensitivity on this same frequency also result in a signal that is equivalent to a signal caused by the base's constant angular velocity. Actually, suppose that the base's angular vibrations are described by expression (2.1).

Then, allowing for the demodulator, the slowly changing component of the signal at the instrument's outlet has the form

$$\tilde{u}_1 = \frac{W(p-i2\omega_0) - (p-i2\omega_0)\left[W_2^+(p-i2\omega_0)\,W_{12}(p-2i\omega_0) + \right.}{\left. + \tilde{W}_2^+(p-i2\omega_0)\,W_{14}(p-i2\omega_0)\right]} \tilde{\omega}_A. \qquad (2.32)$$

In connection with this, signal (2.1) from the base's angular vibrations will be totally identical to the signal from some slowly changing angular velocity $\bar{\omega}_e$, which is determined by the expression

$$\tilde{\omega}_e^* = -\frac{W(p-i2\omega_0) - (p-i2\omega_0)\left[W_2^+(p-i2\omega_0)\,W_{12}(p-i2\omega_0) + \right.}{\left. + \tilde{W}_2^+(p-i2\omega_0)\,W_{14}(p-i2\omega_0)\right]} \tilde{\omega}_A. \qquad (2.33)$$

In order for there to be no error it is necessary that in the instrument there be realized that relationship among the basic parameters so that the right side of (2.33) becomes zero.

As an example, let us examine in some detail several specific setups of MRG's with signal reading on frequency $2\omega_0$. An OMG's error when there are angular vibrations of the base is found from the relationship

$$\tilde{\omega}_e^* = \frac{1}{2}\frac{(1-\varkappa_Y)\nu_C^2 + (1-\varkappa_Z)\nu_B^2}{(1+\varkappa_Y)\nu_C^2 - (1+\varkappa_Z)\nu_B^2}\tilde{\omega}_A. \qquad (2.34)$$

This error can be reduced only by reducing the values of $1 - \varkappa_Y$ and $1 - \varkappa_Z$. The closer to each other the values along the suspension axes are, the greater the adduced instrument error, which is explained by the reduction in their transfer factor with respect to the useful signal.

For a DMG, the suspension of each of the rings of which has only one degree of freedom in the plane of rotation, the expression determining the equivalent velocity $\bar{\omega}_e$ when there are angular vibrations of the base at frequency $2\omega_0$ has the form

$$\tilde{\omega}_e^* = -\frac{2\frac{R_1}{I_{Zn}}(\nu_B^2 - 1 + \varkappa_Y) + \nu_C^2(1-\varkappa_Y) + \nu_B^2(1-\varkappa_{Zn})}{-2\frac{R_1}{I_{Zn}}(\nu_B^2 - 1 - \varkappa_Y) + \nu_C^2(1+\varkappa_Y) - \nu_B^2(1+\varkappa_{Zn})}\tilde{\omega}_A. \qquad (2.35)$$

In contrast to a DMG with signal reading on the zero frequency, in this case the error does not depend on the angle ϕ_{12} between the suspension axes in the plane of rotation. A joint examination of the condition of low instrument sensitivity with respect to the base's constant angular vibrations (2.1) ($\bar{\omega}_e \approx 0$) and dynamic tuning condition (1.66) shows that the simultaneous fulfillment of these conditions is possible only when a nonelastic suspension is realized for one of the rings ($C_B = 0$ or $C_C = 0$).

When the signal is read in a rotating system of coordinates on frequency, ω_0, two cases are possible, depending on the type of reference function used in the demodulator. In one of them, where the reference function has the form $e^{-i\omega_0 t}$, the expression for the instrument error for angular vibrations of the base on frequency $2\omega_0$ coincides with expression (2.3). In the second case, where the reference function $e^{i\omega_0 t}$ is used, the instrument error will be determined by expression (2.33).

Starting with the generalized mathematical model of an RVG, in a manner analogous to the previously discussed cases it is easy to derive expressions for the computation

of modulation RVG errors caused by angular vibrations of the base at frequency $2\omega_0$ when the signal is read from the intermediate suspension rings in any measuring system of coordinates.

2.2. Reaction of Rotor Vibration Gyroscopes to Disturbing Moments

No actually existing instrument can be manufactured with ideal accuracy. During the building of instrument assemblies and the assembly and regulation of the instrument as a whole, some deviations from the given rated parameters are usually allowed. Such deviations also appear when the instrument is used. One of the consequences of this can be the appearance of disturbing moments that affect a gyroscope and result in additional errors.

Let us investigate the errors caused in modulation RVG's by the effect on them of the mechanical part of disturbing moments. From the generalized mathematical model of an RVG (1.20) it follows that when disturbing moments are acting on a gyroscope, the motion in inertial space of the first stage's (for example) rotor is described by the expression

$$\tilde{\chi}_1 = \frac{1}{W(p)}[W_{11}(p)(\overline{M}^{(1)} + e^{-i\varphi_{11}}\overline{M}_n^{(1)}e^{-i\omega_0 t}) + \\ + W_{13}(p)(\overline{M}^{(1)*}e^{-i2\omega_0 t} + e^{i\varphi_{11}}\overline{M}_n^{(1)*}e^{-i\omega_0 t}) + \\ + W_{12}(p)(\overline{M}^{(2)} + \overline{M}_n^{(2)*}e^{-i\omega_0 t}) + W_{14}(\overline{M}^{(2)*}e^{-i2\omega_0 t} + \overline{M}_n^{(2)*}e^{-i\omega_0 t})]. \quad (2.36)$$

From (2.36) it is obvious that the creation of an MRG that is totally invariant when acted upon by disturbing moments is impossible in principle, since the requirement that all the terms in the numerator on the right side of the equation equal zero automatically results in a requirement that its denominator also equals zero.

Let us discuss, in sequence, the errors caused in different types of MRG setups by the effect of different types of disturbing moments. Let the first-stage rotor be subjected to the effect of a constant or slowly changing moment $\overline{M}^{(1)}$. The reason for the appearance of this moment can be displacement of the rotor's center of mass, relative to the suspension axes, along the axis of rotation and the presence of constant or slowly changing linear accelerations of the base, the vector of which lies in a plane perpendicular to the rotor's axis of rotation. In this case, in the nonrotating system of coordinates the rotor can be deflected through some angle and perform oscillations with a frequency of $2\omega_0$ around this angle. When the signal is read in the nonrotating system of coordinates on the zero frequency, the instrument's error will be determined by the expression

$$\tilde{\chi}_1 = \frac{W_{11}(p)}{W(p)}\overline{M}^{(1)}. \quad (2.37)$$

It is obvious that in this case, as in the case when angular vibrations of the base act on an instrument, it is convenient to represent the MRG's error in the form of an equivalent angular velocity, the signal from which is completely identical to the signal from an acting disturbing moment:

$$\tilde{\omega}_e = \frac{pW_{11}(p)}{W(p) - [W_{12}^{\dagger}(p)W_{12}(p) + \tilde{W}_{12}^{\dagger *}(p)W_{14}(p)]p}\overline{M}^{(1)}. \quad (2.38)$$

For an OMG with a single degree of freedom in the plane of rotation, the expression for the equivalent angular velocity in the resonance tuning mode has the form

$$\bar{\omega}_e = \frac{-i}{I_Y(1+\varkappa_Y)\omega_0}\bar{M}^{(1)}. \tag{2.39}$$

The larger the rotor's moment of inertia relative to the axis of the torsion bars and the higher the rotor's frequency of rotation, the smaller this error will be. In the case of two degrees of freedom in the OMG, its error when affected by moment $\bar{M}^{(1)}$ will be found from the expression

$$\bar{\omega}_e = -\frac{I_Y\left[\frac{1}{2}v_B^2-(1-\varkappa_Y)+i\xi_B\right]+I_Z\left[\frac{1}{2}v_C^2-(1-\varkappa_Z)+i\xi_C\right]}{I_Y I_Z\left[i\frac{1}{2}(1+\varkappa_Y)v_C^2+i\frac{1}{2}(1+\varkappa_Z)v_B^2-\right.}\bar{M}^{(1)}. \tag{2.40}$$
$$\left.-i(1-\varkappa_Z)2\frac{I_X}{I_Y}-\xi_C(1+\varkappa_Y)-\xi_B(1+\varkappa_Z)\right]\omega_0$$

Thus, the OMG error caused by disturbing moment $\bar{M}^{(1)}$ cannot be eliminated. It can be reduced by the proper selection of the instrument's parameters and by reducing the disturbing moment itself.

The error in a DMG in which the suspension of each of the rings has one degree of freedom is described by the expression

$$\bar{\omega}_e = -\frac{i}{I_{Zn}\omega_0}\frac{v_B^2+\frac{I_{Zn}}{I_{Yn}}v_C^2+2\frac{R_1}{I_{Yn}}-(1-\varkappa_Y)(1+\cos 2\varphi_{12})}{\frac{1}{2}v_B^2(1+\varkappa_{Zn})+\frac{1}{2}v_C^2(1+\varkappa_Y)+v_B^2\frac{R_1}{I_{Zn}}+}\bar{M}^{(1)}. \tag{2.41}$$
$$+\frac{R_1}{I_{Zn}}(5\varkappa_Y-3)-2\frac{R_2-R_1}{I_{Yn}}(1-\varkappa_{Zn})$$

In order to build an instrument that is not sensitive to moment $\bar{M}^{(1)}$ it is necessary that its parameters have values for which expression (2.41) becomes zero. The condition of equality of the numerator of (2.41) to zero is fulfilled for the following relationship between the rigidities of the rings' suspension:

$$C_C = -2(R_2+R_1)\omega_0^2 - C_B. \tag{2.42}$$

It is not difficult to see that equality (2.42) is satisfied for the rigidity values determined from expressions (2.10), and in connection with this the denominator of (2.41) also becomes zero; that is, the instrument operates in a pseudoresonance mode. In order to find the error in this case, we should take into consideration the viscous friction acting on the suspension axes. The expression for equivalent angular velocity $\bar{\omega}_e$ then takes on the form

$$\bar{\omega}_e = \frac{i}{I_{Yn}I_{Zn}\omega_0}\frac{I_{Yn}\xi_B+I_{Zn}\xi_C}{\xi_B\left(1+\varkappa_{Zn}+2\frac{R_1}{I_{Zn}}\right)+\xi_C(1+\varkappa_Y)}\bar{M}^{(1)}. \tag{2.43}$$

Thus, when operating in a pseudoresonance mode, a DMG realized according to the diagram shown in Figure 12, with a rotor that is acted upon by constant disturbing moment $\bar{M}^{(1)}$ has an error determined by expression (2.43).

If the NR's suspension has two degrees of freedom ($C_C^{(2)} \to \infty$) and $\varphi_{12} = 0$, the condition of nonsensitivity of the instrument to disturbing moment $\bar{M}^{(1)}$ has the form

$$C_B^{(1)}\left[2\left(R_3+R_1\right)\omega_0^2+C_C^{(1)}+C_B^{(1)}\right]+2R_1\omega_0^2\left(2R_3\omega_0^2+C_C^{(1)}\right)+$$
$$+C_B^{(2)}\left(2R_3\omega_0^2+C_C^{(1)}\right)=0. \tag{2.44}$$

It is also fulfilled when conditions (2.16) and (2.19) are observed, since they make it possible to reduce the instrument's sensitivity to angular vibrations with a frequency of $2\omega_0$. If the VR's suspension from the PD's shaft has two degrees of freedome and $\phi_{12} = 0$, the nontrivial conditions for DMG invariance to the effect of moment $\overline{M}^{(1)}$ in the resonance tuning mode is written in the following form:

$$C_C^{(2)}=\frac{-C_B^{(2)}\left(2R_1+R_3\right)\omega_0^2\pm R_3\omega_0^2\sqrt{-R_1\omega_0^2C_B^{(2)}}}{2R_1\omega_0^2+C_B^{(2)}}; \tag{2.45}$$

$$C_B^{(1)}=-\frac{R_1\omega_0^2C_C^{(2)}+\left(R_3+R_1\right)\omega_0^2C_B^{(2)}+\frac{1}{2}C_C^{(2)}C_B^{(2)}+2R_3\omega_0^2R_1\omega_0^2}{\left(R_3+4R_1\right)\omega_0^2+\frac{1}{2}\left(C_C^{(2)}+C_B^{(2)}\right)}. \tag{2.46}$$

These conditions turn out to be incompatible with the conditions of low sensitivity to angular vibrations of the base with a frequency of $2\omega_0$. Therefore, and depending on the instruments' operating conditions, their parameters must satisfy either relationships (2.21) and (2.22) or relationships (2.45) and (2.46).

For a DMG in which each rotor has two degrees of freedom, the condition for the absence of error caused by disturbing moment $\overline{M}^{(1)}$ is determined by the expression

$$R_3\omega_0^2\left(C_C^{(1)}C_B^{(1)}+C_C^{(2)}C_B^{(2)}\right)+2R_3\omega_0^2\left(C_1C_2-\Delta C_1\Delta C_2\cos\varphi_{12}\right)+$$
$$+4R_1\omega_0^2\left(C_1C_2+C_C^{(1)}C_B^{(1)}\right)+4R_3\omega_0^2R_1\omega_0^2\left(C_1+C_2\right)+$$
$$+C_2C_C^{(1)}C_B^{(1)}+C_1C_C^{(2)}C_B^{(2)}=0. \tag{2.47}$$

When each of the rotors has a uniformly rigid suspension, this condition is fulfilled when the condition of dynamic tuning of the instrument is.

Let us examine a TMG in which the suspension of each of the rotors has only one degree of freedom. The condition for nonsensitivity of such an instrument to constant disturbing moment $\overline{M}^{(1)}$ has the form

$$\left[\left(R_3^{(1)}+R_1^{(1)}\right)\omega_0^2+C_1\right]\left[\left(\frac{1}{2}R_3^{(2)}+R_1^{(1)}\left(1+\cos 2\varphi_{12}\right)\right)\omega_0^2+\right.$$
$$\left.+C_1-\Delta C_1\cos 2\varphi_{12}+C_B^{(2)}\right]-\frac{1}{2}\left[\left(R_1^{(1)}\omega_0^2+\Delta C_1\right)^2+\right. \tag{2.48}$$
$$\left.+2\left(R_1^{(1)}\omega_0^2+\Delta C_1\right)\left(-R_1^{(1)}\omega_0^2+C_1\right)\cos 2\varphi_{12}+\left(-R_1^{(1)}\omega_0^2+C_1\right)^2\right]=0.$$

From (2.48) it is possible to derive the dependence of the rigidity of the first rotor's suspension to the PD's shaft on the rigidities of the suspensions of the other two rotors, which--when the suspension axes are orthogonal--is described by the following expressions:
for $\phi_{12} = 0$,

$$C_B^{(2)}=-\frac{\left[\left(R_3^{(1)}+R_1^{(1)}\right)\omega_0^2+C_1\right]\left[\left(\frac{1}{2}R_3^{(2)}+2R_1^{(1)}\right)\omega_0^2+C_B^{(1)}\right]-\frac{1}{2}\left(2R_1^{(1)}\omega_0^2-C_B^{(1)}\right)^2}{\left(R_3^{(1)}+R_1^{(1)}\right)\omega_0^2+C_1}; \tag{2.49}$$

for $\phi_{12} = \pi/2$,

$$C_B^{(2)} = -\frac{[(R_3^{(1)} + R_1^{(1)})\omega_0^2 + C_1]\left(\frac{1}{2}R_3^{(2)}\omega_0^2 + C_C^{(1)}\right) - \frac{1}{2}C_C^{(1)2}}{(R_3^{(1)} + R_1^{(1)})\omega_0^2 + C_1}. \quad (2.50)$$

The joint realization of relationships (2.49) or (2.50) and (1.62) makes it possible to build an instrument that is not sensitive to disturbing moment $\overline{M}^{(1)}$ when operating in the dynamic tuning mode. For the simultaneous fulfillment of the condition for low sensitivity to angular vibrations of the base on frequency $2\omega_0$, relationship (2.26) or (2.28) must be considered jointly with these expressions. In this case we have a system of three nonlinear equations relative to the three rigidities of the the RVG's rotors' suspensions. The selection of the optimum instrument parameters, with due consideration for the mentioned conditions, can be done with the help of a digital computer.

Let us discuss the MRG errors caused by a constant disturbing moment $\overline{M}^{(1)}$ when the useful signal is read on frequency $2\omega_0$ in a nonrotating system of coordinates. Allowing for the signal demodulator at the instrument's outlet, in this case it will have the form

$$\tilde{u}_1 = \frac{W_{13}(p - i2\omega_0)}{W(p - i2\omega_0)}\overline{M}^{(1)*}, \quad (2.51)$$

while the equivalent angular velocity is determined by the expression

$$\tilde{\omega}_e' = -\frac{W_{13}(p - i2\omega_0)}{\tilde{W}_1^+(p)W_{12}(p - i2\omega_0) + W_1^{+*}(p)W_{14}(p - i2\omega_0)}\overline{M}^{(1)*}. \quad (2.52)$$

For a DMG with a single degree of freedom, in the resonance tuning mode this expression takes on the form

$$\tilde{\omega}_e^* = \frac{i}{I_Y(1 + \varkappa)\omega_0}\overline{M}^{(1)*}. \quad (2.53)$$

This relationship coincides with expression (2.39); that is, the method used to read the useful signal has no effect on the error of an OMG with a single degree of freedome that is caused by moment $\overline{M}^{(1)}$.

The error in a DMG in which the suspension of each rotor has a single degree of freedom can be found from the relationship

$$\tilde{\omega}_e^* = \frac{i}{\omega_0}\frac{2\frac{1}{I_Y}\frac{R_1}{I_{Zn}} + \frac{1}{I_Y}\nu_C^2 - \frac{1}{I_{Zn}}\nu_B^2}{(1 + \varkappa_Y)\left(\nu_C^2 + 2\frac{R_1}{I_{Zn}}\right) - \nu_B^2\left(1 + \varkappa_{Zn} + 2\frac{R_1}{I_{Zn}}\right)}\overline{M}^{(1)*}. \quad (2.54)$$

When condition (2.10) is fulfilled, the numerator of (2.54) becomes zero. In connection with this, the instrument operates in a pseudoresonance mode and in order to determine its error it is necessary to take into consideration the internal friction in the torsion bars of the rotors' suspensions.

The condition for nonsensitivity of a TMG with single-stage suspension of each of the rotors to the effect of disturbing moment $\overline{M}^{(1)}$ has the form

$$C_B^{(2)} = -\frac{1}{2}\frac{e^{-i2\varphi_{1s}}\left[R_3^{(2)}\omega_0^{(2)}\left(R_1^{(1)}\omega_0^2+\Delta C_1\right)+2R_1^{(1)}\omega_0^2 C_C^{(1)}\right]+C_C^{(1)}C_B^{(1)}}{e^{-i2\varphi_{1s}}\left(R_1^{(1)}\omega_0^2+\Delta C_1\right)}. \tag{2.55}$$

Condition (2.55), together with dynamic tuning condition (1.62) and the condition for low sensitivity to angular vibrations of the base on frequency $2\omega_0$, makes it possible to select the optimum parameters for an instrument that is being designed.

For an MRG with signal reading in a rotating system of coordinates on frequency ω_0, the error caused by disturbing moment $\bar{M}^{(1)}$--depending on the form of the reference function used in the demodulator--is described by either expression (2.38) or expression (2.52).

If moment $\bar{M}^{(1)}$ is of the harmonic type ($\bar{M}^{(1)} = \bar{m}_A e^{-i2\omega_0 t}$) with a frequency of $2\omega_0$, which can occur (for example) when linear vibrations on the same frequency act on an instrument, the errors in modulation VRG's are determined by the following expressions:
when the signal is read in the nonrotating system on the zero frequency,

$$\bar{\omega}_e = \frac{pW_{13}(p)}{W(p)-\left[W_{\Sigma}^{+}(p)\,W_{12}(p)+\bar{W}_{\Sigma}^{+*}(p)\,W_{14}(p)\right]p}\,\bar{m}_A^*; \tag{2.56}$$

when the signal is read on frequency $2\omega_0$,

$$\bar{\omega}_e^* = -\frac{W_{11}(p-i2\omega_0)}{\bar{W}_{\Sigma}^{+}(p)\,W_{12}(p-i2\omega_0)+W_{\Sigma}^{+*}(p)\,W_{14}(p-i2\omega_0)}\,\bar{m}_A. \tag{2.57}$$

For the MRG's under discussion and a constant amplitude of moment $\bar{m}$, expression (2.56) coincides with expression (2.52) for all practical purposes; that is, the error caused by harmonic moment $\bar{M}^{(1)}$ with frequency $2\omega_0$ for an instrument with reading on the zero frequency is equivalent to the error of an MRG with reading on frequency $2\omega_0$ that appears when the constant disturbing moment $\bar{M}^{(1)}$ acts upon it. When the signal is read on frequency $2\omega_0$, the expressions for OMG and DMG error coincide, respectively, with expressions (2.53) and (2.54). In this case the instruments' errors do not depend on the signal-reading method. For a TMG with one-stage ring suspensions, from the condition of the equality of the numerator of (2.57) to zero it follows that when there is a relationship among its parameters that is defined by the expression

$$C_B^{(2)} = -\frac{1}{2}\frac{R_3^{(2)}\omega_0^2\left(R_1^{(1)}\omega_0^2+C_1\right)+\left(2R_1^{(1)}\omega_0^2+C_B^{(1)}\right)C_C^{(1)}}{R_1^{(1)}\omega_0^2+C_1}, \tag{2.58}$$

the instrument will be insensitive to a harmonic disturbing moment with frequency $2\omega_0$.

From (2.36) it follows that when disturbing moments act on an MRG's suspension axes, there will be an error expressed by the presence at its outlet of a signal that is equivalent to the signal from some constant angular velocity $\bar{\omega}$ only if these moments are of a harmonic type with the frequency of rotation ω_0 of the rotor. These moments include, for example, moments caused by static disbalance of the VR along the PD's axis of rotation and the effect in the plane of rotation of constant linear overloads and vibrations with a frequency of $2\omega_0$, as well as moments generated by static nonequilibrium of the rotors relative to the suspension axes and linear vibrations of the base along the axis of rotation at frequency ω_0.

Let us represent the vector of moments $\bar{M}_{\pi}^{(1)}$ in terms of the amplitudes and phases of harmonic disturbing moments. Let the following disturbing moments act along the suspension axes of an MRG's first stage:

$$M_B^{(1)} = m_B^{(1)} \sin(\omega_0 t + \varphi_{B1}); \qquad M_C^{(1)} = m_C^{(1)} \sin(\omega_0 t + \varphi_{C1}). \tag{2.59}$$

Then, using Euler's formulas, vector $\bar{M}_{\pi}^{(1)}$ can be written in the form

$$\bar{M}_{\pi}^{(1)} = \frac{1}{2}[(-im_B^{(1)} e^{i\varphi_{B1}} + m_C^{(1)} e^{i\varphi_{C1}}) e^{i\omega_0 t} + \\ + (im_B^{(1)} e^{-i\varphi_{B1}} - m_C^{(1)} e^{-i\varphi_{C1}}) e^{-i\omega_0 t}]. \tag{2.60}$$

There are also analogous expressions for the vectors of disturbing moments acting along the other stages' suspension axes. Using relationships (2.36) and (2.60), let us determine the NR's angular deflection in inertial space:

$$\dot{\chi}_1 = \frac{1}{2} \frac{1}{W(p)} [-ie^{i\varphi_{B1}} (e^{-i\varphi_{12}} W_{11}(p) + e^{i\varphi_{12}} W_{13}(p)) m_B^{(1)} + \\ + e^{i\varphi_{C1}} (e^{-i\varphi_{12}} W_{11}(p) - e^{i\varphi_{12}} W_{13}(p)) m_C^{(1)} + \\ + [ie^{-i\varphi_{B1}} (e^{-i\varphi_{12}} W_{11}(p) + e^{i\varphi_{12}} W_{13}(p)) m_B^{(1)} - \\ - e^{i\varphi_{C1}} (e^{-i\varphi_{12}} W_{11}(p) - e^{i\varphi_{12}} W_{13}(p)) m_C^{(1)}] e^{-i2\omega_0 t}]. \tag{2.61}$$

In the case of signal reading on the zero frequency, MRG errors (presented in terms of equivalent angular velocities) are determined by the expression

$$\tilde{\omega}_e = \frac{1}{2} \frac{-ie^{i\varphi_{B1}} \left(e^{-i\varphi_{12}} W_{11}(p) + e^{i\varphi_{12}} W_{13}(p)\right) m_B^{(1)} + \\ + e^{i\varphi_{C1}} \left(e^{-i\varphi_{12}} W_{11}(p) - e^{i\varphi_{12}} W_{13}(p)\right) m_C^{(1)}}{W(p) - [W_{\Sigma}^{+}(p) W_{12}(p) + \tilde{W}_{\Sigma}^{+*}(p) W_{14}(p)]_{p}}, \tag{2.62}$$

while when the signal is read on frequency $2\omega_0$ in a nonrotating system of coordinates, they are determined by the expression

$$\tilde{\omega}_e^{*} = -\frac{1}{2} \frac{ie^{-i\varphi_{B1}} \left(e^{-i\varphi_{12}} W_{11}(p - i2\omega_0) + e^{i\varphi_{12}} W_{13}(p - i2\omega_0)\right) m_B^{(1)} - \\ - e^{-i\varphi_{C1}} \left(e^{-i\varphi_{12}} W_{11}(p - i2\omega_0) - e^{i\varphi_{12}} W_{13}(p - i2\omega_0)\right) m_C^{(1)}}{\tilde{W}_{\Sigma}^{+}(p) W_{12}(p - i2\omega_0) - W_{\Sigma}^{+*}(p) W_{11}(p - i2\omega_0)}. \tag{2.63}$$

Let us discuss the errors in several specific RVG systems. For an OMG with a rotor having a single degree of freedom and with signal reading on the zero frequency in the resonance tuning mode, the equivalent angular velocity in the presence of disturbing moment (2.59) relative to the suspension axis has the form

$$\tilde{\omega}_e = \frac{-1}{I_{Y\Pi}(1 + \varkappa_Y)\omega_0} \frac{1}{2} m_B^{(1)} e^{i\varphi_{B1}}. \tag{2.64}$$

For a DMG that also has only a single degree of suspension freedom for each rotor and from which the signal is read on the zero frequency, in the dynamic tuning mode the error can be determined from the expression

$$\tilde{\omega}_e = -\frac{i}{\omega_0} \frac{-\frac{1}{I_{Z\Pi}} (\nu_B^2 - 1 + \varkappa_Y) m_B e^{i\varphi_B} + \frac{1}{I_{Y\Pi}} \left(\nu_C^2 - 1 + \varkappa_{Z\Pi} + 2\frac{R_1}{I_{Z\Pi}}\right) m_C e^{i\varphi_C}}{\frac{1}{2}\nu_B^2 \left(1 + \varkappa_{Z\Pi} + 2\frac{R_1}{I_{Z\Pi}}\right) + \frac{1}{2}\nu_C^2 (1 + \varkappa_Y) + \frac{R_1}{I_{Z\Pi}}(5\varkappa - 3) - \frac{2R_2 - R_1}{I_{Y\Pi}}} \tag{2.65}$$

When conditions (2.10) are fulfilled, the instrument operates in a pseudoresonance mode and the numerator and denominator of expression (2.65) simultaneously become zero. Therefore, in order to reveal the indeterminacy that is obtained in expression (2.61), it is necessary to take into consideration the damping along the rotors' suspension axes.

For a TMG with a single degree of freedom for the suspension of each rotor, when constant moments $m_B^{(1)}$ and $m_C^{(1)}$ are in action, the numerator of expression (2.61) has the following form:

$$\begin{aligned} D = -ie^{-i\varphi_{B1}}e^{-i\varphi_{12}}\Big\{&C_B^{(2)}\left[\left(R_3^{(1)}+2R_1^{(1)}\right)\omega_0^2+C_C^{(1)}\right]+\frac{1}{2}C_C^{(1)}C_B^{(1)}+\\ &+C_1\left[R_3^{(1)}+\frac{1}{2}R_3^{(2)}+R_1^{(1)}\left(2+\cos 2\varphi_{12}\right)\right]\omega_0^2-\\ &-\Delta C_1\cos 2\varphi_{12}\left(R_3^{(1)}+R_1^{(1)}\right)\omega_0^2+C_B^{(1)}R_1^{(1)}\left(1+\cos 2\varphi_{12}\right)\omega_0^2+\\ &+\frac{1}{2}R_3^{(2)}\omega_0^2\left(R_3^{(1)}+2R_1^{(1)}\right)\omega_0^2+R_1^{(1)}\omega_0^2R_3^{(1)}\left(1+\cos 2\varphi_{12}\right)\omega_0^2+\\ &+\frac{1}{2}C_C^{(1)}C_B^{(1)}e^{+i2\varphi_{12}}+C_C^{(1)}R_1^{(1)}\omega_0^2+\frac{1}{2}\Delta C_1R_3^{(2)}\omega_0^2\Big\}m_B^{(1)}+\\ &+e^{i\varphi_{C1}}e^{-i\varphi_{12}}\Big\{C_B^{(2)}\left(R_3^{(1)}\omega_0^2+C_B^{(1)}\right)+\frac{1}{2}C_C^{(1)}C_B^{(1)}\left(1-e^{i2\varphi_{12}}\right)+\\ &+C_1\left(R_3^{(1)}+\frac{1}{2}R_3^{(2)}+2R_1^{(1)}\right)\omega_0^2-\Delta C_1R_3^{(1)}\cos 2\varphi_{12}\omega_0^2+\\ &+C_B^{(1)}R_1^{(1)}\left(1+2\cos 2\varphi_{12}\right)\omega_0^2-C_C^{(1)}R_1^{(1)}\omega_0^2-\frac{1}{2}\Delta C_1R_3^{(2)}\omega_0^2+\\ &+\frac{1}{2}R_3^{(2)}\omega_0^2R_3^{(1)}\omega_0^2+R_3^{(1)}\omega_0^2R_1^{(1)}\left(1+\cos 2\varphi_{12}\right)\omega_0^2\Big\}m_C^{(1)}. \end{aligned} \tag{2.66}$$

Expression (2.66), together with expression (1.127) for an instrument's transfer factor, makes it possible to determine the equivalent angular velocity $\overline{\omega}_e$ when disturbing moments (2.59) are acting on the suspension axes. The errors in DMG's having signal reading on the zero frequency and a two-stage suspension of the NR from the VR and the VR from the PD's shaft can also be found with the help of expression (2.66) and the corresponding expressions for transfer factor K_g. In order to do this, in (2.66) we should set $R_1^{(1)} = 0$ in the first case and $R_3^{(2)} = 0$ in the second.

When the signal from a TMG is read on frequency $2\omega_0$ in a nonrotating system of coordinates, the numerator of expression (2.63) takes on the form

$$\begin{aligned} D = ie^{-i\varphi_{B1}}e^{-i\varphi_{12}}&\left[\left(2R_1^{(1)}\omega_0^2+C_C^{(1)}\right)\left(\frac{1}{2}R_3^{(2)}\omega_0^2+C_B^{(2)}\right)+\right.\\ &\left.+2R_1^{(1)}\omega_0^2C_C^{(1)}+\frac{1}{2}\left(1+e^{i2\varphi_{12}}\right)C_C^{(1)}C_B^{(1)}\right]m_B^{(1)}-\\ -e^{-i\varphi_{12}}e^{-i\varphi_{C1}}&\left[C_B^{(1)}\left(\frac{1}{2}R_3^{(2)}\omega_0^2+C_B^{(2)}\right)+\frac{1}{2}\left(1-e^{i2\varphi_{12}}\right)C_C^{(1)}C_B^{(1)}\right]. \end{aligned} \tag{2.67}$$

As special cases, from (2.67) we can derive expressions for the errors in DMG's and OMG's having signal reading on frequency $2\omega_0$ when disturbing moments (2.59) are acting on the rings' suspension axes.

The reaction of an MRG to disturbing moments acting on the second stage is analogous to its reaction to moments $\overline{M}^{(1)}$ and $\overline{M}_\pi^{(1)}$. A constant or slowly changing moment $\overline{M}^{(2)}$ will cause in an instrument an error described by the following expressions:

when the signal is read in a nonrotating system of coordinates on the zero carrier frequency--

$$\tilde{\omega}_e = \frac{pW_{12}(p)}{W(p) - [W_2^+(p)\,W_{12}(p) + \tilde{W}_2^{+*}(p)\,W_{14}(p)]\,p}\,\overline{M}^{(2)}; \tag{2.68}$$

when the signal is read on frequency $2\omega_0$--

$$\tilde{\omega}_e^* = -\frac{W_{14}(p - i2\omega_0)}{\tilde{W}_2^+(p)\,W_{12}(p - i2\omega_0) + W_2^{+*}(p)\,W_{14}(p - i2\omega_0)}\,\overline{M}^{(2)*}. \tag{2.69}$$

An error will also appear in an MRG if disturbing moment $\overline{M}^{(2)}$ is of a harmonic nature: $\overline{M}^{(2)} = \overline{m}_A^{(2)} e^{-i2\omega_0 t}$. In this case the expressions for determining the instrument's error have the following form:
when the signal is read in a nonrotating system on the zero frequency--

$$\tilde{\omega}_e = \frac{pW_{11}(p)}{W(p) - [W_2^+(p)\,W_{12}(p) + \tilde{W}_2^{+*}(p)\,W_{14}(p)]}\,\overline{m}_A^{(2)*}; \tag{2.70}$$

when it is read on frequency $2\omega_0$--

$$\tilde{\omega}_e^* = -\frac{W_{12}(p - i2\omega_0)}{\tilde{W}_2^+(p)\,W_{12}(p - i2\omega_0) + W_2^{+*}(p)\,W_{14}(p - i2\omega_0)}\,\overline{m}_A^{(2)}. \tag{2.71}$$

Disturbing moments $\overline{M}_\Pi^{(2)}$ acting on the second stage's suspension axes will cause an error in the instrument only if they are of a harmonic nature with a frequency of change of ω_0. Analogous to (2.60), in general form we will write this moment in the following manner:

$$\overline{M}_\Pi^{(2)} = \frac{1}{2}\left[\left(-im_B^{(2)}e^{i\varphi_{B2}} + m_C^{(2)}e^{i\varphi_{C2}}\right)e^{i\omega_0 t} + \right.$$
$$\left. + \left(im_B^{(2)}e^{-i\varphi_{B2}} - m_C^{(2)}e^{-i\varphi_{C2}}\right)e^{-i\omega_0 t}\right]. \tag{2.72}$$

The MRG errors generated by disturbing moment (2.72) will then be determined by the following expressions:
when the signal is read in a nonrotating system on the zero frequency--

$$\tilde{\omega}_e = \frac{1}{2}\,p\,\frac{-ie^{i\varphi_{B2}}\left[W_{12}(p) + W_{14}(p)\right]m_B^{(2)} + e^{i\varphi_{C2}}\left[W_{12}(p) - W_{14}(p)\right]m_C^{(2)}}{W(p) - [W_2^+(p)\,W_{12}(p) + \tilde{W}_2^{+*}(p)\,W_{11}(p)]\,p}; \tag{2.73}$$

when it is read on frequency $2\omega_0$--

$$\tilde{\omega}_e^* = -\frac{1}{2}\,\frac{ie^{-i\varphi_{B2}}\left[W_{12}(p - i2\omega_0) + W_{14}(p - i2\omega_0)\right]m_B^{(2)} - e^{-i\varphi_{C2}}\left[W_{12}(p - i2\omega_0) - W_{14}(p - i2\omega_0)\right]m_C^{(2)}}{\tilde{W}_2^+(p)\,W_{12}(p - i2\omega_0) + W_2^{+*}(p)\,W_{11}(p - i2\omega_0)}. \tag{2.74}$$

The expressions presented in this section make it possible, when the disturbing moments are known, to determine MRG errors expressed in the form of an equivalent angular velocity of the base, as well as their dependence on the instruments' basic parameters. The latter fact can be used when designing specific instruments with the required accuracy characteristics when operating under given real conditions.

2.3. Operating Errors in Rotor Vibration Gyroscopes

One of the important properties of instruments is their ability to maintain their basic characteristics with given limits when they are in operation. Actually, when

affected by a change in temperature, instability of the power supply, material properties that change with time and other factors, the values of instrument parameters and, consequently, basic instrument characteristics can change during the operating process. The effect of these factors on the characteristics of RVG's is particularly noticeable, since their basic operating mode is the resonance tuning mode, with very little damping, which makes them extremely sensitive to even an insignificant change in their parameters. When designing such instruments, therefore, it is necessary to devote particular attention to the possibility of insuring their stable operation under given real conditions.

Let us discuss how small changes in parameters affect the basic characteristics of an MRG. The basic characteristic of an MRG is its transfer factor K_g with respect to the base's angular velocity, which is a function of the rigidities' of the rotors' suspensions, the rings' moments of inertia and the PD's frequency of rotation:

$$K_g = K_g(C_B^{(i)}, C_C^{(i)}, I_{Xs}^{(i)}, I_{Ys}^{(i)}, I_{Xn}^{(i)}, I_{Yn}^{(i)}, I_{Zs}^{(i)}, I_{Zn}^{(i)}, \omega_n), \quad i = 1, 2, \ldots, n. \tag{2.75}$$

During operation, these parameters can deviate from their rated values; that is, some small increments appear. In order to evaluate the effect of these increments on a change in the transfer factor, let us make use of methods from the theory of sensitivity [37].

The basic factor affecting a change in the value of K_g will be detuning of the instrument from the resonance mode. The transfer factor can be written in the following form:

$$K_g = \frac{\operatorname{Re} A_0 + i \operatorname{Im} A_0}{\operatorname{Re} B_0 + i \operatorname{Im} B_0}, \tag{2.76}$$

while the instrument's dynamic tuning condition has the form Re B_0 = 0. If, during operation, there occur deviations of the instrument parameters listed above from their rated values, the expression for Re B_0 can be written as

$$\operatorname{Re} B_0 = \operatorname{Re} B_0|_{\Delta a_i = 0} + \Delta(\Delta a_i), \tag{2.77}$$

where Δa_i = deviations of the instrument's parameters from their rated values, while Δ characterizes the detuning of the instrument from the resonance mode that arises in connection with this. Substituting (2.77) into expression (2.76) and assuming that the parameters' rated values corresponded to resonance tuning, we obtain the expression for the instrument's transfer factor when it is detuned from the resonance mode:

$$K_g = K_{g.p} \frac{1 + i \frac{\Delta}{\operatorname{Im} B_0}}{1 + \left(\frac{\Delta}{\operatorname{Im} B_0}\right)^2}, \tag{2.78}$$

where $K_{g.p}$ = the instrument's transfer factor in the resonance tuning mode. Thus, when the instrument is detuned its transfer factor is reduced by a factor of $1 + (\Delta/\operatorname{Im} B_0)^2$. In addition to this, as a result of the detuning there appears a cross component of the transfer factor, it being the case that the larger the ratio $\Delta/\operatorname{Im} B_0$ is, the larger it is.

It is completely obvious that the more sensitive an instrument is to detuning from the resonance mode, the higher its sensitivity with respect to the base's angular velocity (and the lower the coefficient of viscous friction along the suspension axes).

In order to evaluate the magnitude of an instrument's detuning when the values of its parameters deviate from their rated values, we will use sensitivity functions of the first type. In this case the expression for detuning can be written in the form

$$\begin{aligned}\Delta = \frac{\partial}{\partial \Delta\omega_0}\operatorname{Re} B_0\Big|_{\Delta\omega_0=0}\Delta\omega_0 + \sum_{i=1}^{n}\Big\{ &\frac{\partial}{\partial \Delta C_B^{(i)}}\operatorname{Re} B_0\Big|_{\Delta C_B^{(i)}=0}\Delta C_B^{(i)} + \\ &+ \frac{\partial}{\partial \Delta C_C^{(i)}}\operatorname{Re} B_0\Big|_{\Delta C_C^{(i)}=0}\Delta C_C^{(i)} + \\ &+ \frac{1}{2}\frac{\partial}{\partial \Delta R_1^{(i)}}\operatorname{Re} B_0\Big|_{\Delta R_1^{(i)}=0}(\Delta l_{X_B}^{(i)} - \Delta l_{Y_B}^{(i)} - \Delta l_{Z_B}^{(i)}) + \\ &+ 2\frac{\partial}{\partial \Delta R_3^{(i)}}\operatorname{Re} B_0\Big|_{\Delta R_3^{(i)}=0}(\Delta l_{X_H}^{(i)} - \Delta l_{Y_H}^{(i)} - \Delta l_{Z_H}^{(i)})\Big\}.\end{aligned} \tag{2.79}$$

For MRG's with VP that are constructed on the basis of two stages of the generalized RVG model, the sensitivity functions of the first type that are part of expression (2.79) take on the following form:

1. When the PD's velocity of rotation changes:

$$\begin{aligned}\frac{\partial}{\partial \Delta\omega_0}\operatorname{Re} B_0\Big|_{\Delta\omega_0=0} = 2\omega_0\{&C_C^{(1)}C_B^{(1)}[(R_3^{(1)} + 4R_1^{(1)} + R_3^{(2)})(2R_1^{(2)}\omega_0^2 + \\ &+ C_2) + 2R_1^{(2)}C_B^{(2)}] + C_C^{(2)}C_B^{(2)}[R_3^{(1)}(2R_1^{(1)}\omega_0^2 + C_1) + 2R_1^{(1)}C_B^{(1)}] + \\ &+ 2\omega_0^2[R_3^{(1)}(R_1^{(1)}\omega_0^2 + C_1) + 2R_1^{(1)}C_B^{(1)}][(R_3^{(1)} + R_1^{(1)} - R_1^{(2)})(R_1^{(2)}\omega_0^2 + \\ &+ C_2) + 2R_1^2C_B^2] + \omega_0^4[R_3^{(1)}(R_3^{(1)} + R_1^{(1)} - R_1^{(2)})(2R_1^{(1)}R_1^{(2)}\omega_0^2 + \\ &+ R_1^{(1)}C_2 + R_1^{(2)}C_1) + 2R_1^{(1)}R_1^{(2)}(R_3^{(1)}(C_B^{(1)} + C_B^{(2)}) + R_1^{(1)}C_B^{(1)} - \\ &- R_1^{(2)}C_B^{(1)})] + 2\omega_0^2R_1^{(1)}R_3^{(1)}C_C^{(1)}(3R_1^{(2)}\omega_0^2 + 2C_2)\}.\end{aligned} \tag{2.80}$$

From (2.80) it is easy to derive the analogous sensitivity functions for simpler MRG layouts. For example, for a TMG with one degree of freedom for the suspension of each rotor, we should set $R_1^{(2)} = 0$, $C_C^{(2)} \to \infty$. As a result, we obtain

$$\begin{aligned}\frac{\partial}{\partial \Delta\omega_0}\operatorname{Re} B_0\Big|_{\Delta\omega_0=0} = 2\omega_0\Big\{&\frac{1}{2}C_C^{(1)}C_B^{(1)}(R_3^{(1)} + 4R_1^{(1)} + R_3^{(2)}) + \\ &+ C_B^{(2)}[R_3^{(1)}(2R_1^{(1)}\omega_0^2 + C_1) + 2R_1^{(1)}C_B^{(1)}] + \\ &+ (R_3^{(1)} + R_1^{(1)})\omega_0^2\Big[R_3^{(1)}\Big(\frac{3}{2}R_1^{(1)}\omega_0^2 + C_1\Big) + \\ &+ 2R_1^{(1)}C_B^{(1)}\Big] + 2\omega_0^2R_1^{(1)}R_3^{(1)}C_C^{(1)}\Big\}.\end{aligned} \tag{2.81}$$

For the DMG in (2.81), we should set $R_3^{(2)} = 0$, $C_B^{(2)} \to \infty$:

$$\frac{\partial}{\partial \Delta\omega_0}\operatorname{Re} B_0\Big|_{\Delta\omega_0=0} = 2\omega_0[R_3^{(1)}(2R_1^{(1)}\omega_0^2 + C_1) + 2R_1^{(1)}C_B^{(1)}]. \tag{2.82}$$

Finally, for an OMG with a single degree of freedom ($R^{(1)} = 0$, $C^{(1)} \to \infty$), the sensitivity function has the form

$$\frac{\partial}{\partial \Delta\omega_0} \operatorname{Re} B_0 \Big|_{\Delta\omega_0=0} = R_3^{(1)}\omega_0. \tag{2.83}$$

2. When the rigidities of the rotors' suspension change:

$$\frac{\partial}{\partial \Delta C_B^{(2)}} \operatorname{Re} B_0 \Big|_{\Delta C_B^{(2)}=0} = C_C^{(1)}C_B^{(1)}\left[\left(\frac{1}{2}R_3^{(1)} + 2R_1^{(1)} + \right.\right.$$
$$\left.\left. + \frac{1}{2}R_3^{(2)} + 2R_1^{(2)}\right)\omega_0^2 + C_C^{(2)}\right] + C_C^{(2)}\omega_0^2\left[R_3^{(1)}\left(R_1^{(1)}\omega_0^2 + C_1\right) + \right.$$
$$\left. + 2R_1^{(1)}C_B^{(1)}\right] + \left[R_3^{(1)}\left(R_1^{(1)}\omega_0^2 + C_1\right) + 2R_1^{(1)}C_B^{(1)}\right]\frac{1}{2}\left(R_3^{(1)} + R_1^{(1)} + \right. \tag{2.84}$$
$$\left. + 3R_3^{(2)}\right)\omega_0^4 + R_1^{(1)}R_3^{(1)}C_C^{(1)}\omega_0^4;$$

$$\frac{\partial}{\partial \Delta C_C^{(2)}} \operatorname{Re} B_0 \Big|_{\Delta C_C^{(2)}=0} = C_C^{(1)}C_B^{(1)}\left[\frac{1}{2}\left(R_3^{(1)} + 4R_1^{(1)} + R_3^{(2)}\right)\omega_0^2 + C_B^{(2)}\right] +$$
$$+ \omega_0^2\left[R_3^{(1)}\left(R_1^{(1)}\omega_0^2 + C_1\right) + 2R_1^{(1)}C_B^{(1)}\right]\left[\frac{1}{2}\left(R_3^{(1)} + R_1^{(1)} - \right.\right. \tag{2.85}$$
$$\left.\left. - R_1^{(2)}\right)\omega_0^2 + C_B^{(2)}\right] + R_1^{(1)}R_3^{(1)}C_C^{(1)}\omega_0^4;$$

$$\frac{\partial}{\partial \Delta C_C^{(1)}} \operatorname{Re} B_0 \Big|_{\Delta C_C^{(1)}=0} = C_B^{(1)}C_C^{(2)}C_B^{(2)} + C_B^{(1)}\omega_0^2\left[\left(R_3^{(1)} + 4R_1^{(1)} + R_3^{(2)}\right)\times\right.$$
$$\left.\times\left(R_1^{(2)}\omega_0^2 + C_2\right) + 2R_1^{(2)}C_B^{(2)}\right] + \frac{1}{2}R_3^{(1)}\omega_0^2\left[\left(R_3^{(1)} + 5R_1^{(1)} - \right.\right. \tag{2.86}$$
$$\left.\left. - R_1^{(2)}\right)\omega_0^2\left(R_1^{(2)}\omega_0^2 + C_2\right) + C_B^{(2)}\left(2R_1^{(2)}\omega_0^2 + C_C^{(2)}\right)\right];$$

$$\frac{\partial}{\partial \Delta C_B^{(1)}} \operatorname{Re} B_0 \Big|_{\Delta C_B^{(1)}=0} = C_C^{(1)}C_C^{(2)}C_B^{(2)} + C_C^{(1)}\omega_0^2\left[\left(R_3^{(1)} + 4R_1^{(1)} + \right.\right.$$
$$\left.\left. + R_3^{(2)}\right)\left(R_1^{(2)}\omega_0^2 + C_2\right) + 2R_1^{(2)}C_B^{(2)}\right] + C_C^{(2)}C_B^{(2)}\left(\frac{1}{2}R_3^{(1)} + 2R_1^{(1)}\right)\omega_0^2 + \tag{2.87}$$
$$+ \left(\frac{1}{2}R_3^{(1)} + 2R_1^{(1)}\right)\left[\left(R_3^{(1)} + R_1^{(1)} - R_1^{(2)}\right)\left(R_1^{(2)}\omega_0^2 + C_2\right) + 2R_1^{(2)}C_B^{(2)}\right]\omega_0^4.$$

3. When the moments of inertia of the rings changes:

$$\frac{\partial}{\partial \Delta R_1^{(2)}} \operatorname{Re} B_0 \Big|_{\Delta R_1^{(2)}=0} = C_C^{(1)}C_B^{(1)}\omega_0^2\left[\left(R_3^{(1)} + 4R_1^{(1)} + R_3^{(2)}\right)\omega_0^2 + 2C_B^{(2)}\right] +$$
$$+ \left[R_3^{(1)}\left(R_1^{(1)}\omega_0^2 + C_1\right) + 2R_1^{(1)}C_B^{(1)}\right]\times \tag{2.88}$$
$$\times\left[\left(R_3^{(1)} + R_1^{(1)} - 2R_1^{(2)}\right)\omega_0^2 + 2C_B^{(2)} - C_2\right] + 2R_1^{(1)}R_3^{(1)}C_C^{(1)}\omega_0^6;$$

$$\frac{\partial}{\partial \Delta R_3^{(2)}} \operatorname{Re} B_0 \Big|_{\Delta R_3^{(2)}=0} = C_C^{(1)}C_B^{(1)}\omega_0^2\left(R_1^{(2)}\omega_0^2 + C_2\right); \tag{2.89}$$

$$\frac{\partial}{\partial \Delta R_1^{(1)}} \operatorname{Re} B_0 \Big|_{\Delta R_1^{(1)}=0} = \left(R_1^{(2)}\omega_0^2 + C_2\right)\omega_0^2\left[R_3^{(1)}\omega_0^2\left(R_1^{(1)}\omega_0^2 + \right.\right.$$
$$\left.\left. + C_1 + 2C_C^{(1)}\right) + 2C_B^{(1)}\left(R_1^{(1)}\omega_0^2 + 2C_C^{(1)}\right)\right] + \left(R_3^{(1)}\omega_0^2 + 2C_B^{(1)}\right)\omega_0^2\times \tag{2.90}$$
$$\times\left[\left(R_3^{(1)} + R_1^{(1)} - R_1^{(2)}\right)\omega_0^2\left(R_1^{(2)}\omega_0^2 + C_2\right) + C_B^{(2)}\left(2R_1^{(2)}\omega_0^2 + C_C^{(2)}\right)\right];$$

$$\frac{\partial}{\partial \Delta R_3^{(1)}} \operatorname{Re} B_0 \Big|_{\Delta R_3^{(1)}=0} = \left(R_1^{(2)}\omega_0^2 + C_2\right)\omega_0^2\left[R_3^{(1)}\left(R_1^{(1)}\omega_0^2 + C_1\right) + \right.$$
$$\left. + 4R_1^{(1)}\omega_0^2C_1 + C_C^{(1)}C_B^{(1)}\right] + \left(R_1^{(1)}\omega_0^2 + C_1\right)\omega_0^2\left[\left(R_3^{(1)} + R_1^{(1)} - \right.\right. \tag{2.91}$$
$$\left.\left. \cdots\cdots\cdots\right.\right.$$

$$\cdots\cdots\cdots$$

$$-R_1^{(2)})\,\omega_0^2\,(R_1^{(2)}\omega_0^2+C_2)+C_B^{(2)}\,(2R_1^{(2)}\omega_0^2+C_C^{(2)})].$$

The expressions for the senstivity functions make it possible to find, for each instrument, the dependence of its sensitivity on a possible change in the basic parameters. Along with the expressions describing an instrument's transfer factor and dynamic characteristics, as well as its basic errors, the sensitivity functions are initial expressions for synthesizing an RVG's basic parameters. All other conditions being equal, it is desirable to have those instrument parameters for which its sensitivity functions will be minimal. Starting with the sensitivity functions and the requirements for an instrument, the allowances for changes in its basic parameters under real operating conditions are calculated.

2.4. Errors in a Single-Rotor Modulation Gyroscope

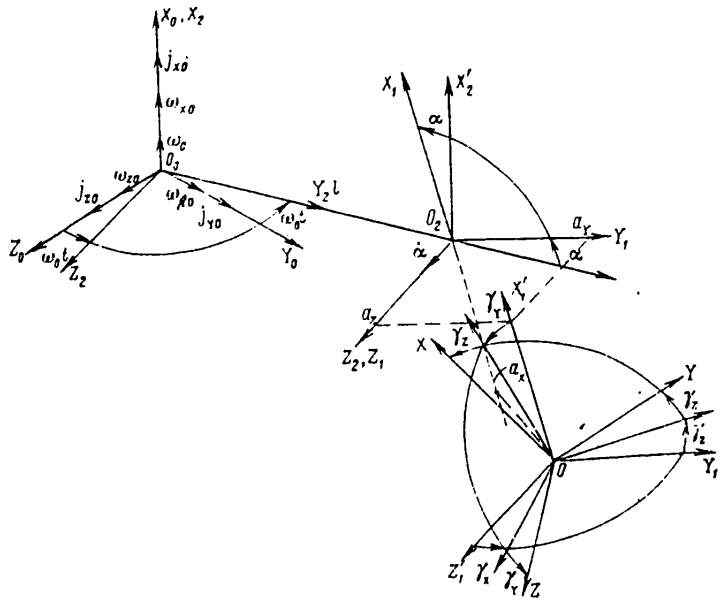

Figure 13. Systems of coordinates.

In the preceding sections of this chapter we have discussed errors in MRG's with VP in general form. As an example, let us investigate in more detail the errors in the simplest of the MRG's: a single-rotor modulation gyroscope with rotating suspension, a diagram of which was presented in Figure 11. Let us discuss the mathematical model of the operation of such an instrument, allowing for the basic technological errors in its construction. In order to do this, we will introduce the following systems of coordinates (Figure 13):

$O_0X_0Y_0Z_0$--a system of coordinates coupled with the instrument's base;
$O_0X_2Y_2Z_2$--a system of coordinates coupled with the PD's shaft;
$O_2X_2'Y_2'Z_2'$--a system of coordinates, the O_2Z_2' axis of which coincides with the torsion bars' axis, while the O_2Y_2' axis lies in the torsion bars' plane of rotation;
$O_2X_1Y_1Z_1$--a system of coordinates coupled with the torsion bars;
$OX_1'Y_1'Z_1'$--a system of coordinates with its origin at the rotor's center of mass and axes that are parallel to the axes of system $O_2X_1Y_1Z_1$;

OXYZ--a system of coordinates, the axes of which coincide with the rotor's main axes of inertia, while its origin is at the rotor's center of mass.

Among the basic technological errors in the production of the instrument we can include:
the presence of some distance l between the motor shaft's axis of rotation and the torsion bars' axis;
static disbalance of the rotor, characterized by the coordinates a_X, a_Y, a_Z of its center of mass in the system of coordinates coupled with the torsion bars;
dynamic disbalance of the rotor, characterized by angles γ_X, γ_Y, γ_Z.

The gyroscope's rotor can be suspended from the PD's shaft with the help of torsion bars of different designs. In connection with this, the general requirement is that the torsion bars' flexural rigidity exceed substantially their torsional rigidity. Assuming that this is observed in a real design, we will consider only the angular motion of the rotor relative to the torsion bars' axis. Assuming that the values of a_X, a_Y, a_Z and γ_X, γ_Y, γ_Z, as well as angle ψ, are sufficiently small and retaining in the equation of motion only terms of no higher than the second order of smallness, we obtain

$$\begin{aligned} T^2\ddot{\psi} + 2\xi T\dot{\psi} + \psi = &-K_n\dot{\omega}_{Z0}\cos(\omega_0 t + \gamma_X) - K_n\dot{\omega}_{Y0}\sin(\omega_0 t - \gamma_X) + \\ &+ K_0\omega_{Z0}\sin(\omega_0 t + \varphi_1) - K_0\omega_{Y0}\cos(\omega_0 t + \varphi_1) - K_1\omega_{X0}\psi - \\ &- K_1\dot{\omega}_{X0} - K_2\omega_{Y0}\omega_{X0}\cos\omega_0 t - K_3 + K_2\omega_{Z0}\omega_{X0}\sin\omega_0 t - \\ &- K_1\gamma_Z\omega_{X0} + m'a_X(j_{Y0}\cos\omega_0 t - j_{Z0}\sin\omega_0 t) + \\ &+ m'a_Y(j_{Y0}\cos\omega_0 t - j_{Z0}\sin\omega_0 t)\psi + m'a_X j_{X0}\psi - m'a_Y j_{X0}, \end{aligned} \tag{2.92}$$

where

$$T^2 = \frac{I_Z}{C_n};\quad 2\xi = \frac{\mu}{\sqrt{I_Z C_n}};\quad K_n = T^2\sqrt{1+\gamma_X^2};$$

$$K_0 = \frac{I_Z\omega_0}{C_n}(1+\varkappa_Z)\sqrt{1+\operatorname{tg}^2\varphi_1};$$

$$K_1 = 2(I_X - I_Y)\frac{\omega_0}{C_n};\quad K_2 = \frac{I_X - I_Y}{C_n};$$

$$K_3 = \frac{\omega_0^2}{C_n}[I_X\gamma_Z + I_Y\gamma_X + I_X\gamma_Y\gamma_X + m(a_Y + l)a_Y];$$

$$K_4 = \frac{I_X - I_Z}{C_n}\gamma_Y;\quad m' = \frac{m}{C_n};\quad \operatorname{tg}\varphi_1 = 2\gamma_X\frac{I_Z - I_Y}{I_X + I_Z - I_Y};$$

j_{X0}, j_{Y0}, j_{Z0} = linear accelerations in the base's motion relative to the corresponding axes; $C_\pi = C + (I_X - I_Y)\frac{2}{0}$ = total rigidity of the elastic system relative to the torsion bars' axis; m = the rotor's mass.

For arbitrary motion of the base, equation (2.92) is a non-steady-state one and its exact solution entails considerable difficulties. Therefore, let us take advantage of the method of successive approximations, which is widely used in gyroscopy [18]. Ignoring the terms of the higher order of smallness in the right side of (2.92), we obtain the OMG's equation of motion in the first approximation:

$$\begin{aligned} T^2\ddot{\psi} + 2\xi T\dot{\psi} + \psi = &-K_n\dot{\omega}_{Z0}\cos\omega_0 t - K_n\dot{\omega}_{Y0}\sin\omega_0 t + \\ &+ K_0\omega_{Z0}\sin\omega_0 t - K_0\omega_{Y0}\cos\omega_0 t + M_{ad}, \end{aligned} \tag{2.93}$$

where M_{ad} = adduced disturbing moment acting, in the first approximation, on the

rotor when the base is in motion. In order to find the motion of the OMG's rotor in the second approximation, we place the solution of the equation of the first approximation on the right side of equation (2.93) and solve the linear differential equation that is obtained, keeping only terms of the second order of smallness in the right side.

We will conduct our investigation of errors after provisionally dividing them into three groups: methodical, instrumental and operational.

Expressions for the signals at the instrument's output, in the presence of harmonic rocking of the base around the axes of sensitivity in the frequency pass band, can be derived from its transfer function (1.81) by replacing p with $i\omega_0$. If, for example, the base performs oscillations around the O_0Y_0 axis:

$$\omega_{Y0} = \omega_{Ya} \sin \omega t, \tag{2.94}$$

the signals at the OMG's demodulator's output have the form

$$\begin{aligned} 4u_1 &= -\{N(\omega_0 - \omega)(K_0 - K_n\omega)\cos[\omega t + \beta(\omega_0 - \omega)] + \\ &+ N(\omega_0 + \omega)(K_0 + K_n\omega)\cos[\omega t + \beta(\omega_0 + \omega)]\} K_{dm}\omega_{Ya}; \\ 4u_2 &= \{-N(\omega_0 - \omega)(K_0 - K_n\omega)\sin[\omega t + \beta(\omega_0 - \omega)] + \\ &+ N(\omega_0 + \omega)(K_0 + K_n\omega)\sin[\omega t + \beta(\omega_0 + \omega)]\} K_{dm}\omega_{Ya}, \end{aligned} \tag{2.95}$$

where

$$N = \sqrt{\frac{1}{(1 - T^2\omega^2)^2 + 4\xi^2T^2\omega^2}}; \quad \beta(\omega) = \operatorname{arctg}\frac{2\xi T\omega}{1 - T^2\omega^2};$$

K_{dm} = the demodulator's transfer factor.

From expressions (2.95) it follows that when there is harmonic rocking of the instrument's base, along with the basic signal (at the demodulator's first outlet) there appears a cross signal (at the second outlet), the magnitude of which with respect to the basic one increases as the frequency of the base's oscillations rises.

As was already stated in Section 2.1, a characteristic feature of RVG's operating on the principle of amplitude modulation is that when there are harmonic oscillations of the base in the instrument's plane of sensitivity that are on frequencies close to $2\omega_0$, at its outlets there appear error signals that are identical to useful signals from slowly changing angular velocities of the base.

The equivalent angular velocity of the base's motion can be found from expression (2.3), while for frequencies equal to $2\omega_0$ it is found from expression (2.5). With the given instrument accuracy, from (2.5) it is easy to obtain the allowable amplitudes of the base's angular oscillations with frequency $2\omega_0$ at the point where the instrument is mounted.

Let us discuss the methodical error that occurs in an OMG when there is angular motion of the base relative to the three axes. Without disrupting the commonality, we will limit ourselves to an investigation of the expression for the interference signal at only one of the demodulator's outlets, which--in the case of resonance tuning of the instrument and the presence of simultaneously permanent rotation of the base at speeds ω_{XC}, ω_{YC}, ω_{ZC} and angular vibrations with amplitudes ω_{Xa}, ω_{Ya}, ω_{Za}--has the following form:

$$2u_1 = K_{dm}\frac{1}{2\xi}\sqrt{\left\{-K_2\left(\omega_{XC}\omega_{YC}+\frac{1}{2}\omega_{Xa}\omega_{Ya}\right)+\right.}$$
$$+\frac{1}{2\xi}K_0K_1\omega_{XC}\omega_{YC}+\frac{1}{2}K_1\omega_{Xa}\omega_{ZYa}\left[-\frac{1}{2}N(\omega_0-\omega)\times\right.}$$
$$\left.\times(K_0-K_n\omega)\sin\beta_1+\frac{1}{2}N(\omega_0+\omega)(K_0+K_n\omega)\sin\beta_2\right]\Big\}^2+$$
$$+\left\{K_2\left(\omega_{XC}\omega_{ZC}+\frac{1}{2}\omega_{Xa}\omega_{Za}\right)-\frac{1}{2\xi}K_0K_1\omega_{XC}\omega_{ZC}-\right.}$$
$$-\frac{1}{2}K_1\omega_{Xa}\omega_{ZYa}\left[\frac{1}{2}N(\omega_0-\omega)(K_0-K_n\omega)\cos\beta_1+\right.}$$
$$\left.+\frac{1}{2}N(\omega_0+\omega)(K_0+K_n\omega)\cos\beta_2\right]\Big\}^2, \tag{2.96}$$

where

$$\omega_{ZY}=\sqrt{\omega_{Za}^2+\omega_{Ya}^2},\quad \beta_1=\operatorname{arctg}\frac{\omega_{Za}}{\omega_{Ya}}+\beta(\omega_0-\omega),\quad \beta_2=$$
$$=\operatorname{arctg}\frac{\omega_{Za}}{\omega_{Ya}}+\beta(\omega_0+\omega).$$

From expression (2.96) it follows that when there is permanent rotation of the instrument's base relative to an arbitrary axis, in it there appears the interference signal

$$2u_1=\frac{1}{2\xi}K_{dm}\left(\frac{1}{2\xi}K_0K_1-K_2\right)\omega_{XC}\omega_{ZYC}. \tag{2.97}$$

The ratio of the interference signal to the useful signal, allowing for the relationship $(1/2\xi)K_0K_1 >> K_2$, can be expressed in the following manner:

$$\Delta u_1\simeq\frac{\varkappa_Z}{\xi}\frac{\omega_{XC}}{\omega_0}\frac{\omega_{ZYC}}{\omega_{YC}}. \tag{2.98}$$

Expression (2.98) makes it possible to evaluate the accuracy of the measurement of the rotor's angular velocity as a function of the base's angular velocity relative to an axis that coincides with the rotor's axis of rotation. The smaller ξ (the greater the instrument's sensitivity) and the rotor's angular velocity ω_0 are, the greater this error is.

An evaluation of the additional error that occurs in connection with low-frequency rocking of the base, as made with expression (2.96), shows that this error is extremely small and does not have to be allowed for in connection with the real parameters involved in the rocking of objects and the real requirements for instrument accuracy. When there is angular vibration of the base, the error signal is evaluated with the simple expression

$$2u_1=\frac{1}{4\xi}K_{dm}K_2\omega_{Xa}\omega_{Za}, \tag{2.99}$$

while the base's equivalent angular velocity can be computed, with sufficient accuracy, with the formula

$$\omega_{eY} = \frac{1}{2}\frac{\varkappa_Z}{1+\varkappa_Z}\frac{\omega_{Za}\omega_{Xa}}{\omega_0}. \tag{2.100}$$

The error under discussion, which is caused by angular vibrations of the base, occurs only when the vibrations take place around an axis that does not coincide with the rotor's axis of rotation and does not lie in the plane of sensitivity.

Thus, expressions (2.97)-(2.100) make it possible to evaluate an instrument's methodical error when it is operating on a movable base. One of the basic factors resulting in instrument error is the presence of static disbalance of the rotor (Figure 13). In this case, when the instrument is operating on a base that is subjected to linear accelerations and vibrations, its rotor is affected by disturbing moments that, in accordance with the results presented in Section 2.2, lead to the appearance of error signals at the instrument's outlets. In the presence of static disbalance along the rotor's axis of rotation (characterized by coordinate a_X) and constant or slowly changing accelerations in the plane of sensitivity j_{ZYC}, these error signals, expressed in terms of equivalent angular velocities of the base, are described by the expressions

$$\left.\begin{aligned}\omega_{eZ} &= -\frac{ma_X}{I_Z(1+\varkappa_Z)\omega_0}j_{ZC};\\ \omega_{eY} &= -\frac{ma_X}{I_Z(1+\varkappa_Z)\omega_0}j_{YC}.\end{aligned}\right\} \tag{2.101}$$

Practical calculations show that high OMG accuracy (on the order of 10^{-2} °/h) under conditions of overloads of up to 10 g and more requires that the static balance along the rotor's axis of rotation be insured with an accuracy of several angstroms. Such high balancing accuracy can be achieved only by the use of special methods that utilize the system for measuring the rotor's angle of rotation that is already available in the instrument.

In the presence of linear vibrations of the base with frequencies $q = \omega_0$ and $q = 2\omega_0$ (as well as frequencies close to them) and amplitudes j_{Xa}, j_{Ya}, j_{Za}, at the instrument's outlets there also appear interference signals. In the second case, when $j_{Z0} = j_{Za}\cos 2\omega_0 t$ and $j_{Y0} = j_{Ya}\cos 2\omega_0 t$, the base's equivalent velocities of rotation have the form

$$\left.\begin{aligned}\omega_{eY} &= \frac{1}{2}\frac{ma_X}{I_Z(1+\varkappa_Z)\omega_0}j_{Ya};\\ \omega_{eZ} &= -\frac{1}{2}\frac{ma_X}{I_Z(1+\varkappa_Z)\omega_0}j_{Za},\end{aligned}\right\} \tag{2.102}$$

and in the first,

$$\left.\begin{aligned}\omega_{eY} &= -\frac{ma_Y}{I_Z(1+\varkappa_Z)\omega_0}j_{Xa}\sin\varphi_a;\\ \omega_{eZ} &= -\frac{ma_Y}{I_Z(1+\varkappa_Z)\omega_0}j_{Xa}\cos\varphi_a,\end{aligned}\right\} \tag{2.103}$$

where φ_B = phase of the vibrations with respect to the rotor's angular velocity. The value of the interference signal for identical overloads is of the same order as when constant linear accelerations are affecting the instrument. In order to reduce this interference it is possible to cushion the instrument, when the parameters of the disturbances are known, to select the rotor's angular velocity so that the vibration overloads in the area of frequencies ω_0 and $2\omega_0$ will be minimal. In addition to this, there exist special methods for reducing this interference [32].

When linear accelerations and vibrations act simultaneously along all three axes of an instrument, the error signal's additional component can be expressed in terms of equivalent angular velocity:

$$\omega_Y = \frac{m}{I_Z(1+\varkappa_Z)\omega_0}\left\{\frac{m'}{2\xi}a_X^2 j_{XC} j_{YC} - \right.$$
$$- a_Y \sqrt{m' a_Y N^2(q) j_{Xa} j_{ZYa} + (m' a_Y j_{XC} + K_3)^2 j_{ZYa}^2 +}$$
$$+ \sqrt{+ 2m' a_Y (m' a_Y j_{XC} + K_3) j_{ZYC} j_{ZYa} j_{Xa} N(q) \sin\beta -} \qquad (2.104)$$
$$\left. - \frac{1}{4} m' a_X^2 j_{Xa} j_{ZYa} [N(\omega_0 + q) - N(\omega_0 - q)]\right\}.$$

It should be mentioned here that in the case of instrument operation on a vibrating base, in addition to those that have already been discussed, in it there can appear additional interference signals with the following relationships of the frequencies of the angular and linear vibrations and the rotor's rotation frequency [5]:

$$\nu_i \approx 0, \qquad (2.105)$$

where

$$\nu_1 = \omega_0 - \omega; \quad \nu_2 = q - \omega_0; \quad \nu_3 = \omega - q;$$
$$\nu_4 = 2\omega_0 - q; \quad \nu_5 = \omega - 2q; \quad \nu_6 = 2\omega - q;$$
$$\nu_7 = 3\omega_0 - q; \quad \nu_{8-9} = 2\omega_0 - q \pm \omega; \quad \nu_{10} = 2\omega_0 + q - \omega;$$
$$\nu_{11-12} = q \pm \omega - \omega_0; \quad \nu_{13-14} = \omega_0 - \omega \pm q; \quad \nu_{15-16} = 3\omega_0 - q \pm \omega.$$

The magnitude of these errors is much less than those presented above. However, when designing an instrument the value of ω_0 should be chosen so as to reduce as much as possible the intensity of the vibrations close to the frequencies found from (2.105).

An investigation of the effect of dynamic disbalance of the rotor on instrument error showed that it is negligibly small for the basic signal and can be manifested only as some increase in the level of the cross signal that appears when there are constant angular velocities of the base and that, in connection with this, is smaller than the basic signal by a factor of $[1/2\gamma_X]/[I_Z(1 + \varkappa_Z)/(I_Z - I_Y)]$.

During the analysis of methodical OMG errors it was shown that one of the basic causes of instrument error is angular vibrations of the base with a frequency of $2\omega_0$. In practice, such vibrations are inherent in any rotating bodies, as well as the rotating part of an OMG. In connection with this, it has been proven experimentally that the vibrations' amplitude depends on the quality of the realization of the supports and the dynamic and static disbalance of the OMG's rotating part. In [13] the author presents a quite complete technique for investigating the reaction of ball-bearing supports to the appearance of vibrations caused by rotating bodies. Therefore, here we will examine the effect of static and dynamic disbalance on the appearance of angular vibrations with a frequency of $2\omega_0$ in the rotating part of an OMG. It is obvious that such a phenomenon takes place when there is varying rigidity in different radial directions in the main rotation supports.

Let the radial rigidity of the main rotation supports be different in different directions. We will designate the radial rigidity of the left support as C_{01} and that of the right support as C_{02} (Figure 14). In the case of an infinitely rigid

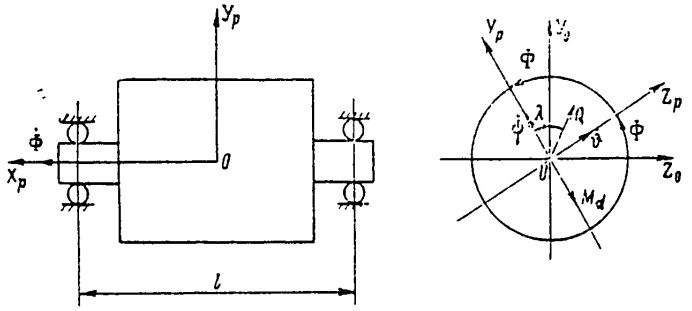

Figure 14. Diagram of effect of disturbing factors on the rotating part of an RVG.

shaft and rotor, the total angular rigidity of the rotor-shaft-support system will then be determined by the expression

$$C_0 = l^2 \frac{C_{01} C_{02}}{C_{01} + C_{02}}, \tag{2.106}$$

where ℓ = distance between the supports.

In the presence of a force acting in a plane perpendicular to the main axis of rotation, from the side of the supports the rotor will be acted on by reaction moment M_p, the vector of which lies in the same plane and is perpendicular to the force's vector. Let us determine the moments acting on the rotor in the system of coordinates that is rotating along with it. Let Q be the force generated by the static disbalance of the OMG's rotating part, while M_d is the moment generated by its dynamic disbalance (Figure 14). According to [21], the expressions for Q and M_d have the form

$$Q = m_p \dot{\Phi}^2 a_{ZY}; \tag{2.107}$$

$$M_d = (I - I_e) \varepsilon \dot{\Phi}^2, \tag{2.108}$$

where m_p = mass of the OMG's rotating part; a_{ZY} = displacement of its center of mass relative to the axis of rotation in the plane of rotation; I, I_e = axial and equatorial moments of inertia; ε = angle between the main axis of inertia and the axis of rotation.

In the $X_p O_p Z_p$ plane, the following radial force acts on the left support:

$$F_1 = \frac{1}{2}\left(Q \sin\lambda - \frac{M_d}{l}\right), \tag{2.109}$$

while on the right support it is

$$F_2 = \frac{1}{2}\left(Q \sin\lambda + \frac{M_d}{l}\right). \tag{2.110}$$

As a result of this the rotor will turn through angle ψ_p, which is determined quite accurately by the expression

$$\psi_p = \frac{1}{l}\left(\frac{F_2}{C_{02}} - \frac{F_1}{C_{01}}\right). \tag{2.111}$$

On the other hand, according to Hooke's Law we have

$$M_{Yp} = C_0 \psi_p, \tag{2.112}$$

where C_0 is determined by expression (2.106). Substituting (2.111) into (2.112), we obtain the expression for the moment acting on the rotor along the O_pY_p axis:

$$M_{Yp} = \frac{1}{2} l \frac{1}{C_{01} + C_{02}} \left[- \left(Q \sin \lambda - \frac{M_d}{l} \right) C_{01} + \right. \\ \left. + \left(Q \sin \lambda + \frac{M_d}{l} \right) C_{02} \right]. \tag{2.113}$$

Analogously we find the moment acting along the OZ axis:

$$M_{Zp} = \frac{1}{2} l \frac{C_{02} - C_{01}}{C_{02} + C_{01}} Q \cos \lambda. \tag{2.114}$$

The radial rigidity of the supports is not the same in different directions because of nonuniformity of the material's properties, deviations of the geometric shapes of the supports' elements from the ideal, and the nonlinear dependence of the supports' pliability on the stresses. Thus, radial rigidity can be regarded as a periodic function of angle $\Phi = \omega_0 t$, with period 2π.

Considering what has been said above, along with conditions (2.113) and (2.114), let us write the equations of motion of the OMG's rotating part in the system of coordinates that is rigidly coupled with it:

$$I_e \ddot{\vartheta}_p + H \dot{\psi}_p + l^2 \frac{C_{01}\left(\Phi + \frac{\pi}{2} \operatorname{sign}(Q \cos \lambda)\right) C_{02}\left(\Phi + \frac{\pi}{2} \operatorname{sign}(Q \cos \lambda)\right)}{C_{01}\left(\Phi + \frac{\pi}{2} \operatorname{sign}(Q \cos \lambda)\right) + C_{02}\left(\Phi + \frac{\pi}{2} \operatorname{sign}(Q \cos \lambda)\right)} \vartheta_p = \\ = -\frac{1}{2} l \frac{C_{01}\left(\Phi + \frac{\pi}{2} \operatorname{sign}(Q \cos \lambda)\right) - C_{02}\left(\Phi + \frac{\pi}{2} \operatorname{sign}(Q \cos \lambda)\right)}{C_{01}\left(\Phi + \frac{\pi}{2} \operatorname{sign}(Q \cos \lambda)\right) + C_{02}\left(\Phi + \frac{\pi}{2} \operatorname{sign}(Q \cos \lambda)\right)} Q \cos \lambda; \tag{2.115}$$

$$I_e \ddot{\psi}_p - H \dot{\vartheta}_p + l^2 \frac{\begin{array}{c} C_{01}\left(\Phi + \frac{\pi}{2} - \frac{\pi}{2} \operatorname{sign}\left(Q \sin \lambda + \frac{M_d}{l}\right)\right) \times \\ \times C_{02}\left(\Phi + \frac{\pi}{2} - \frac{\pi}{2} \operatorname{sign}\left(Q \sin \lambda - \frac{M_d}{l}\right)\right) \end{array}}{\begin{array}{c} C_{01}\left(\Phi + \frac{\pi}{2} - \frac{\pi}{2} \operatorname{sign}\left(Q \sin \lambda + \frac{M_d}{l}\right)\right) + \\ + C_{02}\left(\Phi + \frac{\pi}{2} - \frac{\pi}{2} \operatorname{sign}\left(Q \sin \lambda - \frac{M_d}{l}\right)\right) \end{array}} \psi_p = \\ = -\frac{1}{2} l \frac{\begin{array}{c} C_{01}\left(\Phi + \frac{\pi}{2} - \frac{\pi}{2} \operatorname{sign}\left(Q \sin \lambda + \frac{M_d}{l}\right)\right) - \\ - C_{02}\left(\Phi + \frac{\pi}{2} - \frac{\pi}{2} \operatorname{sign}\left(Q \sin \lambda - \frac{M_d}{l}\right)\right) \end{array}}{\begin{array}{c} C_{01}\left(\Phi + \frac{\pi}{2} - \frac{\pi}{2} \operatorname{sign}\left(Q \sin \lambda + \frac{M_d}{l}\right)\right) + \\ + C_{02}\left(\Phi + \frac{\pi}{2} - \frac{\pi}{2} \operatorname{sign}\left(Q \sin \lambda - \frac{M_d}{l}\right)\right) \end{array}} Q \sin \lambda - M_d.$$

Let us examine the case where $0 < M_d/l < Q \sin \lambda$ and $0 < Q \cos \lambda$. Equations (2.115) will then be written in the form

$$I_e \ddot{\vartheta}_p + H \dot{\psi}_p + l^2 F\left(\Phi + \frac{\pi}{2}\right) \vartheta_p = -\frac{1}{2} l F_d\left(\Phi + \frac{\pi}{2}\right) Q \cos \lambda; \\ I_e \ddot{\psi}_p - H \dot{\vartheta}_p + l^2 F(\Phi) \psi_p = \frac{1}{2} l F_d(\Phi) Q \sin \lambda - M_d. \tag{2.116}$$

Functions F and F_d satisfy Dirichlet's conditions and can be expanded into Fourier series:

$$F(\Phi) = F_0 + \sum_{n=1}^{\infty} \Delta F_n \sin(n\Phi + \varphi_n); \tag{2.117}$$

$$F_d\left(\Phi + \frac{\pi}{2}\right) = F_{d0} + \sum_{n=1}^{\infty} \Delta F_{dn} \sin(n\Phi + \varphi_{dn}), \tag{2.118}$$

where F_{d0} characterizes the average moment (during a single revolution) that is applied to the rotor and appears because of the inequality of the average radial rigidities C°_{01} and C°_{02} of the left and right supports. Monotypical, precision supports are most often used in these instruments, so we can assume that $C^{\circ}_{01} = C^{\circ}_{02}$ and $F_d = 0$.

In equation (2.16), the terms with ΔF_n and ΔF_{dn}, as determined by the nonuniform rigidity of the supports as functions of angle Φ, are terms of a higher order of smallness, so in order to integrate this equation we use the method of successive approximations. In connection with this, the equations of the first approximation have the obvious solution

$$\vartheta_p = 0; \ \psi_p = -\frac{M_d}{l^2 F_0}. \tag{2.119}$$

Substituting solution (2.119) of the first approximation's equations into the right side of the second approximation's equations, we write them as

$$\begin{aligned} I_e\ddot{\vartheta}_p + H\dot{\psi}_p + l^2F_0\vartheta_p &= -\frac{1}{2}Ql\cos\lambda \sum_{n=1}^{\infty} \Delta F_{dn} \sin\left(n\omega_0 t + n\frac{\pi}{2} + \varphi_{dn}\right); \\ I_e\ddot{\psi}_p - H\dot{\vartheta}_p + l^2F_0\psi_p &= -\frac{M_d}{l^2F_0}\sum_{n=1}^{\infty} \Delta F_n \sin(n\omega_0 t + \varphi_n) + \\ &+ \frac{1}{2}Ql\sin\lambda \sum_{n=1}^{\infty} \Delta F_{dn}\sin(n\omega_0 t + \varphi_{dn}), \end{aligned} \tag{2.120}$$

where $\lambda^2 F_0$ = average (during a single revolution) rigidity of the rotor-shaft-support system.

An error can appear in an RVG only if the instrument's rotating part completes oscillations with a frequency of ω_0 in the system of coordinates that is coupled with it; this occurs only when n = 1.

The velocities of the rotating part's angular oscillations around the OZ_p and OY_p axes will be expressed by the relationships

$$\begin{aligned} \dot{\vartheta}_p &= \frac{\omega_0}{(-I_e\omega_0^2 + l^2F_0)^2 + (H\omega_0)^2}\left\{\frac{1}{2}Ql\,\Delta F_{d1}\left[(-I_e\omega_0^2 + l^2F_0)\cos\lambda + \right.\right. \\ &+ H\omega_0\sin\lambda\left]\sin(\omega_0 t + \varphi_{d1}) - \frac{M_d}{l^2F_0}\Delta F_1 H\omega_0\sin(\omega_0 t + \varphi_1)\right\}; \\ \dot{\psi}_p &= \frac{\omega_0}{(-I_e\omega_0^2 + l^2F_0)^2 + (H\omega_0)^2}\left\{\frac{1}{2}Ql\,\Delta F_{d1}\left[H\omega_0\cos\lambda + \right.\right. \\ &+ (-I_e\omega_0^2 + l^2F_0)\sin\lambda\left]\cos(\omega_0 t + \varphi_{d1}) - \right. \\ &\left. - \frac{M_d}{l^2F_0}\Delta F_1(-I_e\omega_0^2 + l^2F_0)\cos(\omega_0 t + \varphi_1)\right\}. \end{aligned} \tag{2.121}$$

Analogous expressions can also be derived for the relationships Q and M_d, as well as angle λ.

In order to determine the OMG error caused by nonuniformity of the supports' rigidity and disbalance of the instrument's rotating part, it is necessary to find the projections of angular velocities $\dot{\vartheta}_p$ and $\dot{\psi}_p$ on the instrument's axes of sensitivity and substitute them into expression (2.5). Overloading in the instrument's plane of sensitivity also results in the appearance of an error when the supports' radial rigidity is not uniform. Its magnitude can be evaluated with the technique presented above. The technical measures contributing to a reduction in the error can be as follows:
careful dynamic and static balancing of the rotating part;
increasing the angular rigidity of the main rotation supports;
reducing the value of the angular nonuniformity of the supports' rigidity, which can be achieved by reducing the permissible tolerances for the geometrical shape of the supports' elements, properly selecting the bearings and the "favorable" mutual orientation of their outer rings, and creating the appropriate axial tightness.

In conclusion, let us discuss the OMG error arising because of a change in the instrument's basic parameters while it is in operation. As has already been pointed out in Section 2.3, the basic source of this error is the disruption of resonance tuning. In accordance with (2.79), detuning for an OMG is determined by the expression

$$\Delta = \frac{\omega_0}{2}\left[(1-\varkappa_Z)\left(\frac{\Delta C}{C}-\frac{\Delta I_Z}{I_Z}-2\frac{\Delta\omega_0}{\omega_0}\right)+\Delta\varkappa_Z\right], \tag{2.122}$$

where ω_0, C, I_Z, $\varkappa_Z$ = rated values of the parameters insuring resonance tuning of an OMG.

From (2.122) it follows that in order to achieve a substantial reduction in the effect of a change in an instrument's basic parameters on its detuning from the resonance mode, it is necessary to provide a rotor configuration such that $\varkappa_Z \to 1$. If the changes in the parameters arise as the result of changes in the temperature conditions, detuning can be reduced by selecting the appropriate materials for the rotor and the torsion bars [31].

Detuning from the resonance mode leads to a change in an instrument's transfer factor that, in accordance with (2.78), can be determined from the expression

$$K_{\frac{q}{r}} = \frac{1+\varkappa_Z}{2\omega_0}\frac{1}{2\xi}\frac{1+i\frac{\Delta}{\xi}}{1+\left(\frac{\Delta}{\xi}\right)^2}. \tag{2.123}$$

In order to maintain stable operation of a highly sensitive instrument it is necessary that the condition $\Delta << \xi$ be fulfilled when it is in operation.

From an analysis of OMG errors it follows that a significant reduction can be achieved in them by adopting a structural solution in which $\varkappa_Z \to 1$. However, from the dynamic tuning condition it follows that in this case the torsion bars' torsional rigidity will converge on zero. Reducing the torsion bars' torsional rigidity results in a reduction in their load-bearing capacity; that is, their capability to insure the instrument's nondestructability and ability to operate under large constant, impact and vibrational overloads.

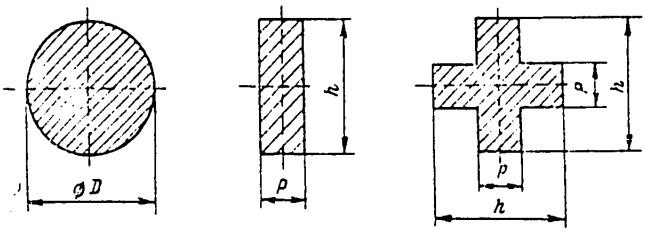

Figure 15. Torsion bar cross-sections.

Let us discuss the dependence of the strength characteristics of torsion bars on an instrument's other parameters. Torsion bars are usually made in the form of tension members that are either in one piece with the rotor or are made separately and then press-fitted into it. Torsion bars can have cross-sections of various shapes. They are most frequently circular, rectangular or cross-shaped (Figure 15). When their cross-section is constant throughout their entire length l_t and there is no axial tightening, the torsional rigidity of such torsion bars is determined by the following expressions [39]:

a) for a circular cross-section--

$$C = \frac{\pi D^4}{32 l_\tau} G, \tag{2.124}$$

where G = shear modulus of the torsion bar's material;

b) for a rectangular cross-section--

$$C = \beta_n p^3 h \frac{G}{l_\tau}, \quad p < h, \tag{2.125}$$

where β_π is a function of the ratio h/p;

c) for a cruciform cross-section--

$$C = \beta_к p^3 h \frac{G}{l_\tau}, \tag{2.126}$$

where $\beta_к$ is a function of the ratio h/2p.

By substituting expressions (2.124)-(2.126) into the dynamic tuning condition, it is possible to relate the torsion bars' geometric dimensions to the moment of inertia of the rotor relative to the torsion bars' axis I_Z and the angular velocity ω_0.

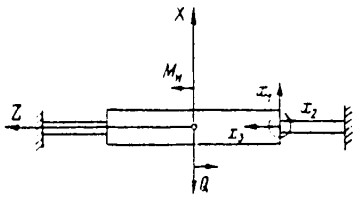

Figure 16. Diagram of effect of force Q and bending moment M_i on an OMG rotor.

In order to calculate the strength of torsion bars, let us determine the stresses arising in them under the influence of two factors: the force Q applied in the rotor's center of mass along its axis of rotation and the bending moment M_i directed along the rotor's OY axis (Figure 16). This system is statically indeterminate. In order to disclose the indeterminacy, we will free the right torsion bar's left end and apply to it forces x_1 and x_3 and moment x_2. The canonical equations of the method of forces [39] will then have the form

$$\delta_{11}x_1 + \delta_{12}x_2 + \delta_{13}x_3 + \delta_{1Q} = 0;$$
$$\cdots\cdots\cdots$$

$$\cdots\cdots\cdots$$

$$\delta_{21}x_1 + \delta_{22}x_2 + \delta_{23}x_3 + \delta_{2Q} = 0; \qquad (2.127)$$

$$\delta_{31}x_1 + \delta_{32}x_2 + \delta_{33}x_3 + \delta_{3Q} = 0,$$

where $\delta_{ik} = \delta_{ki}$ = relative displacement of the system's points in the direction of the i-th force factor when acted upon by a single force factor replacing the k-th factor.

The basic movements in the system under discussion are determined by flexure. Therefore, we will ignore shear and tension, assuming that $\delta_{33} = \delta_{31} = \delta_{32} = \delta_{13} = \delta_{23} = 0$. By using (Mor's) integration, we then obtain the following expressions for the other movements:

$$\delta_{11} = \frac{1}{IE}\left(a^2 + 3a l_\tau + \frac{8}{3} l_\tau^2\right); \quad \delta_{12} = \delta_{21} =$$

$$= \frac{1}{IE} l_\tau (a + 2l_\tau); \quad \delta_{22} = \frac{1}{IE} 2l_\tau;$$

$$\delta_{1Q} = -\frac{Q}{IE}\frac{1}{2} l_\tau \left(a^2 + \frac{5}{2} a l_\tau + \frac{5}{3} l_\tau^2\right); \quad \delta_{2Q} = \qquad (2.128)$$

$$= -\frac{Q}{IE}\frac{1}{2} l_\tau (a + l^\tau);$$

$$\delta_{1M} = -\frac{M_i}{IE}\frac{1}{2} l_\tau (2a + 3l_\tau); \quad \delta_{2M} = -\frac{M_i}{IE} l_\tau,$$

where I = moment of inertia of the torsion bars' cross-section; E = modulus of elasticity of the torsion bars' material. Substituting the values of δ_{ik} from (2.128) into (2.127), we determine the unknown reactions to x_1 and x_2 in the case of being acted upon by:
force Q--

$$x_1 = \frac{1}{2} Q, \; x_2 = -\frac{1}{4} Ql; \qquad (2.129)$$

moment M_i--

$$x_1 = \frac{a + l_\tau}{a^2 + 2al_\tau + \frac{4}{3} l_\tau^2} M_i, \; x_2 = -\frac{\frac{1}{2} l_\tau a + \frac{1}{3} l_\tau^2}{a^2 + 2al_\tau + \frac{4}{3} l_\tau^2} M_i. \qquad (2.130)$$

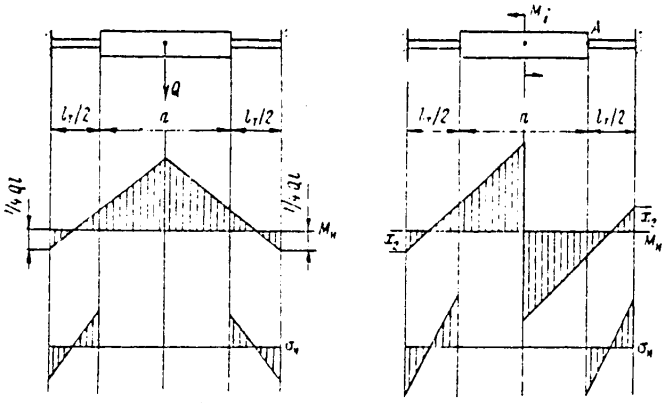

Figure 17. Stress sheets.

The summary diagrams of the bending moments for the first and second cases, as well as the corresponding stress sheets, are presented in Figure 17. From the diagrams

it follows that the greatest stresses occurring when acted upon by transverse force Q arise at the points where the torsion bars are attached and can be calculated with the help of the following expression [39]:

$$\sigma_{max} = \frac{1}{4} Ql \frac{Y_{max}}{I}, \tag{2.131}$$

where Y_{max}/I = moment of resistance of the torsion bars' cross-section.

Using resonance tuning condition (1.68) and expressions (2.129) and (2.131), we obtain the formula for computing the values of the maximum stresses in the cross-sections of the three different types of torsion bars under discussion:
for a circular cross-section--

$$\sigma_{max} = \frac{1}{4} \frac{G}{I_Z (1 - \varkappa_Z) \omega_0^2} DQ; \tag{2.132}$$

for a rectangular cross-section--

$$\sigma_{max} = \frac{3}{4} \beta_n \frac{G}{I_Z (1 - \varkappa_Z) \omega_0^2} pQ, \quad \sigma_{max\ Z} = \sigma_{max\ Y} \frac{p}{h}, \tag{2.133}$$

where β_n = 0.41 when p = h;
for a cruciform cross-section--

$$\sigma_{max} = \frac{3}{4} \beta_k \frac{G}{I_Z (1 - \varkappa_Z) \omega_0^2} \frac{1}{1 + \frac{h^2}{p^2} - \frac{p}{h}} hQ. \tag{2.134}$$

From expressions (2.132)-(2.134) it follows that the higher the rotor's angular velocity, the smaller the stresses in the torsion bars. The maximum stresses do not depend on the length of the torsion bars. Therefore, from the viewpoint of strength it is more favorable to have short and thick torsion bars. In the case of a cruciform cross-section, the larger the value of ratio h/p that can be provided, the smaller the stresses. From the viewpoint of achieving maximum strength, cruciform torsion bars are the most preferable of the three types under discussion. If the maximum possible load on the rotor, the parameters of the torsion bars and the maximum allowable stresses in their material, the limitations on the value of $\varkappa_Z$ can be derived from (2.132)-(2.134).

An important characteristic of the rotor-torsion bar elastic system is its flexural rigidity when acted upon by a moment directed along the rotor's OY axis. Using the stress diagrams that have been compiled and Mor's integration, we obtain the expression for the linear movement of point A (see Figure 16) when acted upon by moment M_i:

$$\delta = \frac{1}{2} l_T^2 \frac{1}{IE} M_i. \tag{2.135}$$

In this case, the system's static flexural rigidity will be determined by the expression

$$C_n = C_{i.t} \frac{a}{l_T}, \tag{2.136}$$

where $C_{i.t}$ = flexural rigidity of the torsion bars, which can be derived from the following relationships:
for a circular cross-section--

$$C_{i.\tau} = \frac{\pi D^4}{64} \frac{E}{l_\tau}; \tag{2.137}$$

for a rectangular cross-section--

$$C_{i.\tau Y} = \frac{1}{6} p^3 h \frac{E}{l_\tau}, \quad C_{i.\tau Z} = \frac{1}{6} h^3 p \frac{E}{l_\tau}; \tag{2.138}$$

for a cruciform cross-section--

$$C_{i.\tau} = \frac{1}{6} p \left[h (p^2 + h^2) - p^3 \right] \frac{E}{l}. \tag{2.139}$$

Let us evaluate the ratio of the torsional and flexural rigidities (when the rotor is rotating relative to the OY and OZ axes, respectively) for torsion bars with different cross-sections. Allowing for the total rigidity of the elastic system and the fulfillment of the resonance tuning condition, this ratio has the form

$$\frac{C_Z}{C_Y} = \frac{1}{\frac{C_{i.\tau}}{I_Z \omega_0^2} + \frac{I_X}{I_Z} - 1}. \tag{2.140}$$

Keeping in mind the relationship between C and $C_{i.t}$, we obtain the following expressions for different torsion bar cross-sections:
for a circular cross-section--

$$\frac{C_Z}{C_Y} = \frac{1}{\frac{a}{l_\tau} \frac{E}{G} (1 - \varkappa_Z) + \frac{I_X}{I_Z} - 1}; \tag{2.141}$$

for a square cross-section--

$$\frac{C_Z}{C_Y} = \frac{1}{1{,}19 \frac{a}{l_\tau} \frac{E}{G} (1 - \varkappa_Z) + \frac{I_X}{I_Z} - 1}; \tag{2.142}$$

for a cruciform cross-section--

$$\frac{C_Z}{C_Y} = \frac{1}{0{,}168 \left(1 + \frac{h^2}{p^2} - \frac{p}{h} \right) \frac{a}{l_\tau} \frac{E}{G} (1 - \varkappa_Z) + \frac{I_X}{I_Z} - 1}. \tag{2.143}$$

Torsion bars with a cruciform cross-section have the smallest C_Z/C_Y ratio. In connection with this, the smaller the value of $1 - \varkappa_Z$, the more commensurate rigidities C_Y and C_Z are. In this case the instrument's errors and dynamics should be defined more precisely according to the equations that describe the functioning of an OMG with two degrees of freedom in the plane of sensitivity.

CHAPTER 3. COMPOSITE ROTOR VIBRATION GYROSCOPES

3.1. Principles of the Construction of Composite Rotor Vibration Gyroscopes

An analysis of the functioning of various RVG systems shows that when the rotor's center of mass is displaced relative to the suspension axes' point of intersection, most of them react to linear accelerations of the base in the same manner as they do to its linear velocities. This leads to errors in the readings that can be reduced only by careful static balancing. At the same time, in the case of segregation of signal components caused by the base's angular velocities and its linear acceleration, this property makes it possible to create an instrument that measures simultaneously both the absolute angular velocities and the linear accelerations of the base's motion. We will call such instruments composite RVG's. The principles of the construction of these RVG's are explained in [43].

In order to segregate signal components, it is necessary to know the characteristic features of each of them. It is obvious that these components can be segregated neither by a frequency nor by a phase feature. The feature used can be only the sign of the component. The signal component that is proportional to the angular velocities changes sign when the direction of the drive motor's angular velocity ω_0 does, while the component that is proportional to the linear accelerations changes sign when the sign of coordinate a_X of the displacement of the rotor's center of mass does.

When constructing a composite RVG it is necessary to have two signals, in one of which only one component differs in sign from the one analogous to it in the other. The other signal parameters must be identical. From this it follows that in order to construct a composite RVG it is necessary to have two identical oscillatory systems that differ from each other either in the drive motor's direction of rotation or by the sign of the coordinate of the displacement of the rotor's center of mass relative to the suspension axes' point of intersection.

In the first case we must have two independent RVG's with parameter values that are extremely close to each other. It should be mentioned here that the creation of a composite instrument according to such a principle is also possible through the use of classical two- and three-stage gyroscopes, although the preservation with the required degree of accuracy of the identity of the parameters in these instruments, which are usually of a complicated, prefabricated type, is practically unrealizable.

In the second case, both oscillatory systems can be mounted on the shaft of a single drive motor. Such a method of instrument construction is most rational, since it

makes it possible to reduce the instrument's dimensions substantially and does not require (as it does in the first case) synchronization of the angular velocities (when different drive motors are used) or the use of reversing (when a single drive motor is used).

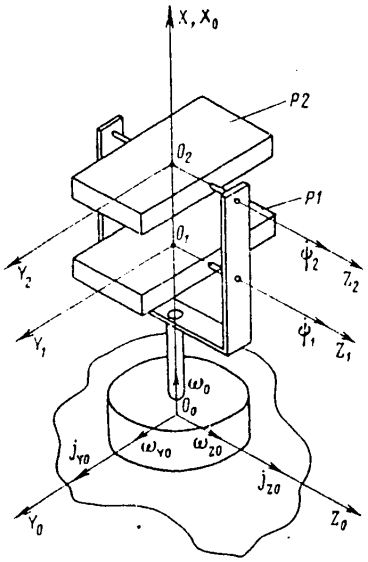

Figure 18. Diagram of composite RVG with independent suspension of the rotors.

A composite RVG can be built on the basis of the different RVG layouts described in the preceding chapters. However, taking into consideration the requirement for the greatest possible overall identity of the oscillatory systems' parameters, preference should be given to the structurally most simply realizable OMG setup.

Figure 18 is a diagram of a composite instrument (KOMG) based on two OMG's. To the shaft of a drive motor rotating with angular velocity ω_0, two rotors are attached, each by its own pair of torsion bars. The rotors' suspension (measuring) axes are situated parallel to each other in a single plane. The rotors' centers of mass are displaced, relative to their suspension axis, along axis of rotation OX by the values a_{X1} and a_{X2}.

As was demonstrated in [43], it is also possible for the torsion bars' axes to be placed perpendicular to each other. However, although in the first case angular vibrations of the PD's shaft with frequency $2\omega_0$, which give rise to errors in the measurement of absolute angular velocities, have practically no effect on the accuracy of the measurement of linear accelerations, in the second case the opposite is true: their effect on the accuracy of the measurement of absolute angular velocities is insignificant, but during the measurement of linear accelerations it is very tangible. Thus, the advantage can be given to either system, depending on the formulation of the problem. There are no other differences in systems with parallel and perpendicular positioning of the torsion bars, so let us discuss the former.

From (2.92) it follows that, in the first approximation, the rotors' equations of motion relative to the measuring axes have the form

$$\left.\begin{aligned} &I_{X1}\ddot{\psi}_1 + \mu_1\dot{\psi}_1 + [(I_{X1} - I_{Y1})\,\omega_0^2 + C_1]\,\psi_1 = -I_{Z1}\dot{\omega}_{Z0}\cos\omega_0 t - \\ &- I_{Z1}\dot{\omega}_{Y0}\sin\omega_0 t + (I_{Z1} + I_{X1} - I_{Y1})\,\omega_0\omega_{Z0}\sin\omega_0 t - \\ &- (I_{Z1} + I_{X1} - I_{Y1})\,\omega_0\omega_{Y0}\cos\omega_0 t + m_{p1}a_{X1}j_{Z0}\sin\omega_0 t - \\ &- m_{p1}a_{X1}j_{Y0}\cos\omega_0 t; \\ &I_{Z2}\ddot{\psi}_2 + \mu_2\dot{\psi}_2 + [(I_{X2} - I_{Y2})\,\omega_0^2 + C_2]\,\psi_2 = -I_{Z2}\dot{\omega}_{Z0}\cos\omega_0 t - \\ &- I_{Z2}\dot{\omega}_{Y0}\sin\omega_0 t + (I_{Z2} + I_{X2} - I_{Y2})\,\omega_0\omega_{Z0}\sin\omega_0 t - (I_{Z2} + \\ &+ I_{X2} - I_{Y2})\,\omega_0\omega_{Y0}\cos\omega_0 t + m_{p2}a_{X2}j_{Z0}\sin\omega_0 t - \\ &- m_{p2}a_{X2}j_{Y0}\cos\omega_0 t. \end{aligned}\right| \qquad (3.1)$$

In equations (3.1), subscript "1" refers to the first rotor (R1), and "2" to the second rotor (R2).

Let us discuss the case where the values of the parameters of both oscillatory systems equal each other, while the rotors' centers of mass are displaced to different sides at equal distances from the suspension axis ($a_{X2} = -a_{X1}$). By subtracting and adding, term-by-term, the equations in system (3.1), we obtain

$$I_Z\ddot{\alpha}_C + \mu\dot{\alpha}_C + [(I_X - I_Y)\omega_0^2 + C]\alpha_C = -2I_Z\dot{\omega}_{Z0}\cos\omega_0 t - \\ - 2I_Z\dot{\omega}_{Y0}\sin\omega_0 t + 2(I_Z + I_X - I_Y)\omega_0\omega_{Z0}\sin\omega_0 t - \\ - 2(I_Z + I_X - I_Y)\omega_0\omega_{Y0}\cos\omega_0 t; \qquad (3.2)$$

$$I_Z\ddot{\alpha}_\pi + \mu\dot{\alpha}_\pi + [(I_X - I_Y)\omega_0^2 + C]\alpha_\pi = m_p a_X j_{Z0}\sin\omega_0 t - \\ - m_p a_X j_{Y0}\cos\omega_0 t,$$

where

$$\alpha_C = \psi_1 + \psi_2;\ \alpha_\pi = \psi_1 - \psi_2.$$

Thus, the rotors' total angle of rotation relative to their measuring axes will be proportional to the base's angular velocity in the instrument's plane of sensitivity, while the difference between the rotors' angles of rotation is proportional to the base's linear accelerations in the same plane.

The information can be extracted by three different methods. First, by summing and subtracting the appropriate signals at the demodulators' outlets. In this case each OMG has its own signal reading and processing system. Secondly, by summing and subtracting the amplitude-modulated signals at the outputs of the sensors of the rotors' angles of rotation. Here, each OMG has its own rotor rotation angle sensor, while further processing of the information takes place individually, over an angular velocity measurement channel and a linear acceleration measurement channel. Finally, in the third case signal separation by channels is possible by using angle measurers, one of which measures the rotors' total angle of rotation α_C directly, while the other measures the difference angle α_π. It is obvious that such measurers can be constructed on the basic of well-known inductance and capacitance angle measurers. Of the three signal separation methods listed, the last is the most preferable, since it eliminates completely the effect of nonidentity of the parameters of the different information reading and processing system channels on cross communications between the angular velocity and linear acceleration measurement channels.

From (3.2) it follows that the functioning of a KOMG with respect to the angular velocity measurement channel is practically the same as that of the OMG, the features of which were described in Chapter 2, except for the fact that its transfer factor is doubled.

Let us evaluate how the instrument's basic parameters are related to the characteristics of the linear acceleration measurement channel. It is not difficult to see that motion of the base in the instrument's plane of sensitivity ZOY, with constant linear accelerations $\bar{j}$, leads to a signal at the KOMG's output that is equivalent to the signal that appears when the base rotates at a constant angular velocity $\bar{\omega}_e$, as determined by the expression

$$\bar{\omega}_e = \frac{m_p a_X}{I_z(1 + \varkappa_Z)\omega_0}\bar{j}. \qquad (3.3)$$

This expression makes it possible to relate the basic characteristics (such as sensitivity, linearity of the characteristic, sensitivity threshold and measurement range) of a composite instrument used to measure linears accelerations to the analogous characteristics of an OMG. The sensitivity threshold for the measurement of linear accelerations $|\bar{j}_\pi|$ can be evaluated with the expression

$$|j_\pi| = \frac{I_Z(1+\varkappa_Z)\omega_0}{m_p a_X}|\bar{\omega}_\pi|, \tag{3.4}$$

where $|\omega_\pi|$ = the OMG's sensitivity threshold with respect to the base's absolute angular velocity.

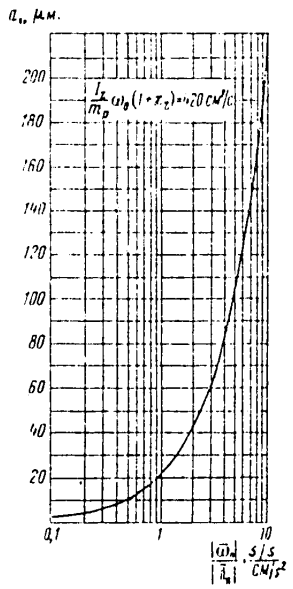

Figure 19. Graph of dependence of displacement a_X on the value of $|\bar{\omega}_\pi/j_\pi|$.

The relationship between an instrument's sensitivity thresholds relative to angular velocity and linear acceleration depends on the rotor's rotation frequency and geometric dimensions and the displacement of its center of mass along the axis of rotation. Figure 19 is a graph of the dependence of a_X on the value of $|\bar{\omega}_\pi|/|j_\pi|$ for a structural coefficient value $(I_Z m_p)\omega_0(1 + \varkappa_Z) = 420$ cm^2/s. It is obvious that the lower limit of the relationship of the sensitivity thresholds, as well as the sensitivities themselves, is determined by the technological capabilities for creating such a small displacement of the rotor's center of mass and maintaining it during the operating process. All other conditions being equal, this limit can be lowered by increasing the rotor's frequency of rotation and selecting the appropriate geometric dimensions (for example: for a rotor in the shape of a parallelepiped, the required value of a_X is practically proportional to the square of its length (b^2)).

From an analysis of expression (3.4) it is possible to assume that however low a threshold of instrument sensitivity to linear acceleration is desired can be achieved by increasing the displacement a_X of the rotor's center of mass. However, this is not so. Analyzing equations of motion (2.92), we find that for quite large values of a_X we should take into consideration moment

$$\frac{m_p a_X}{(I_X - I_Y)\omega_0^2 + C} j_{X0}\psi,$$

which we previously ignored as being a value of a higher order of smallness in comparison with the equation's basic terms. Linear vibrations of the base relative to the OX axis can lead to parametric resonance and the disruption of the instrument's stable operation, while constant linear accelerations can result in detuning from the resonance mode. In accordance with expression (2.122), the relative detuning can be computed with the formula

$$\delta = \frac{1}{2}\frac{1-\varkappa_Z}{C} m_p a_X j_{X0}. \tag{3.5}$$

From (3.5) it is possible to determine the maximum allowable value of a_x as a function of the instrument parameters, the linear accelerations acting on it, and the requirements for its accuracy characteristics.

The creation in a KOMG of the required ranges for measuring angular velocities and linear accelerations is an important question. The design of the torsion bars and the rotor rotation angle measurer is such that angle ψ is limited by some maximum value ψ_{max}. Since the amplitude of the rotor's angle of rotation is determined simultaneously by both the velocity and the linear acceleration being measured, their ranges depend on each other. When only small angular velocities are being measured, the range of the linear accelerations is enlarged, and vice versa.

Let us discuss how to evaluate an instrument's maximum range for linear accelerations and angular velocities. When resonance tuning condition (1.68) is fulfilled, from equations (3.2) we find that the maximum angle of rotation of the rotor is determined by the expression

$$\psi_{max} = \frac{1}{2\xi\omega_0}\left\{(1+\varkappa_Z)|\bar{\omega}_{max}| + \frac{m_p a_x}{J_Z\omega_0}|\bar{j}_{max}|\right\}, \tag{3.6}$$

where $|\bar{\omega}_{max}|$, $|\bar{j}_{max}|$ = absolute values of the maximum measured angular velocity and linear acceleration, respectively. Introducing designators $d_\omega = |\bar{\omega}_{max}|/|\bar{\omega}_\pi|$ and $d_j = |\bar{j}_{max}|/|\bar{j}_\pi|$ for the angular velocity and linear acceleration measurement ranges, respectively, and taking expression (3.4) in consideration, we obtain

$$d_\omega + d_j = \frac{2\xi\omega_0}{1+\varkappa_Z}\frac{\psi_{max}}{|\bar{\omega}_n|}. \tag{3.7}$$

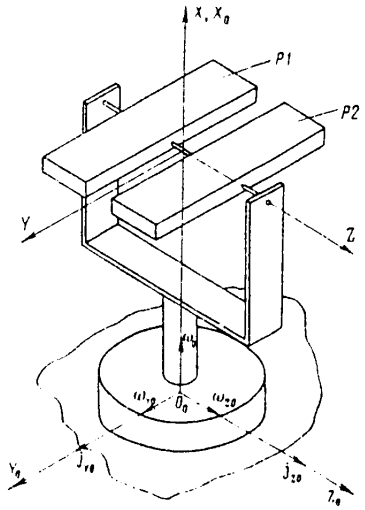

Figure 20. Diagram of composite RVG with common rotor suspension.

From (3.7) it follows that for a highly sensitive instrument, even when the measurement range for angular velocity is extremely limited (when the instrument is mounted on a stabilized base) its linear acceleration measurement range is still 10^3-10^5, which is inadequate for many problems. We should also mention here that the measurement range is coupled with the instrument's pass band and increases as it is expanded.

The KOMG system under discussion contains two independent oscillatory systems. Since it is impossible to achieve complete identity of these systems' parameters during the production process, instrument tuning consists of achieving equality of the frequencies of their natural oscillations to the angular velocity ω_0 of the drive motor's shaft. Individual parameters of the oscillatory systems, such as the rotor's moments of inertia and the torsion bars' rigidity, can differ noticeably from each other. A change in these parameters during the operating process leads to different relative detuning of the systems from resonance and, as will be shown below, to substantial instrument errors.

From (3.7) it follows that a substantial enlargement of the range of linear accelerations that can be measured is impossible without reducing the instrument's sensitivity to angular velocity, and vice versa. The KOMG layout depicted in Figure 20 was proposed for the purpose of eliminating this defect. In this setup both rotors have a common suspension axis OZ. In the general case, the angular rigidity of the torsion bar connecting rotor R1 to the shaft equals C_1, that of the torsion bar connecting rotor R2 to the shaft is C_2, and that of the intermediate torsion bar connecting the two rotors is C_i. As in the preceding case, the rotors' centers of mass are displaced along the OX axis relative to the OZ axis by distances a_{X1} and a_{X2} (in connection with this, it is necessary to try to insure that $a_{X1} = -a_{X2} = a_X$). In comparison with the layout discussed earlier, this one makes it possible to achieve a significant reduction in the instrument's size and is more convenient from the viewpoint of the manufacturing process, since both rotors and the torsion bars can be made from a single blank. Besides this, any errors related to nonparallelism of both rotors' measuring axes are eliminated.

The equations of motion of a KOMG realized according to the layout depicted in Figure 20 have the form

$$\left.\begin{aligned}
&I_{Z1}\ddot{\psi}_1 + \mu_1\dot{\psi}_1 + [(I_{X1} - I_{Y1})\,\omega_0^2 + C_1]\,\psi_1 + C_n\alpha_n = -\\
&-I_{Z1}\dot{\omega}_{Z0}\cos\omega_0 t - I_{Z1}\dot{\omega}_{Y0}\sin\omega_0 t + (I_{Z1} + I_{X1} - I_{Y1})\,\omega_0\omega_{Z0}\times\\
&\times\sin\omega_0 t - (I_{Z1} + I_{X1} - I_{Y1})\,\omega_0\omega_{Y0}\cos\omega_0 t +\\
&+ m_{p1}a_{X1}j_{Z0}\sin\omega_0 t - m_{p1}a_{X1}j_{Y0}\cos\omega_0 t;\\
&I_{Z2}\ddot{\psi}_2 + \mu_2\dot{\psi}_2 + [(I_{X2} - I_{Y2})\,\omega_0^2 + C_2]\,\psi_2 - C_n\alpha_n = -\\
&-I_{Z2}\dot{\omega}_{Z0}\cos\omega_0 t - I_{Z2}\dot{\omega}_{Y0}\sin\omega_0 t + (I_{Z2} + I_{X2} - I_{Y2})\,\omega_0\omega_{Z0}\times\\
&\times\sin\omega_0 t - (I_{Z2} + I_{X2} - I_{Y2})\,\omega_0\omega_{Y0}\cos\omega_0 t +\\
&+ m_{p2}a_{X2}j_{Z0}\sin\omega_0 t - m_{p2}a_{X2}j_{Y0}\cos\omega_0 t.
\end{aligned}\right| \qquad (3.8)$$

If the parameters of both rotors are identical, then--by adding and subtracting equations (3.8) on a term-by-term basis--we obtain the following KOMG equations of motion:

$$\left.\begin{aligned}
&I_Z\ddot{\alpha}_C + \mu\dot{\alpha}_C + [(I_X - I_Y)\,\omega_0^2 + C]\,\alpha_C = 2I_Z\dot{\omega}_{Z0}\cos\omega_0 t -\\
&-2I_Z\dot{\omega}_{Y0}\sin\omega_0 t + 2\,(I_Z + I_X - I_Y)\,\omega_0\omega_{Z0}\sin\omega_0 t - 2(I_Z +\\
&+ I_X - I_Y)\,\omega_0\omega_{Y0}\cos\omega_0 t;\\
&I_Z\ddot{\alpha}_n + \mu\dot{\alpha}_n + [(I_X - I_Y)\,\omega_0^2 + C + 2C_n]\,\alpha_n = 2m_p a_X\times\\
&\times(j_Y\cos\omega_0 t - j_Z\sin\omega_0 t).
\end{aligned}\right| \qquad (3.9)$$

Thus, as with the preceding setup, the rotors' total angle of rotation α_C is proportional to the base's angular velocity in the plane of sensitivity, while difference angle α_π is proportional to the linear accelerations in the same plane. The essential difference between the second KOMG construction plan and the first is that in the second one, resonance tuning with respect to the angular velocity and linear acceleration measurement channels cannot be realized simultaneously. When one of the channels is tuned into resonance, the second will have the relative detuning

$$\delta = \pm(1 - \varkappa_Z)\frac{C_n}{C}. \qquad (3.10)$$

By varying the value of C_π, this makes it possible to change the relationship

between the instrument's sensitivity thresholds for angular velocity and linear acceleration. Actually, if (for example) resonance tuning is carried out with respect to the angular velocity measurement channel, the relationship between the equivalent angular velocity and the linear acceleration has the form (allowing for expression (3.10))

$$\bar{\omega}_e = \frac{m_p a_x}{I_z(1+\varkappa_z)\omega_0} \frac{1}{1+\left(\frac{1-\varkappa_z}{\xi}\frac{C_\pi}{C}\right)^2} \bar{j}, \tag{3.11}$$

which for $C_\pi/C \neq 0$ results in a corresponding decrease in $|\bar{\omega}_\pi|/|\bar{j}_\pi|$. The smaller ξ is (that is, the higher the instrument's sensitivity), the more significant this reduction is.

3.2. Dynamic Characteristics and Basic Errors in Composite Rotor Vibration Gyroscopes

Let us discuss in more detail the operation of a KOMG setup (see Figure 18) containing two independent oscillatory systems, as described by equations (3.1). From (3.2) it follows that when the parameters of both oscillatory systems are identical and the measuring axes are parallel, the instrument consists, as it were, of two independent channels for measuring angular velocity and linear acceleration, each of which--in turn--also contains two channels corresponding to the instrument's axes of sensitivity. The dynamic characteristics of the angular velocity measurement channel are described by transfer function $W_g(p)$, as determined by expression (1.81), while the linear acceleration measurement channel is described by the transfer function

$$\frac{m_p a_x}{I_z(1+\varkappa_z)\omega_n} W_g(p).$$

Thus, both channels have the same pass band, in which the frequency distortions are quite small. From (1.86) it follows that the narrower this band is, the higher the instrument's sensitivity.

There exist a number of technical problems in which, along with a highly sensitive measurer of angular velocities, a less accurate but broad-band measurer of linear accelerations is required. Within the framework of the setup we are discussing, such an instrument can be realized only by the creation of zero displacement of the center of mass of one of the oscillatory systems, which will operate as a normal OMG, and the creation of the required dynamic characteristics in the second oscillatory system, which has a displaced center of mass. In connection with this, in order to obtain a signal that is proportional to the linear accelerations, after preliminary processing (for the purpose of obtaining identical characteristics with respect to the angular velocity) the signal from the first oscillatory system should be subtracted from the signal from the second. In this trivial way it is possible to achieve full independence of the angular velocity measuring channel from linear accelerations of the base.

Figure 21 is the structural diagram of a KOMG constructed according to the setup shown in Figure 18 and in accordance with equations (3.1). The characteristic feature of this setup is the presence in it of cross-couplings between the measuring channels when the oscillatory systems' parameters are not identical. Let us evaluate the level and nature of these couplings. Allowing for the presence at the instrument's outlet of a phase-sensitive demodulator, we will consider only signals

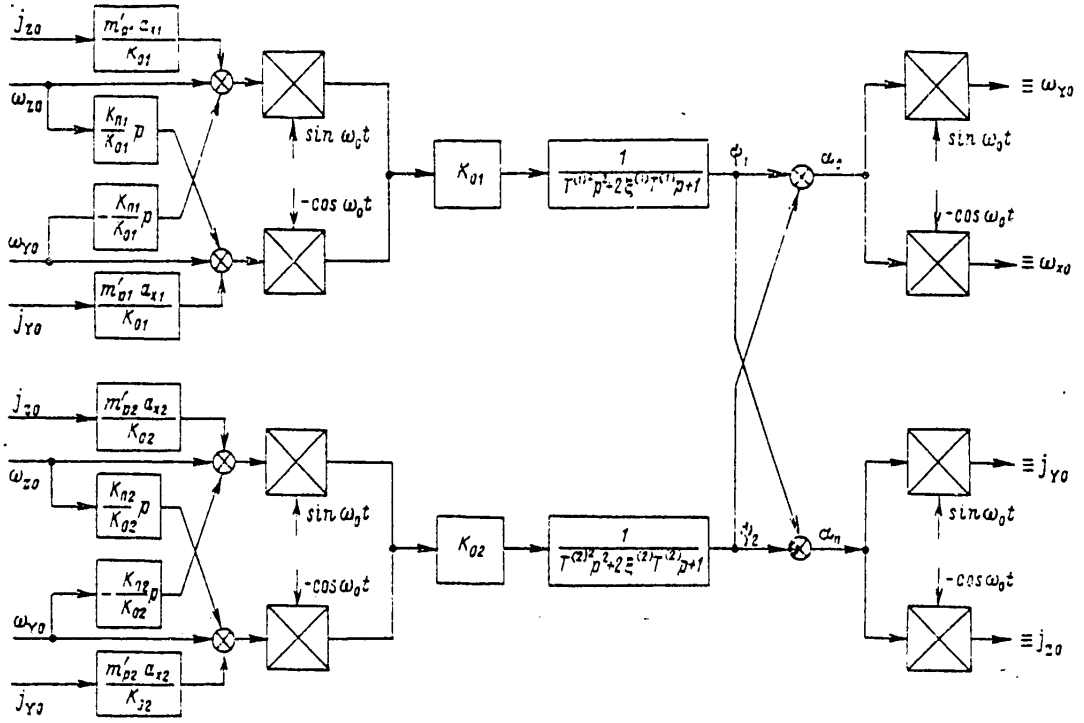

Figure 21. Structural diagram of composite RVG with independent rotor suspension.

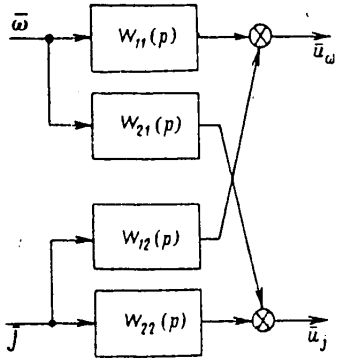

Figure 22. Vector structural diagram of composite RVG.

that are proportional to the envelopes of the rotors' angular oscillations with frequency ω_0. In order to do this, as we did previously we will make use of vector coordinates and complex transfer functions. In this case the instrument's structural diagram is converted into the form depicted in Figure 22, where the following additional definitions have also been introduced: $W_{11}(p) = W_{g1}(p) + W_{g2}(p)$ = sum of the transfer functions of the first and second MRG's with respect to signals that are proportional to the base's angular velocity:

$$W_{21}(p) = -W_{g1}(p) + W_{g2}(p);$$

$$W_{12}(p) = \frac{m_{p1} a_{X1}}{I_{Z1}(1 + \varkappa_{Z1})\omega_0} W_{g1}(p) - \frac{m_{p2} a_{X2}}{I_{Z2}(1 + \varkappa_{Z2})\omega_0} W_{g2}(p) -$$

is the difference between the transfer functions of the first and second MRG's with respect to signals that are proportional to the base's linear acceleration;

$$W_{22}(p) = \frac{m_{p1} a_{X1}}{I_{Z1}(1 + \varkappa_{Z1})\omega_0} W_{g1}(p) + \frac{m_{p2} a_{X2}}{I_{Z2}(1 + \varkappa_{Z2})\omega_0} W_{g2}(p).$$

Transfer functions $W_{g1}(p)$ and $W_{g2}(p)$ are determined from expression (1.81) by substituting the values of the parameters of the first and second oscillatory systems, respectively.

In order to evaluate the effect of individual instrument parameters on the cross-couplings between the measuring channels described by transfer functions $W_{12}(p)$ and $W_{21}(p)$, we will make use of methods from sensitivity theory [37]. Let one of the oscillatory systems have the following parameter values:

$$\omega_{M1} = \sqrt{\frac{C_1}{I_{Z1}}} = \omega_M,\ \varkappa_{Z1} = \varkappa_Z,\ \xi = \xi_1,\ m_{p1} = m_p,\ a_{X1} = a_X,\ I_{Z1} = I_Z,$$

while the second has

$$\omega_{M2} = \omega_M + \Delta\omega_M,\quad \varkappa_{Z2} = \varkappa + \Delta\varkappa,\quad \xi_2 = \xi + \Delta\xi,\quad m_{p2} = m_p + \Delta m_p,\ a_{X2} = a_X + \Delta a_X,\quad I_{X2} = I_X + \Delta I_X,$$

where $\Delta\omega_m$, Δ , $\Delta\xi$, Δm_p, Δa_X, ΔI_Z = small variations in the parameters.

Using sensitivity functions of the first type and limiting ourselves to the band of frequencies $\omega << \omega_0$, the expression for $W_{21}(p)$ can, with a sufficient degree of accuracy, be represented as

$$W_{21}(p) = \frac{W_g(p)}{p - \frac{1}{T_2} i + \frac{\mu_2}{T_2}} \left\{ \frac{\varkappa}{1+\varkappa} \Delta\varkappa p - \left[\left(\frac{1}{T_2} \frac{\varkappa}{1+\varkappa} + \frac{T_3}{1+\mu_3^2} \omega_0^2 \right) \Delta\varkappa + \frac{T_3}{1+\mu_3^2} 2\omega_0 \left(\frac{\omega_M}{\omega_0} \Delta\omega_M - \frac{1}{T} \mu_3 \Delta\xi \right) \right] i + \left[\frac{\mu_2}{T_2} \frac{\varkappa}{1+\varkappa} - \frac{T_3 \mu_3}{1+\mu_3^2} \omega_0^2 \right) \Delta\varkappa - \frac{T_3}{1+\mu_3^2} 2\omega_0 \left(\mu_3 \frac{\omega_M}{\omega_0} \Delta\omega_M + \frac{1}{T} \Delta\xi \right) \Big] \right\}, \tag{3.12}$$

while the expression for $W_{12}(p)$ is

$$W_{12}(p) = \frac{W_g(p)}{p - \frac{1}{T_2} i + \frac{\mu_2}{T_2}} \left\{ \left(\frac{\Delta m_p}{m_p} + \frac{\Delta a_X}{a_X} - \frac{\Delta I_Z}{I_Z} - \frac{1-\varkappa}{1+\varkappa} \Delta\varkappa \right) p - \left[\frac{1}{T_2} \left(\frac{\Delta m_p}{m_p} + \frac{\Delta a_X}{a_X} - \frac{\Delta I_Z}{I_Z} - \frac{1-\varkappa}{1+\varkappa} \Delta\varkappa \right) + \frac{T_3}{1+\mu_3^2} \omega_0^2 \Delta\varkappa + \frac{T_3}{1+\mu_3^2} 2\omega_0 \left(\frac{\omega_M}{\omega_0} \Delta\omega_M - \frac{1}{T} \mu_3 \Delta\xi \right) \right] i + \left[\frac{\mu_2}{T_2} \left(\frac{\Delta m_p}{m_p} + \frac{\Delta a_X}{a_X} - \frac{\Delta I_Z}{I_Z} - \frac{1-\varkappa}{1+\varkappa} \Delta\varkappa \right) - \frac{T_3}{1+\mu_3^2} \omega_0 \left(\mu_3 \omega_0 \Delta\varkappa + 2\mu_3 \frac{\omega_M}{\omega_0} \Delta\omega_M + \frac{2}{T} \Delta\xi \right) \right] \right\} \frac{m_p a_X}{I_Z (1+\varkappa) \omega_0}. \tag{3.13}$$

The variations Δ , $\Delta\omega_m$ and $\Delta\xi$ of the oscillatory systems' parameters that are used in expressions (3.12) and (3.13) are expressed in terms of the oscillatory systems' elementary parameters with the help of the following relationships:

$$\Delta\varkappa = \frac{\Delta I_X - \Delta I_Y - \varkappa \Delta I_Z}{I_Z}; \tag{3.14}$$

$$\Delta\omega_M = \frac{\omega_M}{2} \left(\frac{\Delta C}{C} - \frac{\Delta I_Z}{I_Z} \right); \tag{3.15}$$

$$\Delta\xi = \frac{\mu}{2I_Z \sqrt{\varkappa\omega_0^2 + \omega_M^2}} \left[\frac{\Delta\mu}{\mu} - \frac{1}{2} \frac{\Delta I_Z}{I_Z} - \frac{1}{2} \frac{1}{\varkappa\omega_0^2 + \omega_M^2} \left(\omega_0^2 \frac{\Delta I_X - \Delta I_Y}{I_Z} + \frac{C}{I_Z} \right) \right]. \tag{3.16}$$

From expressions (3.12) and (3.13) it follows that the cross-couplings are the greatest in a highly sensitive instrument that is operating in a resonance tuning mode. The relationships $\varkappa \approx 1$, $\xi << 1$ usually occur for such instruments. Taking into consideration the relationships between instrument parameters that occur during operation in the resonance tuning mode, and using expressions (3.12)-(3.16), in accordance with the structural diagram depicted in Figure 22 we obtain the following expressions for the equivalent linear acceleration $|\bar{j}_e|$ and angular velocity $\bar{\omega}_e$:

$$\bar{j}_e \approx \frac{I_Z(1+\varkappa)\omega_0}{m_p a_X}\frac{i}{2\xi}\left\{-\left[\frac{1}{2}\frac{\Delta I_X-\Delta I_Y-\varkappa\Delta I_Z}{I_Z}-\frac{1-\varkappa}{2}\times\right.\right. \tag{3.17}$$
$$\left.\left.\times\left(\frac{\Delta C}{C}-\frac{\Delta I_Z}{I_Z}\right)\right]i-\xi\frac{\Delta\mu}{\mu}\right\}\frac{\bar{\omega}}{T_g p+1},$$

$$\omega_e \approx \frac{m_p a_X}{I_Z(1+\varkappa)\omega_0}\frac{i}{2\xi}\left\{-i\left(\frac{\Delta m_p}{m_p}+\frac{\Delta a_X}{a_X}-\frac{\Delta I_Z}{I_Z}-\frac{1-\varkappa}{1+\varkappa}\Delta\varkappa\right)\right.$$
$$\times 2\xi(T_g p+1)-\left[\frac{1}{2}\frac{\Delta I_X-\Delta I_Y-\varkappa\Delta I_Z}{I_Z}-\frac{1-\varkappa}{2}\left(\frac{\Delta C}{C}-\right.\right. \tag{3.18}$$
$$\left.\left.\left.-\frac{\Delta I_Z}{I_Z}\right)\right]i-\xi\frac{\Delta\mu}{\mu}\right\}\frac{1}{T_g p+1}\bar{j},$$

where $\bar{j}_e$ = linear acceleration causing a signal identical to the signal from the angular velocity $\bar{\omega}$ of the base's rotation at the linear acceleration measurement channel's output; $\bar{\omega}_e$ = angular velocity of the base, the signal from which is identical to the signal from the base's linear accelerations $\bar{j}$ at the angular velocity measurement channel's output.

From expression (3.17) and (3.18) it follows that the greatest effect on the level of the cross-couplings is exerted by nonidentity of the oscillatory systems with respect to parameter $\varkappa$. This is explained by the fact that determines the value of the dynamic rigidity along the rotors' suspension axis, which is 98-99 percent of the total rigidity along this axis. When $\xi << 1$, even an insignificant change in will move the system out of the resonance tuning mode and cause a sharp change in its transfer factor and the signals' phase relationships. For example, given identical sensitivity of the instrument's measuring channels and $\xi \lesssim 10^{-3}$, in order to obtain a cross-coupling level of $\bar{\omega}_e/\bar{j} = \bar{j}_e/\bar{\omega} \lesssim 10^{-2}$, it is necessary to achieve identity of the oscillatory systems' with respect to parameter $\varkappa$ with better than 0.004-percent accuracy. An instrument constructed according to this plan can operate only in a narrow band of measurable values. In order to enlarge the measurement band, a plan in which one of the oscillatory systems has zero displacement of the center of mass (for example, $a_{Z1} = 0$) can be used. In this case the instrument's transfer functions have the form

$$W_{11}(p) = W_{g1}(p);$$
$$W_{12}(p) = 0;$$
$$W_{21}(p) = W_{g2}(p) - W_{g1}(p);$$
$$W_{22}(p) = \frac{m_p a_{X2}}{I_{X2}(1-\varkappa_2)\omega_0}W_{12}(p).$$

Here there is no dependence of the angular velocity measurement channel on the acceleration measurement channel, while the effect of the first on the second can be reduced by creating the appropriate relationship between the instrument's channels' sensitivities.

The effect on the cross-couplings' level of nonidentity of the torsion bars' torsional rigidities C is directly proportional to the share of these rigidities in the system's total rigidity along the suspension axis; that is, the smaller the value of $1 - \varkappa$, the less the effect. Practically, for identical conditions the requirements for accuracy in maintaining C are two orders of magnitude smaller than the analogous requirements for parameter $\varkappa$. The requirements for the identity of the coefficients of viscous friction in both oscillatory systems are smaller by a factor of $1/\xi$ than the requirements for $\varkappa$ and are comparatively easily realizable for small values of ξ.

There is yet one more factor that can lead to cross-couplings between the measuring channels in this setup: nonparallelism of the rotors' suspension axes. Actually, between the projections of the rotors' suspension axes on a plane perpendicular to the axis of rotatin, let there exist a small angle $\Delta\phi$. If the first OMG's transfer factor then equals unity, the second's will equal $e^{i\Delta\phi}$. The inequality of the transfer factors results in cross-couplings between the measuring channels. In connection with this it is obvious that $\bar{j}_e$ and $\bar{\omega}_e$ can be determined with the help of the following expressions:

$$\bar{j}_e = i\,\Delta\varphi\,\frac{I_Z(1+\varkappa_Z)\omega_0}{m_p a_X}\,\bar{\omega}; \tag{3.19}$$

$$\bar{\omega}_e = i\,\Delta\varphi\,\frac{m_p a_X}{I_Z(1+\varkappa_Z)\omega_0}\,\bar{j}. \tag{3.20}$$

Analogous cross-couplings will occur when the suspension axes are not parallel in the XOY plane. In comparison with the others, the level of these couplings is insignificant and can be limited by introducing the appropriate tolerances in the instrument production and assembly process.

Let us discuss the cross-couplings between the measuring channels that occur during the operation of a KOMG built according to the second plan. By adding and subtracting equations (3.8) on a term-by-term basis, we obtain equations that describe this setup's operating features when the oscillatory systems have nonidentical parameters:

$$\left.\begin{aligned}
&I_{ZC}\ddot{\alpha}_C + \mu_C\dot{\alpha}_C + [(I_{XC} - I_{YC})\omega_0^2 + C_C]\alpha_C + I_{Zn}\ddot{\alpha}_n + \mu_n\dot{\alpha}_n + \\
&+ [(I_{Xn} - I_{Yn})\omega_0^2 + C_{np}]\alpha_n = -2I_{ZC}\dot{\omega}_{Z0}\cos\omega_0 t - \\
&- 2I_{ZC}\dot{\omega}_{Y0}\sin\omega_0 t + 2(I_{ZC} + I_{XC} - I_{YC})\omega_0\omega_{Z0}\sin\omega_0 t - \\
&- 2(I_{ZC} + I_{XC} - I_{YC})\omega_0\omega_{Y0}\cos\omega_0 t + (m_{p2}a_{X2} - m_{p1}a_{X1})j_Y \times \\
&\times\cos\omega_0 t + (m_{p2}a_{X2} - m_{p1}a_{X1})j_Z\sin\omega_0 t; \\
&I_{ZC}\ddot{\alpha}_n + \mu_C\dot{\alpha}_n + [(I_{XC} - I_{YC})\omega_0^2 + C_C + 2C_n]\alpha_n + I_{Zn}\ddot{\alpha}_C + \\
&+ \mu_n\dot{\alpha}_C + [(I_{Xn} - I_{Yn})\omega_0^2 + C_{np}]\alpha_C = -2I_{Zn}\dot{\omega}_{Z0}\cos\omega_0 t - \\
&- 2I_{Zn}\dot{\omega}_{Y0}\sin\omega_0 t + 2(I_{Zn} + I_{Xn} - I_{Yn})\omega_0\omega_{Z0}\sin\omega_0 t - \\
&- 2(I_{Zn} + I_{Xn} - I_{Yn})\omega_0\omega_{Y0}\cos\omega_0 t + (m_{p2}a_{X2} + m_{p1}a_{X1})\times \\
&\times j_Y\cos\omega_0 t + (m_{p2}a_{X2} + m_{p1}a_{X1})j_Z\sin\omega_0 t,
\end{aligned}\right| \tag{3.21}$$

where

$$I_{ZC} = \frac{I_{Z2} + I_{Z1}}{2};\quad I_{YC} = \frac{I_{Y2} + I_{Y1}}{2};$$

$$I_{XC} = \frac{I_{X2} + I_{X1}}{2};\quad \mu_C = \frac{\mu_2 + \mu_1}{2};$$

$$I_{Xn} = \frac{I_{X2} - I_{X1}}{2}; \quad C_C = \frac{C_2 + C_1}{2};$$
$$\mu_n = \frac{\mu_2 - \mu_1}{2}; \quad C_{np} = \frac{C_2 - C_1}{2}.$$
$$I_{Yn} = \frac{I_{Y2} - I_{Y1}}{2}; \quad I_{Zn} = \frac{I_{Z2} - I_{Z1}}{2};$$

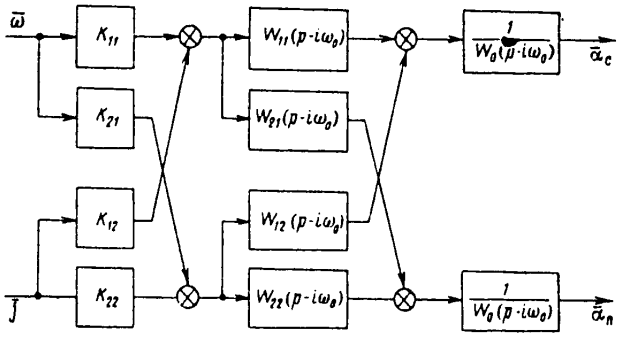

Figure 23. Structural diagram of a composite RVG with common suspension of the rotors.

On the basis of equations (3.21) and allowing for the presence of a phase-sensitive demodulator at the instrument's outlet, the structural diagram for the signals' envelopes has the form presented in Figure 23. In connection with this, we introduce the following definitions:

$$\left.\begin{aligned}
K_{11} &= 2(I_{ZC} + I_{XC} - I_{YC})\,\omega_0;\\
K_{21} &= 2(I_{Zn} + I_{Xn} - I_{Yn})\,\omega_0;\\
K_{22} &= m_{p2}a_{X2} + m_{p1}a_{X1};\quad K_{12} = m_{p2}a_{X2} - m_{p1}a_{X1};\\
W_{11}(p) &= I_{ZC}p^2 + \mu_C p + [(I_{XC} - I_{YC})\,\omega_0^2 + C_C + 2C_n];\\
W_{21}(p) &= W_{12}(p) = I_{Zn}p^2 + \mu_n p + [(I_{Xn} - I_{Yn})\,\omega_0^2 + C_{np}];\\
W_{22}(p) &= I_{ZC}p^2 + \mu_C p + [(I_{XC} - I_{YC})\,\omega_0^2 + C_C];\\
W_0(p) &= \{I_{ZC}p^2 + \mu_C p + [(I_{XC} - I_{YC})\,\omega_0^2 + C_C]\}\{I_{ZC}p^2 +\\
&\quad + \mu_C p + [(I_{XC} - I_{YC})\,\omega_0^2 + C_C + 2C_n]\} -\\
&\quad - \{I_{Zn}p^2 + \mu_n p + [(I_{Xn} - I_{Yn})\,\omega_0^2 + C_{np}]\}^2.
\end{aligned}\right\} \qquad (3.22)$$

In accordance with the structural diagram, the signals at the instrument's outlet are described by the following expressions:

$$\left.\begin{aligned}
\tilde{\alpha}_c &= \frac{1}{W_0(p - i\omega_0)}\{[K_{11}W_{11}(p - i\omega_0) + K_{21}W_{12}(p - i\omega_0)]\,\bar{\omega} +\\
&\quad + [K_{12}W_{11}(p - i\omega_0) + K_{22}W_{12}(p - i\omega_0)]\,\bar{J}\};\\
\tilde{\alpha}_n &= \frac{1}{W_0(p - i\omega_0)}\{[K_{22}W_{22}(p - i\omega_0) + K_{12}W_{21}(p - i\omega_0)]\,\bar{J} +\\
&\quad + [K_{21}W_{22}(p - i\omega_0) + K_{11}W_{21}(p - i\omega_0)]\,\bar{\omega}\}.
\end{aligned}\right\} \qquad (3.23)$$

Equations (3.22) and (3.23) make it possible to derive quite easily the expressions for equivalent angular velocity and linear acceleration when there is an input value

in the other measuring channel:

$$\left.\begin{aligned}\bar{\omega}_e &= \frac{K_{12}W_{11}(p-i\omega_0)+K_{22}W_{12}(p-i\omega_0)}{K_{11}W_{11}(p-i\omega_0)+K_{21}W_{12}(p-i\omega_0)}\,\bar{j};\\ \bar{j}_e &= \frac{K_{21}W_{22}(p-i\omega_0)+K_{11}W_{21}(p-i\omega_0)}{K_{22}W_{22}(p-i\omega_0)+K_{12}W_{21}(p-i\omega_0)}\,\bar{\omega}.\end{aligned}\right\} \tag{3.24}$$

Assuming, as before, that the instrument's parameters can differ from the nominal ones--which are identical for both interrelated oscillatory systems--by only small amounts that are determined by the variations in these parameters, for the area of essential frequencies we obtain the following expressions for $\bar{\omega}_e$ and $\bar{j}_e$ in the first approximation:

$$\begin{aligned}\bar{\omega}_e \approx i\frac{m_p a_X}{I_Z(1+\varkappa)}\times\\ \times\frac{1}{p-i\left(1-\sqrt{\varkappa+\nu^2+\frac{C_\pi}{I_Z\omega_0^2}}\sqrt{1-\xi^2}\right)\omega_0+\xi\omega_0\sqrt{\varkappa+\nu^2+\frac{C_\pi}{I_Z\omega_0^2}}}\times\\ \times\frac{1}{2}\left\{\frac{1}{\omega_0^2}\left(\frac{\Delta m_p}{m_p}+\frac{\Delta a_X}{a_X}+\frac{\Delta I_Z}{I_Z}\right)p^2+\frac{2}{\omega_0}\left[\left(\frac{\Delta m_p}{m_p}+\frac{\Delta a_X}{a_X}-\frac{\Delta\mu}{\mu}\right)\xi-\right.\right.\\ -i\left(\frac{\Delta m_p}{m_p}+\frac{\Delta a_X}{a_X}+\frac{\Delta I_Z}{I_Z}\right)\Big]p+\Delta\varkappa-(1-\varkappa)\frac{\Delta I_Z}{I_Z}+\\ +\left(1-\varkappa+\nu^2+\frac{C_\pi}{I_Z\omega_0^2}\right)\left(\frac{\Delta m_p}{m_p}+\frac{\Delta a_X}{a_X}\right)+\nu^2\frac{\Delta C}{C+C_\pi}-\\ \left.-i\xi\left(\frac{\Delta\mu}{\mu}+2\frac{\Delta m_p}{m_p}+2\frac{\Delta a_X}{a_X}\right)\right\}\bar{j},\end{aligned} \tag{3.25}$$

where $\nu=\sqrt{(C+C_\pi)/I_Z\omega_0^2}$ is the ratio of the frequency of one rotor's natural oscillations to angular velocity ω_0 when $\omega_0=0$ and the second rotor has lost a degree of freedom relative to the torsion bars' axis;

$$\begin{aligned}\bar{j}_e \approx i\frac{I_Z(1+\varkappa)}{m_p a_X}\times\\ \times\frac{\omega_0^2}{p-i\left(1-\sqrt{\varkappa+\nu^2-\frac{C_\pi}{I_Z\omega_0^2}}\sqrt{1-\xi^2}\right)\omega_0+\xi\omega_0\sqrt{\varkappa+\nu^2-\frac{C_\pi}{I_Z\omega_0^2}}}\times\\ \times\frac{1}{2}\left\{\frac{1}{\omega_0^2}\left(\Delta\varkappa+(2+\varkappa)\frac{\Delta I_Z}{I_Z}\right)p^2-i\frac{2}{\omega_0}\left(\Delta\varkappa+(2+\varkappa)\frac{\Delta I_Z}{I_Z}\right)p+\right.\\ +\Delta\varkappa-(1-\varkappa)\frac{\Delta I_Z}{I_Z}+\left(1-\varkappa+\nu^2-\frac{C_\pi}{I_Z\omega_0^2}\right)\left[\Delta\varkappa+(1+\varkappa)\frac{\Delta I_Z}{I_Z}\right]+\\ \left.+\nu^2\frac{\Delta C}{C+C_\pi}-i\xi 2\left(\frac{\Delta\mu}{\mu}+\Delta\varkappa+(1+\varkappa)\frac{\Delta I_Z}{I_Z}\right)\right\}\bar{\omega}_e.\end{aligned} \tag{3.26}$$

From expressions (3.25) and (3.26) it follows that, as was the case for the first setup, the greatest influence on the level of the cross-couplings between the measuring channels is exerted by the nonidentical natural of the rotors with respect to parameter $\varkappa$. In contrast to the first setup, however, the level of the cross-couplings depends on which of the measuring channels is used to realize resonance tuning. If resonance tuning takes place along the angular velocity measurement

channel, the cross-coupling from the first channel to the second has a high level, and vice versa. The level of the cross-coupling from the channel not having resonance tuning to the other is determined by the magnitude of this channel's detuning from resonance, which is regulated by the intermediate torsion bar's rigidity C_i. Thus, by selecting the appropriate value of C_i, it is possible to change the channels' dynamic characteristics, their measurement range and the level of the cross-couplings.

From the expressions for the transfer functions of an OMG (1.86) and a KOMG it follows that during the creation of a highly sensitive instrument (when resonance tuning is realized and the relative damping factor ξ is extremely small), its time constant T_g can be quite large. As a result of this, in a KOMG there can arise large errors in the determination of angular velocities and linear accelerations. These errors are especially large when the instrument is operating in an open system (for example, the acceleration measurement channel's dynamic errors for an inertial navigation system and so on). Taking (1.81) into consideration, the expression for the acceleration measurement channel's dynamic error can be written, with a sufficient degree of accuracy, in the form

$$\tilde{u}_d(t) = K_i L^{-1}\left[\left(\frac{1}{T_2 p - 1 + \mu_2} - \frac{1}{-1 + \mu_2}\right) j(p)\right], \tag{3.27}$$

where

$$K_i = i\,\frac{2m_p a_\chi}{(T\omega_0 - \sqrt{1-\xi^2})(T\omega_0 + 1)};$$

L^{-1} = operator of an inverse Laplace transform.

Suppose that the law governing the change in acceleration can be approximated by the first n terms of the exponential series

$$j = \tilde{a}_0 + \tilde{a}_1 t + \cdots + \tilde{a}_n t^n. \tag{3.28}$$

The expression for the dynamic error then takes on the form

$$\tilde{u}_d(p) = -K_i \frac{T_2}{T_2 p - 1 + \mu_2} \frac{\tilde{a}_n p^n + \tilde{a}_1 p^{n-1} + \cdots + n!\,\tilde{a}_n}{p^n} \frac{1}{-1 + \mu_2}. \tag{3.29}$$

By breaking the right side of (3.29) down into elementary fractions and applying the inverse Laplace transform to both sides, we obtain an expression for an instrument's dynamic error signal when acceleration (3.28) is acting on it:

$$\begin{aligned}\bar{u}_d(t) = -K_i \Big\{ &\bar{A}_1 + \bar{A}_2 t + \cdots + \bar{A}_n t^{n-1} + \bar{B}_1 T_2 e^{-\frac{\mu_2}{T_2} t} \sin\frac{t}{T_2} + \\ &+ \bar{B}_2\left[-\mu_2 \sin\frac{t}{T_2} + \cos\frac{t}{T_2}\right] e^{-\frac{\mu_2}{T_2} t}\Big\} \frac{1}{-1 + \mu_2}.\end{aligned} \tag{3.30}$$

The unknown coefficients A_i and B_i can be found from the following equalities:

$$\left.\begin{aligned} &p^{n+1}\,\mathrm{Re}\,\bar{B}_2 + p^n\,\mathrm{Re}\,\bar{B}_1 + \\ &+ [p^{n-1}\,\mathrm{Re}\,\bar{A}_1 + p^{n-2}\,\mathrm{Re}\,\bar{A}_2 + \cdots + (n-1)!\,\mathrm{Re}\,\bar{A}_n] \times \\ &\times\left(p^2 + 2\frac{\xi}{T} p + \frac{1+\mu_2^2}{T_2^2}\right) = \\ &\cdots\cdots\cdots\end{aligned}\right\}$$

$$\left.\begin{aligned} &\cdots\cdots\cdots \\ &= \left[(T_2 p + \mu_2)\sum_{i=0}^{n} p^{n-i}\,\mathrm{Re}\,\bar{a}_i - \sum_{i=0}^{n} p^{n-i}\,\mathrm{Im}\,\bar{a}_i\right]; \\ &p^{n+1}\,\mathrm{Im}\,\bar{B}_2 + p^n\,\mathrm{Im}\,\bar{B}_1 + \\ &+ [p^{n-1}\,\mathrm{Im}\,\bar{A}_1 + p^{n-2}\,\mathrm{Im}\,\bar{A}_2 + \cdots + (n-1)!\,\mathrm{Im}\,\bar{A}_n]\times \\ &\times\left(p^2 + 2\frac{\xi}{T}p + \frac{1+\mu_2^2}{T_2^2}\right) = \\ &= \left[(T_2 p + \mu_2)\sum_{i=0}^{n} p^{n-i}\,\mathrm{Im}\,\bar{a}_i + \sum_{i=0}^{n} p^{n-i}\,\mathrm{Re}\,\bar{a}_i\right]. \end{aligned}\right\} \qquad (3.31)$$

By equating in (3.31) the coefficients for identical powers of p in the left and right sides, we obtain a system of 2(n + 2) linear algebraic equations in order to find the 2(n + 2) unknowns ReA_i, ImA_i, ReB_i and ImB_i.

When the instrument is acted upon by a discontinuous disturbance and the measuring channel is tuned into the resonance mode, the dynamic error will be described by the expression

$$\begin{aligned} \tilde{u}\ (t) &= im_p a_\chi \frac{1}{2\xi}\,\tilde{a}_n\left(\cos 2\xi\frac{t}{T_g} + i\sin 2\xi\frac{t}{T_g}\right)e^{-\frac{t}{T_g}} \approx \\ &\approx -im_p a_\chi \frac{1}{2\xi}\,\tilde{a}_n e^{-\frac{t}{T_g}}. \end{aligned} \qquad (3.32)$$

Thus, the larger the value of T_g, the greater the instrument's dynamic error. At the same time, as was shown in Section 1.6, the higher the instrument's sensitivity (the smaller ξ is), the greater the value of T_g. Therefore, the realization of an instrument that has both high sensitivity and small dynamic errors is fundamentally impossible within the framework of the layout we are discussing.

In addition to the specific errors we have discussed, a KOMG also has all the errors that are typical of an OMG (see Section 2.4). In this case the errors related to angular motion of the instrument's base and synchronous interference are doubled in the velocity measurement channel. In the acceleration measurement channel they are determined by the nonidentity of the oscillatory systems' parameters. Thus, the linear acceleration measurement channel's errors are much smaller than those of the angular acceleration measurement channel. Thanks to this, the instrument's second channel's sensitivity threshold is lower and the cross-couplings from the second channel to the first can be reduced. The second channel's dynamic errors can be reduced by introducing detuning from the resonance mode.

3.3. Synthesizing the Parameters of an Output Filter for Composite Rotor Vibration Gyroscopes

In Section 3.2 it was shown that composite MRG's have significant dynamic errors that cannot be reduced without lowering the instrument's sensitivity. These errors have the greatest effect on the instrument's functioning in the linear acceleration measurement channel if the signals from the channel are used for an inertial navigation system. Integration of these signals results in inadmissibly large errors in determining velocity and the path that has been covered. Into the channel's input there also enter disturbances related to angular and linear oscillations of the

base, which are a source of additional errors. Besides this, both the instrument itself and the signal extraction and processing devices have internal noise, on which the instrument's sensitivity threshold depends to a considerable extent. Thus, there arises the problem of optimum signal processing at the linear acceleration measurement channel's outlet for the purpose of obtaining the most reliable information about the linear accelerations acting on the object, with due consideration for the factors listed above. Such processing can be carried out with the help of a special filter installed at the instrument's output. Let us determine the parameters of this filter.

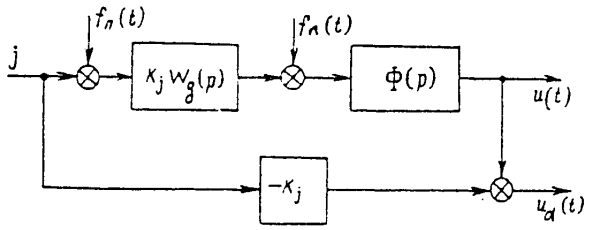

Figure 24. Diagram of formation of composite RVG errors.

Figure 24 is a structural diagram of the formation of instrument errors in the acceleration measurement channel. Let us introduce the following definitions: $\bar{f}_\pi(t)$ = the disturbance caused by angular and linear oscillations of the base, reduced to an equivalent linear acceleration; $\bar{f}_n(t)$ = the instrument's internal noises, as heard at its outlet; $\Phi(p)$ = transfer function of the filter at the instrument's outlet. Disturbance $\bar{f}_\pi(t)$ is of a random nature and depends on the characteristics of the specific object in which the instrument is installed, as well as the conditions of its motion. Therefore, we will ignore this disturbance in our further discussion. An instrument's internal noises are also of a random nature and are usually approximated by "white noise." We will also assume $\bar{f}_n(t)$ to be "white noise" with the same power B^2 at both channel outputs.

We will determine transfer function $\Phi(p)$ on the basis of the minimum mean-square error in the measurement of the linear acceleration's absolute value and the given limitation on the dispersion of the noise at the instrument's outlet. This means that it is necessary to bring to a minimum the functional

$$I = \int_0^\infty |\bar{u}_d(t)|^2\, dt + k^2 D_{\bar{u}}(t), \tag{3.33}$$

where k = an indeterminate Lagrange multiplier; $D_{\bar{u}}(t)$ = dispersion of the modulus of the linear acceleration measurement channel's output signal.

An instrument has the greatest dynamic errors when operating in the resonance tuning mode. In connection with this, the cross-couplings between the channels can be ignored with a sufficient degree of accuracy, while the instrument's transfer function is written in the form of (1.86). In this case the problem reduces to the synthesis of a filter that is optimum, in the sense of criterion (3.33), for each linear acceleration measurement channel. We will use the method of synthesis in a frequency area, the basic ideas of which are explained in [41]. According to (Parseval''s) theorem, in the area of images the expression for functional (3.33) can be written--allowing for the assumptions we have made--in the following form:

$$I = \frac{1}{2\pi i}\int_{-i\infty}^{i\infty} [u_d(p)\,u_d(-p) + k^2B^2\Phi(p)\,\Phi(-p)]\,dp, \tag{3.34}$$

where $u_d(p)$ = error signal at one of the linear acceleration measurement channel's outputs.

Using the structural diagram presented in Figure 24 and introducing error factors C_l [23], we will rewrite expressions (3.34), substituting the dynamic error's value in terms of the acting disturbances and the instrument's parameters:

$$I = \frac{1}{2\pi i}\int_{-i\infty}^{i\infty}\left\{\left[K_i W_{\vartheta}(p)\Phi(p) - K_j + \sum_{l=1}^{n}\frac{C_l}{l!}p^l\right]\times\right.$$
$$\times\left[K_i W_{\vartheta}(-p)\Phi(-p) - K_j + \sum_{l=1}^{n}\frac{C_l}{l!}(-p)^l\right] j(p)\,j(-p) + \tag{3.35}$$
$$\left. + k^2B^2\Phi(p)\,\Phi(-p)\right\} dp.$$

The necessary and sufficient condition for achieving a minimum of functional (3.35) is the requirement that all poles of function $X(p)$, which is determined by the expression

$$X(p) = \Phi_0(p)\,[K_j^2 W_{\vartheta}(p)\,W_{\vartheta}(-p)\,j(p)\,j(-p) + k^2B^2] +$$
$$+\left(-K_j + \sum_{l=1}^{n}\frac{C_l}{l!}p^l\right) W_{\vartheta}(-p)\,K_j\,j(p)\,j(-p), \tag{3.36}$$

where $\Phi_0(p)$ = transfer function of the forming filter, which is optimum in the sense of the adopted criterion, lie in the right semiplane.

Let us adopt a law governing the change in acceleration in the form of (3.28). When determining $\Phi_0(p)$ we will require that the optimum filter be stable; that is, that all poles of $\Phi_0(p)$ lie in the left semiplane. Substituting (3.29) and (1.86) into (3.36), we will write the multiplier standing in front of $\Phi_0(p)$ as:

$$Y(p) = K_j^2\,\frac{a_0p^n + a_1p^{n-1} + \cdots + n!\,a_n}{p^{n+1}}\times$$
$$\times\,\frac{(-1)^n a_0p^n + (-1)^{n-1}a_1p^{n-1} + \cdots + n!\,a_n}{(-1)^{n+1}p^{n+1}}\,\frac{1}{T_{\vartheta}p+1}\,\frac{1}{-T_{\vartheta}p+1} + k^2B^2. \tag{3.37}$$

When p is replaced by -p in expression (3.37), it does not change, so we can represent it as two cofactors $Y(p) = Y^+(p)Y^-(p)$, where $Y^+(p)$ has all zeroes and poles in the left semiplane, while $Y^-(p)$ corresponds to it in the right semiplane:

$$\left.\begin{aligned} Y^+(p) &= \frac{b_{n+2}p^{n+2} + b_{n+1}p^{n+1} + \cdots + b_0}{p^{n+1}(T_{\vartheta}p+1)};\\ Y^-(p) &= \frac{(-1)^{n+2}b_{n+2}p^{n+2} + (-1)^{n+1}b_{n+1}p^{n+1} + \cdots + b_0}{(-1)^{n+1}p^{n+1}(-T_{\vartheta}p+1)}. \end{aligned}\right\} \tag{3.38}$$

In order to determine the unknown coefficients b_i it is necessary to find the roots of the algebraic equation

$$\begin{aligned}(-1)^{n+1}p^{2n+2}(1-T_g^2p^2)\,k^2B^2+\\+k_j^2[(-1)^n a_0p^n+(-1)^{n-1}a_1p^{n-1}+\cdots+n!\,a_n]\times\\\times(a_0p^n+a_1p^{n-1}+\cdots+n!\,a_n)=0,\end{aligned}\tag{3.39}$$

and then carry out factorization of the polynomial in the left side of (3.37).

Let us divide the right and left sides of (3.36) by $Y^-(p)$:

$$Y^+(p)\Phi_0(p)-K_j\left(K_j-\sum_{l=1}^{n}\frac{C_l}{l!}p^l\right)\frac{W_0(-p)}{Y^-(p)}\,j(p)\,j(-p)=\frac{X(p)}{Y^-(p)},\tag{3.40}$$

where

$$K_j\left(K_j-\sum_{l=1}^{n}\frac{C_l}{l!}p^l\right)\frac{W_0(-p)}{Y^-(p)}\,j(p)\,j(-p)=K_j\left(K_j-\sum_{l=1}^{n}\frac{C_l}{l!}p^l\right)\times$$
$$\times\frac{(a_0p^n+a_1p^{n-1}+\cdots+n!\,a_n)[(-1)^n a_0p^n+(-1)^{n-1}a_1p^{n-1}+n!\,a_n]}{p^{n+1}[(-1)^{n+2}b_{n+2}p^{n+2}+(-1)^{n+1}b_{n+1}p^{n+1}+b_0}.$$

Breaking down the rational-fraction expression into elementary fractions, we have

$$\begin{aligned}K_j\left(K_j-\sum_{l=1}^{n}\frac{C_l}{l!}p^l\right)\frac{W_0(-p)}{Y^-(p)}\,j(p)\,j(-p)=\\=K_j\left[\left(K_j-\sum_{l=1}^{n}\frac{C_l}{l!}p^l\right)\frac{W_0(-p)}{Y^-(p)}\,j(p)\,j(-p)\right]_+ +\\+K_j\left[\left(K_j-\sum_{l=1}^{n}\frac{C_l}{l!}p^l\right)\frac{W_0(-p)}{Y^-(p)}\,j(p)\,j(-p)\right]_-,\end{aligned}\tag{3.41}$$

where the function in the first square brackets has poles in the left semiplane only, while the one in the second square brackets has them in the right semiplane only:

$$\begin{aligned}K_j\left[\left(K_j-\sum_{l=1}^{n}\frac{C_l}{l!}p^l\right)\frac{W_0(-p)}{Y^-(p)}\,j(p)\,j(-p)\right]_+=\\=K_j\left(\frac{L_1}{p}+\frac{L_2}{p^2}+\cdots+\frac{L_{n+1}}{p^{n+1}}\right),\end{aligned}\tag{3.42}$$

here the expressions for the unknown L_i can be found, by the method of indeterminate coefficients, by expansion into the simplest fractions.

Substituting (3.42) into (3.40) and taking into consideration the requirement that $X(p)/Y^-(p)$ be analyzable in the left semiplane, we obtain the final expression for for the transfer function of the optimum forming filter for the acceleration measurement channel's signal:

$$\Phi_0(p)=K_j\frac{(T_gp+1)(L_1p^n+L_2p^{n+1}+\cdots+L_{n+1})}{b_{n+2}p^{n+2}+b_{n+1}p^{n+1}+\cdots+b_0}.\tag{3.43}$$

Thus, when the law governing the change in linear acceleration and the instrument's parameters are known, expression (3.43) makes it possible to reduce the instrument's dynamic error by realizing optimum (under the indicated conditions) filtration of the output signal. For example, if the linear acceleration at the instrument's input changes rapidly ($j = a_0$), the expression for the optimum filter's transfer function has the form

$$\Phi_0(p) = \frac{T_\beta p + 1}{\frac{BT_\beta}{jK_j} p^2 + \frac{B}{jK_j}\sqrt{1 + \frac{j}{B} T_\beta p + 1}}. \tag{3.44}$$

The realization of such a filter presents no significant difficulties. Filtration effectiveness and feasibility can be determined for any specific problem. In order to do this, after the parameters of the filter are computed, it is necessary to re-evaluate the instrument's dynamic errors. It should be mentioned here that a synthesized filter is optimal only for specific disturbances and instrument parameters, for which their mathematical expectations can be used. For a conclusive evaluation of the effectiveness of filtration, the sensitivity function for changing disturbances and instrument parameters should be derived and the additional dynamic errors appearing in connection with these disturbances should be evaluated.

CHAPTER 4. STABILIZATION SYSTEMS UTILIZING ROTOR VIBRATIONS GYROSCOPES AS THE BASIC SENSITIVE ELEMENTS

4.1. Stabilization System Equations of Motion, Structural Diagrams and Transfer Functions

The specific nature of RVG's, which are small, highly sensitive measurers of absolute angular velocities, determines their basic area of utilization as sensitive elements in the construction of systems that are stabilized in inertial space. These systems are installed in ships for the purpose of creating a reference system of coordinates and are usually built to operate with gyroscopic sensors of different types. There are two fundamentally different ways of using RVG's in stabilization systems.

The first way involves the use of RVG's as the basic sensors that measure the deviation of a stabilized platform from the position it initially occupied in inertial space and generate and send an appropriate signal to the system that controls the stabilizing engines, which must compensate for the effect of the disturbing moments. This way provides for the creation of relatively more accurate and cheaper stabilized platforms than platforms based on gyroscopes of the classical type [15]. The use of RVG's makes it possible to miniaturize platforms, which for many objects is extremely important. In this case, a number of demands are made on an RVG acting as a sensor for a stabilization system. In addition to a low sensitivity threshold, it must have rather broad ranges of measurable velocities and frequencies, as well as high accuracy when operating on a base subjected to a broad spectrum of disturbances.

The second way involves the use of RVG's to increase the accuracy of gyroscopically stabilized platforms (GSP) by integration with traditional two-stage gyroscopic sensors.

The simplest stabilization systems that can be built using RVG's are unaxial stabilized platforms (OSP). In this case one of the RVG's sensitivity axes coincides with the axis of stabilization. As a result, at the output of the instrument's appropriate channel there forms a signal that is proportional to the platform's angular velocity of rotation around the axis of stabilization in inertial space. The absolute angular velocity of rotation of the platform around an unstabilized axis that coincides with the RVG's second axis of sensitivity, leads to the appearance at the RVG's output of an error signal because of the cross-coupling that takes place in the RVG itself.

A structural diagram of an OSP is shown in a linear and stationary approximation in Figure 25. The following definitions are used in the system: M_B = disturbing

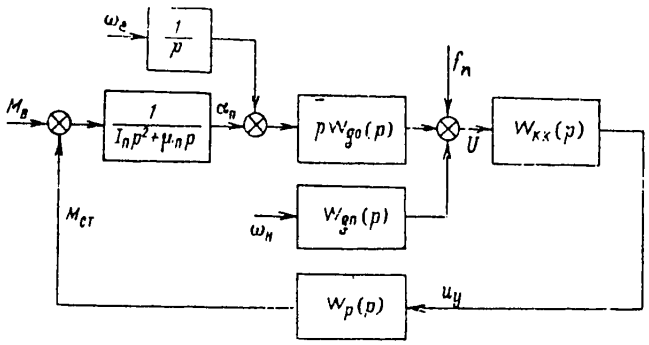

Figure 25. Structural diagram of uniaxial stabilization system.

moment acting on the platform along the stabilization axis; α_π = angle of rotation of the platform in inertial space around the stabilization axis; u = signal at the RVG's output; u_y = signal on the stabilizing engine's control winding; M_{CT} = moment developed by the stabilizing engine; ω_H = absolute velocity of the platform relative to the unstabilized axis that coincides with one of the RVG's sensitivity axes; ω_e = = RVG error signal, reduced to an equivalent angular velocity at the instrument's input; f_n = interference signal, reduced to equivalent noise at the RVG's output; $W_{g.o}(p)$, $W_{g.\pi}(p)$ = transfer functions of the RVG for direct and cross signals, respectively; $W_{k.k}(p)$ = transfer function of the correcting circuit in the stabilizing circuit; $W_p(p)$ = transfer function of the stabilizing engine.

An analysis of the system represented by the structural diagram in Figure 25 makes it possible to study its basic properties (in the first approximation) and realize a preliminary synthesis of the regulator's parameters. For a more detailed investigation of OSP's based on RVG's, their specific features should be taken into consideration. As was shown in Chapter 1, the signal of a modulation RVG (an MRG) contains two components: a slowly changing one (the signal on the zero frequency) and an amplitude-modulated one that has a carrier frequency equal to the doubled frequency of rotation of the rotor. For structural considerations the latter component cannot be overly high and is usually 200-400 Hz. This component must be filtered reliably, for otherwise it can cause an undesirable angular vibration of the platform on frequency $2\omega_0$. It is obvious that for large amplification factors, the filter for the doubled frequency of rotation can have noticeable effect on the system's dynamics. Therefore, the OSP's basic characteristics should be defined precisely, allowing for the nonstationary nature of the RVG's signal.

The structural diagram of such a system, allowing for the RVG transfer functions derived in Chapter 1, has the form shown in Figure 26. For an MRG there is only one nonstationary parallel connection between the instrument's input and output, which in the diagram is reflected by the presence of multiplying elements that modulate the signal on frequency $2\omega_0$. For RVG's with double modulation and single modulation by motor PD1, for which condition (1.22) is not fulfilled, there will be (generally speaking) an infinite set of such parallel connections. In connection with this, modulation frequencies n will be both multiples of frequency $2\omega_0$ and composites of frequencies ω_0 and $\dot{\phi}_1$. The cross-couplings from the instrument's second measuring channel will also contain a full set of amplitude-modulated signals, which in the structural diagram are shown by the signals $\tilde{u}_{H1},\ldots,\tilde{u}_{Hn}$ at the RVG's output. The errors caused by disturbing moments with the appropriate modulation frequencies are allowed for in the form of equivalent angular velocities ω_e.

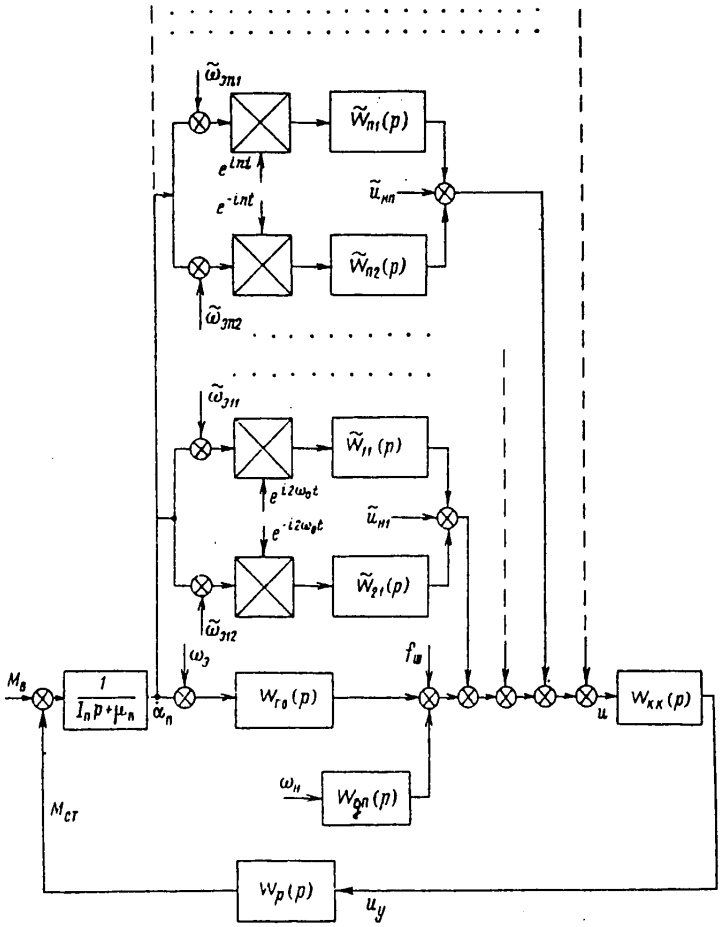

Figure 26. Structural diagram of OSP, allowing for the nonstationary nature of the RVG.

Real OSP's based on RVG's are not linear systems, so when determining their properties we should allow for the effect on their operation of the basic nonlinearities. Above all, this means nonlinearity of the type of saturation in the measurer of the RVG's rotor's angle of rotation. It is caused by the presence of arresting devices that limit the rotor's angle of rotation and protect the torsion bars against fracturing, as well as the limitation on the range of the change in voltage in each individual channel of the signal processing system. The second essential nonlinearity is the moment of dry friction in the platform's suspension axis. It can be particularly large when a direct-current moment sensor with a brush commutator is used as the stabilizing engine. When saturation in each channel of the signal processing system and the moments of dry friction are allowed for, the structural diagram of an OSP with an RVG takes on the form depicted in Figure 27.

The analytical expression for nonlinearity of the saturation type in the signal processing system's channel can be approximated with a piecewise-linear function of the type

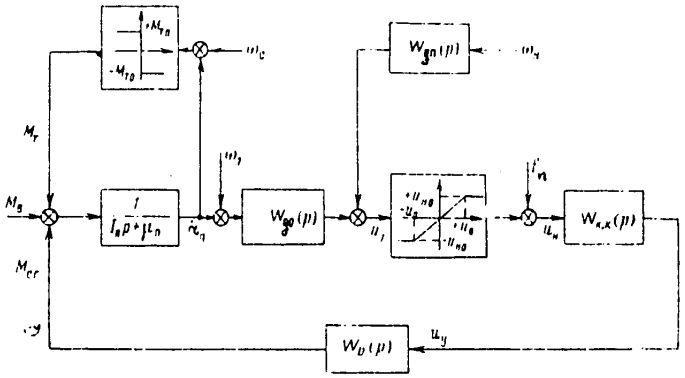

Figure 27. Structural diagram of OSP, taking the basic nonlinearities into consideration.

$$u_{\text{н}} = \begin{cases} u & \text{for } |u| < u_0; \\ u_{\text{н}0} & \text{for } u > u_0; \\ u_{\text{н}0} & \text{for } u < -u_0. \end{cases} \tag{4.1}$$

"Dry" friction is usually approximated by so-called Coulomb friction [22], which--depending on the platform's and base's relative angular velocity--is described by a relay characteristic that is indeterminate at zero. We will predefine this characteristic in the following manner:

$$M_{\text{т}} = \begin{cases} -M_{\text{т}0} & \text{for } \dot{\alpha}_{\text{п}} - \omega_C > 0; \\ M_{\text{т}0} & \text{for } \dot{\alpha}_{\text{п}} - \omega_C < 0; \\ M_{\text{п}} + M_{\text{ст}} & \text{for } \dot{\alpha}_{\text{п}} - \omega_C = 0, \end{cases} \tag{4.2}$$

where ω_C = absolute angular velocity of the base relative to the axis coinciding with the platform's suspension axis.

A problem of particular complexity is allowing for the presence of arresting devices that limit the angles of rotation of the RVG rotors. Limitation of the rotors' degrees of freedom leads to a change in the equations of motion, which become essentially nonlinear, so that the MRG transfer functions derived in Chapter 1 lose their meaning.

Taking into consideration the nonstationary nature of the RVG and the described nonlinearities that are inherent in OSP's and RVG's, we are now able to investigate an OSP's basic properties.

Let us examine the special features of the description of multiaxial stabilized platforms. Figure 28 is a diagram of a triaxial stabilized platform (TSP). Either two or three RVG's can be used in its construction. In view of the fact that each RVG is a two-dimensional measurer, the first variant makes it possible to achieve duplication of one channel, while the second makes it possible to duplicated all three stabilization channels. The most natural orientation of the RVG's on the platform is the one in which their axes of sensitivity coincide with the stabilization axes.

In order to describe such a system, we will use a vector-matrix apparatus. In this case, given assumptions that enable us to regard the system as being stationary and

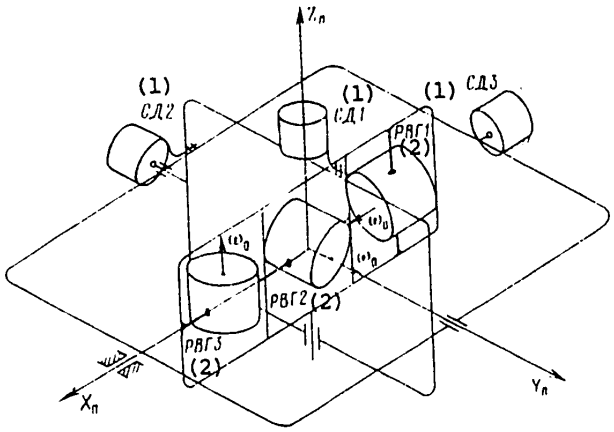

Figure 28. Diagram of TSP based on RVG's.

Key:
1. SD. [stabilizing engine] 2. RVG.

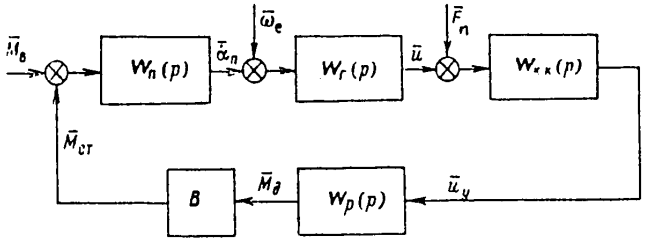

Figure 29. Structural diagram of TSP based on RVG's.

linear, its structural diagram can be represented in the form depicted in Figure 29. In the structural diagram we have introduced the vectors of the system's generalized coordinates and the disturbances acting on it, as well as the transfer matrices of its basic elements. When constructing the platform's transfer matrix $W_п(p)$, along with the cross-couplings between the channels with respect to the platform's centrifugal moments of inertia [22], the cross-couplings with respect to the gyroscopic moments should also be taken into consideration. The latter arise because of the fact that the rotating parts of each RVG, which are rotor PD2, have some kinetic moment h_i. Allowing for this, the elements a_{ij} of the platform's transfer matrix are written in the form

$$\left.\begin{aligned}
a_{11} &= \frac{1}{d(p)}\left[1-(I_{XY}p+h_3)(I_{XY}p-h_3)W_{п2}(p)W_{п3}(p)\right]W_{п1}(p);\\
a_{12} &= \frac{1}{d(p)}\left[h_1+h_2(I_{XY}p+h_3)W_{п3}(p)\right]W_{п1}(p)W_{п2}(p);\\
a_{13} &= -\frac{1}{d(p)}\left[h_1(I_{XY}p-h_3)W_{п1}(p)W_{п2}(p)+h_2W_{п1}(p)\right]W_{п3}(p);\\
a_{21} &= -\frac{1}{d(p)}\left[h_1+h_2(I_{XY}p-h_3)W_{п3}(p)\right]W_{п1}(p)W_{п2}(p);\\
a_{22} &= \frac{1}{d(p)}\left[1+h_2^2W_{п1}(p)W_{п3}(p)\right]W_{п2}(p);\\
a_{23} &= -\frac{1}{d(p)}\left[I_{XY}p-h_3-h_1h_2W_{п1}(p)\right]W_{п2}(p)W_{п3}(p);\\
a_{31} &= \frac{1}{d(p)}\left[h_1(I_{XY}p+h_3)W_{п2}(p)+h_2\right]W_{п3}(p)W_{п1}(p);
\end{aligned}\right\} \qquad (4.3)$$

$$a_{32} = -\frac{1}{d(p)}[I_{XY}p + h_3 - h_1h_2W_{n1}(p)]\,W_{n3}(p)W_{n2}(p),$$
$$a_{33} = \frac{1}{d(p)}[1 + h_1^2W_{n1}(p)\,W_{n2}(p)]\,W_{n3}(p),$$

where

$$d(p) = 1 + h_1^2W_{n1}(p)\,W_{n2}(p) + h_2^2W_{n1}(p)\,W_{n3}(p) + h_3^2W_{n2}(p)\,W_{n3}(p) - (I_{XY}p)^2\,W_{n2}(p)\,W_{n3}(p) + 2h_1h_2I_{XY}p\,W_{n1}(p)\,W_{n2}(p)\,W_{n3}(p);$$
$$W_{ni}(p) = \frac{1}{T_{ni}p + \mu_{ni}}.$$

The measurers' transfer matrix $W_g(p)$ allows for the operation of each of the three RVG's on two channels and the presence of internal cross-couplings between the channels that is inherent in RVG's. This matrix has the form

$$\mathbf{W}_g(p) = \begin{Vmatrix} W_{g.n1}(p) + W_{g.n2}(p) & W_{g.n1}(p) & -W_{g.n2}(p) \\ -W_{g.n1}(p) & W_{g.n1}(p) + W_{g.n3}(p) & W_{g.n3}(p) \\ W_{g.n2}(p) & -W_{g.n3}(p) & W_{g.n2}(p) + W_{g.n3}(p) \end{Vmatrix}. \quad (4.4)$$

Matrix $W_{k.k}(p)$ can be an arbitrary operator matrix with 3 x 3 dimensionality. Its elements must be selected in such a manner that for a given unchanging part of the system, desirable dynamic characteristics are obtained in it. In particular, when the cross-couplings are weak, this matrix can be a diagonal one.

Matrix $BW_p(p)$ allows for the transfer functions $W_{pi}(p)$ of the regulators in each of the channels, as well as the cross-couplings between the stabilization channels with respect to the stabilizing engines' moments [22]. In the general case this matrix is written in the form

$$\mathbf{BW}_p(p) = \begin{Vmatrix} W_{p1}(p) & 0 & 0 \\ \sin\beta_1 \operatorname{tg}\beta_2 W_{p1}(p) & \cos\beta_1 W_{p2}(p) & \sin\beta_1 \sec\beta_2 W_{p3}(p) \\ \cos\beta_1 \operatorname{tg}\beta_2 W_{p1}(p) & -\sin\beta_1 W_{p2}(p) & \cos\beta_1 \sec\beta_2 W_{p3}(p) \end{Vmatrix}, \quad (4.5)$$

where β_1, β_2 = relative angles of rotation, respectively, of the platform and the intermediate suspension ring and the intermediate and outer suspension rings.

The cross-couplings in the regulator are eliminated almost completely when a device that realizes spatial conversion of the coordinates is used [24]. Plane conversion of the coordinates eliminates cross-couplings caused by the platform's angle of rotation β_1 alone. It should be mentioned here that in some cases the structural features of an RVG make it possible to simplify substantially the solution of the problem of plane conversion of the coordinates. When RVG's with signal reading in a rotating system of coordinates and single signal modulation are used in a TSP based on two RVG's (RVG1 and RVG3) in which only the signals from RVG3 are used for stabilization along the 2-2 and 3-3 axes, it is sufficient to attach the receiving coils of RVG3's GOI directly to the intermediate ring. In this case, even when the platform rotates through angle β_1 the sensitivity axes of RVG3 will always coincide with the suspension axes on which the corresponding stabilizing engines are mounted.

Allowing for the nonstationary nature of RVG's in multidimensional systems when normal instrument transfer functions are used leads to an extremely cumbersome form of

both the equations of motion and the system's structural diagrams. Therefore, it is more convenient to use the complex RVG transfer functions derived in Chapter 1.

In order to do this, let us introduce additional matrix transformations of the system's coordinates:

$$\bar{\omega}_{\text{п}} = \left\| \begin{matrix} \bar{\omega}_1 \\ \bar{\omega}_2 \\ \bar{\omega}_3 \end{matrix} \right\| = \mathrm{J}\bar{\alpha}_{\text{п}}, \tag{4.6}$$

where

$$\mathrm{J} = \left\| \begin{matrix} i & 0 & 1 \\ i & 0 & 1 \\ 0 & 1 & i \end{matrix} \right\|.$$

Vectors $\bar{\omega}_1$, $\bar{\omega}_2$, $\bar{\omega}_3$ are absolute angular velocity vectors lying in the plane of sensitivity of the first, second and third RVG's, respectively. The vectors of the output signals from each RVG are $\bar{u}_1$, $\bar{u}_2$, $\bar{u}_3$. The transition from these vectors to the vector of the signals going from the RVG's into the stabilization system is accomplished by the following transformation:

$$\bar{u} = \frac{1}{2}\mathrm{A}_1 \left\| \begin{matrix} \bar{u}_1 \\ \bar{u}_2 \\ \bar{u}_3 \end{matrix} \right\| + \frac{1}{2}\mathrm{A}_2 \left\| \begin{matrix} \bar{u}_1^* \\ \bar{u}_2^* \\ \bar{u}_3^* \end{matrix} \right\|, \tag{4.7}$$

where

$$\mathrm{A}_1 = \left\| \begin{matrix} -i & -i & 0 \\ 1 & 0 & 1 \\ 0 & 1 & -i \end{matrix} \right\|; \quad \mathrm{A}_2 = \left\| \begin{matrix} -i & -i & 0 \\ 1 & 0 & 1 \\ 0 & 1 & i \end{matrix} \right\|.$$

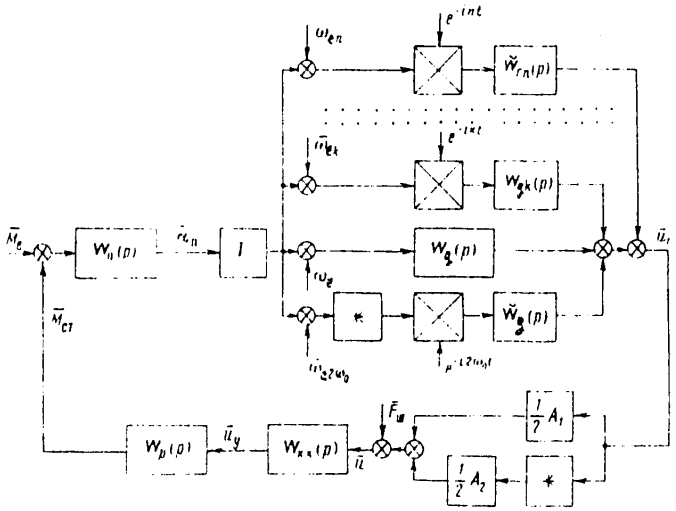

Figure 30. Structural diagram of TSP, allowing for the nonstationary nature of the RVG's signals.

When transformations (4.6) and (4.7) are taken into consideration, the TSP's structural diagram can be represented in the form depicted in Figure 30. As in the

unidimensional case, for systems with single modulation by the PD2 motor and systems with modulation by the PD1 motor, for which condition (1.22) is fulfilled, in this system there is only a single nonstationary, parallel coupling with modulation on frequency $2\omega_0$. For other RVG setups there is an infinite set of such couplings with modulating frequencies that are both multiples of $2\omega_0$ and composite frequencies. Transfer matrices $W_g(p)$, $\tilde{W}_g(p)$ and $\tilde{W}_{g.k}(p)$ are diagonal matrices, along the main diagonals of which the corresponding complex RVG transfer functions are located.

Let us discuss a method of representing, with the help of a matrix structural diagram, a TSP in which the basic nonlinearities of the type of saturation in the RVG (4.1) and the type of dry friction in the suspension axes (4.2) are taken into consideration. In order to do this, we will introduce so-called nonlinearity units BH1 and BH2, which are diagonal matrices of dimensionality 3 x 3 in which the piecewise-linear functions u_{Hi} and M_{Ti}, as determined by expressions (4.1) and (4.2), are located along the respective main diagonals. The input for BH2 should be the vector of the platform's relative angular velocities in the suspension axes. When the base is immobile, the conversion from the absolute angular velocities of the platform to its relative velocities in the suspension axes is accomplished by multiplication from the left of matrix B^T by vector $\bar{\alpha}_\pi$ [22]. When the system of coordinates is given as indicated in [24], the relationship between the vector of relative velocities in the suspension axes and the base's angular velocities is determined by matrix B_1:

$$B_1 = \begin{Vmatrix} \cos\beta_1 \cos\beta_2 & \sin\beta_1 \cos\beta_2 & -\sin\beta_2 \\ -\sin\beta_1 & \cos\beta_1 & 0 \\ 0 & 0 & 1 \end{Vmatrix}. \qquad (4.8)$$

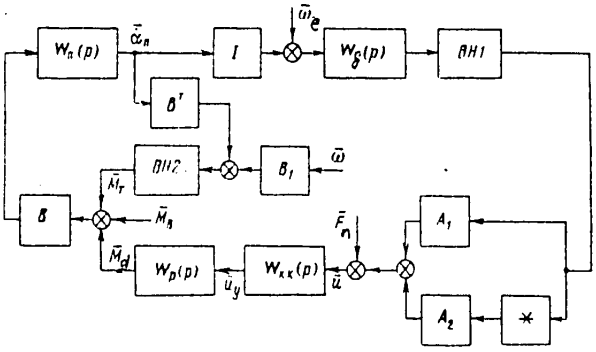

Figure 31. Structural diagram of TSP, with basic nonlinearities allowed for.

In the suspension axes there occurs summation of the moments of the "dry" friction forces, the stabilizing engines' moments and the disturbing moments, which should be regarded as being reduced to the platform's suspension axes. With the help of matrix B, the total moment is converted to the moment acting along the platform's axes.

Saturation is allowed for in the signal processing system by simply connecting nonlinearity unit BH1 to the structural diagram, in series, after transfer matrix $W_g(p)$. Figure 31 is the structural diagram of such a system, with BH2 also having been taken into consideration.

4.2. Static Characteristics of Stabilization Systems

Let us discuss the simplest OST layout. From the structural diagram depicted in Figure 25 it is easy to derive the transfer function of an open system:

$$W(p) = \frac{1}{\mu_n} \frac{1}{T_n p + 1} W_{g^0}(p) W_{к.к}(p) W_p(p), \tag{4.9}$$

where $T_\pi = J_\pi/\mu_\pi$. The transfer function of a closed system, with respect to a disturbing moment acting on the platform, has the form

$$K(p) = \frac{1}{\mu_n p} \frac{1}{T_n p + 1} \frac{1}{1 + W(p)}, \tag{4.10}$$

while with respect to the equivalent angular velocity acting at the RVG's output, it is

$$K_{\omega e}(p) = \frac{W(p)}{1 + W(p)} \frac{1}{p}. \tag{4.11}$$

In expressions (4.10) and (4.11) let us make the maximum transition for $p \to 0$. In the absence in the stabilization circuit of purely differentiating or integrating components, for $p \to 0$ the maximum of the product $W_{k.k}(p)W_p(p)$ is K_p.

As has already been stated, in connection with dynamic tuning an RVG can be characterized by two operating modes. The first of them is the integrating mode, which occurs in the initial period of the transient process in connection with the effect on the instrument's input of a discontinuity in the angular velocity. Since the length of the transient process is quite long for highly sensitive RVG's, for a GSP this mode will be caused by the effect of the disturbance resulting from some static error appearing after the conclusion of the short-period component of the transient process in the stabilization system. The second mode is a differentiating one and is the RVG's steady-state reaction to a constant angular velocity. In this mode the instrument's properties will determine the GSP's drifts when acted upon by constant disturbing moments along the stabilization axes.

In the first case, with respect to the base's absolute angular velocity the following relationship occurs:

$$W_{g^0}(p) \underset{p \to 0}{=} -K_g, \tag{4.12}$$

and in the second:

$$W_{g^0}(p) \underset{p \to 0}{=} -\frac{K_{ii}}{p}. \tag{4.13}$$

When acted upon by a constant disturbing moment, the OSP's static error then has the following forms:
in the differentiating mode--

$$\dot{\alpha} = \frac{1}{\mu_n} \frac{1}{1 + \frac{K_g K_p}{\mu_n}} M, \tag{4.14}$$

in the integrating mode--

$$\alpha_n = \frac{1}{K_i K_p} M. \tag{4.15}$$

A constant equivalent angular velocity at the RVG's input results in the following OSP static errors:
in the differentiating mode--

$$\dot{\alpha}_n = \frac{K_g K_p}{\mu_n + K_g K_p}\,\dot{\omega}_e, \tag{4.16}$$

in the integrating mode--

$$\dot{\alpha}_n = \dot{\omega}_e. \tag{4.17}$$

When the RVG is operating in the differentiating mode and the requirements for OSP accuracy are real, it is necessary that amplification factor K_p be one or two orders of magnitude greater than when the RVG is operating in the integrating mode. In the case of large values of K_p, OSP drifts are determined by RVG errors expressed in terms of the equivalent angular velocities at its input.

Let us discuss the static characteristics of multidimensional stabilization systems. When a system is represented in linear and stationary form, in accordance with the structural diagram depicted in Figure 29, its equation of motion has the form

$$\begin{aligned}\bar{\alpha}_n = {} & [E + W_n(p)\,BW_p(p)\,W_{k.k}(p)\,W_g(p)]^{-1}\,W_n(p)\times \\ & \times [\bar{M} - BW_p(p)\,W_{k.k}(p)\,W_g(p)\,\bar{\omega}_e].\end{aligned} \tag{4.18}$$

Let us derive the static characteristics of a DSP [biaxial stabilized platform] based on a single RVG. In connection with this we will assume that, in the general form, in the system it is possible to realize mixed control of the stabilizing engines; that is, all the elements of matrix $W_{k.k}(p)$ do not equal zero. It is then the case that, in the differentiating mode,

$$\begin{aligned}\bar{\dot{\alpha}}_n = {} & \left\| \begin{array}{c} \frac{1}{\mu_{n3}K_3} + \frac{h^2}{\mu_{n2}\mu_{n3}} - K_{c2}\frac{h}{\mu_{n3}}\bar{K}_{23} + K_{n.g}\left(K_{c2}\bar{K}_{32} - K_{c3}\frac{h}{\mu_{n3}}\right); \\ K_{c2}\frac{h}{\mu_{n3}} - K_{c3}\bar{K}_{32} - K_{n.g}\left(K_{c2}\frac{h}{\mu_{n3}}\bar{K}_{23} - K_{c3}\right); \end{array} \right. \\ & \left. \begin{array}{c} -K_{c3}\frac{h}{\mu_{n2}} - K_{c2}\bar{K}_{23} + K_{n.g}\left(K_{c3}\frac{h}{\mu_{n2}}\bar{K}_{32} - K_{c2}\right); \\ \frac{1}{\mu_{n2}K_2} + \frac{h^2}{\mu_{n2}\mu_{n3}} + K_{c3}\frac{h}{\mu_{n2}}\bar{K}_{32} - K_{n.g}\left(K_{c2}\bar{K}_{23} + K_{c3}\frac{h}{\mu_{n2}}\right) \end{array} \right\| \times \\ & \times \left\| \begin{array}{cc} \frac{1}{\mu_{n2}} & \frac{h}{\mu_{n2}\mu_{n3}} \\ -\frac{h}{\mu_{n2}\mu_{n3}} & \frac{1}{\mu_{n3}} \end{array} \right\| \frac{1}{d}\,\bar{M},\end{aligned} \tag{4.19}$$

where

$$\begin{aligned} d = {} & \frac{1}{\mu_{n2}K_2}\,\frac{1}{\mu_{n3}K_3}\times \\ & \times \left\{ \left[1 + K_2\left(\frac{h^2}{\mu_{n3}} + K_{c3}\bar{K}_{32}h - K_{n.g}(K_{c2}\bar{K}_{23}\mu_{n2} + K_{c3}h\bar{K}_{32})\right)\right]\times \right. \\ & \times \left[1 + K_3\left(\frac{h^2}{\mu_{n2}} - K_{c2}\bar{K}_{23}h + K_{n.g}(K_{c3}\bar{K}_{32}\mu_{n3} - K_{c2}h)\right)\right] - \\ & - K_2K_3[(K_{c2}\bar{K}_{23}\mu_{n2} + hK_{c3}) + K_{n.g}(K_{c2}\mu_{n2} + hK_{c3}\bar{K}_{32})]\times \\ & \left. \times [(K_{c3}\bar{K}_{32}\mu_{n3} - hK_{c2}) - K_{n.g}(K_{c3}\mu_{n3} - hK_{c2}\bar{K}_{23})]\right\}; \end{aligned}$$

K_2, K_3 = amplification factors of isolated stabilization channels in the closed state; K_{c2}, K_{c3} = amplification factors of open isolated stabilization channels $\overline{K}_{32} = K_{k32}/K_{k33}$, $\overline{K}_{23} = K_{k23}/K_{k22}$ are relative transfer factors of cross-signals in the correcting circuit; $K_{\pi.g} = W_{g.\pi}(0)/W_{g.o}(0)$ = relative transfer factor of cross-signals in the RVG.

Let us make some simplifications in expressions (4.19). As was shown in Section 1.6, the RVG's transfer factor with respect to the cross-signal relative to the base's angular velocity is determined by the detuning of the instrument from the resonance mode or by a phase shift in the demodulator. In real instruments these values should be quite small, so in (4.19) we can ignore the terms containing $K_{\pi.g}$. The transfer factor of an open, isolated stabilization channel is usually greater than unity, so the following relationship is fulfilled:

$$K_{ci} = \frac{1}{K_i \mu_n}.$$

Considering what has been said, let us derive the expression for a DSP's static errors in a simpler form:

$$\bar{\alpha}_n = \left\| \begin{matrix} K_2\left[1 + \frac{h^2}{\mu_{n2}}\left(\frac{1}{\mu_{n3}} + K_3\right)\right] \\ -K_2\left[\overline{K}_{32}\left(1 + \frac{h^2}{\mu_{n2}\mu_{n3}}\right) + K_3\frac{h^3}{\mu_{n2}\mu_{n3}}\right] \\ -K_3\left[\overline{K}_{23}\left(1 + \frac{h^2}{\mu_{n2}\mu_{n3}}\right) - K_2\frac{h^3}{\mu_{n2}\mu_{n3}}\right] \\ K_3\left[1 + \frac{h^2}{\mu_{n3}}\left(\frac{1}{\mu_{n2}} + K_2\right)\right] \end{matrix} \right\| \times \quad (4.20)$$

$$\times \frac{1}{\left(1 + K_1\frac{h^2}{\mu_{n2}}\right)\left(1 + K_2\frac{h^2}{\mu_{n3}}\right) + \frac{h^2}{\mu_{n2}\mu_{n3}} - \overline{K}_{32}\overline{K}_{23}\left(1 + \frac{h^2}{\mu_{n2}\mu_{n3}}\right) + \frac{h^3}{\mu_{n2}\mu_{n3}}(K_2\overline{K}_{32} - K_1\overline{K}_{23})} \overline{M}.$$

From (4.20) it follows that a DSP's static errors can be reduced by increasing the amplification factor in the circuit for the direct control of the stabilizing engines and in the cross-control circuit, as well as by increasing the kinetic moment h. In connection with direct control, it is sufficient to set $K_{23} = K_{32} = 0$ in expression (4.20). In the case of cross-control alone, expression (4.20) is transformed into

$$\bar{\alpha}_n = \left\| \begin{matrix} K_{2n}K_{3n}\frac{h^2}{\mu_{n2}} \\ -K_{2n}\left(1 + \frac{h^2}{\mu_{n2}\mu_{n3}} + K_{3n}\frac{h^3}{\mu_{n2}\mu_{n3}}\right) \\ -K_{3n}\left(1 + \frac{h^2}{\mu_{n2}\mu_{n3}} - K_{2n}\frac{h^3}{\mu_{n2}\mu_{n3}}\right) \\ K_{2n}K_{3n}\frac{h^2}{\mu_{n3}} \end{matrix} \right\| \quad (4.21)$$

$$\times \frac{\overline{M}}{K_{2n}K_{3n}\frac{h^4}{\mu_{n2}\mu_{n3}} - 1 - \frac{h^2}{\mu_{n2}\mu_{n3}} + (K_{2n} - K_{3n})\frac{h^3}{\mu_{n2}\mu_{n3}}},$$

where

$$K_{2n} = K_{c2}\frac{K_{K22}}{K_{K33}}; \quad K_{3n} = K_{c3}\frac{K_{K12}}{K_{K33}}.$$

Given the assumptions made above, disturbances applied to the system in the form of an equivalent angular velocity at the RVG's input result in static errors described by the following expressions:

$$\bar{\alpha}_n = \left\| \begin{array}{c} \left(1+\frac{h^2}{\mu_{n2}}K_3\right)+\frac{h^2}{\mu_{n2}\mu_{n3}}(1+h\bar{K}_{32}K_2)-\bar{K}_{32}\bar{K}_{23}\left(1+\frac{h^2}{\mu_{n2}\mu_{n3}}\right) \\ -\bar{K}_{32}\left(K_3\frac{h}{\mu_{n2}}-K_2\right) \\ -\bar{K}_{23}\frac{h^2}{\mu_{n2}}\left(K_2\frac{h}{\mu_{n3}}-K_3\right) \\ \left(1+\frac{h^2}{\mu_{n3}}K_2\right)+\frac{h^2}{\mu_{n2}\mu_{n3}}(1-h\bar{K}_{23}K_3)-\bar{K}_{23}\bar{K}_{32}\left(1+\frac{h^2}{\mu_{n2}\mu_{n3}}\right) \end{array} \right\| \times \frac{\bar{\omega}_2}{\left(1+K_3\frac{h^2}{\mu_{n2}}\right)\left(1+K_2\frac{h^2}{\mu_{n3}}\right)+\frac{h^2}{\mu_{n2}\mu_{n3}}-\bar{K}_{32}\bar{K}_{23}\left(1+\frac{h^2}{\mu_{n2}\mu_{n3}}\right)+\frac{h^3}{\mu_{n2}\mu_{n3}}(K_2\bar{K}_{32}-K_3\bar{K}_{23})}. \tag{4.22}$$

From (4.22) follows the trivial conclusion that the larger kinetic moment h is relative to the stabilization circuits' amplification factors, the smaller the systematic DSP drifts caused by RVG errors. For small kinetic moments and high amplification factors in the stabilization circuit:

$$\bar{\alpha}_n \approx \left\| \begin{array}{cc} 1 & 0 \\ 0 & 1 \end{array} \right\| \bar{\omega}_e \tag{4.23}$$

that is, for all practical purposes the DSP drifts equal the RVG errors.

In an analogous manner let us determine the DSP's static errors when the RVG is operating in the integrating mode. When a disturbing moment is acting along the stabilization axes, they can be defined as

$$\bar{\alpha}_n = \left\| \begin{array}{cc} \frac{1}{K_{c2}} & -\bar{K}_{23}\frac{1}{K_{c3}} \\ -\bar{K}_{32}\frac{1}{K_{c2}} & \frac{1}{K_{c3}} \end{array} \right\| \frac{1}{1-\bar{K}_{23}\bar{K}_{32}}\bar{M}, \tag{4.24}$$

while when an equivalent angular velocity is acting on the RVG's input, they are determined from the expression

$$\bar{\alpha}_n = \left\| \begin{array}{cc} 1 & 0 \\ 0 & 1 \end{array} \right\| \frac{1}{1+\frac{h}{\mu_{n2}\mu_{n3}}}\bar{\omega}_e. \tag{4.25}$$

Thus, when the RVG is operating in the integrating mode, constant disturbing moments result in permanent angular deviations of the DSP from the position it initially occupied in inertial space, it being the case that the higher the open system's amplification factor, the smaller the deviations are. In connection with this, both direct and cross control prove to be effective.

4.3. Choosing the Structure and Parameters of a Uniaxial Stabilization System

Let us discuss OSP's that are described by the structural diagram presented in Figure 25. We will choose the structure and parameters of the correcting circuit on the basis of the requirement of realizing a given value of K_p in the system while insuring its stable operation with given indicators for the quality of the transient processes.

Let us examine an OSP based on a single-rotor MRG featuring signal reading in a rotating system of coordinates. In the dynamic tuning mode, its transfer function with respect to the basic signal is described by expression (1.86). As the indicator of the transient process's quality we will take the value of the cutoff frequency ω_2 of the open system's LAKh [logarithmic frequency response characteristic] and its deviation in the area of this frequency, as well as the system's stability reserves with respect to phase ϕ_3 and amplitude A_3 [2]. From an examination of the open system's frequency characteristics it follows directly that it is easy to obtain the given values of the quality indicators by using a series-connected correcting circuit with the following transfer function:

$$W_{к.к}(p) = \frac{T_{к1}p + 1}{T_{к2}p + 1}; \quad T_{к1} > T_{к2}. \tag{4.26}$$

Let us establish the relationship between the values of the time constants T_{k1} and T_{k2}, the regulator's amplification factor K_p, cutoff frequency ω_2 and the values of the stability reserves relative to amplitude and phase when the LAKh's deviation in the area of the cutoff frequency is -20 dB/decade.

Considering the fact that for real systems the time constants $T_\pi = J_\pi/\mu_\pi$ and T_g are large and that the frequencies corresponding to them are considerably lower than the cutoff frequency, we obtain the following systems of equations:

$$\left.\begin{aligned} &\frac{K_g K_p}{\mu_\pi}\sqrt{\frac{T_{к1}^2\omega_1^2+1}{T_{к2}^2\omega_1^2+1}}\frac{1}{T_\pi T_g\omega_1^2}\frac{1}{\sqrt{T_p^2\omega_1^2+1}} = A_3;\\ &\operatorname{arctg} T_{к1}\omega_1 - \operatorname{arctg} T_{к2}\omega_1 - \operatorname{arctg} T_p\omega_1 = 0;\\ &\frac{K_g K_p}{\mu_\pi}\sqrt{\frac{T_{к1}^2\omega_2^2+1}{T_{к2}^2\omega_2^2+1}}\frac{1}{T_\pi T_g\omega_2^2}\frac{1}{\sqrt{T_p^2\omega_2^2+1}} = 1; \end{aligned}\right\} \tag{4.27}$$

where ω_1 = the frequency on which the open system's phase characteristic equals $-\pi$; T_p = a time constant that allows for the stabilizing engine's inertial lag.

We will assume that the condition $1/T_p >> \omega_2$ is fulfilled in the system. It is then obvious that the maximum ratio $T_{k2}/T_{k1} = \nu$ for which the required stability reserve with respect to phase is insured is determined by the expression

$$\nu = 1 + 2\operatorname{tg}^2\varphi_3 - \sqrt{(1 + 2\operatorname{tg}^2\varphi_3)^2 - 1}, \tag{4.29}$$

while the cutoff frequency is

$$\omega_2 = \frac{1-\nu}{2T_{к1}\nu}. \tag{4.30}$$

Substituting (4.30) into the first equation in system (4.28), we obtain the open system's amplification factor:

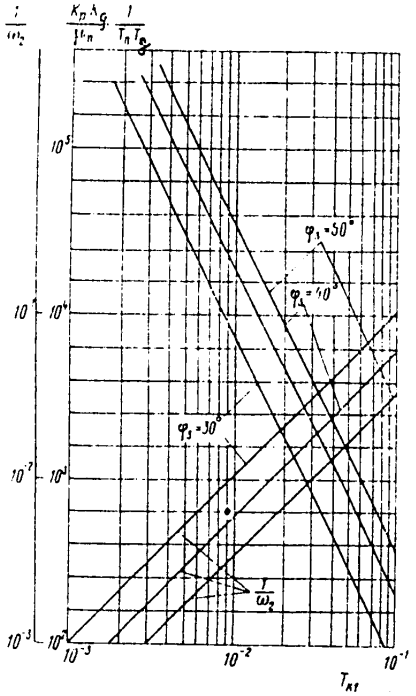

Figure 32. Graphs for selecting the correcting circuit's time constant.

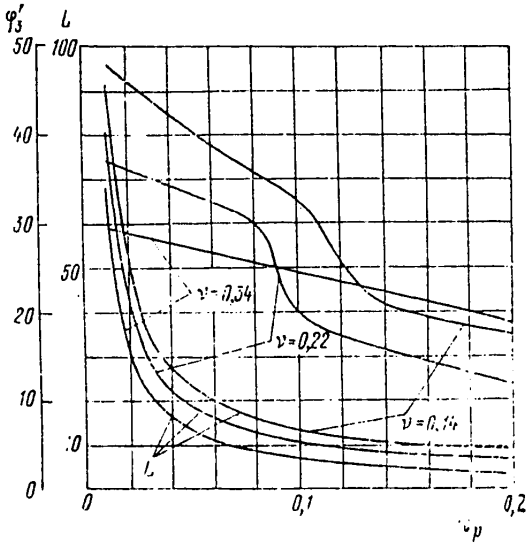

Figure 33. Areas of OSP stability and stability reserve with respect to phase as a function of the regulator's time lag.

$$\frac{K_p K_g}{\mu_n} = \frac{T_n T_r}{T_{kl}^2}\frac{(1-\nu)^2}{4\nu}\sqrt{\frac{5-2\nu+\nu^2}{1-2\nu+5\nu^2}}. \qquad (4.31)$$

Figure 32 depicts the graphs of the dependence of $(K_pK_g/\mu_\pi)/(1/T_\pi T_g)$ and $1/\omega_2$ on T_{kl} for different system stability reserves with respect to phase. These graphs and relationship (4.29) make it possible to make a preliminary selection of the correcting circuit parameters (4.26) that provide the desired regulation process quality.

The stabilizing engine's time lag T_p imposes additional limitations on the choice of the open system's amplification factor. In connection with this, the stability reserve with respect to phase takes on the value

$$\varphi_3' = \varphi_3 - \operatorname{arctg}\frac{1}{2}\frac{1-\nu}{\nu}\tau_p, \qquad (4.32)$$

while the open system's amplification factor, allowing for the required quality reserve with respect to amplitude, satisfies the inequality

$$\frac{\left[1-\tau_p^2+\left(\frac{1}{\nu}-1\right)\tau_p\right](\tau_p+\nu)(1-\nu-\tau_p)^2}{\nu\tau_p^2(1-\tau_p)} \geqslant \left(\frac{K_pK_g}{\mu_n T_n T_g}\frac{T_{kl}^2}{A_3}\right)^2 = L^2, \qquad (4.33)$$

where $\tau_p = T_p/T_k < 1$. In accordance with (4.33), in Figure 33 we have plotted the areas of allowable values of L that relate the values of the system's parameters and its stability reserve A_3.

Calculations made for specific systems show that a correcting circuit with transfer function (4.26) makes it possible to insure small stabilization errors, as determined by expression (4.15). When acted upon by real disturbances, however, the

drifts in such systems (as found with expression (4.14)) can become quite large. Reducing the drifts by one or two orders of magnitude causes a significant enlargement of the system's pass band. As a result, the requirements for the stabilization system elements that are related to the expansion of their dynamic range are raised and the noise level in each of the elements is reduced. Thus, the stabilization circuit structure under discussion can be used as a basis for correcting systems or systems in which the requirements for the magnitude of the drift are not quite so high.

The easiest way to increase an open system's amplification factor is to include an integrating-differentiating element in the stabilization circuit. The correcting circuit's transfer function then acquires the form

$$W_{к.к}(p) = \frac{T_{к3}p + 1}{T_{к4}p + 1} \frac{T_{к1}p + 1}{T_{к2}p + 1}, \qquad (4.34)$$

where $T_{k4} > T_{k3} >> T_{k1} > T_{k2}$. In connection with this it can be assumed that the amplification factor increases by a factor of T_{k3}/T_{k4} while the open system's LAKh's cutoff frequency remains unchanged. The required value of the open system's amplification factor also determines the relationship between the time constants T_{k3} and T_{k4}. Time constant T_{k3} should be selected in such a fashion that relationship $T_{k3} >> T_{k1}$ is satisfied. In this case the technique for selecting time constants T_{k1} and T_{k2} and allowing for the effect of the stabilizing engine's time constant T_p is analogous to the one described above. Let us mention, however, that the given system will have two stability reserves with respect to amplitude; that is, it is provisionally stable.

As follows from an analysis of the equations of motion, the dynamic characteristics of a DMG differ substantially from the characteristics of an OMG. Let us discuss an OSP based on the use of one of the most highly developed types of RVG: a DMG with single modulation by motor PD2 and signal reading in a nonrotating system of coordinates on the zero frequency (a Khaui gyroscope). We will make use of its transfer functions, as approximated in the band of essential frequencies by expressions (1.109). An oscillatory component with time constant T_π describes the precession motion and determines the gyroscope's deflection in inertial space. In connection with the discussion of a system's stability, this oscillatory component and the component with the introduction of a derivative in the area of its frequency cutoff can be approximated by the expression $(T_\pi^2/T_\pi^2)/(1/p)$. An oscillatory component with time constant T_H describes the gyroscope's nutational oscillations and affects the system's dynamic characteristics.

One of the simplest correcting circuits in a stabilization circuit, which makes it possible to increase the regulator's amplification factor K_p, is a nonminimal-phase, series-connected circuit with a transfer function in the form

$$W_{к.к}(p) = \frac{T_{к3}p + 1}{T_{к3}p + 1} \frac{-T_{к1}p + 1}{T_{к1}p + 1}, \qquad (4.35)$$

where $T_{k3} < T_{k2}$.

Using (as before) the frequency criterion of stability, let us determine the correcting circuit's parameters and, in connection with them, the maximally achievable amplification factor of the open system. (We will assume that $1/T_{k3}$ and $1/T_p$ are much larger than the nutational frequency $1/T_H$ and that the effect of the

corresponding components on the system's dynamic characteristics can be ignored in the first approximation.)

It is obvious that in order to achieve the maximum amplification factor it is necessary that the open system's phase frequency characteristic take on the value $-\pi$ at frequency ω_0, as determined from the relationship

$$\nu_0 = \omega_0 T_н = \sqrt{\frac{2}{3}\left(1 - 2\xi_н^2 - \sqrt{(1-2\xi_н^2)^2 - \frac{3}{4}}\right)} \approx \frac{1}{\sqrt{3}}. \tag{4.36}$$

Frequencies ω_1, on which the amplitude frequency characteristic equals unity, is then determined as the roots of the cubic equation

$$\nu_1^3 - \nu_1 + A_п \nu_0 \sqrt{(1-\nu_0^2)^2 - 4\xi_н^2 \nu_0^2} = 0, \tag{4.37}$$

where $\nu_1 = \omega_1 T_н$. Taking into consideration the fact that $\xi_н << 1$ and giving (for example) a stability reserve with respect to amplitude of 6 dB, we obtain the following solution for equation (4.37):

$$\nu_{11} \approx \frac{2}{\sqrt{3}} \cdot 0{,}173\,6; \quad \nu_{12} \approx \frac{2}{\sqrt{3}} \cdot 0{,}766\,0; \quad \nu_{13} \approx \frac{2}{\sqrt{3}} \cdot 0{,}939\,7.$$

Having obtained ν_0 and ν_1 from equations (4.36) and (4.37), the values of the correcting circuit's normalized time constants $\tau_{k1} = T_{k1}/T_н$ and $\tau_{k2} = T_{k2}/T_н$ can be determined by solving the following system of nonlinear algebraic equations:

$$\left.\begin{aligned} \tau_{к2} &= \frac{2(1+\tau_п\nu_0 \operatorname{tg}\psi_0)\,\nu_0\tau_{к1} + (\tau_п\nu_0 - \operatorname{tg}\psi_0)(1-\nu_0^2\tau_{к1}^2)}{\nu_0(1+\tau_п\nu_0\operatorname{tg}\psi_0)(1-\nu_0^2\tau_{к1}^2) - 2(\tau_п\nu_0 - \operatorname{tg}\psi_0)\nu_0^2\tau_{к1}}; \\ \tau_{к2} &= \frac{2(1+\tau_п\nu_{11}\operatorname{tg}\psi_1)\,\nu_{11}\tau_{к1} + (\tau_п\nu_{11} - \operatorname{tg}\psi_1)(1-\nu_{11}^2\tau_{к1}^2)}{\nu_{11}(1+\tau_п\nu_{11}\operatorname{tg}\psi_1)(1-\nu_{11}^2\tau_{к1}^2) - 2(\tau_п\nu_{11} - \operatorname{tg}\psi_1)\nu_{11}^2\tau_{к1}}; \end{aligned}\right\} \tag{4.38}$$

where

$$-\psi_0 = -\frac{\pi}{2} + \operatorname{arctg}\frac{2\xi_н\nu_0}{1-\nu_0^2}; \quad -\psi_1 = \varphi_3 - \frac{\pi}{2} + \operatorname{arctg}\frac{2\xi_н\nu_{11}}{1-\nu_{11}^2},$$

$$\tau_п = \frac{T_п}{T_н}.$$

The open system's amplification factor can be evaluated approximately with the expression

$$K \approx \nu_{11}\frac{1}{T_н}\frac{\tau_п}{\tau_{к2}}K_ф. \tag{4.39}$$

Figures 34 and 35 show the graphs of the dependence of τ_{k1} and τ_{k2} on $\tau_п$ for different values of the reserve with respect to phase ϕ_3, while Figure 36 is a graph of the dependence of $(K/K_0)T_H$ on the platform's time constant τ_0. From these graphs it follows that for real instrument parameters and the chosen correction structure, the maximum value of the amplification factor of the open system of an OSP with a Khaui gyroscope proves to be less than for the system with the single-rotor MRG that was discussed above. Its value is determined by the frequency of the gyroscope's nutational oscillations. Therefore, when designing this type of instrument, one of the basic requirements is to obtain the maximum possible value of ω_H. It is also

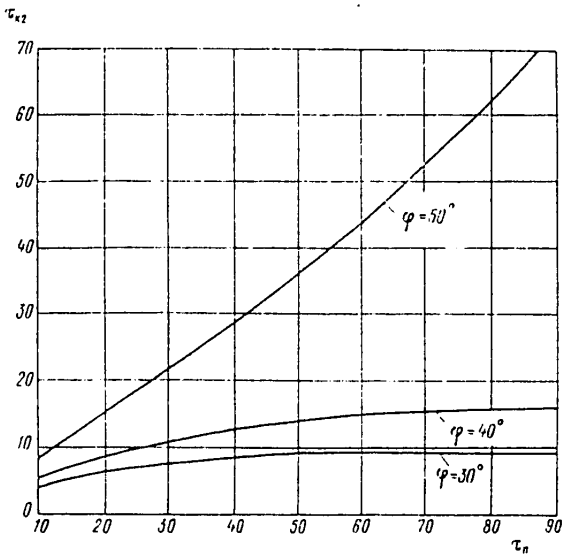

Figure 34. Dependences of τ_{k1} on platform's time lag.

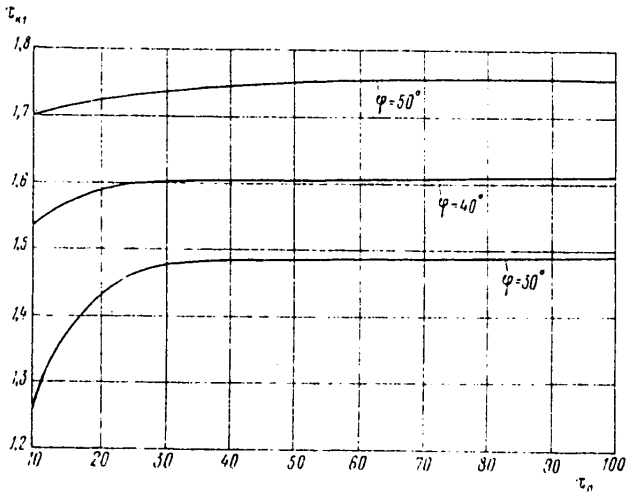

Figure 35. Dependences of τ_{k2} on platform's time lag.

possible to increase the amplification factor by introducing an additional integrating-differentiating component into the stabilization circuit. The use of correction of the boosting type to increase amplification factor K_p is hardly feasible, since it entails expansion of the pass band and a corresponding increase in the requirements for all its components.

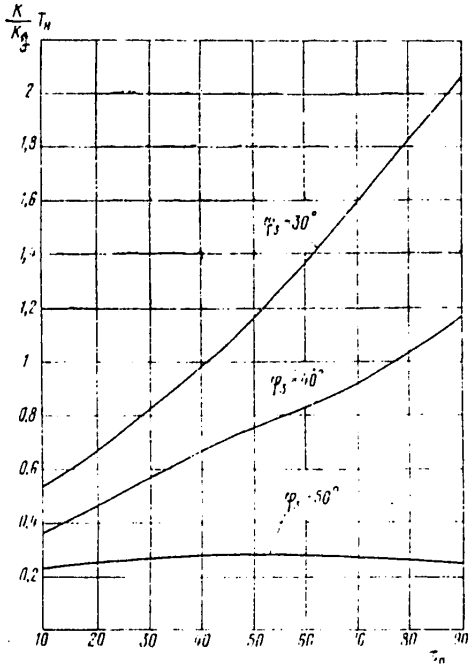

Figure 36. Dependence of amplification factor on the platform's time constant.

4.4. Dynamic Errors in a Uniaxial Stabilization System

The overwhelming majority of stabilized platforms are intended for operation on mobile objects. The presence of angular oscillations and vibrations is a characteristic of these objects. Angular oscillations and vibrations of an object at the point where a stabilized platform is installed contribute to the appearance of harmonic disturbing moments that affect the stabilization system. The causes of these moments are residual disbalance of the platform, moments of dry and viscous friction in the suspension axes, stress moments and so on that result in harmonic oscillations of the platform. The amplitude of these oscillations determines the stabilization system's dynamic error, the allowable magnitude of which is assigned during the planning of stabilized platforms. Let us discuss the dynamic errors of OSP's based on MRG's.

In engineering practice, dynamic errors are determined with the help of a system's transfer functions. In order to do this, the closed system's transfer function with respect to the stabilization angle caused by the disturbing moment is found either analytically or with the help of closing nomograms. The modulus of this transfer function for each frequency equals the amplitude of the platform's angular oscillations when acted upon by a unit disturbing moment along the stabilization axis. For an OSP, the closed system's transfer function is determined by expression (4.10). In our analysis of dynamic errors we will discuss three characteristic frequency areas: low frequencies, where $\left|W(p)\right|_{p=i\omega} \gg 1$; resonance frequencies, in which modulus $\left|W(p)\right|_{p=i\omega}$ is commensurate with unity; postresonance frequencies, for which the relationship $\left|W(p)\right|_{p=i\omega} \ll 1$ occurs.

Let us first discuss an OSP based on an OMG with VP and signal reading on the PD's rotation frequency. Taking into consideration the correcting circuit transfer function (4.34) that was derived in Section 4.3, the closed system's transfer function in the low-frequency area can be approximated by the expression

$$K(p) = \frac{1}{K_g K_p} \frac{(T_g p + 1)(T_{k4} p + 1)}{p(T_{k3} p + 1)}. \qquad (4.40)$$

Thus, when the disturbing moment's frequency is increased to approximately $1/\max(T_g, T_{k4})$, the closed system's transfer factor and, consequently, dynamic error decrease. Then, approximately to the frequency $\min(1/T_g, 1/T_{k3})$ or to frequency $1/T_{k4}$ (if $T_g > T_{k4}$), the system's transfer factor does not change for all practical purposes, but beginning with frequency $\max(1/T_g, 1/T_{k4})$ it increases if $T_g > T_{k4}$. However, if $T_g < T_{k3}$, then, beginning with frequency $1/T_{k4}$ the transfer factor decreases. For frequencies higher than $\max(1/T_g, 1/T_{k4})$, the transfer factor's value again remains practically constant. The expressions for evaluating the system's transfer factor with respect to a disturbing moment can be derived quite easily from (4.40) and have the following form for $T_g > T_{k4}$:

$$\omega < \frac{1}{T_r}, \quad |K(i\omega)| \approx \frac{1}{K_g K_p} \frac{1}{\omega}; \qquad (4.41)$$

$$\frac{1}{T_{k4}} > \omega > \frac{1}{T_g}, \quad |K(i\omega)| \approx \frac{T_r}{K_g K_p}; \qquad (4.42)$$

$$\frac{1}{T_{к3}} > \omega > \frac{1}{T_{к4}}, \quad |K(i\omega)| \approx \frac{T_g T_{к4}}{K_g K_p}\omega; \tag{4.43}$$

$$\omega > \frac{1}{T_{к3}}, \quad |K(i\omega)| \approx \frac{T_g}{K_g K_p}\frac{T_{к4}}{T_{к3}}. \tag{4.44}$$

When $T_{k3} < T_g < T_{k4}$, the expression for the second band of frequencies takes on the form

$$\frac{1}{T_g} > \omega \frac{1}{T_{к4}}, \quad |K(i\omega)| \approx \frac{T_{к4}}{K_g K_p}, \tag{4.45}$$

while when $T_g < T_{k3}$, the expression for the transmission factor in the third band of frequencies also changes:

$$\frac{1}{T_g} > \omega > \frac{1}{T_{к3}}, \quad |K(i\omega)| = \frac{1}{K_g K_p \omega}\frac{T_{к3}}{T_{к4}}. \tag{4.46}$$

When analyzing the closed system's transfer function in the area of cutoff frequency ω_2, its expression can be written, with an adequate degree of accuracy, in the form

$$K(p) = \frac{1}{K_g K_p}\frac{mT_g(T_p p+1)(T_{к2}p+1)}{m\frac{l_n T_g}{K_g K_p}T_p T_{к2}p^4 + ml_n T_g\frac{T_p+T_{к2}}{K_g K_p}p^3 + m\frac{l_n T_g}{K_g K_p}p^2 + T_{к1}p+1}, \tag{4.47}$$

where $m = T_4/T_{k3}$.

In (4.47), expressing the values of the system's parameters in terms of the correcting circuit's time constant T_{k1}, we obtain

$$K(p) = \frac{T_g m}{K_g K_p}\frac{(T_{к1}\tau_p p+1)(T_{к1}\nu p+1)}{\frac{\nu}{a(\nu)}T_{к1}^4\tau_p p^4 + \frac{1}{a(\nu)}T_{к1}^3(\tau_p+\nu)p^3 + \frac{1}{a(\nu)}T_{к1}^2 p^2 + T_{к1}p+1}, \tag{4.48}$$

where $a(\nu) = \frac{(1-\nu)^2}{4\nu}\sqrt{\frac{5-2\nu+\nu^2}{1-2\nu+5\nu^2}}$.

For the sake of simplicity, we will ignore the stabilizing engine's time constant τ_p and introduce normalized operator $\bar{p} = T_{k1}p$. Expression (4.48) will then take on the form

$$K(\bar{p}) = \frac{T_g m}{K_g K_p}\frac{\nu\bar{p}+1}{\frac{\nu}{a(\nu)}\bar{p}^3 + \frac{1}{a(\nu)}\bar{p}^2 + \bar{p}+1}. \tag{4.49}$$

Substituting into (4.49) the values for ν and $a(\nu)$ that occur for real system stability reserves with respect to phase, it can be shown that the discriminant of the cubic equation corresponding to the polynomial in the denominator of (4.49) is always greater than zero. This means that the polynomial has one real and two imaginary roots. When this is taken into consideration, transfer function K(p) can be represented by the following expression:

$$K(\bar{p}) = \frac{T_g m}{K_g K_p}\frac{\nu\bar{p}+1}{(\tau_{1e}\bar{p}+1)(\tau_{2e}^2\bar{p}^2 + 2\xi_{2e}\tau_{2e}\bar{p}+1)}. \tag{4.50}$$

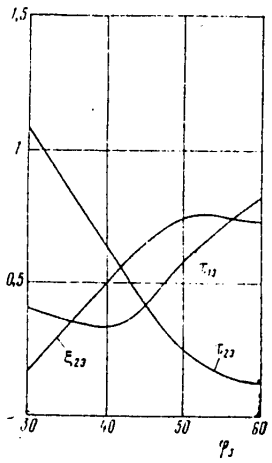

Figure 37. Dependence of τ_{1e}, τ_{2e} and ξ_{2e} on system's phase-stability reserve.

The dependence of τ_{1e}, τ_{2e} and ξ_{2e} on the system's phase-stability reserve is shown in Figure 37. It is obvious that frequency $1/(\tau_{2e}T_{k1})$ is the OSP's resonance frequency, while the value of relative damping factor ξ_{2e} determines the height of the resonance peak in the closed system's AChKh [amplitude-frequency characteristic]. In accordance with this, the closed system's transmission factor on the resonance frequency can be written as

$$K_{res} = \frac{1}{2\xi_{2e}} \frac{T_g/n}{K_g^2 K_p} \sqrt{\frac{\nu^2 + \tau_{2e}^2}{\tau_{1e}^2 + \tau_{2e}^2}}. \qquad (4.51)$$

In the area of postresonance frequencies the stabilization system's effect on platform oscillations can be ignored and the closed system's transfer function is assumed to be equal to that of the platform. The exemplary form of the OSP's closed system's transfer function is shown in Figure 38.

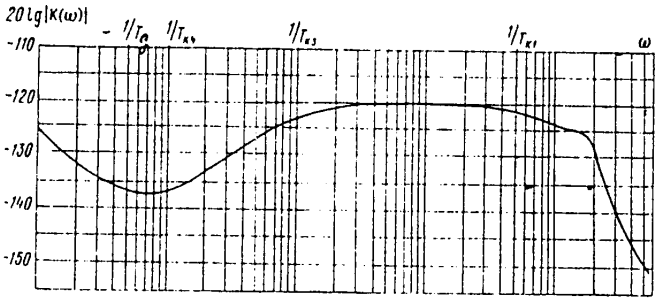

Figure 38. LAKh of a uniaxial GSP based on a DMG.

The expressions that have been derived make it possible to determine the dynamic errors of an OSP when real disturbances act on the platform, as well as to select during the planning stage those stabilization system parameters that insure that the magnitude of the dynamic errors does not exceed the figure given in the specifications.

Let us discuss the dynamic error in an OSP based on a DMG with VP and signal reading on the zero frequency. Considering the simplified gyroscope transfer function derived in Section 1.6 and the correcting circuit transfer function obtained in Section 4.3, we can write the open system's transfer function as

$$W(p) = \frac{K_g K_p}{\mu_n} \frac{1}{T_n p + 1} \frac{T_1 p + 1}{(T_{np}^2 p^2 + 2T_{np}\xi_{np}p + 1)(T_n^2 p^2 + 2\xi_n T_n p + 1)} \times \frac{T_{k3}p + 1}{T_{k3}p + 1} \frac{-T_{k1}p + 1}{T_{k1}p + 1} \frac{T_{k5}p + 1}{T_{k4}p + 1} \frac{1}{T_p p + 1}. \qquad (4.52)$$

Table 2.

Относительный коэффициент демпфирования предшественных колебаний (1)	Соотношение между постоянными времени звеньев системы [по (4.53)] (2)	Диапазон изменения частот возмущающего момента (3)	Аналитическое выражение для коэффициента передачи $K(\omega)$ (4)
$\xi_{пр} \ll 1$	$\frac{1}{T_{пр}} > \frac{1}{T_{к4}}$	$\omega < \frac{1}{T_{пр}}$	$\simeq \frac{T_{к4}}{K_g K_p}$
	$\frac{1}{T_{к4}} > \frac{1}{T_{пр}}$	$\omega < \frac{1}{T_{к4}}$	$\simeq \frac{1}{K_p}$
		$\omega < \frac{1}{T_{к3}}$	$\simeq \frac{T_{к4}\omega}{K_p}$
		$\omega < \min\left(\frac{1}{T_{к4}}, \frac{1}{T_{пр}}\right)$	$\simeq \frac{1}{K_g K_p \omega}$
	$\frac{1}{T_{к4}} < \frac{\xi_{пр} - \sqrt{\xi_{пр}^2 - 1}}{T_{пр}}$	$\omega < \frac{\xi_{пр} - \sqrt{\xi_{пр}^2 - 1}}{T_{пр}}$	$\simeq \frac{T_{к4}}{K_g K_p}$
$\xi_{пр} > 1$	$\frac{1}{T_{к4}} < \frac{\xi_{пр} - \sqrt{\xi_{пр}^2 - 1}}{T_{пр}}$	$\omega < \frac{1}{T_{пр}}$	$\simeq \frac{\omega}{\xi_{пр} - \sqrt{\xi_{пр}^2 - 1}} \frac{T_{к4}}{K_p}$
		$\frac{1}{T_{пр}} < \omega < \frac{\xi_{пр} + \sqrt{\xi_{пр}^2 - 1}}{T_{пр}}$	$\simeq \frac{T_{к4}}{K_p T_{пр}\left(\xi_{пр} - \sqrt{\xi_{пр}^2 - 1}\right)}$

[continued on next page]

$\xi_{np} > 1$	$\frac{1}{T_{к4}} > \frac{1}{T_{np}}$	$\omega > \frac{\xi_{np} + \sqrt{\xi_{np}^2 - 1}}{T_{np}}$	$\approx \frac{T_{к1}\omega}{K_p}$
	$\frac{1}{T_{np}} < \frac{1}{T_{к4}} < \frac{\xi_{np} + \sqrt{\xi_{np}^2 - 1}}{T_{np}}$	$\omega < \min\left(\frac{1}{T_{к4}}, \frac{\xi_{np} - \sqrt{\xi_{np}^2 - 1}}{T_{np}}\right)$	$\approx \frac{1}{K_p K_g \omega}$
		$\omega \ll \frac{1}{T_{к3}}$	$\approx \frac{T_{к4}}{T_{к3} K_p}$
		$\omega < \min\left(\frac{1}{T_{к4}}, \frac{\xi_{np} + \sqrt{\xi_{np}^2 - 1}}{T_{np}}\right)$	$\approx \frac{T_{к1}\omega}{K_g K_p T_1 (\xi_{np} - \sqrt{\xi_{np}^2 - 1})}$
	$\frac{1}{T_{к4}} > \frac{\xi_{np} - \sqrt{\xi_{np}^2 - 1}}{T_{np}}$	$\omega < \frac{\xi_{np} + \sqrt{\xi_{np}^2 - 1}}{T_{np}}$	$\approx \frac{T_{к1}}{K_g K_p (\xi_{np} - \sqrt{\xi_{np}^2 - 1})}$
		$\omega > \frac{\xi_{np} + \sqrt{\xi_{np}^2 - 1}}{T_{np}}$	$\frac{T_{к4}\omega}{K_p}$
	$\frac{1}{T_{к4}} > \frac{\xi_{np} - \sqrt{\xi_{np}^2 - 1}}{T_{np}}$	$\omega < \frac{1}{T_{к4}}$	$\frac{1}{K_p (\xi_{np} - \sqrt{\xi_{np}^2 - 1})}$
	$\frac{1}{T_{к4}} > \frac{\xi_{np} + \sqrt{\xi_{np}^2 - 1}}{T_{np}}$	$\omega < \frac{1}{T_{к4}}$	$\frac{1}{K_p}$
		$\omega < \frac{1}{T_{к1}}$	$\frac{T_{к4}\omega}{K_p}$

Key:
1. Relative damping factor of precessional oscillations
2. Relationship between time constants of system's components (after (4.53))
3. Range of change in frequencies of disturbing moment
4. Analytical expression for transmission factor K(ω)

As we did previously, for simplicity's sake we will assume T_p and T_{k3} to be sufficiently small values and ignore them. Let us now obtain the transfer function of the closed system for the different frequency areas.

In the low-frequency area, the expression for the closed system's transfer function with respect to the stabilization angle takes on the form

$$K(p) = \frac{1}{p} \frac{T_{пр}^2 p^2 + 2\xi_{пр} T_{пр} p + 1}{K_p K_g (T_1 p + 1)} \frac{T_{к4} p + 1}{T_{кп} p + 1}. \qquad (4.53)$$

As follows from (1.111), depending on the state of the MRG's parameters, the relative damping factor $\xi_{пр}$ of the precessional oscillations can be either smaller or greater than unity. In the second case, the second-order component in the numerator of (4.53) decomposes into the product of two first-order components. The values of transmission factor $K(\omega)$, as a function of the ratio of the time constants of the dynamic components of transfer function (4.53) in different ranges of changes in the disturbing moment's frequencies, are presented in Table 2.

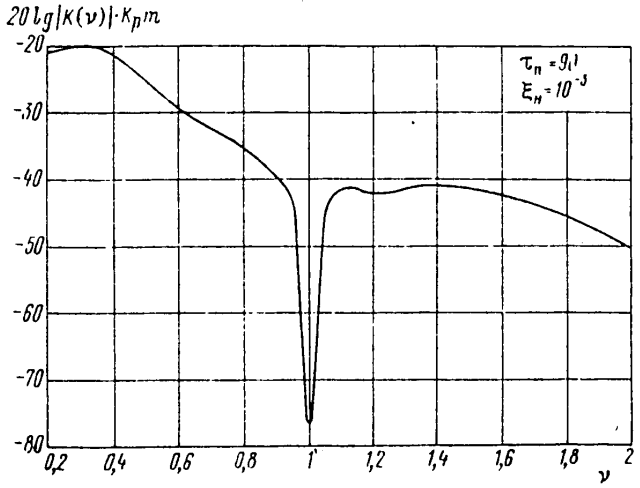

Figure 39. AChKh of a uniaxial GSP based on a DMG in the area of resonance frequencies.

In the area of resonance frequencies, the closed system's transfer function can be written, with an adequate degree of accuracy, as

$$K(p) = \frac{(T_н^2 p^2 + 2\xi_н T_н p + 1)(T_{к1} p + 1)}{I_п p^2 (T_н^2 p^2 + 2\xi_н T_н p + 1)(T_{к1} p + 1) + K_p m (T_{к2} p + 1)(-T_{к1} p + 1)}, \qquad (4.54)$$

where $T_{k5}/T_{k4} = m$.

Taking into consideration the expression for the open system's amplification factor (4.39) and introducing dimensionless time constants related to the nutational oscillations' time constant, as well as operator $\bar{p} = T_н p$, we obtain

$$K(\bar{p}) = \frac{1}{K_{pm}} \frac{(\bar{p}^2 + 2\xi_H \bar{p} + 1)(\tau_{K1}\bar{p} + 1)}{\frac{1}{\nu_{11}}\tau_{K2}\tau_{K1}\bar{p}^5 + \frac{\tau_{K2}}{\nu_{11}}(1 + \xi_H 2\tau_{K1})\bar{p}^4 + \frac{\tau_{K2}}{\nu_{11}}(\tau_{K1} + 2\xi_H)\bar{p}^3 + \left(\frac{1}{\nu_{11}} - \tau_{K1}\right)\tau_{K2}p^2 + (\tau_{K2} - \tau_{K1})p + 1} \quad (4.55)$$

By substituting in (4.55) the values of the correcting circuit's time constants τ_{k1} and τ_{k2} and the dimensionless frequency ν_{11}, as found in the preceding paragraph, we can construct the system's AChKh in the area of resonance frequencies. These characteristics are presented in Figure 39.

In the area of frequencies considerably higher than the resonance ones, the stabilization circuit can be regarded as opn, while the OSP's transfer function equals that of the platform itself.

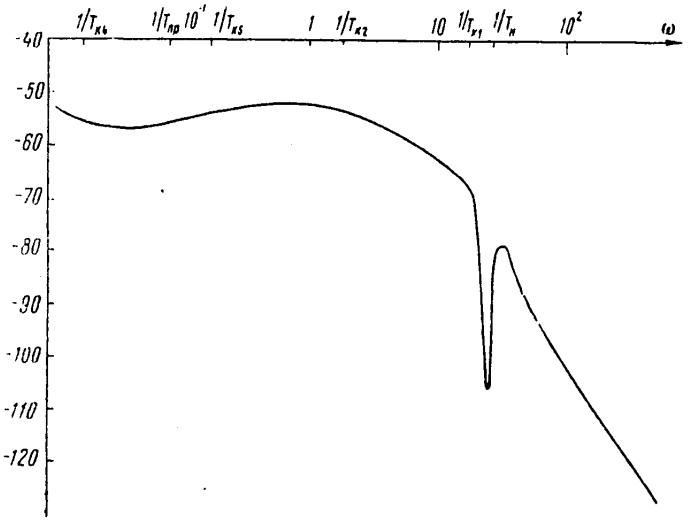

Figure 40. AChKh of transfer function of OSP's closed system.

The exemplary form of the OSP's closed system's transfer function's AChKh is shown in Figure 40.

4.5. Effect of Non-Steady-State Feedback on the Operation of a Uniaxial Stabilization System

It has already been said that a characteristic feature of an RVG is the presence at its outlet, along with the slowly changing component of the signal, harmonic components with amplitudes that are proportional to the input angular velocity and frequencies that are close to being multiples and composite frequencies of rotation of the PD. Since stabilization systems based on RVG's assume the realization of extremely high amplification factors in the stabilization circuit, when inadequate filtration is present the signal from the RVG can cause oscillation of the platform with inadmissibly large amplitudes or even loss of stability on the part of the system. Therefore, when designing such systems it is necessary to analyze their stability and dynamic accuracy, with due consideration for the non-steady-state

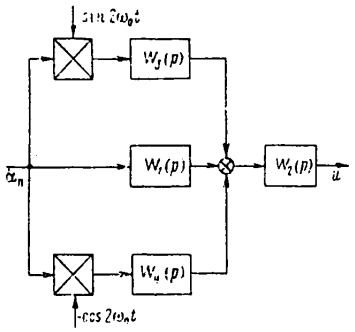

Figure 41. Structural diagram of OMG with transient nature of output signal allowed for.

feedback contributed by the RVG, and make the correct choice of the filter used at its outlet.

Let us discuss the effect of non-steady-state (or transient) feedback on the operation of an OSP based on an OMG with VP and signal reading on the rotor's rotation frequency. In order to do this, we will use the technique of reducing equations with periodic coefficients to stationary form, as explained in Section 1.5. First, let us derive the RVG transfer functions with respect to the basic signal without any assumptions about filtration of the harmonic component, but with due consideration for the RVG's resonance tuning. In accordance with expression (1.81), the structural diagram of an instrument with the carrier frequency eliminated is presented in Figure 41. The values of the operators in the structural diagram are determined by expressions that are derived directly from the OMG transfer functions described in Section 1.6:

$$\frac{1}{W_2(p)} = i\frac{4}{K_0}\left(\frac{1}{2}\frac{T^2}{1+\sqrt{1-\xi^2}}p^2 + \frac{\xi T}{1+\sqrt{1-\xi^2}}p + 1\right)(T_g p + 1)^2; \tag{4.56}$$

$$W_1(p) = \frac{2}{\xi}\left(\frac{1}{2}\frac{T^2 T_g}{1+\varkappa}p^3 + \frac{T^2}{1+\varkappa}p^2 + T_g p + 1\right) \approx$$
$$\approx \frac{2}{\xi}\left(\frac{1}{2}\frac{T^2}{1+\varkappa}p^2 + \frac{1}{2}\frac{\xi T}{1+\varkappa}p + 1\right)(T_g p + 1); \tag{4.57}$$

$$W_3(p) = \frac{2}{\xi}\frac{1-\varkappa}{1+\varkappa}\left(\frac{1}{2}\frac{T^2 T_g}{1-\varkappa}p^3 + \frac{T^2}{1-\varkappa}p^2 + T_g p + 1\right); \tag{4.58}$$

$$W_4(p) = 2\frac{\varkappa}{1+\varkappa}T_g p\left(\frac{1+\varkappa}{2\varkappa}T_g p + 1\right). \tag{4.59}$$

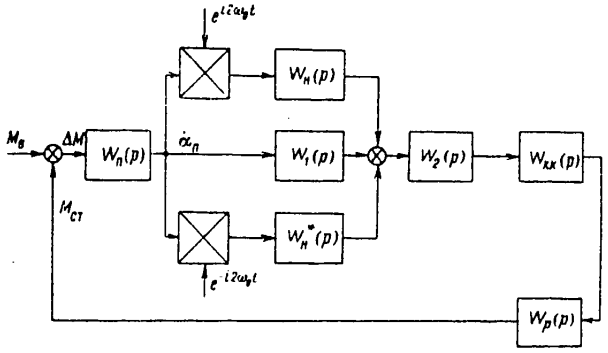

Figure 42. Structural diagram of an OSP, allowing for the non-steady-state nature of the signal from the OMG.

The OSP's structural diagram then takes on the form shown in Figure 42, where we have also introduced the definition of the RVG's transient part's operator:

$$W_{\text{п}}(p) = \frac{1}{2}[W_1(p) + iW_3(p)], \tag{4.60}$$

while the system's equation of motion in operator form is written as follows:

$$\frac{1}{pK(p)}\dot{\alpha}_{\text{п}} + W_{\text{р}}(p)\,W_{\text{к.к}}(p)\,W_2(p)\,[W^*_{\text{н}}(p)\,\dot{\alpha}_{\text{п}}e^{-i2\omega_0 t} + W_{\text{н}}(p)\,\dot{\alpha}_{\text{п}}e^{i2\omega_0 t}] = M_{\text{в}}. \tag{4.61}$$

Let us reduce equation (4.61) to the form of (1.31), by introducing the definitions

$$\left.\begin{aligned} \Phi_2(p) &= pK(p)\,W_{\text{п}}(p)\,W_{\text{р}}(p)\,W_{\text{к.к}}(p)\,W_2(p);\\ \Phi_3(p) &= pK(p)\,W^*_{\text{н}}(p)\,W_{\text{р}}(p)\,W_{\text{к.к}}(p)\,W_2^2(p);\\ R(p) &= pK(p). \end{aligned}\right\} \tag{4.62}$$

In accordance with the technique for reducing equation (1.31) to stationary form, we derive the operators that determine the first-step equation:

$$\begin{aligned} \Phi_1^{(1)}(p) = 1 - pK(p)\,W_{\text{р}}(p)\,W_{\text{к.к}}(p)\,W_2(p)\,[W_{\text{н}}(p)(p - i2\omega_0)\times\\ \times K(p - i2\omega_0)\,W_{\text{р}}(p - i2\omega_0)\,W_{\text{к.к}}(p - i2\omega_0)\,W_2(p - i2\omega_0)\times\\ \times W^*_{\text{н}}(p - i2\omega_0) + W^*_{\text{н}}(p)(p + i2\omega_0)\,K(p + i2\omega_0)\times\\ \times W_{\text{р}}(p + i2\omega_0)\,W_{\text{к.к}}(p + i2\omega_0)\,W_2(p + i2\omega_0)\,W_{\text{н}}(p + i2\omega_0)]; \end{aligned} \tag{4.63}$$

$$\Phi_2^{(1)}(p) = p(p - i2\omega_0)\,K(p)\,K(p - i2\omega_0)\,W_{\text{н}}(p)\,W_{\text{н}}(p - i2\omega_0)\times \tag{4.64}$$
$$\times W_{\text{р}}(p)\,W_{\text{р}}(p - i2\omega_0)\,W_{\text{к.к}}(p)\,W_{\text{к.к}}(p - i2\omega_0)\,W_2(p)\,W_2(p - i2\omega_0);$$

$$\Phi_3^{(1)}(p) = p(p + i2\omega_0)\,K(p)\,K(p + i2\omega_0)\,W^*_{\text{н}}(p)\,W^*_{\text{н}}(p + i2\omega_0)\times \tag{4.65}$$
$$\times W_{\text{р}}(p)\,W_{\text{р}}(p + i2\omega_0)\,W_{\text{к.к}}(p)\,W_{\text{к.к}}(p + i2\omega_0)\,W_2(p)\,W_2(p + i2\omega_0);$$

$$A_0(p) + B_0(p) = pK(p); \tag{4.66}$$

$$A_1^{(1)}(p) = pK(p)\,W_{\text{н}}(p)\,W_{\text{р}}(p)\,W_{\text{к.к}}(p)\,W_2(p)(p - i2\omega_0)\,K(p - i2\omega_0); \tag{4.67}$$

$$B_1^{(1)}(p) = p(p + i2\omega_0)\,K(p)\,K(p + i2\omega_0)\,W^*_{\text{н}}(p)\,W_{\text{р}}(p)\,W_{\text{к.к}}(p)\,W_2(p). \tag{4.68}$$

Introducing the additional definition $W_c(p)$ for the transfer function of the stationary part of the system from the RVG's input to the stabilizing engine's output, we will rewrite expressions (4.63), (4.67) and (4.68) as

$$\begin{aligned} \Phi_1^{(1)}(p) = 1 - pK(p)\,W_{\text{c}}(p)\left[\frac{W_{\text{н}}(p)}{W_1(p)}\,\frac{W^*_{\text{н}}(p - i2\omega_0)}{W_1(p - i2\omega_0)}\times\right.\\ \times(p - i2\omega_0)\,K(p - i2\omega_0)\,W_{\text{c}}(p - i2\omega_0) + \frac{W^*_{\text{н}}(p)}{W_1(p)}\,\frac{W_{\text{н}}(p + i2\omega_0)}{W_1(p + i2\omega_0)}\times\\ \left.\times(p + i2\omega_0)\,K(p + i2\omega_0)\,W_{\text{c}}(p + i2\omega_0)\right]; \end{aligned} \tag{4.69}$$

$$A_1^{(1)}(p) = \frac{W_{\text{п}}(p)}{W_1(p)}(p - i2\omega_0)\,K(p - i2\omega_0)\,pK(p)\,W_{\text{c}}(p); \tag{4.70}$$

$$B_1^{(1)}(p) = \frac{W^*_{\text{н}}(p)}{W_1(p)}(p + i2\omega_0)\,K(p + i2\omega_0)\,pK(p)\,W_{\text{c}}(p). \tag{4.71}$$

Ignoring the effect on the system's operation of oscillations at frequency $4\omega_0$ (that is, by limiting ourselves to the approximation obtained in the first step), we obtain the characteristics of the platform's settled motion when a constant disturbing moment is acting on the axis of stabilization. The OSP's settled motion is composed of the constant deflection velocity in inertial space and the harmonic oscillations relative to the stabilization axis. The platform's constant deflection velocity can be found from the expression

$$\dot{\alpha}_{\text{п}} = \lim_{p\to 0} \frac{pK_{\cdot}(p)}{\Phi_1^{(1)}(p)} M, \tag{4.72}$$

which, when the values of the operators in terms of the system's parameters are substituted into it, takes on the form

$$\dot{\alpha}_{\text{п}} = \left\{ 1 + 4K_{\text{н}} \frac{\begin{array}{c}[q_{\text{р}} - K_{\text{н}} \operatorname{Re} W_{\text{к.к}}(i2\omega_0)] \operatorname{Re} W_{\text{к.к}}(i2\omega_0) - \\ - [1 + K_{\text{н}} \operatorname{Im} W_{\text{к.к}}(i2\omega_0)] \operatorname{Im} W_{\text{к.к}}(i2\omega_0)\end{array}}{\begin{array}{c}[q_{\text{р}} - K_{\text{н}} \operatorname{Re} W_{\text{к.к}}(i2\omega_0)]^2 + \\ + [1 + K_{\text{н}} \operatorname{Im} W_{\text{к.к}}(i2\omega_0)]^2\end{array}} \right\}^{-1} \times \\ \times \frac{1}{\mu_{\text{п}}} \frac{1}{1 + \frac{K_{\text{д}} K_{\text{р}}}{\mu_{\text{п}}}} M, \tag{4.73}$$

where

$$K_{\text{н}} = \frac{1-\varkappa}{1+\varkappa} \frac{1}{I_{\text{п}}} \frac{K_{\text{д}} K_{\text{р}}}{4\omega_0}; \quad q_{\text{р}} = 2\omega_0 T_{\text{р}}.$$

The amplitude of the platform's angular oscillations with frequency $2\omega_0$ will be determined from the expression

$$A_2 = \operatorname{mod} \frac{A_1^{(1)}(p)}{\Phi_1^{(1)}(p)}\Big|_{p=i2\omega_0} \frac{M}{\omega_0}. \tag{4.74}$$

Substituting the value of operator $A_1^{(1)}p$ from expression (4.70) into (4.74), we obtain

$$A_2 \approx \frac{1}{I_{\text{п}}} \frac{1}{2\omega_0^2} \left\{ \frac{1}{[q_{\text{р}} + K_{\text{н}} \operatorname{Re} W_{\text{к.к}}(i2\omega_0)]^2 + [1 - K_{\text{н}} \operatorname{Im} W_{\text{к.к}}(i2\omega_0)]^2} \right\}^{\frac{1}{2}} \times \\ \times \operatorname{mod} W_{\text{к.к}}(i2\omega_0) M. \tag{4.75}$$

Thus, the effect of the OMG's non-steady-state nature on the system's static characteristics is determined by coefficient $K_{\text{н}}$ and coefficient $q_{\text{р}}$, which characterizes the width of the stabilizing engine's pass band relative to frequency $2\omega_0$, as well as the values of the amplitude and phase of the correcting circuit's frequency characteristic on frequency $2\omega_0$. The smaller coefficient $K_{\text{н}}$ is (and it has smaller values for platforms with large moments of inertia and when the OMG's rotor has high frequencies of rotation), the less the effect of the non-steady-state nature. The significant reduction in the effect of the non-steady-state nature is explained by the fact that when the parameters of the OMG's rotor are chosen appropriately ($\varkappa \to 1$), the oscillations on the doubled frequency of rotation of the rotor are attenuated. Narrowing the stabilizing engine's relative pass band (increasing $q_{\text{р}}$) also reduces the effect of the non-steady-state nature on the OSP's settled motion. Expressions (4.73) and (4.74) make it possible to select the correcting circuit's parameters in such a fashion as to insure the obtaining of the OSP's required static characteristics.

When the stabilizing circuit's parameters are selected in accordance with the recommendations made in Section 4.3, without allowing for the effect of the OMG's non-steady-state nature, the static characteristics will acquire the form

$$\alpha_{\text{п}} = \left\{ 1 + 4K_{\text{н}} \frac{\begin{array}{c}q_{\text{р}}[1 + q^2\nu(1 + \nu + q^2\nu^2) - q(1-\nu)(1+\nu^2q^2)] - \\ - K_{\text{н}}[1 + q^2(1 - \upsilon^2 + q^2\upsilon^2)]\end{array}}{\begin{array}{c}[1 + \nu^2q^2 + q(1-\nu)K_{\text{н}}]^2 + \\ + [q_{\text{р}}(1 + \nu^2q^2) - K_{\text{н}}(1 + q^2\nu)]^2\end{array}} \right\}^{-1} \times \\ \times \frac{1}{\mu_{\text{п}} + K_{\text{д}}K_{\text{р}}} M; \tag{4.76}$$

$$A_2 = \frac{1}{I_n}\frac{1}{2\omega_0^2}\left\{\frac{(1+q^2\nu^2)^2}{[q_p(1+q^2\nu^2)+K_u(1+q^2\nu)]^2+[1+q^2\nu^2-K_{uq}(1-\nu)]^2}\right\}^{\frac{1}{2}} \times$$
$$\times \sqrt{\frac{1+q^2}{1+\nu^2q^2}}\,M, \tag{4.77}$$

where $q = 2\omega_0 T_{kl}$.

Coefficient q characterizes the width of the steady-state stabilization system's pass band. The broader the system's relative pass band (the smaller q is), the greater the effect of the OMG's non-steady-state nature on its dynamic characteristics.

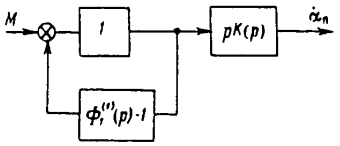

Figure 43. Equivalent structural diagram of OSP based on an OMG.

In order to evaluate the effect of the OMG's non-steady-state nature on the OSP's stability, we will present its structural diagram in the form depicted in Figure 43. The system consists of two series-connected components. In order for it to be stable it is sufficient that each component individually be stable. The first component is a closed stabilization system that does not allow for the OMG's non-steady-state nature. Its stability is insured with the help of the methods explained in Section 4.3. The second component, in which the effect of the OMG's non-steady-state nature is allowed for, is a component with positive feedback. Its stability can be investigated with the help of frequency methods. The corresponding open system's transfer function has the form

$$W_{раз}(p) = \Phi_1^{(1)}(p) - 1. \tag{4.78}$$

Substituting the value of $\Phi_1^{(1)}(p)$ from (4.69) into (4.78), we obtain

$$W_{раз}(p) = -2pK(p)\,W_c(p)\,\mathrm{Re}\left[\frac{W_u''(p)\,W_u^*(p-i2\omega_0)}{W_1(p)\,W_1(p-i2\omega_0)}\right] \times$$
$$\times (p-i2\omega_0)\,K(p-i2\omega_0)\,W_c(p-i2\omega_0)\Big]. \tag{4.79}$$

Expressing the operators in (4.79) in terms of the system's parameters, its transfer function in the open state can be written as

$$W_{раз}(p) = -2\frac{K_g K_p}{I_n p+\mu_n}\,\frac{\frac{1}{2}\frac{T^2}{1+\varkappa}p^2+\frac{1}{2}\frac{\xi T}{1+\varkappa}p+1}{\frac{1}{4}T^2p^2+\frac{1}{2}\xi Tp+1}\,\frac{1}{T_\Gamma p+1} \times$$
$$\times \frac{W_{к.к}(p)}{T_p p+1}\left[1+\frac{K_g K_p}{I_n p+\mu_n}\,\frac{\frac{1}{2}\frac{T^2}{1+\varkappa}p^2+\frac{1}{2}\frac{\xi T}{1+\varkappa}p+1}{\frac{1}{4}T^2p^2+\frac{1}{2}\xi Tp+1} \times\right.$$
$$\left.\times \frac{1}{T_g p+1}\,\frac{W_{к.к}(p)}{T_p p+1}\right]^{-1}\mathrm{Re}\left\{2\,\frac{\left(\frac{T}{1-\varkappa}p-i\right)\left(\frac{T}{2}p+\frac{\xi}{2}+i\right)}{\frac{1}{2}\frac{T^2}{1+\varkappa}p^2+\frac{1}{2}\frac{\xi T}{1+\varkappa}p+1} \times\right.$$
$$\times \frac{\frac{T}{1-\varkappa}p-i}{\frac{2T}{1-\varkappa}p+\frac{\xi}{1-\varkappa}-1}\,\frac{K_u}{q_p}\,\frac{1}{\frac{1}{2}Tp-i+\frac{1}{2}T\frac{\mu_n}{I_n}} \times \tag{4.80}$$
. . . . . .

$$\cdot\ \cdot\ \cdot\ \cdot\ \cdot\ \cdot\ \cdot\ \cdot\ \cdot$$

$$\times \frac{\frac{2T}{1-\varkappa}p - i + \frac{\xi}{4}}{\frac{1}{2}Tp - i + \frac{1}{q_p}} \frac{1}{\frac{1}{2}Tp - i + \frac{\xi}{2}} \frac{W_{к.к}(p - i2\omega_0)}{T_{ф}p + 1} \times$$

$$\times \left[1 + \frac{K_и}{q_p} \frac{1}{\frac{1}{2}Tp - i + \frac{1}{2}T\frac{\mu_п}{I_п}} \times \right.$$

$$\left. \times \frac{\frac{2T}{1-\varkappa}p - i + \frac{\xi}{4}}{\left(\frac{1}{2}Tp - i + \frac{1}{q_p}\right)\left(\frac{1}{2}Tp - i + \frac{\xi}{2}\right)} \frac{W_{к.к}(p - i2\omega_0)}{T_{ф}p + 1}\right]^{-1}\Bigg\}.$$

From (4.80) it follows that the necessary condition for stability of the system is the fulfillment of the inequality

$$4K_и \frac{K_н \operatorname{mod}^2 W_{к.к}(i2\omega_0) + \operatorname{Im} W_{к.к}(i2\omega_0) - q_p \operatorname{Re} W_{к.к}(i2\omega_0)}{[1 + K_н \operatorname{Im} W_{к.к}(i2\omega_0)]^2 + [q_p - K_н \operatorname{Re} W_{к.к}(i2\omega_0)]^2} < 1, \tag{4.81}$$

which, when the stabilizing engine's pass band is infinite and there is no special correction on frequency $2\omega_0$, takes on the form

$$\frac{4K_и^2}{1 + K_и^2} < 1. \tag{4.82}$$

An analysis of transfer function (4.82) shows that for most systems with real parameters, these conditions are adequate. Expression (4.82) imposes an additional limitation on the value of the open stabilization system's transmission factor. If this inequality is not fulfilled, it is necessary to design the correcting circuit so that inequality (4.81) is fulfilled. In connection with this, the designer should check to see what effect this correcting circuit has on the stability and quality indicators of the closed system described by transfer function K(p).

4.6. Multidimensional Stabilization Systems Using Rotor Vibration Gyroscopes

At the present time, OSP's are in extremely limited practical use. The construction of OSP's operating on nonstabilized bases with RVG's as sensitive elements makes practically no sense. This is related to the specific nature of the RVG's themselves. Actually, they are fundamentally two-dimensional measurers of the base's absolute velocities with identical sensitivity along both measuring axes. Therefore, for a highly sensitive instrument even comparatively small angular velocities of the base along an unstabilized axis either saturate its single-channel part or result in contact between the rotor and the stops, which has a strong effect on the instrument's basic characteristics or makes it generally incapable of functioning. At the same time, the two-dimensional nature of the RVG makes it possible to use only one instrument for the construction of a biaxial stabilized platform. Such platforms are widely used in different branches of technology, such as for the stabilization of the sighting line of radio engineering and optical devices, for the determination of the plane of the horizon on a moving object, and so forth.

Let us discuss the special features of the dynamics of a DSP based on a single RVG, assuming the system to be stationary and linear and using the vector-matrix description presented in Section 4.1. In this case the platform's transfer matrix has the form

$$W_n(p)=\begin{Vmatrix} \frac{W_{n2}(p)}{1+h^2W_{n2}(p)W_{n3}(p)} & h\frac{W_{n2}(p)W_{n3}(p)}{1+h^2W_{n2}(p)W_{n3}(p)} \\ -h\frac{W_{n3}(p)W_{n3}(p)}{1+h^2W_{n2}(p)W_{n3}(p)} & \frac{W_{n3}(p)}{1+h^2W_{n2}(p)W_{n3}(p)} \end{Vmatrix}, \tag{4.83}$$

while the RVG's transfer function is

$$W_g(p)=\begin{Vmatrix} W_{g0}(p) & W_{g\,n}(p) \\ -W_{g\,n}(p) & W_{g0}(p) \end{Vmatrix}. \tag{4.84}$$

The outer diagonal elements of matrices (4.83) and (4.84) characterize the cross-couplings between the stabilization channels that appear as a result of the presence of kinetic moment h of the RVG's rotating part and cross-couplings in the signals read from the RVG. Assuming that the RVG is operating in the resonance mode and the level of the cross-couplings in its signals in the band of essential frequencies is insignificant, we will first examine only the couplings with respect to the gyroscopic moments. If the correcting circuit and the regulator do not have specially introduced cross-couplings and are described by diagonal transfer matrices, the closed system's transfer matrix has the form

$$K(p)=\frac{1}{D(p)}\times$$

$$\times\begin{Vmatrix} 1+h^2W_{n3}(p)W_{n3}(p)+W_3(p) & -hW_{n2}(p)W_3(p) \\ hW_{n3}(p)W_2(p) & 1+h^2W_{n2}(p)W_{n3}(p)+W_2(p) \end{Vmatrix} W_n(p), \tag{4.85}$$

where $D(p) = (1 + W_2(p))(1 + W_3(p))(1 + h^2pK_2(p)K_3(p))$; $W_2(p)$, $W_3(p)$, $K_2(p)$, $K_3(p)$ = transfer functions of the open and closed stabilization channels, respectively, without allowing for cross-couplings.

For stable operation of the system it is necessary and sufficient that each element of the matrix that is the first cofactor of the product in the right side of (4.85) be stable. These elements are determined by the expressions

$$\left.\begin{aligned} K_{22}(p)&=pK_2(p)\frac{1+h^2W_{n3}(p)K_3(p)}{1+h^2p^2K_2(p)K_3(p)};\\ K_{23}(p)&=-hpK_2(p)\frac{W_3(p)}{1+W_3(p)}\frac{1}{1+h^2p^2K_2(p)K_3(p)};\\ K_{32}(p)&=hpK_3(p)\frac{W_2(p)}{1+W_2(p)}\frac{1}{1+h^2p^2K_2(p)K_3(p)};\\ K_{33}(p)&=pK_3(p)\frac{1+h^2W_{n3}(p)K_2(p)}{1+h^2p^2K_2(p)K_3(p)}. \end{aligned}\right\} \tag{4.86}$$

Let us assume that the structure and parameters of each channel's stabilization circuits have been chosen in accordance with the recommendations presented in Section 4.3. In this case, transfer functions $K_2(p)$ and $K_3(p)$, as well as $W_3(p)/(1 + W_3(p))$ and $W_2(p)/(1 + W_2(p))$ have bands [sic--possibly poles] only in the left half-plane. Then, for stability of the closed circuits relative to the summary moments that act along the stabilization axes and are described by transfer functions (4.86), it is required that the closed circuit that corresponds to the following transfer function be stable:

$$K_\Phi(p)\frac{1}{1+h^2p^2K_2(p)K_3(p)}. \tag{4.87}$$

In order to determine the stability of the closed circuit with the transfer function $K_\Phi(p)$ it is possible to use the stability criterion for the open system's frequency

characteristics, the transfer function of which has the form

$$W_{\psi}(p) = h^2 p^2 K_2(p) K_3(p). \tag{4.88}$$

Let us discuss how kinetic moment h affects the stability of DSP's based on different types of RVG's. In order to do this, we will make use of the transfer functions for closed systems that were presented in Section 4.4. The precise values of h for which a system loses its stability can be obtained either graphically or with the help of computational methods. We will limit ourselves to approximate evaluations.

For an OMG with VP and reading on the rotation frequency, the phase characteristic corresponding to transfer function (4.88) can equal $-\pi$ in the area where the amplitude characteristic reaches its maximum value. Thus, in order to insure a system's stability it is sufficient that the amplitude-frequency characteristic corresponding to transfer function (4.88) be less than unity. This occurs when the following condition is met:

$$h < T_{\kappa 1} K_{\partial} K_{\rho} 2\xi_{2e}\tau_{2e}^2 \sqrt{\frac{\tau_{1e}^2+\tau_{2e}^2}{\nu^2+\tau_{2e}^2}} \frac{1}{T_{\underline{\partial} m}}. \tag{4.89}$$

When condition (4.89) is fulfilled, The effect on a DSP's stability of the cross-couplings with respect to the gyroscopic moment that arise because of the presence of kinetic moment h in the MRG's rotating part can be ignored.

For systems based on RVG's that have a transfer function that is the same as that of a DMG with VP and reading on the zero frequency, an analogous estimate can be obtained from the closed system transfer function described by expression (4.54). In connection with this, the sufficient condition for the system's stability will, obviously, be the fulfillment of the inequality

$$h < \max |\operatorname{mod}(i\omega) K(i\omega)|. \tag{4.90}$$

Having determined the maximum value of the system's AChKh, we obtain the limitations imposed on the MRG's kinetic moment. When these limitations are observed, the effect of h on a DSP's stability can be ignored.

Let us assume that the kinetic moment of the MRG's rotating part is small and that its effect on a system's stability can be ignored. Now we will discuss the effect on a DSP's stability of the cross-couplings in the MRG's signal that are determined by the outer diagonal elements of matrix (4.4). In this case the closed system's transfer function has the form

$$K(p) = \frac{1}{d(p)} \begin{Vmatrix} 1 + W_3(p) & -\frac{W_{\partial n}(p)}{W_{\xi^0}(p)} W_2(p) \\ \frac{W_{\partial n}(p)}{W_{\xi^0}(p)} W_3(p) & 1 + W_2(p) \end{Vmatrix} W_n(p), \tag{4.91}$$

where

$$d(p) = (1 + W_2(p))(1 + W_3(p)) + \left[\frac{W_{\varepsilon n}(p)}{W_{\xi^0}(p)}\right]^2 W_2(p) W_3(p).$$

It is obvious that the system will be stable if the closed circuits described by the following transfer functions are stable:

$$\left.\begin{aligned}
K_{22}(p) &= \frac{K_2(p)}{W_{n2}(p)} \frac{1}{1+\left[\frac{W_{p.n}(p)}{W_{go}(p)}\right]^2 \frac{W_2(p)}{1+W_2(p)} \frac{W_3(p)}{1+W_3(p)}};\\
K_{23}(p) &= -\frac{W_{p.n}(p)}{W_{go}(p)} \frac{W_2(p)}{1+W_2(p)} \frac{1}{1+W_3(p)} \times\\
&\times \frac{1}{1+\left[\frac{W_{p.n}(p)}{W_{go}(p)}\right]^2 \frac{W_2(p)}{1+W_2(p)} \frac{W_3(p)}{1+W_3(p)}};\\
K_{32}(p) &= \frac{W_{p.n}(p)}{W_{go}(p)} \frac{W_3(p)}{1+W_3(p)} \frac{1}{1+W_2(p)} \times\\
&\times \frac{1}{1+\left[\frac{W_{p.n}(p)}{W_{go}(p)}\right]^2 \frac{W_2(p)}{1+W_2(p)} \frac{W_3(p)}{1+W_3(p)}};\\
K_{33}(p) &= \frac{K_3(p)}{W_{n3}(p)} \frac{1}{1+\left[\frac{W_{p.n}(p)}{W_{go}(p)}\right]^2 \frac{W_2(p)}{1+W_2(p)} \frac{W_3(p)}{1+W_3(p)}}.
\end{aligned}\right\} \quad (4.92)$$

We will assume that stability is provided in each stabilization channel by the method explained in Section 4.3. The closed circuits described by transfer functions (4.92) will then be stable if the open system's transfer function

$$W_\phi(p) = \left[\frac{W_{p.n}(p)}{W_{go}(p)}\right]^2 p^2 K_2(p) K_3(p) W_{k.k2}(p) W_{k.k3}(p) \times \times W_{p1}(p) W_{p2}(p) W_{go}^2(p). \quad (4.93)$$

meets the stability criterion with respect to the frequency characteristic of the open system.

In the right side of (4.93), let us substitute the expressions for the transfer functions of a system's components, allowing for possible minor detuning δ of the MRG from the resonance mode. For an OMG with VP and reading on the rotation frequency we then obtain

$$W_\phi(p) = \left(\frac{\delta}{\xi}\right)^2 \left(\frac{\frac{T^2}{2\delta}p^2+1}{T_r p+1}\right)^2 \frac{T_{k12}p+1}{(T_{1e_1}p+1)(T_{2e_1}^2 p^2+2\xi_{2e_1}T_{2e_1}p+1)} \times \times \frac{T_{k13}p+1}{(T_{1e_2}p+1)(T_{2e_2}^2 p^2+2\xi_{2e_2}T_{2e_2}p+1)} \frac{1}{(T_{p2}p+1)(T_{p3}p+1)}. \quad (4.94)$$

The system's stability is determined by the behavior of frequency characteristic $W_\phi(i\omega)$ in the section where the phase characteristic takes on the value π. In connection with this, a sufficient condition for stability is the requirement that the frequency characteristic's absolute value remain less than unity at all times. From (4.94) it follows that for minor detunings of the instrument from the resonance mode ($\delta << \xi$), when the approximation of the MRG's transfer functions is made competently the detuning has practically no effect on the DSP's stability. An analysis of the frequency characteristic in the area where its absolute value reaches a maximum, with due consideration for the basic relationships derived in Sections 4.3 and 4.4, shows that the signal cross-couplings existing in the MRG as the result of the platform's angular accelerations also do not affect the DSP's stability.

By using the transfer functions for different RVG layouts that were derived in Chapter 1, in an analogous manner we can--with the help of the transfer function (4.93) of some open system--evaluate according to the frequency criterion the effect of cross-couplings in the RVG on the DSP's stability.

An investigation of cross-couplings in a DSP showed that for sufficiently large values of h, the correction discussed in Section 4.3 may not provide the system with the required amplification factors and dynamic characteristics. A special case of such systems is an astatic gyroscope, corrected with respect to deflection velocity with the help of signals from an MRG installed in the gyro chamber [7]. Therefore, let us discuss a DSP with due consideration for the cross-couplings between channels with respect to the gyroscopic moment. For the sake of simplification, we will assume that the values of the stabilization channels' parameters are approximately the same. It can be shown that nonfulfillment of this condition within quite broad limits does not lead to substantial quantitative changes in the results that are obtained. At the same time, such an assumption makes it possible to use the previously mentioned method of complex transfer functions and to reduce the order of magnitude of the investigated system by a factor of two. The structural diagram of a DSP constructed with the use of complex transfer functions for the components and vector coordinates, without allowing for transience, is presented in Figure 44.

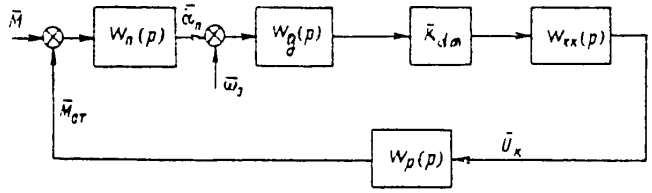

Figure 44. Structural diagram of a DSP with identical channels.

The platform's complex transfer function has the form

$$W_n(p) = \frac{1}{h} \frac{1}{T_n p - i + \lambda_n}, \tag{4.95}$$

where $T_\pi = I_\pi/h$; $\lambda = \mu_\pi/h$. The MRG's transfer functions were derived in complex form in Section 1.6 and can usually be approximated in the band of essential frequencies by simpler expressions. In the diagram we have introduced the demodulator's vector transmission factor

$$\bar{K}_{dm} = \frac{1}{2} e^{i\varepsilon}, \tag{4.96}$$

which allows for a possible phase shift ε in the demodulator or (which is the same) rotation through angle ε of the MRG's sensitivity axes relative to the stabilization axes. If there are no cross-couplings with respect to the MRG's signals between the channels, ε determines the nature of the control of the stabilizing engines. For $\varepsilon = 0$ we will call it cross control, while for $\varepsilon = \pi/2$ we will call it direct control and for $0 < \varepsilon < \pi/2$ it is mixed control. In general form, the correcting circuit can introduce additional cross-couplings between the channels for the purpose of obtaining maximum amplification factors in the stabilization circuit. The regulator's transfer function describes the dynamics of the stabilizing engines.

Let us discuss DSP's based on an MRG of a different type. When an OMG with VP and reading on the rotor's rotation frequency is used, when $T_p << T_\pi$ and the amplification factor equals unity, the frequency characteristic of the open system takes on the form depicted in Figure 45. From Figure 45 it follows that when the open system's amplification factor is

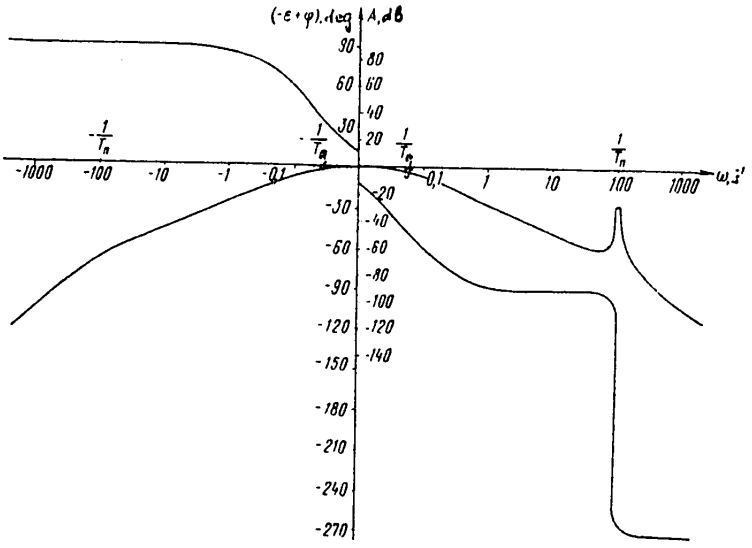

Figure 45. LAKh of open system for a DSP based on an OMG with identical channels.

$$K < \frac{\mu_п}{I_п} \sqrt{T_д^2 + T_д^2} \approx \sqrt{1 + \left(\frac{T_д}{T_п}\right)^2} \frac{\mu_п}{h} \qquad (4.97)$$

the closed system is absolutely stable. Without using correcting elements in the stabilization circuit, for large amplification factors DSP operational stability can be insured only in the case of direct control of the stabilizing engines ($\varepsilon = \pi/2$). However, the system is then almost at the limit of stability, so that allowing for small time constants for the stabilizing engine, amplifiers and other elements in the system leads it into instability.

The achievement of stable operation of a system by including series-connected correcting elements in the stabilization circuit can be accomplished in two ways. The first presumes that the system's cutoff frequency is higher than the frequency $1/T_п$ of the platform's nutational oscillations, so that it is advisable to use direct control of the stabilizing engines, while the correcting circuit's structure should be the one explained in Section 4.3. This way makes it possible to realize extremely high amplification factors in the stabilization circuit, but at the same time it broadens the system's pass band considerably. Therefore, it is used primarily for "heavy" platforms (with large moments of inertia $I_п$) based on an MRG with a small kinetic moment h. For "light" platforms with a high nutation frequency it is possible to use a nonminimal-phase correcting circuit with a transfer function of the type of (4.35) and a time constant $T_{kl} \approx \sqrt{3}T_п$. In this case, the stabilizing engines should be cross-controlled. With such correction and amplitude stability reserve A_3 = 6 dB, the open system's amplification factor can be estimated from the expression

$$K \approx \sqrt{1 + 0{,}04\left(\frac{T_д}{T_п}\right)^2}. \qquad (4.98)$$

The increase in the amplification factor is achieved by the appropriate choice of time constants T_{k3} and T_{k4} of the integrating-differentiating component.

Let us discuss a DSP based on a DMG with VP and reading on the zero frequency. For our analysis we will use its approximated transfer function (1.109) For a unit amplification factor, the open system's frequency characteristics have the form shown in Figure 46. An analysis of the frequency characteristics shows that in the case of a "heavy" platform, for which $1/T_{\pi} << 1/T_{H}$, the correcting circuit's structure and the technique for selecting the parameters remains the same as for an OSP. In connection with this, direct control of the stabilizing engines is realized.

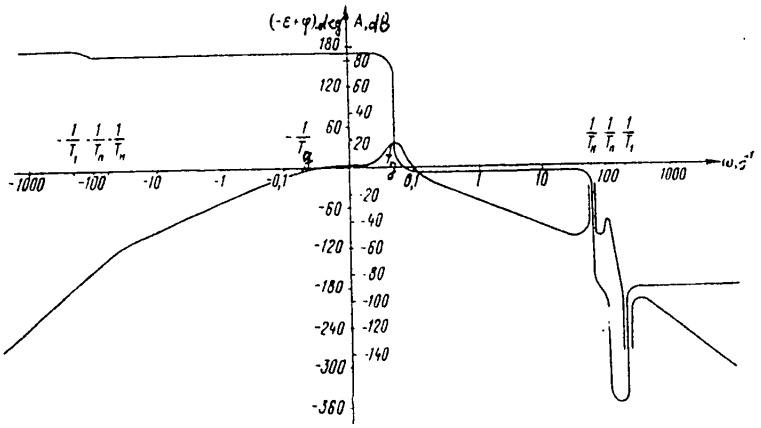

Figure 46. LAKh of open system for a DSP with identical channels that is based on a DMG.

For a "light" platform, where the frequencies of the MRG's and platform's nutational oscillations are close to each other, preliminary so-called "phasing in" of the system is required. This is achieved by additional cross control of the stabilizing engines ($\varepsilon \neq 0$). In order to insure stability of the phased-in system it is possible to use a series-connected nonminimal-phase correcting element with transfer function (4.35) and time constant $T_{k1} \approx \sqrt{3}T$ for $1/T_{\pi} < 1/T_{H}$ or $T_{k1} \approx \sqrt{3}T_{H}$ for $1/T_{H} < 1/T_{\pi}$. In connection with this, the system's amplification factor can be found from expression (4.39), while the increase in it is achieved because of the appropriate choice of T_{k3} and T_{k4}.

Let us discuss the effect of cross-couplings with respect to the gyroscopic moments of the MRG's rotating part and the MRG's signals on the stability of a TSP. From equations of motion (4.18) it follows that if we ignore the other cross-couplings in the TSP and assume each separate channel described by transfer function $K_i(p)$ to be stable, the system coupled with respect to the MRG's gyroscopic moments will be stable when the component with a transfer function of the following type is stable:

$$K_{\Phi}(p) = \frac{1}{1 + h_1^2 p^2 K_1(p) K_2(p) + h_2^2 p^2 K_1(p) K_3(p) + h_3^2 p^2 K_2(p) K_3(p)}. \qquad (4.99)$$

If the TSP is based on two MRG's, then--depending on which channels are duplicated--one of the h_i must be set equal to zero. The stability of this element can be checked with the help of frequency methods, according to its transfer function in

the open state:

$$W_\Phi(p) = h_1^2 p^2 K_1(p) K_2(p) + h_2^2 p^2 K_1(p) K_3(p) + h_3^2 p^2 K_2(p) K_3(p). \tag{4.100}$$

The sufficient condition for stability that states that the absolute value of $W_\Phi(i\omega)$ not exceed unity can serve as an approximate evaluation of the effect of the MRG's kinetic moments on the TSP's stability. In connection with this, if the channels are assumed to be identical, several understated maximally allowable values are obtained for h, as determined by the inequality

$$\sqrt{h_1^2 + h_2^2 + h_3^2} < \max[\operatorname{mod} K^{-1}(i\omega)]. \tag{4.101}$$

When three identical MRG's are used, this equality takes on the form

$$h < \frac{1}{\sqrt{3}} \max[\operatorname{mod} K^{-1}(i\omega)], \tag{4.102}$$

while when the TSP is based on two identical MRG's, it is

$$h < \frac{1}{\sqrt{2}} \max[\operatorname{mod} K^{-1}(i\omega)]. \tag{4.103}$$

The limitations obtained for the magnitude of the MRG's kinetic moment differ from the analogous limitations for a DSP only by coefficients $1/\sqrt{3}$ or $1/\sqrt{2}$. In view of this, the condition under which we can ignore the effect of h on the stability of a TSP based on an OMG with VP and having stabilization circuits with the structure described in Section 4.3, is obtained from (4.89) by premultiplying the right side of the inequality by $1/\sqrt{3}$ or $1/\sqrt{2}$, depending on whether the system is based on three or two MRG's. Thus, when condition (4.101) is fulfilled, the effect of cross-couplings with respect to the gyroscopic moments of the MRG's rotating parts on the dynamics of a TSP can be ignored.

The necessary and sufficient condition for stability of a TSP with cross-couplings with respect to the MRG's signals, when stability of each separate channel is insured and other cross-couplings are ignored, is stability of the component with the transfer function

$$K_\Phi(p) = \frac{1}{1 + \frac{[W_{g.n1}(p)]^2}{W_{g.o1}(p) W_{g.o2}(p)} K_{c1}(p) K_{c2}(p) + \frac{[W_{g.n2}(p)]^2}{W_{g.o1}(p) W_{g.o3}(p)} K_{c1}(p) K_{c3}(p) + \frac{[W_{g.n3}(p)]^2}{W_{g.o2}(p) W_{g.o3}(p)} K_{c2}(p) K_{c3}(p)}, \tag{4.104}$$

where $K_{ci}(p) = K_i(p) W_{g.oi}(p) W_{pi}(p)$ = transfer functions of the closed, separate channels with respect to the stabilizing engines' moments. Its transfer function in the open state corresponds to this component:

$$W_\Phi(p) = \frac{[W_{g.n1}(p)]^2}{W_{g.o1}(p) W_{g.o2}(p)} K_{c1}(p) K_{c2}(p) + \frac{[W_{g.n2}(p)]^2}{W_{g.o1}(p) W_{g.o3}(p)} K_{c1}(p) K_{c3}(p) + \frac{[W_{g.n3}(p)]^2}{W_{g.o2}(p) W_{g.o3}(p)} K_{c2}(p) K_{c3}(p), \tag{4.105}$$

on the basis of which the system's stability can be investigated with the help of frequency methods.

For identical MRG's and values of the separate stabilization channels' parameters that are about the same, transfer function (4.105) differs from the analogous function for the DSP only in that its absolute value is premultiplied by a factor of three when three MRG's are used and two when two are used.

Thus, as was the case for a DSP, when a platform is based on an OMG with VP, cross-couplings with respect to the MRG's signals have practically no effect on the stability of a TSP when detunings of the signals from the resonance mode are quite minor.

4.7. Effect of Transient Feedback on the Operation of a Multidimensional Stabilization System

A mathematical description of a linear, multidimensional stabilization system based on RVG's, with due consideration for the transient signal components existing in the RVG's, was presented in Section 4.1. In this section we will concentrate in more detail on the investigation of the effect of the non-steady-state nature (transience) of the sensitive elements' signals on the operation of multidimensional stabilization systems. In connection with this, we will limit ourselves only to systems based on RVG's with single modulation and VP and with single modulation and KP for which condition (1.22) is fulfilled. Figure 47 is a structural diagram of such a system. In accordance with this diagram, the closed system's equation of motion can be written as:

$$\left\{ \mathrm{E} - \frac{1}{2} \mathrm{W}_{\mathrm{п}}(p)\, W_{\mathrm{р}}(p)\, \mathrm{W}_{\mathrm{к.\,к}}(p) [\mathrm{A}_2 \mathrm{W}^{*}_{\mathrm{д}}(p)\, I^{*} + \mathrm{A}_1 \mathrm{W}_{\mathrm{г}}(p)\, I] \right\} \bar{\alpha}_{\mathrm{п}} - \\ - \frac{1}{2} \mathrm{W}_{\mathrm{п}}(p)\, \mathrm{W}_{\mathrm{р}}(p)\, W_{\mathrm{к.\,к}}(p) [\mathrm{A}_2 \tilde{\mathrm{W}}^{*}_{\mathrm{д}}(p)\, I \bar{\alpha}_{\mathrm{п}} e^{i2\omega_0 t} + \\ + A_1 \tilde{\mathrm{W}}_{\mathrm{г}}(p)\, I^{*} \bar{\alpha}_{\mathrm{п}} e^{-2i\omega_0 t}] = \mathrm{W}_{\mathrm{п}}(p)\, \overline{M}_{\mathrm{и}}. \tag{4.106}$$

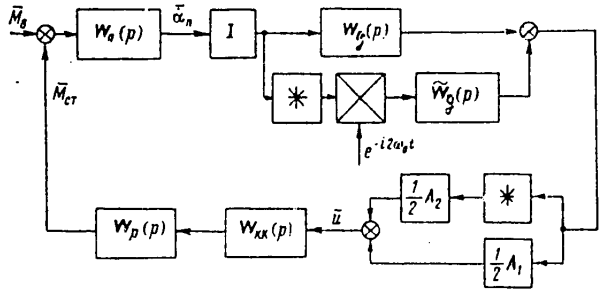

Figure 47. Structural diagram of a multidimensional GSP, allowing for transience of RVG signals.

In order to investigate the effect of the transience, we will make use of the technique explained in Section 1.5. In order to do it, we rewrite equation of motion (4.106) in a more convenient form:

$$\bar{\alpha}_{\mathrm{п}} - \Phi_1(p)\, \bar{\alpha}_{\mathrm{п}} e^{i2\omega_0 t} - \Phi_2(p)\, \bar{\alpha}_{\mathrm{п}} e^{-i2\omega_0 t} = \mathrm{K}(p)\, \overline{M}_{\mathrm{и}}, \tag{4.107}$$

where

$$\mathrm{K}(p) = \left\{ \mathrm{E} - \frac{1}{2} \mathrm{W}_{\mathrm{п}}(p)\, \mathrm{W}_{\mathrm{р}}(p)\, \mathrm{W}_{\mathrm{к.\,к}}(p) [\mathrm{A}_2 \mathrm{W}^{*}_{\mathrm{д}}(p)\, I^{*} + \mathrm{A}_1 \mathrm{W}_{\mathrm{г}}(p)\, I] \right\}^{-1} \mathrm{W}_{\mathrm{п}}(p)$$

is the transfer matrix of the closed stabilization system with respect to the angular velocity vector of the platform's motion in inertial space,

$$\Phi_2(p) = \frac{1}{2} \mathrm{K}(p)\, \mathrm{W}_{\mathrm{р}}(p)\, \mathrm{W}_{\mathrm{к.\,к}}(p)\, \mathrm{A}_2 \tilde{\mathrm{W}}^{*}_{\mathrm{д}}(p)\, I;$$

$$\Phi_3(p) = \frac{1}{2} K(p) W_p(p) W_{к.к}(p) A_1 \tilde{W}_g(p) I^*.$$

Using the indicated technique, as the first-step equation, which allows for the presence in the system of oscillations with a frequency of $2\omega_0$, we will have

$$\begin{aligned}[E - \Phi_2(p)\Phi_3(p-i2\omega_0) - \Phi_3(p)\Phi_2(p+i2\omega_0)] - \Phi_3(p)\Phi_3(p+i2\omega_0) \times \\ \times \bar{\alpha}_n e^{-i4\omega_0 t} - \Phi_2(p)\Phi_2(p-i2\omega_0)\bar{\alpha}_n e^{i4\omega_0 t} = \\ = K(p)\overline{M}_n + \Phi_2(p) K(p-i2\omega_0)\overline{M}_n e^{i2\omega_0 t} + \\ + \Phi_3(p) K(p+i2\omega_0)\overline{M}_n e^{-i2\omega_0 t}.\end{aligned} \tag{4.108}$$

If the system's filtering properties are such that we can ignore the components on the left side of (4.108) that contain harmonic factors changing with frequency $4\omega_0$, then for the analysis of the system's properties we obtain a stationary linear matrix equation that is investigatable by well-known techniques. In this case, when acted upon by a constant disturbing moment M_B, an SP's steady motion is composed of the SP's permanent deflection velocity in inertial space, which can be found from the expression

$$\bar{\alpha}_{n.ст} = [E - \Phi_2(0)\Phi_3(-i2\omega_0) - \Phi_3(0)\Phi_2(i2\omega_0)]^{-1} K(0)\overline{M}_n, \tag{4.109}$$

and the SP's harmonic oscillations with respect to the stabilization axes with frequency $2\omega_0$, which oscillations are described by the expression

$$\begin{aligned}\bar{\alpha}_n = [E - \Phi_2(i2\omega_0)\Phi_3(0) - \Phi_3(i2\omega_0)\Phi_2(i4\omega_0)]^{-1}\Phi_2(i2\omega_0)(K(0) \times \\ \times \frac{1}{i2\omega_0}\overline{M}_n e^{i2\omega_0 t} - [E - \Phi_2(-i2\omega_0)\Phi_3(-i4\omega_0) - \Phi_3(-i2\omega_0) \times \\ \times \Phi_2(0)]^{-1}\Phi_3(-i2\omega_0) K(0)\frac{1}{i2\omega_0}\overline{M}_n e^{-i2\omega_0 t}.\end{aligned} \tag{4.110}$$

When investigating the effect of RVG transience on a stabilization system's stability, the latter can be represented as two series-connected multidimensional systems. One of them is described by the transfer matrix K(p) of a closed stabilization system, with no allowance for RVG transience. This system's stability is insured without fail when the parameters of the regulators and the correcting elements in the stabilization circuits are chosen properly. Therefore, in order for the SP to be stable while allowing for RVG transience, it is necessary and sufficient that the multidimensional closed system with the following transfer function be stable:

$$\Phi_1^{(1)}(p) = [E - \Phi_2(p)\Phi_3(p-i2\omega_0) - \Phi_3(p)\Phi_2(p+i2\omega_0)]^{-1}. \tag{4.111}$$

If the system's filtering properties are not sufficient so as to be limited by allowing for the second harmonic of the PD's rotation frequency in accordance with the technique explained in Section 1.5, it is necessary to derive the second-step equation and so on, until the accuracy required for the investigation is achieved.

Let us discuss in more detail a DSP based on a single MRG. If the values of the stabilization channels' parameters are about the same and the differences between them can be ignored, the system should be investigated with the help of the technique developed in [16]. By introducing complex transfer functions and system coordinates, we will represent its structural diagram in the form depicted in Figure

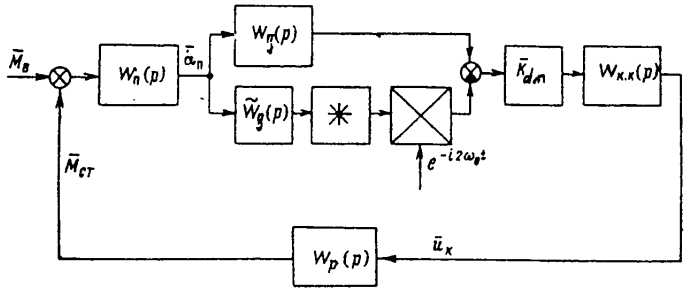

Figure 48. Structural diagram of DSP with identical channels, with transience of RVG signal taken into consideration.

48, where $W_г(p)$ is a settled and $\tilde{W}_г(p)$ a transient transfer function of the RVG, the expressions for which were derived in Section 1.6. In accordance with the structural diagram, the equation of such a DSP takes on the form

$$\bar{\alpha}_п - K(p)\,\bar{K}_{dm}\tilde{W}^*_г(p+i2\omega_0)\,W_{к.к}(p)W_р(p)\bar{\alpha}^*_п e^{-i2\omega_0 t} = K(p)\,\bar{M}_в, \tag{4.112}$$

where K(p) is the closed system's transfer function with no allowance made for the MRG's transience. By writing complexly conjugate equation (4.112) and applying the operator $e^{-i2\omega_0 t}$ to both its sides, we obtain a second equation that, when solved jointly with the first, gives the system's stationary equation of motion:

$$\begin{gathered}[1 - K(p)\,K^*(p+i2\omega_0)\,\bar{K}_{dm}\bar{K}^*_{dm}\,\tilde{W}_г(p)\,\tilde{W}^*_г(p+i2\omega_0)\times \\ \times W_{к.к}(p)\,W^*_{к.к}(p+i2\omega_0)\times \\ \times W_р(p)\,W^*_р(p+i2\omega_0)]\,\bar{\alpha}_п = K(p)\,\bar{M}_в + K(p)\,K^*(p+i2\omega_0)\times \\ \times \bar{K}_{dm}\tilde{W}^*_г(p+i2\omega_0)\,W_{к.к}(p)\,W_р(p)\,\bar{M}^*_в e^{-i2\omega_0 t}.\end{gathered} \tag{4.113}$$

From equation (4.113) it is not difficult to determine the characteristics of the DSP's settled motion when it is acted upon by a constant disturbing moment. The DSP will have a systematic deflection in inertial space with velocity

$$\begin{gathered}\bar{\alpha}_п = \frac{K(0)}{1 - K(0)\,K^*(i2\omega_0)\,\bar{K}_{dm}\bar{K}^*_{dm}\tilde{W}_г(0)\,\tilde{W}^*_г(i2\omega_0)\,W_{к.к}(0)\times} \bar{M}_в, \\ \times W^*_{к.к}(i2\omega_0)\,W_р(0)\,W^*_р(i2\omega_0)\end{gathered} \tag{4.114}$$

and will also perform angular oscillations relative to the stabilization axes according to the rule

$$\begin{gathered}\bar{\alpha}_п = -\frac{K(-i2\omega_0)\,K^*(0)\,\bar{K}_{dm}\tilde{W}^*_г(0)\,W_{к.к}(-i2\omega_0)\,W_р(-i2\omega_0)}{1 - K(-i2\omega_0)\,K^*(0)\,\bar{K}_{dm}\bar{K}^*_{dm}\tilde{W}_г(-i2\omega_0)\times} \times \\ \times \tilde{W}^*_г(0)\,W_{к.к}(-i2\omega_0)\,W^*_{к.к}(0)\,W_р(-i2\omega_0)\,W^*_р(0) \\ \times \frac{\bar{M}^*_в}{i2\omega_0} e^{-i2\omega_0 t}.\end{gathered} \tag{4.115}$$

Provided that the stationary closed circuit is stable, the DSP's stability with the MRG's transience allowed for is easy to determine with respect to the frequency criteria for the open system's transfer functions with complex coefficients:

$$W_\Phi(p) = K(p)\,K^*(p+i2\omega_0)\,\overline{K}_{dm}\,\overline{K}^*_{dn}\tilde{W}_g(p)\,\tilde{W}^*_r(p+i2\omega_0)\times$$
$$\times W_{к.к}(p)\,W^*_{к.к}(p+i2\omega_0)\,W_p(p)\,W^*_p(p+i2\omega_0), \qquad (4.116)$$

(the feedback is positive).

From static characteristics (4.114) it follows that there exist two ways for a signal to pass through the system. This makes it possible to raise the question of creating a static DSP that does not have systematic deflection when acted upon by a constant disturbing moment. Actually, when the condition

$$K^*(p+i2\omega_0) \underset{p\to 0}{\longrightarrow} \infty \qquad (4.117)$$

is fulfilled and the system's stability is insured, the rate of platform deflection moves toward zero and the settled motion is characterized by the platform's angle of rotation in inertial space:

$$\tilde{\alpha}_{п.ст} \underset{p\to 0}{=} -\frac{1}{pK^*(p+i2\omega_0)}\times$$
$$\times \frac{1}{\overline{K}_{dm}\,\overline{K}^*_{dn}\,\tilde{W}_g(0)\,\tilde{W}^*_g(i2\omega_0)\,W_{к.к}(0)\,W^*_{к.к}(i2\omega_0)\,W_p(0)\,W^*_p(i2\omega_0)}\,\overline{M}_в \qquad (4.118)$$

and its angular oscillations with frequency $2\omega_0$ are determined from the expression

$$\tilde{\alpha}_п = \frac{1}{\overline{K}^*_{dm}\,\tilde{W}_g(-i2\omega_0)\,W^*_{к.к}(0)\,W^*_p(0)}\,\frac{\overline{M}^*_в}{i2\omega_0}\,e^{-i2\omega_0 t}. \qquad (4.119)$$

Condition (4.117) is fulfilled when there is simultaneous fulfillment of the equality

$$\mathrm{Re}\,W^*_c(i2\omega_0) = -1;\ \mathrm{Im}\,W^*_c(i2\omega_0) = 0, \qquad (4.120)$$

where $W_c(p)$ = transfer function of the DSP's open, stationary circuit.

Let us discuss the possibility of the simultaneous fulfillment of conditions (4.120) and the conditions for stability of a DSP based on an OMG with VP. Since for such an instrument there is equality of the operators describing the stationary and transient parts of the transfer function, we will rewrite the system's equation of motion in the following form:

$$[1 + W_c(p) + W^*_c(p+i2\omega_0)]\,\tilde{\alpha}_п = [1 + W^*_c(p+i2\omega_0)]\,W_п(p)\,\overline{M}_в +$$
$$+ W_п(p)\,W^*_п(p+i2\omega_0)\,\overline{K}^*_{dm}\,\tilde{W}^*_g(p+i2\omega_0)\,W_{к.к}(p)\,W_p(p)\,\overline{M}^*_в e^{-i2\omega_0 t}. \qquad (4.121)$$

Replacing (for the sake of convenience) the sign in front of ω_0 with the opposite one, we will make use of the expression for the open system's transfer function

$$W_c(p) = -i\,\frac{1}{2}\,e^{i\varepsilon}\,\frac{K_{дв}K_p}{J_п}\,\frac{1}{\xi^2}\,\frac{T_1 p - i}{(T_3 p - i + \mu_3)(T_2 p - i + \mu_2)}\times$$
$$\times \frac{W_{к.к}(p)}{T_p p + 1}\,\frac{1}{T_п p - i + \lambda_п}. \qquad (4.122)$$

We will examine two cases. In the first, we will assume h to be quite small ($h << I_п 2\omega_0$). This will make it possible to ignore the cross-couplings between the DSP's channels with respect to the gyroscopic moments created by the rotating part of the MRG. Conditions (4.119) then take on the form

$$-\varepsilon + \mathrm{arctg}\,W^*_{к.к}(-i2\omega_0) - \mathrm{arctg}\,q_p = \pi + 2k\pi,\ k = 1, 2, \ldots, \qquad (4.123)$$

When the system's parameters are known, expressions (4.123) make it possible to determine the additional requirements for the correcting circuit in the stabilization circuit. What these requirements come down to is that on frequency $2\omega_0$ the circuit must amplify the signal and form the required value of its phase. Since h is small, system stability is insured (without allowing for transience) by the methods described in Section 4.3 when direct control of the stabilizing engines is used. Then, provided that the stabilizing engine's aperiodic lag is compensated for ($q_p << 1$, $\operatorname{arctg} q_{p\approx 0}$), as an additional correcting circuit it is possible to use a series-connected resonance amplifier with the transfer function

$$W_y(p) = \frac{1}{\frac{1}{4\omega_0^2}p^2 + \frac{K_n}{4\omega_0 \nu}p + 1}. \tag{4.124}$$

The system under discussion will be stable if the open system's transfer function fulfills the condition for stability with respect to the frequency criterion:

$$W_\phi(p) = W_c^*(p) + W_c^*(p - i2\omega_0). \tag{4.125}$$

Transfer function (4.125) has complex coefficients, so in order to judge the system's stability it is necessary to examine the corresponding frequency characteristic in the frequency band $-\infty < \omega < \infty$. From expression (4.125) it is obvious that when correcting circuits (4.34) and (4.124) are used, the behavior of frequency characteristic (4.125) in the band $\omega < -\omega_2$, where ω_2 is the cutoff frequency of the steady-state system's frequency characteristic, meets the stability criterion. Since frequency characteristic (4.125) is symmetrical relative to frequency ω_0, of which one can convince oneself from (4.122), it is sufficient to examine its behavior in the band of essential frequencies of the system's steady-state part. In this range ($\omega < \omega_0$), mod $W_c^*(i\omega - i2\omega_0) < 1$. Let us determine how component $W_c^*(i\omega - i2\omega_0)$ affects the frequency characteristic's behavior near the steady-state system's cutoff frequency ω_2.

On frequency $\omega = \omega_2$, the value of frequency characteristic $W_c^*(i\omega - i2\omega_0)$ can be determined from the expression

$$\begin{aligned} W_c^*(i\omega_2 - i2\omega_0) = -e^{-i\varphi} \frac{K_p K_p}{2\xi} \frac{1}{i[1 - 2\omega_0 T_n(1 - \nu_2)] + \lambda_n} \times \\ \times \frac{\nu_2}{i\nu_2 + \frac{1}{2}\xi} \frac{1}{-i\frac{4}{\xi^2}(1 - \nu_2) + i + \frac{2}{\xi}} \frac{-T_{K1} i2\omega_0(1 - \nu_2) + 1}{-\nu T_{K1} i2\omega_0(1 - \nu_2) + 1} \times \\ \times \frac{1}{1 - (1 - \nu_2)^2 - i\frac{K_n}{2\nu}(1 - \nu_2)} \frac{1}{-iq_p(1 - \nu_2) + 1}, \end{aligned} \tag{4.126}$$

where $\nu_2 = \omega_2/2\omega_0$ characterizes the pass band of the open system's steady-state part relative to the rotation frequency of the MRG's rotor. Allowing for the assumptions that we have made and substituting the values of the system's parameters from Section 4.3, we find the modulus of frequency characteristic (4.126):

$$\begin{aligned} \operatorname{mod} W_c^*(i\omega_2 - i2\omega_0) \approx 2a(\nu) \frac{\nu\nu_2}{(1 - \nu)^2(1 - \nu_2)^2} \times \\ \times \sqrt{\frac{4\nu^2\nu_2^2 + (1 - \nu)^2(1 - \nu_2^2)^2}{4\nu_2^2 + (1 - \nu)^2(1 - \nu_2)^2}} \times \\ \cdots\cdots\cdots \end{aligned} \tag{4.127}$$

$$\times \frac{1}{\sqrt{(2-\nu_2)^2+\frac{4}{\nu_2}\left[a(\nu)\frac{1-\varkappa}{1+\varkappa}\frac{\nu}{\xi}\frac{1-\nu_2}{1-\nu}\right]^2}},$$

which, when $\nu < 1$ and $\nu_2 << 1$ can be evaluated with the help of the inequality

$$\operatorname{mod} W_c^*(i\omega_2 - i2\omega_0) < \frac{\nu_2\nu}{(1-\nu)(1-\nu_2)^3}\xi\frac{1+\varkappa}{1-\varkappa}. \qquad (4.128)$$

From (4.128) it follows that in the area of frequency ω_2, where mod $W_c(i\omega)$ of the frequency characteristic of the steady-state part of the system takes on values close to unity, mod $W_c^*(i\omega_2 - i2\omega_0) << 1$. Therefore, when determining stability the second component in the right side of the open system's transfer equation (4.125) can be ignored. Thus, for the chosen correcting circuit parameters, the presence of RVG transience does not affect a DSP's stability.

Let us discuss the static characteristics of a DSP based on an OMG with VP when additional correcting circuit (4.124) is used. When acted upon by a constant disturbing moment, the platform is deflected from its initial position through a constant angle that is determined from the expression

$$\bar{\alpha}_{n.\,ст} = \lim_{p\to 0}\frac{1+W_c^*(p+i2\omega_0)}{pW_c(p)}\overline{M}_в. \qquad (4.129)$$

By discovering the values of the operators in expression (4.129), we obtain the dependence of the DSP's static error on the stabilization signal's parameters:

$$\bar{\alpha}_{n.\,ст} \approx \frac{i\nu+\frac{K_и}{2\xi}}{K_и\omega_0}\frac{\overline{M}_в}{K_в K_р}. \qquad (4.130)$$

When the given operational accuracy and the known values of the disturbances are taken into consideration, from expression (4.130) it is possible to find the required amplification factor in the stabilization circuit.

A constant disturbing moment also leads to harmonic oscillations of the platform with frequency $2\omega_0$. The expression describing the rule governing the platform's oscillations has the form

$$\bar{\alpha}_n = i\frac{\overline{K}_{дт}W_n(-i2\omega_0)W_n^*(0)\tilde{W}_в^*(0)W_{к.к}(-i2\omega_0)W_р(-i2\omega_0)}{1+W_c(-i2\omega_0)+W_c^*(0)}\frac{\overline{M}_в^*}{2\omega_0}e^{-i2\omega_0 t}. \qquad (4.131)$$

Allowing for the accepted change of sign for ω_0 and substituting into (4.131) the operators' values expressed in terms of the system's parameters, for $T_р = 0$ we obtain

$$\bar{\alpha}_n \approx i\frac{1}{K_и}\frac{1}{2I_n\omega_0^2}\overline{M}_в^* e^{i2\omega_0 t}. \qquad (4.132)$$

From (4.132) it follows that in order to compensate for real disturbing moments, a platform must perform angular oscillations with frequency $2\omega_0$, the amplitude of which is on the order of angular seconds and can reach tens of angular seconds. When such oscillation amplitudes are not allowable, it is not feasible to use correcting circuit (4.123) to eliminate systematic platform deflections caused by constant disturbing moments.

When platform deflections caused by the effect of constant disturbing moments are eliminated, the platform--as follows from (4.113)--will still have a systematic

deflection if the disturbing moments are of a harmonic type with frequency $2\omega_0$:

$$\overline{M}_n = M_{nA} e^{-i2\omega_0 t}. \tag{4.133}$$

The expression for determining the magnitude of the deflection as a function of the disturbing moment's amplitude is found easily from (4.113) and has the form

$$\bar{\alpha}_n = \frac{W_n^*(i2\omega_0)\,\tilde{W}_g^*(i2\omega_0)}{W_g(0)}\,\overline{M}_{nA}^*. \tag{4.134}$$

The dependence of the platform's deflection on M_{BA}^*, expressed in terms of the system's parameters, is determined quite accurately by the simple expression

$$\bar{\alpha}_n \approx i\,\frac{1}{2I_n\omega_0}\,\frac{1-\varkappa}{1+\varkappa}\,M_{nA}^*. \tag{4.135}$$

RVG errors can also lead to both systematic deflections of the platform and the appearance of a constant angle of its deflection from the position it initially occupied in inertial space.

As was shown in Chapter 2, MRG errors can be represented in the form of an equivalent angular velocity $\bar{\omega}_e$ acting on the instrument's input. The effect of angular velocity $\bar{\omega}_e$ on an MRG's input is equivalent to the effect on the stabilization axes of equivalent disturbing moment

$$\overline{M}_{n.e} = \overline{K}_{dn} W_p(p)\, W_{\kappa.\kappa}(p)\,[W_g(p) - \tilde{W}_g^*(p + i2\omega_0)\, e^{-i2\omega_0 t}]\,\bar{\omega}_e. \tag{4.136}$$

We will discuss only those errors that result in the equivalent angular velocity described by the expression

$$\bar{\omega}_e = \bar{\omega}_{e0} + \bar{\omega}_{eA} e^{-i2\omega_0 t}, \tag{4.137}$$

where $\bar{\omega}_{e0}$ = constant angular velocity, while $\bar{\omega}_{eA}$ = amplitude of the angular vibrations with frequency $2\omega_0$. In this case the expression for the equivalent disturbing moment will take on the form

$$\begin{aligned}\overline{M}_{n.e} = {} & \overline{K}_{dn} W_p(0)\, W_{\kappa.\kappa}(0)\,[W_g(0)\,\bar{\omega}_{e0} - \tilde{W}_g^*(i2\omega_0)\,\bar{\omega}_{eA}] + \\ & + \overline{K}_{dn} W_p(-i2\omega_0)\, W_{\kappa.\kappa}(-i2\omega_0)\,[W_g(-i2\omega_0)\,\bar{\omega}_{eA} - \\ & - \tilde{W}_g^*(0)\,\bar{\omega}_{e0}]\, e^{-i2\omega_0 t}.\end{aligned} \tag{4.138}$$

By substituting (4.138) into expressions (4.131) and (4.134), we obtain the dependence of the velocity of the platform's systematic deflection and its angular deflection in inertial space on MRG errors:

$$\bar{\alpha}_n = 2\left(\frac{1-\varkappa}{1+\varkappa}\,\bar{\omega}_{e1} - \bar{\omega}_{e0}\right); \tag{4.139}$$

$$\bar{\alpha}_{n.\,ст} \approx 2\left(i\nu + \frac{K_H}{2\xi}\right)\left(\bar{\omega}_{e0} + \frac{1-\varkappa}{1+\varkappa}\,\bar{\omega}_{eA}\right). \tag{4.140}$$

Thus, when the method under discussion is used to construct a stabilization system, the platform's systematic deflections are determined by the base's linear and angular vibrations with frequency $2\omega_0$, the angular vibrations of the MRG's rotating part in the main rotation supports relative to its axes of sensitivity on the same frequency, and the errors in the MRG itself.

Let us discuss the possibility of eliminating systematic DSP deflection caused by the effect of constant disturbing moments on the stabilization axes when the MRG's

rotating part has a large kinetic moment. From Section 4.6 it follows that in this case it is advisable to use cross-control of the stabilizing engines ($\varepsilon = 0$), while in order to achieve system stability for large amplification factors it is possible to use a series-connected, nonminimal-phase correcting circuit with transfer function (4.34). It is obvious that when $K_H < 1$ and the aperiodic lag in the stabilizing engines is compensated for, conditions (4.120) can be fulfilled by (for example) the additional connection in series in the stabilizing circuit of a resonance amplifier and a nonminimal-phase correcting element. The transfer function of such an additional correcting circuit takes on the form

$$W_y(p) = \frac{-\frac{1}{2\omega_0}p + 1}{\frac{1}{2\omega_0}p + 1} \cdot \frac{1}{\frac{1}{4\omega_0^2}p^2 + \frac{K_H}{4\omega_0}p + 1}. \qquad (4.141)$$

As in the case of small values of h, it can be shown that when the amplification factors are sufficiently large and $1/T_\pi << \omega_0$, the inclusion of such a circuit does not have any substantial effect on the system's stability.

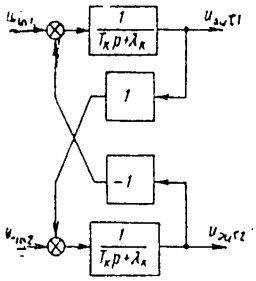

Figure 49. Structural diagram of two-dimensional correcting circuit.

For values of the frequency of the platform's nutational oscillations and frequency $\omega_0/(1 + \varkappa)$ ($1/T_\pi < \omega_0/(1 + \varkappa)$) that are close to each other, when $K_H \geqslant 1$ condition (4.120) is fulfilled by using an additional two-dimensional, series-connected correcting element with the transfer function

$$W_y(p) = -\frac{i}{K_H}\frac{1}{T_K p - i + \lambda_K}, \qquad (4.142)$$

where $(1 + \varkappa)/\omega_0 < T_K < T_\pi$, while $\lambda_K << 1$. Such an element can be realized by introducing into the system direct control of the stabilizing engines ($\varepsilon = -\pi/2$), reducing the open system's amplification factor by a factor of K_H, and including in the stabilizing circuit a correcting element with the structural diagram shown in Figure 49. If these frequencies are so close together that the additional correcting circuit has an effect on the dynamics of the entire system, the choice of the structure and parameters of the stabilizing circuit must be made from the very beginning with due consideration for MRG transience.

The elimination of systematic DSP deflections because of the effect of constant disturbing moments takes place only when conditions (4.120) are fulfilled exactly. In practice, however, the precise realization of a system's desired frequency characteristic and its maintenance during operation are impossible, since the parameters of the system's elements can change in time, depending on the temperature and other operating conditions. This leads to a change in the values of the modulus and argument of frequency characteristic $W_C^*(i\omega)$ on frequency $\omega = 2\omega_0$. Let us give these changes in the form of small increments of the rated values:

$$\left.\begin{aligned} \operatorname{mod} W_c^*(i2\omega_0) &= 1 + \Delta; \\ \arg W_c^*(i2\omega_0) &= -\pi + \Delta\varphi. \end{aligned}\right\} \qquad (4.143)$$

By substituting the values of the modulus and argument of $W_C^*(i\omega)$ from (4.143) into equation (4.113) and directing p to zero, we determine the systematic DSP deflection caused by constant disturbing moments when conditions (4.120) are not fulfilled

accurately:

$$\bar{\alpha}_n = \frac{-\Delta + i\Delta\varphi}{K_g K_p} \bar{M}_0. \qquad (4.144)$$

Inaccurate realization of the open system's frequency characteristic with respect to amplitude leads to DSP deflections relative to the same axis around which the disturbing moment acts, while a phase error results in deflection with respect to the cross axis. Expression (4.144) makes it possible to evaluate the requirements for accuracy in maintaining the values of the system's parameters as a function of the acting disturbing moments and the allowable systematic DSP deflections.

Thus, the special MRG features, which consist of the presence at its output of two useful signal components--one slowly changing, while the other is amplitude modulated, with a carrier frequency that is double the rotor's frequency of rotation--makes it possible to realize a fundamentally new approach to the construction of a stabilization system. It presumes the creation of those conditions for the passage through the system of a signal on the doubled frequency of rotation of the rotor for which there occurs full compensation for the constant disturbing moments acting on the system. Such an approach makes it possible to reduce significantly the systematic deflections of an SP based on a RVG that are caused by constant disturbing moments, without any substantial increase in the amplification factor in the stabilization circuit, which usually entails a number of technical difficulties.

CHAPTER 5. ROTOR VIBRATION GYROSCOPES IN THE DEFLECTION CORRECTION CIRCUIT OF A GYROSCOPIC STABILIZATION SYSTEM

5.1. Description of Stabilization Systems With a Deflection Correction Circuit

In Chapter 4 we discussed the possibility of using MRG's as the basic sensitive elements in stabilization systems. It was shown that the construction of such systems with deflections on a level close to the MRG's threshold of sensitivity involves overcoming a whole series of difficulties engendered by the requirement for realizing high amplification factors in the stabilization circuit.

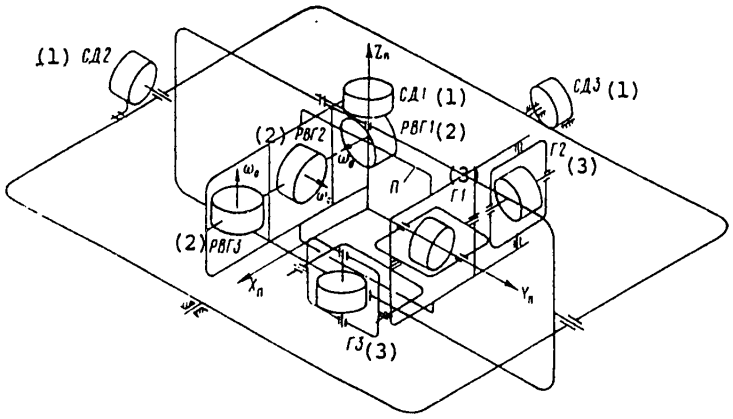

Figure 50. Kinematic diagram of GSP.

Key:
1. SD.
2. RVG.
3. G. [gyroscope]

There is another way to use RVG's in stabilization systems: the construction of an additional GSP deflection correction (KU) circuit. In this case the GSP is built according to the well-known principle, using two-stage gyroscopic units of the traditional type. On the platform there are additional RVG's that measure its rate of deflection in inertial space. Figure 50 is a kinematic diagram of such a GSP. The signals from the RVG's are fed into DM's [demodulator] mounted on the precession axes of the corresponding gyroscopes or on the stabilizing motors in such a fashion as to compensate for the GSP's deflections.

Such integration in a system of traditional gyroscopes and RVG's makes it possible to obtain a whole series of advantages. In the first place, the accuracy

requirements for the GSP's basic gyroscopic units are lowered, which makes it possible to use small and inexpensive gyroscopes, since the realization of the required deflection value is insured by the KU circuit. Secondly, the accuracy of the RVG's operation is improved because they are mounted on a stabilized area and the basic disturbances are countered by a stabilization circuit with a traditional gyroscope. In the third place, the division of the basic functions between a stabilization circuit with a traditional gyroscope, which provides the system's required dynamic characteristics, and a KU circuit with an RVG, which provides the required systematic deflection value, makes it possible to realize both circuits with simpler means. Finally, there is an improvement in the system's reliability because if the RVG goes out of order there is no cessation of the GSP's functioning.

The shortcoming in this way of using RVG's is the limited possibility of miniaturizing the GSP, since the system's instrument complement includes three traditional gyroscopic units with moment sensors and at least two RVG's. The use in the system of a single RVG, for deflection correction with respect to the platform's two most critical axes, can be assumed.

Let us examine a single gyroscopic stabilization channel. Its structural diagram is represented by two closed circuits [2], of which the inner one reflects feedback with respect to the gyroscopic moment, while the outer one reflects it with respect to the stabilizing engine's moment. Such a layout is easily reduced to single-circuit form and is usually analyzed as a unidimensional system with two inputs with respect to the disturbing moments acting along the stabilization and precession axes. Possible circuits for external correction and control of a GSP usually differ substantially with respect to the frequency pass band, so their operation is discussed separately only within the framework of precession theory [25], which simplifies the investigation considerably. When building a GSP KU circuit, as has been shown in a number of works [7-9], in order to reduce the deflections to values close to the RVG's threshold of sensitivity, it is necessary to realize high amplification factors in the KU. This makes it impossible to discuss the operation of the KU and stabilization circuits separately, since such an approach can result in fundamentally incorrect results.

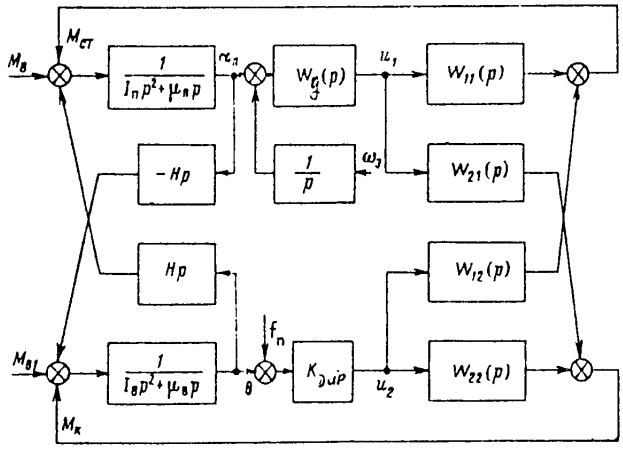

Figure 51. Structural diagram of GSP stabilization channel with a deflection correction circuit.

With due consideration for the remarks that have been made, let us examine, in a linear and steady-state formulation of the problem, the structural diagram of a single GSP channel with a KU circuit, as depicted in Figure 51. A GSP channel with a KU circuit is a two-dimensional, two-channel system with cross-couplings. The input of one channel in the system is the disturbing moment M_B with respect to the stabilization axis, while its output is the platform stabilization angle α_π. The second channel's input is the disturbing moment M_{B1} with respect to the gyroscope's precession axes, while its output is the gyroscope precession angle θ. Between the channels in the object being regulated there exists a negative, antisymmetrical cross-coupling with respect to the gyroscopic moments. Angles α_π and θ are measured, respectively, by an RVG with transfer function $W_g(p)$ and a precession angle sensor (DUP) with transmission factor K_{DUP}. The signals from the RVG (U_1) and the DUP (U_2) enter a regulator, which in general form can also be represented as a two-dimensional element with direct cross-couplings.

Let us discuss in more detail the physical meaning of the transfer functions that describe the regulator. Function $W_{21}(p)$ is the transfer function of the stabilization circuit, which contains transforming and amplifying elements, a correcting circuit and a stabilizing engine. Function $W_{22}(p)$ reflects the feedback that can encompass the gyroscope itself. When a GSP is based on integrating gyroscopes, there is usually no feedback. However, when angular velocity sensors (DUS) with an electric spring are used as the basic sensitive elements, this connection describes the properties of the circuit forming the electric spring. It can also be used to change the GSP's dynamics and, in particular, to limit the precession angles. Transfer functions $W_{11}(p)$ and $W_{21}(p)$ describe the circuits in the KU circuit. The signal from the RVG can be used simultaneously for deflection correction through the circuit described by transfer function $W_{21}(p)$ and to counter disturbances acting along the stabilization axis, as occurs when an RVG is used as the basic sensitive element of a stabilization system, through the circuit described by transfer function $W_{11}(p)$.

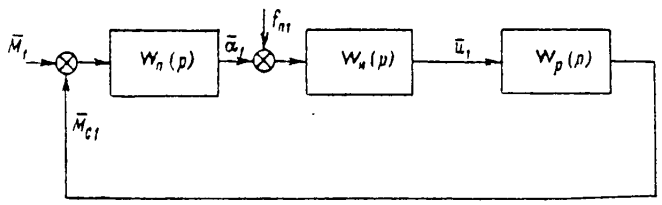

Figure 52. Vector structural diagram of GSP stabilization. circuit.

Since a GSP channel with a KU circuit is described as a two-dimensional automatic regulation system, in order to investigate a GSP with a KU circuit it is advisable to use a vector-matrix mathematical apparatus. A vector-matrix structural diagram corresponding to the structural diagram of a single GSP channel with a KU circuit (see Figure 51) is depicted in Figure 52. The following definitions are introduced in this diagram:
vector of the disturbing moment with respect to the stabilization channel--

$$\overline{M}_1 = \left\| \begin{matrix} M_B \\ M_{B1} \end{matrix} \right\|;$$

vector of the platform's angular rotation with respect to one axis--

$$\bar{\alpha}_1 = \left\| \begin{matrix} \alpha_n \\ 0 \end{matrix} \right\|;$$

vector of the signal at the measurer's output--

$$\bar{u}_1 = \left\| \begin{matrix} u_1 \\ u_2 \end{matrix} \right\|;$$

vector of the stabilizing moment with respect to the stabilization channel--

$$\overline{M}_{c1} = \left\| \begin{matrix} M_{c\tau} \\ M_к \end{matrix} \right\|;$$

transfer matrix of the platform with respect to a single stabilization axis--

$$W_n(p) = \frac{1}{H^2 + \mu_{n1}\mu_n} \frac{1}{p} \times$$

$$\times \frac{1}{\frac{I_n I_n}{H^2 + \mu_n\mu_n} p^2 + \frac{I_n\mu_n + I_n\mu_n}{H^2 + \mu_n\mu_n} p + 1} \left\| \begin{matrix} I_n p + \mu_n & H \\ -H & I_n p + \mu_n \end{matrix} \right\|; \quad (5.1)$$

transfer matrix of the stabilization channel's measurer--

$$W_i(p) = \left\| \begin{matrix} W_n(p) & 0 \\ 0 & K_{\text{зам}} \end{matrix} \right\|; \quad (5.2)$$

transfer matrix of the stabilization channel's regulator--

$$W_p(p) = \left\| \begin{matrix} W_{11}(p) & W_{12}(p) \\ W_{21}(p) & W_{22}(p) \end{matrix} \right\|; \quad (5.3)$$

vector of the stabilization channel's interference signal--

$$\bar{f}_{n1} = \left\| \begin{matrix} \frac{\omega_p}{p} \\ f_n \end{matrix} \right\|. \quad (5.4)$$

Since each GSP stabilization channel is a two-dimensional system and is described by matrix transfer functions, in order to describe bi- and triaxial GSP's it is completely natural to use block matrices for the purpose of achieving greater compactness and better visibility [11]. In order to do this, we will introduce the system's coordinates in the following manner:
the vector of the GSP's angles of rotation, in which each element of the column is a vector column consisting of the platform's angle of rotation in inertial space relative to the corresponding stabilization axis and the angle of rotation of the gyroscope operating along this stabilization axis and around the precession axis--

$$\bar{\alpha} = \left\| \begin{matrix} \bar{\alpha}_1 \\ \bar{\alpha}_2 \\ \bar{\alpha}_3 \end{matrix} \right\|;$$

the vector of the control signals, in which each element of the column is a vector column consisting of the signal from the KU circuit's sensitive element and the signal from the precession angle sensor for the gyroscope along the corresponding stabilization channel--

$$\bar{u} = \left\| \begin{matrix} \bar{u}_1 \\ \bar{u}_2 \\ \bar{u}_3 \end{matrix} \right\|;$$

the vector of the control moments, each element of which is a vector column consisting of the moment with respect to the corresponding platform stabilization axis and the gyroscope's precession axis--

$$\overline{M}_c = \left\| \begin{matrix} \overline{M}_{c1} \\ \overline{M}_{c2} \\ \overline{M}_{c3} \end{matrix} \right\|;$$

the vector of the disturbing moments, which contains as elements vector columns consisting of the disturbing moments with respect to the stabilization and precession axes of each of the stabilization channels--

$$\overline{M} = \left\| \begin{matrix} \overline{M}_1 \\ \overline{M}_2 \\ \overline{M}_3 \end{matrix} \right\|.$$

The connections between the system's coordinates is described by the following vector-matrix relationships:

$$\left.\begin{aligned} \bar{\alpha} &= W_\pi(p)(\overline{M} + M_c); \\ \bar{u} &= W_i'(p)\bar{\alpha}; \\ \overline{M}_c &= W_p(p)\overline{U}, \end{aligned}\right\} \qquad (5.5)$$

where $W_\pi(p)$, $W_i(p)$, $W_p(p)$ = block transfer matrices of the platform, the measurer and the regulator, respectively. Let us explain in more detail the meaning of the elements of the block transfer matrices of a GSP with a KU circuit.

Along the main diagonal of the platform's transfer matrix $W_\pi(p)$ there are transfer matrices that characterize for each stabilization channel the relationship between the vector of the platform's deflection angle $\bar{\alpha}_i$ and the moment acting along the corresponding stabilizing axis $(\overline{M}_i + \overline{M}_{ci})$. The nondiagonal elements of matrix $W_\pi(p)$ describe the cross-couplings existing in the platform between the stabilization channels. These couplings are engendered by the platform's centrifugal moments of inertia, its motion relative to the gyroscopes' axes of precession and the kinetic moments of the driven motors of the RVG's mounted directly on the platform. In accordance with the well-known equations of motion of a GSP [24], the elements of matrix $W_\pi(p)$ can be determined from the following equation:

$$W_\pi(p) = A[E - W_\pi'(p)W_{o\pi}(p)]^{-1}W_\pi'(p), \qquad (5.6)$$

where $W_\pi'(p)$ = a quasidiagonal block matrix, along the main diagonal of which stand matrices of the type of (5.1) that determine the relationship between the platform's and gyroscopes' deflection angles and the disturbing moments in the absence of cross-couplings between the channels; $W_{o\pi}(p)$ = a matrix describing the reverse cross-couplings in the platform caused by the platform's centrifugal moment of inertia and the kinetic moments of the RVG's rotating parts:

$$W_{on}(p) =$$

$$= \left\| \begin{array}{cc:cc:cc} 0 & 0 & h_1 p & 0 & -h_2 p & 0 \\ 0 & 0 & 0 & 0 & 0 & 0 \\ \hdashline -h_1 p & 0 & 0 & 0 & -I_{XY}p^2 + h_3 p & 0 \\ 0 & 0 & 0 & 0 & 0 & 0 \\ \hdashline h_2 p & 0 & -I_{XY}p^2 - h_3 p & 0 & 0 & 0 \\ 0 & 0 & 0 & 0 & 0 & 0 \end{array} \right\|; \qquad (5.7)$$

A = a matrix describing the transition from the gyroscopes' absolute angles of rotation to their relative angles of rotation around the precession axes; that is, allowing for the cross-coupling between the stabilization channels because of the platform's transient motion around the gyroscopes' precession axes:

$$A = \left\| \begin{array}{cc:cc:cc} 1 & 0 & 0 & 0 & 0 & 0 \\ 0 & 1 & \sin\lambda_1 & 0 & \cos\lambda_1 & 0 \\ \hdashline 0 & 0 & 1 & 0 & 0 & 0 \\ \cos\lambda_2 & 0 & 0 & 1 & \sin\lambda_2 & 0 \\ \hdashline 0 & 0 & 0 & 0 & 1 & 0 \\ \sin\lambda_3 & 0 & \cos\lambda_3 & 0 & 0 & 1 \end{array} \right\|, \qquad (5.8)$$

where λ_i = angles of installation of the gyroscopes on the platform, which are given in accordance with Figure 53.

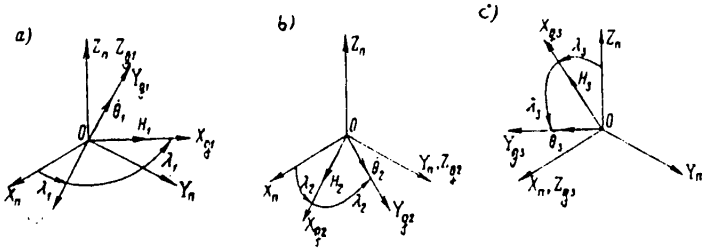

Figure 53. Diagram of arrangement of gyroscopes on a platform.

The measurers' transfer function $W_i(p)$ includes the transfer functions of the RVG's that measure the platform's motion relative to the stabilization axes and the precession angle sensors, which in the simplest case are represented by amplifying elements with transmission factors $K_{DUP\ i}$. Cross-couplings between the channels are formed because of the cross-couplings in the RVG's:

$$W_i(p) =$$

$$= \left\| \begin{array}{cc:cc:cc} W_{go1}(p)+W_{go2}(p) & 0 & W_{g.n1}(p) & 0 & -W_{g.n2}(p) & 0 \\ 0 & K_{DUP\ 1} & 0 & 0 & 0 & 0 \\ \hdashline -W_{g.n1}(p) & 0 & W_{go1}(p)+W_{go3}(p) & 0 & W_{g.n3}(p) & 0 \\ 0 & 0 & 0 & K_{DUP\ 2} & 0 & 0 \\ \hdashline W_{g.n2}(p) & 0 & -W_{g.n3}(p) & 0 & W_{go2}(p)+W_{go3}(p) & 0 \\ 0 & 0 & 0 & 0 & 0 & K_{DUP\ 3} \end{array} \right\| \qquad (5.9)$$

The transfer matrix $W_p(p)$ of the regulator can be represented as the product of two matrices:

$$W_p(p) = W_c(p)\, W_\phi(p), \tag{5.10}$$

where $W_\phi(p)$ = transfer matrix of the formulating component, which matrix characterizes the control law for the stabilizing engines and the moment sensors along the precession axes. In the absence of special cross-couplings between the channels it is a quasidiagonal block matrix, the form of the diagonal element of which depends on the type of GSP and the way the KU circuit is constructed.

Transfer matrix $W_c(p)$ reflects the relationship between the stabilizing and correcting moments acting on the platform and gyroscopes and the control signals entering the stabilizing engines and moment sensors. Cross signals appear here because of misalignment of the suspension axes and the platform's axes and the effect on the platform of the reactive moments of the moment sensors along the gyroscopes' precession axes:

$$W_c(p) = \left\|\begin{array}{cccccc}
W_{c.d1}(p) & 0 & 0 & \cos\lambda_2 W_{d.m2}(p) & 0 & \sin\lambda_3 W_{d.m3}(p) \\
0 & W_{d.m1}(p) & 0 & 0 & 0 & 0 \\
\hline
\sin\beta_1 \operatorname{tg}\beta_2 W_{c.d1}(p) & \sin\lambda_1 W_{d.m1}(p) & \cos\beta_1 W_{c.d2}(p) & 0 & \frac{\sin\beta_1}{\cos\beta_2} W_{c.d3}(p) & \cos\lambda_3 W_{d.m3}(p) \\
0 & 0 & 0 & W_{d.m2}(p) & 0 & 0 \\
\hline
\cos\beta_1 \operatorname{tg}\beta_2 W_{c.d1}(p) & \cos\lambda_1 W_{d.m1}(p) & -\sin\beta_1 W_{c.d2}(p) & \sin\lambda_2 W_{d.m2}(p) & \frac{\cos\beta_1}{\cos\beta_2} W_{c.d3}(p) & 0 \\
0 & 0 & 0 & 0 & 0 & W_{d.m3}(p)
\end{array}\right\| \tag{5.11}$$

where $W_{c.d\,i}(p)$ = transfer function of the stabilizing engine; $W_{d.m\,i}$ = transfer function of the moment sensor with respect to the precession axis; β_i = relative angles of rotation of the platform in the cardan suspension.

Allowing for (5.5), when block matrices are used a GSP's equation of motion in operator form takes on the form

$$\tilde{\alpha}_n = [E - W_n(p)\, W_p(p)\, W_i(p)]^{-1} W_n(p)\, \overline{M}. \tag{5.12}$$

Such a form simplifies the analysis of the system considerably by making all the computations more graphic physically, and also makes it easier to formulate algorithms for use with a digital computer.

5.2. Static Characteristics of Gyroscopic Stabilization Systems With a Deflection Correction Circuit

The static characteristics are one of the most important indicators of the quality of a GSP's performance. Let us see how the addition of a KU circuit affects a GSP's static characteristics. We will consider a single GSP channel. The solution of a GSP's equation of motion written in operator form can be obtained from the structural diagram shown in Figure 52, and has the following form:

$$\tilde{\alpha}_1 = [E - W_n(p)\,W_p(p)\,W_i(p)]^{-1}\,W_n(p)\,\overline{M}_1, \tag{5.13}$$

where $[E - W_\pi(p)W_p(p)W_i(p)]^{-1}W_\pi(p) = K(p)$ is the closed system's transfer matrix. The static characteristics of a GSP with a KU circuit can then be found in the case of a maximum transition to (5.13) for $p \to 0$:

$$\tilde{\alpha}_1 = K(0)\,\overline{M}_1. \tag{5.14}$$

Giving the elements of matrix K(0) in terms of the system's parameters, we obtain a general expression that makes it possible to determine the static characteristics of a GSP with a KU circuit for different types of GSP's. It is obvious that for K(0) this expression has the form

$$K(0) = \frac{1}{1 - \frac{\mu}{H}\frac{W_{22}(0)}{W_{12}(0)} + \frac{W_D(0)}{HP}\left[\frac{W_{22}(0)}{W_{12}(0)}W_{11}(0) - W_{21}(0)\right]} \times$$

$$\times \begin{Vmatrix} \frac{1}{H}\left[\frac{\mu_n}{K_{\text{дин}}\,W_{12}(0)} - \frac{1}{P}\frac{W_{22}(0)}{W_{12}(0)}\right] & \frac{1}{HP} \\ \frac{1}{K_{\text{дин}}\,W_{12}(0)}\left[-1 + \frac{W_D(0)}{HP}W_{21}(0)\right] & \frac{1}{K_{\text{дин}}\,W_{12}(0)}\left[\frac{\mu_n}{H} - \frac{W_D(0)}{HP}W_{11}(0)\right] \end{Vmatrix}. \tag{5.15}$$

In Chapter 1 it was shown that an RVG's functioning can be discussed in both the differentiating and integrating modes. In connection with this, with respect to the platform's angle of rotation α_π for the first mode, we have the following relationship:

$$W_{\text{дг}}(p)_{p\to 0} = -K_{\text{дг}}P,$$

while for the second it is

$$W_{\text{дг}}(p)_{p\to 0} = -K_i.$$

We will also assume that the realization of "pure" integrals and derivatives is not required in the regulator, since this is an exceptionally complicated technical problem. In this case, for a GSP with a KU circuit, in the differentiating mode of RVG operation expression (5.15) is written as

$$K(0) = \frac{1}{1 + \frac{\mu_n}{H}\frac{K_{22}}{K_{12}} + \frac{K_D}{H^2}\left(K_{21} + K_{11}\frac{K_{22}}{K_{12}}\right)} \times$$

$$\times \begin{Vmatrix} \frac{1}{H}\left(\frac{\mu_n}{K_{\text{дин}}\,K_{12}} + \frac{1}{P}\frac{K_{22}}{K_{12}}\right) & \frac{1}{HP} \\ -\frac{1}{K_{\text{дин}}\,K_{12}}\left(\frac{K_D}{H}K_{21} + 1\right) & \frac{1}{K_{\text{дин}}\,K_{12}}\left(\frac{K_D}{H}K_{11} + \frac{\mu_n}{H}\right) \end{Vmatrix}, \tag{5.16}$$

while for a GSP with a KU circuit, in the integrating mode it is

$$K(0) = \frac{1}{K_i}\frac{1}{K_{21} + K_{11}\frac{K_{22}}{K_{12}}} \begin{Vmatrix} \frac{K_{22}}{K_{12}} & 1 \\ -\frac{K_i K_{21}}{K_{\text{дин}}\,K_{12}} & \frac{K_i K_{11}}{K_{\text{дин}}\,K_{12}} \end{Vmatrix}. \tag{5.17}$$

Let us examine the static characteristics of different types of GSP's. For GSP's based on two-stage integrating gyroscopes with ball-bearing supports along the precession axes (so-called "dry" gyroscopes), the small amount of viscous friction along the precession axes is typically negligible ($\mu_B = 0$). In these gyroscopes there is no positional feedback; that is, $K_{22} = 0$. The static characteristics for a GSP of this type that uses a differentiating RVG in the KU circuit take on the form

$$\bar{\alpha}_1 = \frac{1}{1+\frac{K_g K_{21}}{H}} \times$$

$$\times \left\| \begin{matrix} 0 & \frac{1}{HP} \\ -\frac{1}{K_{DUP} K_{12}}\left(\frac{K_g K_{21}}{H}+1\right) & \frac{1}{K_{DUP} K_{12}}\left(\frac{K_g K_{11}}{H}+\frac{\mu_n}{H}\right) \end{matrix} \right\| \left\| \begin{matrix} M_n \\ M_{n1} \end{matrix} \right\|, \tag{5.18}$$

while when the RVG operates in the integrating mode they are

$$\bar{\alpha}_1 = \frac{1}{K_i K_{21}} \left\| \begin{matrix} 0 & 1 \\ -\frac{K_i K_{21}}{K_{DUP} K_{12}} & \frac{K_i K_{11}}{K_{DUP} K_{12}} \end{matrix} \right\| \left\| \begin{matrix} M_n \\ M_{n1} \end{matrix} \right\|. \tag{5.19}$$

Thus, when a KU circuit with a differentiating RVG is used, relative to the disturbing moment acting along the stabilization axis, the GSP remains astatic, with first-order astaticism, with respect to stabilization angle α_π. When a constant disturbing moment acts along the precession axis, the systematic deflection in inertial space of a GSP with KU is n times smaller than for an analogous GSP without a KU circuit:

$$n = 1 + \frac{K_g K_{21}}{H}. \tag{5.20}$$

From (5.20) it follows that the realization in the KU circuit of quite large amplification factors is required in order for a substantial reduction in GSP deflection to be achieved. Depending on the accuracy of the GSP itself, these factors can reach values of $(10^3\text{-}10^4)H$. A GSP's static characteristics with respect to the gyroscope's precession angle do not change, for all practical purposes. The precession angle of a GSP with KU remains the same as for a noncorrected GSP, but when acted upon by M_{B1} it can increase because of the introduction of a feedback circuit with transmission factor K_{11}.

With respect to the stabilization angle, a GSP with a KU circuit based on an integrating RVG has second-order astaticism relative to disturbing moment M_B. In connection with this, a disturbing moment along the precession axis leads to a static error relative to the stabilization angle that is inversely proportional to the correction circuit's transmission factor $K_i K_{21}$. The larger the stabilization circuit's transmission factors $K_{DUP}K_{12}$ are, the smaller the deflections with respect to the gyroscope's angle of precession.

In GSP's based on flotation integrating gyroscopes (PIG), there is also no positional feedback encompassing the gyroscope ($K_{22} = 0$), although the value of μ_B is quite large. The static characteristics of these GSP's with a KU circuit are described by the following expressions:
when the RVG is operating in the differentiating mode--

$$\bar{\alpha}_1 = \frac{1}{1+\frac{K_g K_{21}}{H}} \times$$

$$\times \begin{Vmatrix} \frac{1}{H}\frac{\mu_B}{K_{DUP}K_{12}} & \frac{1}{HP} \\ -\frac{1}{K_{DUP}K_{12}}\left(1+\frac{K_g}{H}K_{21}\right) & \frac{1}{K_{DUP}K_{12}}\left(\frac{\mu_n}{H}+\frac{K_g}{H}K_{11}\right) \end{Vmatrix} \begin{Vmatrix} M_B \\ M_{B1} \end{Vmatrix}; \quad (5.21)$$

when it is operating in the integrating mode--

$$\bar{\alpha}_1 = \frac{1}{K_i K_{21}} \begin{Vmatrix} 0 & 1 \\ -\frac{K_i K_{21}}{K_{DUP}K_{12}} & \frac{K_i K_{11}}{K_{DUP}K_{12}} \end{Vmatrix} \begin{Vmatrix} M_n \\ M_{n1} \end{Vmatrix}. \quad (5.22)$$

In the first mode, the systematic deflections and static error of a GSP with a KU circuit are reduced in comparison with a standard GSP by a factor as large as that that occurs in a GSP based on "dry" gyroscopes. In the second mode, the GSP becomes astatic with respect to moment M_B, while when a moment acts along the precession axis the static error is inversely proportional to the correction circuit's transmission factor $K_i K_{21}$. In both cases, the higher the stabilization circuit's transmission factor $K_{DUP}K_{12}$, the smaller the deflections with respect to the gyroscope's precession angle.

The static characteristics of a GSP based on angular velocity sensors and having a KU circuit are determined directly from (5.16) and (5.17). For differentiating RVG's they have the form

$$\bar{\alpha}_1 = \frac{1}{1+\frac{\mu_n}{H}\frac{K_{22}}{K_{12}}+\frac{K_g}{H}\left(K_{21}+K_{11}\frac{K_{22}}{K_{12}}\right)} \times$$

$$\times \begin{Vmatrix} \frac{1}{HP}\frac{K_{22}}{K_{12}} & \frac{1}{HP} \\ -\frac{1}{K_{DUP}K_{12}}\left(\frac{K_g}{H}K_{21}+1\right) & \frac{1}{K_{DUP}K_{12}}\left(K_g\frac{K_{11}}{H}+\frac{\mu_n}{H}\right) \end{Vmatrix} \begin{Vmatrix} \dot{M}_n \\ \dot{M}_{n1} \end{Vmatrix}, \quad (5.23)$$

while for integrating ones they are

$$\bar{\alpha}_1 = \frac{1}{K_i}\frac{1}{K_{21}+K_{11}\frac{K_{22}}{K_{12}}} \begin{Vmatrix} \frac{K_{22}}{K_{12}} & 1 \\ -\frac{K_i K_{21}}{K_{DUP}K_{12}} & \frac{K_i K_{11}}{K_{DUP}K_{12}} \end{Vmatrix} \begin{Vmatrix} M_n \\ M_{n1} \end{Vmatrix}. \quad (5.24)$$

Since the existing DUS's based on traditional two-stage gyroscopes have a high sensitivity threshold, quite high GSP accuracy can be obtained because of a KU circuit alone. A reduction in systematic deflections (in the case of the use of differentiating RVG's) and static errors (in the case of RVG operating in the integrating mode) when the system is acted upon by disturbing moments M_B and M_{B1} can be achieved by increasing transmission factor $K_{21}K_g$ or transmission factor $K_{11}K_g$. The effectiveness of each of these methods is determined by the ratio of the rigidity along the gyroscope's precession axis $K_{DUP}K_{22}$ to the stabilization circuit's transmission factor $K_{DUP}K_{12}$. The larger this ratio is, the more effective (from the viewpoint of improving static characteristics) is the use of a correcting circuit with transmission factor K_{11}. As K_{12} is increased, there is a decrease in the gyroscope's steady

angle of rotation with respect to the precession axis when the system is acted upon by constant moment M_{B1}, while when K_{11} is increased, the same thing occurs when moment M_B is acting upon the system.

Thus, although for the first two types of GSP's a circuit with transmission factor K_{11} played only a negative role from the viewpoint of improving the static characteristics, because it enlarged angle θ when moment M_{B1} was present, for a GSP based on a DUS this circuit turns out to have a positive effect.

Let us discuss the static errors of a GSP acted upon by an interference signal described by vector $\bar{f}$. Directly from the structural diagram in Figure 52, it follows that the dependence of $\bar{\alpha}_1$ on $\bar{f}$ is described by the expression

$$\bar{\alpha}_1 = \mathbf{K}(p)\,\mathbf{W}_p(p)\,\mathbf{W}_i(p)\bar{f}. \tag{5.25}$$

Giving this expression in terms of the system's parameters and converting to the limit for $p \to 0$, we obtain expressions for determining the GSP's static errors. When a differentiating RVG is used in the KU circuit, the expression takes the form

$$\bar{\alpha}_1 = \frac{1}{1+\frac{\mu_n}{H}\frac{K_{22}}{K_{12}}+\frac{K_B}{H^2}\left(K_{21}+K_{11}\frac{K_{22}}{K_{12}}\right)} \times$$

$$\times \left\| \begin{array}{ll} -\frac{1}{1+\frac{\mu_n\mu_B}{H^2}}\frac{K_B}{H}\left[K_{21}+\frac{K_{22}K_{11}}{K_{22}}+\right. & \frac{1}{K_{12}}\left(\frac{\mu_B}{H}-K_{22}\right) \\ \left.+\frac{\mu_B\mu_{11}}{H^2}\left(K_{11}+\frac{K_{22}K_{\text{дир}}}{K_{22}}\right)\right] & \\ -\frac{K_B}{K_{\text{дир}}K_{12}}\left(\frac{\mu_n}{H}-K_{11}\right) & -\frac{1}{K_{12}}\left(\frac{\mu_B}{H}K_{22}+1\right) \end{array} \right\| \left\| \begin{array}{l} \frac{\omega_e}{p} \\ \\ f_n \end{array} \right\|, \tag{5.26}$$

while when the RVG is operating in the integrating mode, it is

$$\bar{\alpha}_1 = \frac{1}{K_{21}+K_{11}\frac{K_{22}}{K_{12}}} \times$$

$$\times \left\| \begin{array}{ll} -\frac{1}{1+\frac{\mu_n\mu_B}{H^2}}\frac{1}{H}\left[K_{21}+\frac{K_{22}K_{11}}{K_{12}}+\frac{\mu_B\mu_n}{H^2}\left(K_{11}+\frac{K_{22}K_{\text{дир}}}{K_{12}}\right)\right. & 0 \\ & \\ -\frac{1}{K_{\text{дир}}K_{12}}\left(\frac{\mu_{11}}{H}-K_{11}\right) & 0 \end{array} \right\| \left\| \begin{array}{l} \frac{\omega_e}{P} \\ \\ f_n \end{array} \right\|. \tag{5.27}$$

From expressions (5.26) and (5.27) it follows that for a GSP with a KU circuit, when the amplification factors in the KU circuit are sufficiently high, the systematic deflections are determined basically by the magnitude of the RVG's error, as reduced to an equivalent angular velocity at its output, and cannot be changed substantially by the choice of the stabilization or correction circuit's parameters. In order to control such a GSP in the presence of external signals, the point of application of the control actions must be in the RVG's output circuit. The rate of generation of the control action is also determined from expressions (5.26) or (5.27).

5.3. Selecting the Structure and Parameters of a Deflection Correction Circuit for a Uniaxial Gyroscopic Stabilizer

As was already pointed out in Section 5.1, the basic purpose of a systematic deflection correction circuit is to reduce GSP deflections arising because of the effect of slowly changing disturbing moments. From an analysis of the static errors of a GSP with a KU circuit it follows that for the successful solution of this problem, it is necessary to realize in the KU circuit extremely high amplification factors, which usually comes into conflict with the requirement for stable operation of the system. Therefore, as an original prerequisite for the determination of the KU circuit's structure and parameters we will adopt the requirement that the maximum possible amplification factors be obtained in it while maintaining sufficient system stability reserves with respect to phase and amplitude.

From expression (5.13) it follows that the closed system's transfer matrix can be written in the form

$$\mathbf{K}(p) = \frac{1}{D(p)} \begin{Vmatrix} K_{11}(p) & K_{12}(p) \\ K_{21}(p) & K_{22}(p) \end{Vmatrix}, \tag{5.28}$$

where

$$\begin{aligned}
D(p) &= (I_n p + \mu_n)(I_n p + \mu_n)[p(I_n p + \mu_n) - W_g(p) W_{11}(p)] \times \\
&\times [p(I_n p + \mu_n) - W_{22}(p)] + H(I_n p + \mu_n)[Hp + W_{12}(p)] \times \\
&\times [p(I_n + \mu_n) - W_g(p) W_{11}(p)] + H(I_n p + \mu_n)[Hp - W_g(p) W_{21}(p)] \times \\
&\times [p(I_n p + \mu_n) - W_{22}(p)] + H^2[Hp - W_g(p) W_{21}(p)][Hp + W_{12}(p)] - \\
&- W_g(p)[(I_n p + \mu_n) W_{21}(p) - HW_{11}(p)][(I_n p + \mu_n) W_{12}(p) + HW_{22}(p)]; \\
K_{11}(p) &= [(I_n p + \mu_n)[(I_n p + \mu_n)[p(I_n p + \mu_n) - W_{22}(p)] + H^2 p] - \\
&- H^2 W_{22}(p)] D^{-1}(p); \\
K_{12}(p) &= [H(I_n p + \mu_n)[p(I_n p + \mu_n) - W_{22}(p)] + H^2[W_{12}(p) + \\
&+ Hp] + (I_n p + \mu_n)[(I_n p + \mu_n) W_{12}(p) + HW_{22}(p)]] D^{-1}(p); \\
K_{21}(p) &= [-(I_n p + \mu_n) W_g(p)[(I_n p + \mu_n) W_{21}(p) - HW_{11}(p)] - \\
&- H^2[Hp - W_g(p) W_{21}(p)] - \\
&- H(I_n p + \mu_n)[(I_n p + \mu_n) p - W_g(p) W_{11}(p)]] D^{-1}(p); \\
K_{22}(p) &= [-HW_g(p)[(I_n p + \mu_n) W_{21}(p) - HW_{11}(p)] + \\
&+ (I_n p + \mu_n) H[Hp - W_{21}(p) W_g(p)] + \\
&+ (I_n p + \mu_n)(I_n p + \mu_n)[(I_n p + \mu_n) p - W_g(p) W_{11}(p)]] D^{-1}(p).
\end{aligned}$$

In order that the system be stable, it is necessary and sufficient that all the components of transfer matrix K(p) be stable. This occurs when the regulator is stable and the system's characteristic polynomial has all its roots in the left half-plane of the complex plane. We will assume the first condition to be fulfilled and turn to the analysis of the second.

Allowing for the fact that for GSP's based on integrating gyroscopes there is no feedback encompassing the gyroscope, while feedback described by transfer function $W_{11}(p)$ is not feasible from the viewpoint of the static characteristics, for the discussion of this type of GSP we will set $W_{11}(p) = W_{22}(p) = 0$. The characteristic polynomial then acquires a simpler form:

$$\begin{aligned}
D(p) = p[(I_n p + \mu_n)(I_n p + \mu_n) + H^2]\Big\{&p[(I_n p + \mu_n)(I_n p + \mu_n) + H^2] + \\
&+ HW_{12}(p) - \frac{1}{p} W_g(p) W_{21}(p)[Hp + W_{12}(p)]\Big\}.
\end{aligned} \tag{5.29}$$

In order to analyze the stability of polynomial (5.29), we will use frequency methods. In order that D(p) have stable roots, it is necessary and sufficient that transfer function

$$W(p)=\frac{1}{p}\frac{Hp+W_{12}(p)}{p\left[(I_B p+\mu_B)(I_n p+\mu_n)+H^2\right]+HW_{12}(p)}W_g(p)W_{21}(p), \tag{5.30}$$

satisfy one of the stability criteria with respect to an open system's transfer function [36].

Providing the required dynamic characteristics in a GSP depends primarily on the stabilization circuit, so we will assume that the latter's structure and parameters have been selected to be the same as those of an uncorrected GSP. With due consideration for this assumption, let us discuss separately two types of GSP's based on integrating gyroscopes.

For a GSP of an astatic type, the most preferable for of correction in the stabilization circuit is a nonminimal-phase correcting circuit with a transfer function of the same type as (4.35) for $T_{k3} = T_{k2} = 0$ [12]. Let us write transfer function (5.30) in dimensionless form, relating operator p to the platform's nutational frequency $\omega_0 = H/\sqrt{J_\pi J_B}$;

$$W(\bar{p})=\frac{1}{\omega_0\bar{p}H}\frac{\left[\omega_0\tau_\kappa\frac{H}{K_{12}}\bar{p}^2+\left(\omega_0\frac{H}{K_{12}}-\tau_\kappa\right)\bar{p}+1\right]W_g(\bar{p})W_{21}(\bar{p})}{\omega_0\tau_\kappa\frac{H}{K_{12}}\bar{p}^4+\omega_0\frac{H}{K_{12}}\left(1+\frac{\tau_\kappa}{\tau_n}\right)\bar{p}^3+\omega_0\frac{H}{K_{12}}\times}\cdot \tag{5.31}$$
$$\times\left(\tau_\kappa+\frac{1}{\tau_n}\right)\bar{p}^2+\omega_0\frac{H}{K_{12}}\left(1-\tau_\kappa\omega_0^{-1}\frac{K_{12}}{H}\right)\bar{p}+1$$

For normal stability reserves with respect to phase and amplitude, the stabilization circuit has the following parameters [12]: $\tau_k \approx 1.7$; $K_{12}/H\omega_0 \approx 0.2$; $\tau_\pi \gg 1$. For such parameters and a GSP using an OMG with VP in the deflection correction circuit, transfer function (5.31) is approximated quite accurately in the area of essential frequencies by the simple expression

$$W(\bar{p})\approx\frac{K_g K_{21}}{H}\frac{1}{\tau_0^2\bar{p}^2+2\xi_0\tau_0\bar{p}+1}\frac{1}{\tau_g\bar{p}+1}W_{21}(\bar{p}), \tag{5.32}$$

where $\tau_0 \approx 0.944$; $2\xi_0 \approx 0.13$. It follows directly from (5.32) that if the value of the amplification factor in the deflection correction circuit is

$$K_g=\frac{K_g K_{21}}{H}<2\xi_0\tau_g\approx 0{,}13\tau_g, \tag{5.33}$$

the system will remain stable without additional correcting circuits in this circuit ($W_{21}(p) = K_{21}$); that is, the correction system has practically no effect on the operation of the stabilization system. Thus, the better the MRG's filtering properties (the larger τ_g is), the higher the values of the amplification factors in the correction circuit that can be obtained without using additional correcting components. An increase in the allowable amplification factor K_d can be achieved by the inclusion in the deflection correction circuit of a series-connected filtering element with the transfer function

$$W_{21}(\bar{p})=\frac{K_{21}}{\tau_{21}\bar{p}+1}. \tag{5.34}$$

For the formation of such an element in the deflection correction circuit it is possible to use the time lag of the moment sensor for the gyroscope's precession axis. If $\tau_{21} >> 1$, the allowable values of coefficient K_d will be determined from the inequality

$$K_d < 2\xi_0 \tau_g \tau_{21}. \tag{5.35}$$

By selecting the appropriate values of τ_{21} it is possible to realize practically any values of K_d in the system, which means that its deflections will be determined only by the MRG errors.

In addition to nonminimal-phase elements, aperiodic correcting elements are used for correcting GSP's of the astatic type. In these cases the closed system's frequency characteristics differ little from each other, although when aperiodic elements are used the platform's nutational oscillations are damped more weakly, so the allowable values of K_d turn out to be smaller. It is also possible to increase K_d by using additional correcting element (5.34).

The dynamic characteristics of a GSP with a KU circuit are determined by the closed system's transfer function $K_{11}(p)$. When conditions $\tau_g >> 1$, $\tau_{21} >> 1$, $\tau_\pi >> 1$ are fulfilled, the expression for $K_{11}(p)$ can be represented as

$$K_{11}(\bar{p}) = \frac{(\tau_g \bar{p} + 1)(\tau_{21}\bar{p} + 1)}{\frac{\tau_{21}\tau_g}{1 + K_d}\bar{p}^2 + \frac{\tau_{21} + \tau_g}{1 + K_d}\bar{p} + 1} \frac{1}{1 + K_d} K_{11}^0(\bar{p}), \tag{5.36}$$

where $K_{11}^0(\bar{p})$ = normalized transfer function of a GSP without a KU circuit. Thus, along with decreasing a GSP's systematic deflections by a factor of $1 + K_d$, a KU circuit also reduces the amplitude of its induced oscillations when it is acted upon by low-frequency disturbances. The boundary of the area of frequencies in which the reduction of the amplitude of the forced oscillations takes place depends on the transmission factor in the KU circuit. If

$$K_d < \frac{1}{4} \frac{(\tau_{21} - \tau_g)^2}{\tau_{21}\tau_g}, \tag{5.37}$$

the denominator in expression (5.36) breaks down into two aperiodic components. In connection with this, the boundary of the area in which the reduction of the GSP's forced oscillations takes place because of the KU circuit is determined by the expression

$$\omega = \frac{1}{2}\left[\frac{1}{\tau_g} + \frac{1}{\tau_{21}} + \sqrt{\left(\frac{1}{\tau_g} - \frac{1}{\tau_{21}}\right)^2 - \frac{4K_d}{\tau_g\tau_{21}}}\right]\omega_0. \tag{5.38}$$

If the denominator of (5.36) does not break down into aperiodic components, the frequency acquires the value

$$\omega = \sqrt{\frac{1 + K_d}{\tau_g\tau_{21}}}\omega_0. \tag{5.39}$$

The relative damping factor in the denominator of (5.36) of the oscillatory component depends both on K_d and on the relationship of the time constants τ_g and τ_{21} of the GSP and the correcting element, respectively:

$$\xi_K = \frac{1}{2}\left[\sqrt{\frac{\tau_{21}}{\tau_g}} + \sqrt{\frac{\tau_g}{\tau_{21}}}\right]\frac{1}{\sqrt{1+K_d}}. \qquad (5.40)$$

In order to reduce the effect of resonance phenomena on frequency (5.40) on the accuracy of stabilization, the correcting circuit time constant that is chosen should be one for which the value of the relative damping factor is at its highest.

If there is no correcting element in the KU circuit, the denominator of (5.36) is an aperiodic component with conjugating frequency

$$\nu = \frac{1+K_d}{\tau_g}. \qquad (5.41)$$

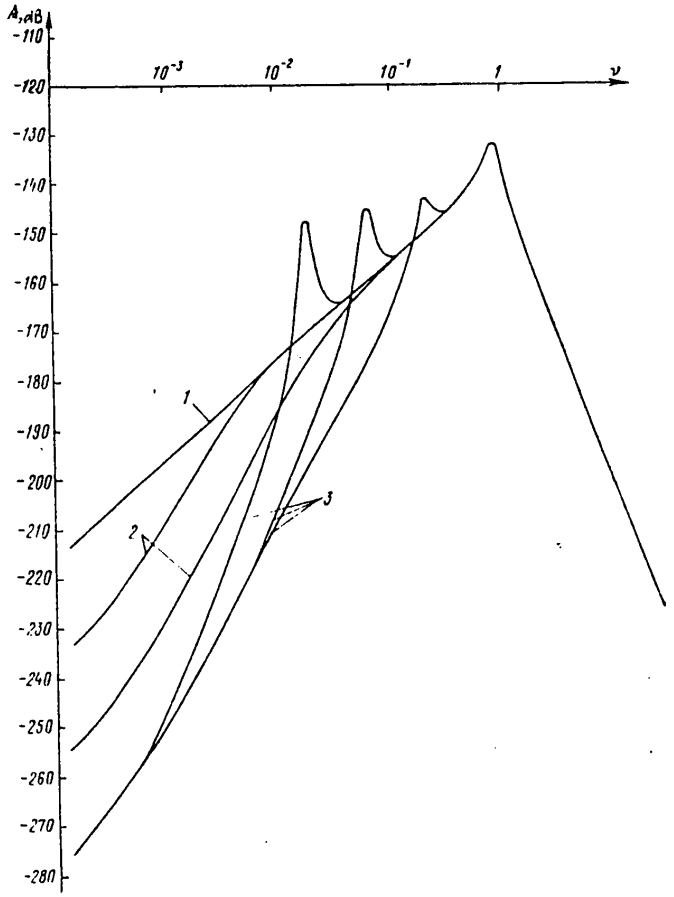

Figure 54. Amplitude-frequency characteristics of a GSP.

The value of ν also determines the boundary of the frequency area in which the KU circuit exerts its influence. Figure 54 shows the approximate form of the frequency characteristics of a GSP without a KU circuit (curve 1), as well as a GSP with a KU circuit with and without a correcting element (curves 3 and 2, respectively).

When a DMG with VP or any other RVG having a transfer function of the form of (1.109) is used as the sensitive element in a deflection correction circuit, the frequency of the DMG's nutational oscillations can be greater ($\omega_H > \omega_0$) or less ($\omega_H < \omega_0$) than the frequency of the platform's nutational oscillations. Coincidence of the nutational frequencies of the DMG and the platform should be avoided, since this mode (as is obvious from (5.31)) is most unfavorable for the operation of a GSP with a deflection correction circuit. If $\omega_H > \omega_0$, the system's stability is determined by the behavior of the frequency characteristic corresponding to transfer function (5.31) in the area of frequency ω_H. In this case the allowable value of K_d is

$$K_d < 2\xi_\pi T_\pi \omega_\pi, \tag{5.42}$$

where T_π = time constant of the DMG's precessional oscillations.

When $\omega_0 < \omega_H$ [sic], all the discussions taking place for a GSP with an OMG are correct, while the allowable values of K_d can be found from (5.33) and (5.35) if τ_g in them is replaced by the time constant of the DMG's precessional oscillations.

In all of the described cases, it is also possible to increase amplification factor K_d by including in the deflection correction circuit a series-connected nonminimal-phase correcting element of the type of (4.35), with a time constant $\tau_K \approx \sqrt{3}$ or, for $\omega_H < \omega_0$, $T_K = \sqrt{3}(1/\omega_H)$. In this case, however, for large values of K_d the deflection correction circuit actually determines the GSP's dynamics.

The second type of GSP's in widespread use at the present time are the so-called static GSP's, which are based on flotation integrating gyroscopes. They are characterized by quite strong damping with respect to the gyroscope's precession axis, in connection with which the oscillatory component in the numerator of the controlled object's transfer function usually breaks down into two aperiodic components. In order to insure stability and the high quality of the regulation process while maintaining the required amplification factors in the stabilization circuit, series-connected correcting components with the introduction of derivatives are used [12]. In the simplest case a component with the introduction of the first derivative is used; its transfer function is:

$$W_{12}(p) = K_{12}\frac{T_1 p + 1}{T_2 p + 1}, \quad T_1 > T_2. \tag{5.43}$$

In this case, in the band of essential frequencies of the system, transfer function (5.30) is approximated by the following expression [12]:

$$W(p) = \frac{1}{pH}\frac{T_1 p + 1}{T_0^2 p^2 + 2\xi_0 T_0 p + 1} W_3(p) W_{21}(p), \tag{5.44}$$

where $1/T_0$ is close to the corrected open system's cutoff frequency, which determines amplification factor K_{12}; ξ_0 is close to unity;

$$\frac{1}{T_3} = \frac{1}{2T_2}\left(1 + \frac{K_{12}}{H}\right)\left(1 - \sqrt{1 - 4\frac{K_{12}T_2}{H\left(1 + \frac{K_{12}}{H}T_1\right)^2}}\right).$$

When an OMG with VP is used to correct platform deflections, a sufficient condition for stability of the system is the requirement that the modulus of the frequency characteristic corresponding to transfer function (5.44) not exceed unity in the

area of frequencies close to $1/T_0$. When $T_3 > T_0$ and there is no additional correcting component in the deflection correction circuit, the sufficient condition is fulfilled if the amplification factor in the deflection correction circuit satisfies the inequality

$$K_d < \frac{T_0}{T_3} = \frac{1}{2}\frac{T_0}{T_2^2}\left(1+\frac{K_{12}}{H}T_1\right)\left(1-\sqrt{1-4\frac{K_{12}}{H}\frac{1}{\left(1+\frac{K_{12}}{H}T_1\right)^2}}\right). \tag{5.45}$$

As in the case of an astatic GSP, an increase in amplification factor K_d can be achieved by intensifying the correction circuit's filtering properties by connecting inertial components with (for example) a transfer function of the type of (5.34).

When MRG's having a transfer function of the (1.109) type (such as a DMG with VP) are used in the deflection correction circuit, the relationship between frequency $1/T_0$ and the MRG's nutational frequency is of considerable importance. If the MRG's nutational frequency is considerably higher than $1/T_0$, the allowable values of K_d can be evaluated with the help of inequality (5.45). In the opposite case, the system's stability will be determined by the behavior of the frequency characteristic close to frequency ω_H. When inequality

$$K_d < \frac{T_3\omega_H}{\sqrt{1+T_3^2\omega_H^2}}2\xi_H, \tag{5.46}$$

is not fulfilled, without the use of additional correcting components the system either loses its stability or is close to the limit of stability. In this case, depending on the specific parameters of the GSP and the RVG, K_d can be increased either by intensifying the deflection correction circuit's filtering properties, or by using a series-connected correcting component with the introduction of the first derivative of $T_3 > T_H$, or by using a nonminimal-phase component $T_3 < T_0$.

Let us now discuss GSP's in which the gyroscope is encompassed by direct feedback, or GSP's based on angular velocity sensors. For simplicity's sake we will assume that the feedback is realized in an ideal manner; that is, $W_{22}(p) = K_{22}$. This occurs when a mechanical spring having rigidity K_{22} is installed on the gyroscope's precession axis. The simplest type of such platforms are direct gyrostabilizers (NGS) [26], in which the gyroscope serves to reduce the amplitude of the platform's forced oscillations in a certain frequency band. NGS's are built on the principle of a mechanical oscillation absorber, so the coupling described by transfer function $W_{12}(p)$ is usually absent in them. In practice it is frequently required to have a simultaneous reduction in the forced oscillations of a platform caused by the base's low-frequency oscillations and its vibrations, the spectrum of which has explicitly expressed maximums. The solution of this problem by expanding the stabilization system's working frequency band meets with obvious difficulties. Therefore, there is interest in a system realized as if with two stabilization circuits, the first of which is based on an RVG and reduces the platform oscillations caused by the low-frequency disturbing moments, while the second utilizes the principle of a gyroscopic oscillation absorber and reduces the platform's forced oscillations in the given frequency band of vibrations of the base. The transform function of this closed system with respect to the stabilization angle is derived easily from (5.28) and has the form

$$K(p) = K_{\text{н.э}}(p)\left[1 - W_{\text{э}}(p)\,W_{11}(p)\,K_{\text{н.э}}(p)\right]. \tag{5.47}$$

The transfer function of the direct gyrostabilizer is

$$K_{\text{п. g}}(p) = \frac{1}{\mu_{\text{п}} p} \frac{T_m^2 p^2 + 2\xi_m T_m p + 1}{T_m^2 T_{\text{п}} p^3 + T_m (T_m + T_{\text{п}} 2\xi_m) p^2 + (T_{\text{п}} + 2\xi_m T_m + T_{\text{п}} T_m^2 \omega_0^2) p + 1},$$

where $1/T_m$ = intrinsic frequency of the gyroscope's oscillations that corresponds to the frequency of maximum suppression of the forced oscillations; ξ_m = relative damping factor of the gyroscope's natural oscillations; ω_0 = frequency of the platform's nutational oscillations; $T_{\pi} = I_{\pi}/\mu_{\pi}$.

Since the condition $H^2/(I_{\pi}K_{22}) >> 1$ must be fulfilled for efficient NGS operation, its transfer function can be represented in the form

$$K_{\text{п. g}}(p) = \frac{1}{\mu_{\text{п}} p} \frac{T_m^2 p^2 + 2\xi_m T_m p + 1}{(\omega_0^2 T_m^2 T_{\text{п}} p + 1)\left[T_0^2 p^2 + \left(\frac{1}{T_{\text{п}}} + \frac{1}{T_m}\right) T_0^2 p + 1\right]}. \quad (5.48)$$

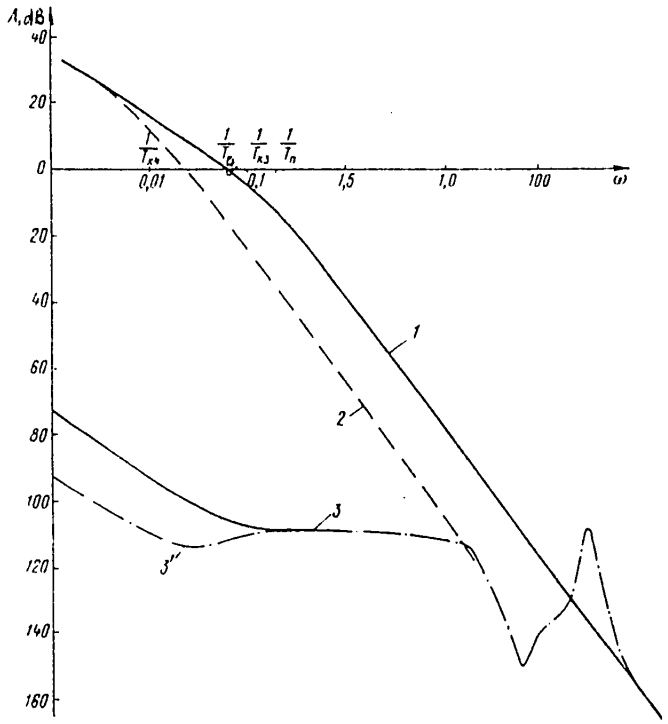

Figure 55. LAKh of stabilization channel.

From (5.48) it is possible to select the NGS parameters for which the given reduction in the amplitude of the platform's forced oscillations in the required frequency band is insured. The effect of the reduction in the oscillations' amplitude takes place in the band of frequencies from $(1/\omega_0^2 T_m^2)(1/T_{\pi})$ to a frequency that is slightly lower than the platform's nutational frequency. Beginning with frequency $1/T_{\pi}$, the forced oscillations' amplitude is reduced by a factor of $\omega_0^2 T_m^2$, while on frequency $1/T_m$ the maximum reduction, by a factor of $\omega_0^2 T_m^2 (1/2\xi m)$, occurs. Figure 55 depicts the frequency characteristics of a platform (curve 1) and a platform with an NGS (curve 2). The essential shortcoming of the latter is the presence in the

frequency characteristic of a peak in the area of the nutational frequency, so the latter must be located in the band of frequencies where the disturbances are minimal.

It is obvious that when designing an additional stabilization circuit using an RVG, the goal of which is to reduce the amplitude of the platform oscillations caused by low-frequency disturbing effects, it is advisable that this circuit's cutoff frequency in the open state ω_2 be made lower than $1/T_m$. In this case the technique for selecting the stabilization circuit's structure and parameters described in Section 4.3 is used. In connection with this, instead of the platform's moment of inertia, in the calculations we should use its equivalent moment of inertia, as determined by the relationship

$$I_{\text{э.п}} = \omega_0^2 T_m^2 I_n. \tag{5.49}$$

Since in this case it is as if the controlled object becomes more inertial, the problem of constructing a stabilization circuit with an RVG is made easier. For the same amplification factors in the stabilization circuit, there is a reduction in its cutoff frequency in the open state, which lowers the requirements for the stabilization circuit's elements. At the same time, because of the use of an NGS, the closed system's band of working frequencies in which there is a reduction in the amplitude of the platform's forced oscillations is expanded substantially. In Figure 55 we see the frequency characteristics of such a closed system when an OMG with VP is used (curves 3 and 3'). Curve 3 corresponds to the case of the utilization in the stabilization circuit of a correcting component with transfer function (4.26).

There is an entire class of GSP's in which DUS's are used as the basic sensitive elements. DUS's with small kinetic moments are normally used for this purpose. The basic shortcoming of such DUS's is their large systematic deflections, since DUS's based on the traditional layout have, as a rule, an inadmissibly high threshold of sensitivity. This flaw can be eliminated by the creation in such GSP's of a KU circuit utilizing highly sensitive measurers of absolute angular velocities, such as RVG's. The structural diagram of such a system is derived easily from the structural diagram depicted in Figure 51. In connection with this we will assume that the direct feedback encompassing the gyroscope is ideal ($W_{22}(p) = -K_{22}$). From (5.23) it follows that for sufficiently high values of K_{22}, cross-control of the platform from the KU circuit through the DUS is not effective, so we will assume that $W_{21}(p) = 0$. Considering the assumptions that have been made, the GSP's transfer function with respect to the stabilization angle takes on the following form:

$$K(p) = K_{\text{g.т}}(p) \frac{1}{1 - W_{\text{g}}(p)\, W_{11}(p)\, K_{\text{g.т}}(p)}, \tag{5.50}$$

where $K_{g.t}$ = transfer function of a GSP using DUS's as sensitive elements, without a KU circuit:

$$K_{\text{g.т}}(p) = \frac{1}{p} \frac{I_n^2 p + \mu_n p + K_{22}}{(I_n p + \mu_n)(I_0 p^2 + \mu_n p + K_{22}) + H^2 p + H K_{22}}.$$

For GSP's based on DUS's it is recommended that the gyroscope's relative damping factor be 0.5-0.7, while the gyroscope's natural frequency ω_T should exceed the system's cutoff frequency ω_{cp} by a factor of 3-10 [12]. In the absence of special correcting components in the stabilization circuit, the relationship between the open system's cutoff frequency and its amplification factor is determined by the expression

$$\omega_{cp} = \frac{1}{I_n} H \frac{K_{12}}{K_{22}}. \tag{5.51}$$

Allowing for expression (5.51), let us rewrite the transfer function of a GSP without a KU in the form

$$K_{g.t}(p) = \frac{1}{I_n p} \frac{p^2 + \frac{\mu_s}{I_s} p + \omega_T^2}{p^3 + \left(\frac{\mu_s}{I_s} + \frac{\mu_n}{I_n}\right)p^2 + \left(\omega_T^2 + \omega_n^2 + \frac{\mu_n}{I_n}\frac{\mu_s}{I_s}\right)p + \omega_T^2 \omega_{cp}}. \tag{5.52}$$

Since DUS's with small kinetic moments are normally used to build GSP's, the relationship $\omega_H << \omega_T$ usually occurs. Besides this, the parameters of real systems (as a rule) satisfy the inequalities

$$\frac{\mu_n}{I_n} \ll \omega_{cp}, \quad \frac{\mu_n}{I_n}\frac{\mu_s}{I_s} \ll \omega_T^2, \quad \frac{\mu_s}{I_s} \gg \frac{\mu_n}{I_n}.$$

Taking these relationships into consideration and introducing the dimensionless operator $\bar{p} = p/\omega_T$, we rewrite the approximated expression for transfer function (5.52) as

$$K_{g.t}(\bar{p}) = \frac{1}{I_n \omega_T^2} \frac{1}{\bar{p}} \frac{\bar{p}^2 + \eta\bar{p} + 1}{\bar{p}^3 + \eta\bar{p}^2 + \bar{p} + \lambda}, \tag{5.53}$$

where η = 1-1.4; λ = 0.1-0.33.

The denominator of $K_{g.t}(p)$ has one real and two complexly conjugated roots and represents, correspondingly, the product of an aperiodic and an oscillatory component. For η = 1 and λ = 0.1, transfer function $K_{g.t}(p)$ is approximated quite accurately by the expression

$$K_{g.t}(\bar{p}) \approx \frac{10}{I_n \omega_T^2} \frac{1}{\bar{p}} \frac{1}{10\bar{p} + 1}. \tag{5.54}$$

In the band of essential frequencies, such a system is represented, for all practical purposes, by an integrating component with a coefficient of integration $K_i = 10/(I_\pi \omega_T^2)$. The greater the platform's moment of inertia and the DUS's natural frequency, the smaller K_i, the systematic GSP deflection and its forced oscillations are when acted upon by disturbing moments. The platform's moment of inertia depends on the engineering problem that it must solve in each specific case, while the increase in ω_T is limited by the DUS's required threshold of sensitivity and the quality of the elements in the stabilization system. Therefore, a decrease in K_i is achieved by introducing integrating-differentiating components without increasing the open system's cutoff frequency. A decrease in the systematic deflections of a GSP based on a DUS can be achieved by basing the KU on an RVG. Let us discuss the special features of such a system when an OMG with VP is used in the deflection correction circuit.

The transfer function of the open system corresponding to the closed system is described by the second cofactor on the right side of (5.50), and in this case has the form

$$W(\bar{p}) = \frac{10 K_{11} K_g}{I_n \omega_T} \frac{1}{10\bar{p} + 1} \frac{1}{\tau_1 \bar{p} + 1} \frac{1}{\tau_n \bar{p} + 1}, \tag{5.55}$$

where $\tau_g = T_g\omega_T$; $\tau_p = T_p\omega_T$. If $\tau_p << 1$ and the open correction system's cutoff frequency ω_{cp} is lower than the stabilization system's cutoff frequency, a GSP with KU proves to be stable and with respect to the stabilization angle has the transfer function

$$K(\bar{p}) = \frac{K_i T_{ii}\omega_T}{10K_{11}K_g\bar{p}} \frac{\tau_g\bar{p}+1}{\frac{\tau_g I_{ii}\omega_T}{K_{11}K_g}\bar{p}^2 + 0{,}1\frac{I_{ii}\omega_T}{K_{11}K_g}\tau_g\bar{p}+1}. \quad (5.56)$$

It is obvious that the value

$$n = 10\frac{K_{11}K_g}{I_{ii}\omega_T} \quad (5.57)$$

shows by what factor the GSP's systematic deflections are reduced when a KU circuit is created in it. The roots of the denominator of transfer function (5.56) are determined by the expression

$$\bar{p}_{1,2} = -0{,}05 \pm \sqrt{2{,}5\cdot 10^{-3} - 0{,}1\frac{n}{T_g\omega_T}}. \quad (5.58)$$

If it is required that the cutoff frequency of a GSP with an open KU circuit be lower than that of the open stabilization system, the following limitation is imposed on the value of n:

$$n < 10T_g\omega_T\lambda^2. \quad (5.59)$$

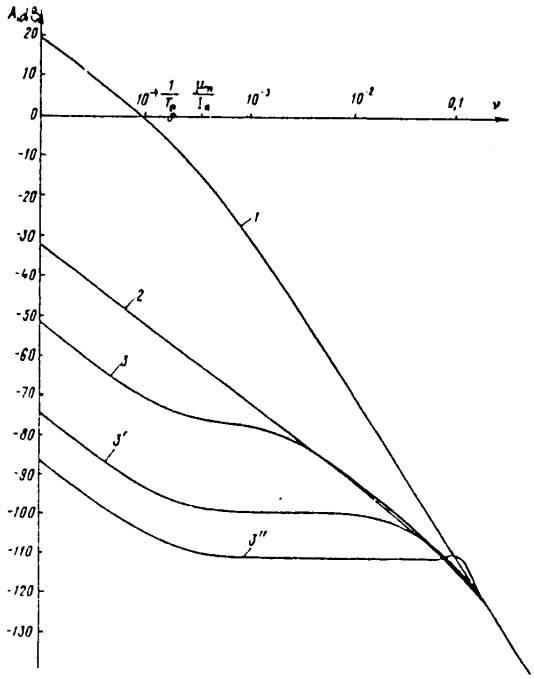

Figure 56. LAKh of the stabilization channel of a GSP based on a DUS with a KU circuit.

In this case the transfer function's denominator represents an oscillatory component with a relative damping factor $\xi \geq 0.5$. For $n \leq 2.5 \cdot 10^{-2} T_g \omega_T$, the denominator of (5.56) breaks down into two aperiodic components. A reduction in n leads to a reduction in the cutoff frequency of the open system with KU. Figure 56 shows the approximate form of the frequency characteristic of an unstabilized platform (curve 1), a GSP based on a DUS (curve 2) and a GSP based on a DUS with a KU circuit based on an OMG with VP for different values of n (curves 3, 3' and 3"), while in Figure 57 we see the same for a GSP based on a DUS with a KU circuit based on an OMG with VP for different values of the OMG's time constant T_g (curves 2, 2' and 3").

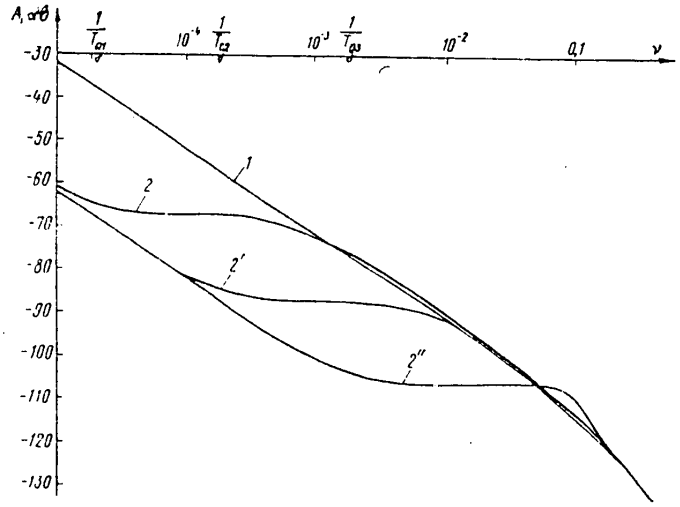

Figure 57. LAKh of a stabilization channel based on a DUS with a KU circuit.

From the graphs it is obvious that when the parameters are chosen appropriately, a KU circuit makes it possible not only to reduce the systematic deflections of a DUS-based GSP, but also to reduce substantially the amplitudes of the platform's forced oscillations when it is acted upon by low-frequency disturbances. On the other hand, the presence on the platform of a DUS-based stabilization circuit lowers the requirements for the RVG-based correction circuit in comparison with the case where only the latter is used to solve the problem of platform stabilization. Actually, in order to obtain identical systematic deflections and dynamic errors, the amplification factor of the circuit with the RVG and its pass band for a GSP based on a DUS prove to be much smaller than for the case of a stabilized platform based on an OMG with VP. When RVG's with a transfer function of the (1.109) type are used as the KU circuit's sensitive elements, it is necessary that the frequency of the RVG's nutational oscillations be considerably higher than the cutoff frequency of the DUS-based open stabilization circuit. In this case all that was said above remains true.

Reductions in the systematic deflections of a GSP with KU can be achieved by increasing the amplification factor in the stabilization circuit or in the correction circuit and simultaneously adding to these circuits a series-connected integrating-differentiating component with appropriately chosen parameters. In connection with this, the pass band of both the stabilization circuit and the correction circuit can remain the same.

The examples of the structure of a KU circuit for GSP's of different types that we have discussed show that when the KU circuit has adequate filtering properties (which can be provided by extremely simple correcting components), in it it is possible to realize high amplification factors. This makes it possible to reduce GSP deflections almost to the level of the RVG's threshold of sensitivity.

Conclusion

Practical problems encountered in applied gyroscopy have made it necessary to place on the agenda questions relating to the development of the theory of RVG's and systems utilizing them. The generalized model proposed in this book makes it possible to evaluate the prospects for the use of various RVG layouts to solve different technical problems. The use of operator methods simplified considerably the analysis of the equations of motion and the obtaining in analytical form of the dependences of an instrument's basic characteristics on its parameters. For OMG's and DMG's these dependences are fully visible and can be used directly in the designing of such instruments. When synthesizing the parameters of more complex RVG systems, they remain the basis of the computational algorithms for computers.

One of the main goals of designers is to minimize instrument error under given operating conditions. The dependences of MRG errors on different disturbing factors related to motion of the base, inaccuracy in instrument production, and special features of instrument operation, as derived in this book, along with the dependences of RVG characteristics on their parameters, make it possible to work out a criterion for selecting an instrument layout and making an optimum synthesis of its basic parameters.

The results of the theoretical investigations presented in this book make it possible to determine the possibility of creating KRVG's [expansion unknown] with the required technical characteristics, as well as to determine the requirements for production accuracy and accuracy in the tuning of element, assemblies and an entire instrument as a whole.

The questions on the theory of GSP's based on RVG's that have been discussed in this book make it possible, using simple engineering methods, to carry out a preliminary selection of the structure of stabilization and correction circuits and their parameters. The specific nature of systems with RVG's consists of the presence of harmonic components in the RVG signal and additional cross-couplings between the stabilization channels. In this book we have made simple estimates of the effect of these cross-couplings on the dynamics of a GSP. We have developed a technique for allowing for transient feedback that makes it possible to define the basic characteristics of a GSP more accurately, allowing for the harmonic component in the RVG signal. For stabilization systems using an RVG in an additional deflection correction circuit, we have obtained limitations on the parameters of the deflection correction circuit, the observance of which makes it possible to discuss it separately from the stabilization circuit.

The area of possible use of RVG's, in which they can compete successfully with gyroscopes of other types, is extremely extensive, beginning with the creation of measurers and absolute angular velocities and linear accelerations and ending with ISN's and ISO's. Therefore, the need for the creation of a comprehensive theory of instruments and systems based on RVG's is an unarguable one.

This book can be regarded as one of the first steps in this direction. Beyond its scope were such important questions as special features of the use of RVG's in ISN's and ISO's, questions in the nonlinear theory of RVG's and stabilized platforms based on RVG's, and many other. The solution of these problems, along with problems emanating from the practical realization of RVG's with the desired technical characteristics, will make it possible to create stabilization and navigation instruments and systems distinguished by their high accuracy, small size and low cost.

BIBLIOGRAPHY

1. Barskiy, A.G., Orlova, M.S., and Khorol, D.M., "Dinamicheskiye sistemy s odnokanal'nymi izmeritelyami" [Dynamic Systems With Single-Channel Measurers], Moscow, Izdatel'stvo "Mashinostroyeniye", 1976.

2. Bessekerskiy, V.A., and Fabrikant, Ye.A., "Dinamicheskiy sintez sistem giroskopicheskoy stabilizatsii" [Dynamic Synthesis of Gyroscopic Stabilization Systems], Leningrad, Izdatel'stvo "Sudostroyeniye", 1968.

3. Brozgul', L.I., and Smirnov, Ye.L., "Vibratsionnyye giroskopy" [Vibration Gyroscopes], Moscow, Izdatel'stvo "Mashinostroyeniye", 1970.

4. Brozgul', L.I., and Smirnov, Ye.L., "Vibration Gyroscopes," in "Istoriya mekhaniki giroskopicheskikh sistem" [History of the Mechanics of Gyroscopic Systems], Moscow, Izdatel'stvo "Nauka", 1975.

5. Vlasov, Yu.B., "Giroskopy na novykh fizicheskikh printsipakh. Vibratsionnyye giroskopy i ikh primeneniye. Uchebnoye posobiye" [Gyroscopes Based on New Physical Principles: Vibration Gyroscopes and Their Use; Textbook], Izdatel'stvo "LETI" [Leningrad Electrotechnical Institute imeni V.I. Ul'yanov (Lenin)], 1976.

6. Vlasov, Yu.B., "O metode resheniya differentsial'nykh uravneniy s periodicheskimi koeffitsiyentami. Mezhvuzovskiy sbornik" [On a Method for Solving Differential Equations With Periodic Coefficients; Inter-VUZ Collection of Works], LIAP [Leningrad Institute of Aviation Instruments], No 117, 1977.

7. Vlasov, Yu.B., and Filonov, O.M., "A Uniaxial Gyroscopic Stabilizer With a Systematic Deflection Compensation Circuit," IZV. VUZOV. SER. PRIBOROSTROYENIYE, No 2, 1975.

8. Vlasov, Yu.B., Masalov, V.P., and Sukhanov, B.N., "On Errors in a Two-Dimensional, Single-Channel Measurer of Absolute Angular Velocities Mounted on a Vibrating and Rocking Base," in "Prikladnaya giroskopiya" [Applied Gyroscopy], Izdatel'stvo LGU [Leningrad State University], 1974.

9. Vlasov, Yu.B., Tikhonov, R.Ye., and Filonov, O.M., "On the Possibility of Correcting the Systematic Deflections of an Astatic Three-Stage Gyroscope With a 'Nonsymmetrical' Rotor," ELEKTROTEKHNIKA, No 12, 1974.

10. Vlasov, Yu.B., Severov, L.A., and Filonov, O.M., "Using a Rotor Vibration Gyroscope to Improve the Accuracy of Gyroscopic Instruments and Systems," TRUDY LIAP, No 91, 1975.

11. Gantmakher, F.R., "Teoriya matrits" [Theory of Matrices], Moscow, Izdatel'stvo "Nauka", 1967.

12. Pel'por, D.S., editor, "Giroskopicheskiye sistemy" [Gyroscopic Systems], Moscow, Izdatel'stvo "Vysshaya shkola", Vol 2, 1977.

13. Zhuravlev, V.F., "Teoriya vibratsii giroskopov" [Theory of Vibration of Gyroscopes], Moscow, Institute of Problems of Mechanics, USSR Academy of Sciences, Preprint No 22, 1972.

14. Zade, L., and Dezoyer, I., "Teoriya lineynykh sistem" [Theory of Linear Systems], Moscow, Izdatel'stvo "Nauka", 1970.

15. "Inertial Navigation Systems Based on Dynamically Tunable Gyroscopes (Review)," VOPROSY RAKETNOY TEKHNIKI, No 2/230, 1974.

16. Kazamarov, A.A., Palatnik, A.M., and Rodnyanskiy, L.O., "Dinamika dvukhmernykh sistem avtomaticheskogo regulirovaniya" [Dynamics of Two-Dimensional Automatic Regulation Systems], Moscow, Izdatel'stvo "Nauka", 1967.

17. Krasovskiy, A.A., "On Two-Channel Automatic Regulation Systems With Antisymmetrical Couplings," AVTOMATIKA I TELEMEKHANIKA, Vol 3, No 2, 1957.

18. Lunts, Ya.L., "Oshibki giroskopicheskikh priborov" [Errors in Gyroscopic Instruments], Leningrad, Izdatel'stvo "Sudostroyeniye", 1968.

19. Maleyev, P.I., "Novyye tipy giroskopov" [New Types of Gyroscopes], Leningrad, Izdatel'stvo "Sudostroyeniye", 1971.

20. N'yuton, Dzh., Jr., "A Vibration Gyroscope Instrument With Rotor Drive," "Trudy Mezhdunarodnogo kongressa po avtomaticheskomu upravleniyu. Tekhnicheskiye sredstva avtomatiki" [Works of the International Congress on Automatic Control: Automation Equipment], 1965.

21. Pavlov, V.A., "Osnovy proyektirovaniya i rascheta giroskopicheskikh priborov" [Principles of the Planning and Designing of Gyroscopic Instruments], Leningrad, Izdatel'stvo "Sudostroyeniye", 1967.

22. Pel'por, D.S., "Giroskopicheskiye sistemy" [Gyroscopic Systems], Moscow, Izdatel'stvo "Vysshaya shkola", Vol 1, 1971.

23. Ponomarev, V.K., and Khovanskiy, Yu.M., "Analiticheskoye konstruirovaniye regulyatorov v sistemakh upravleniya s uchetom ustanovivshikhsya reaktsiy" [Analytical Designing of Regulators in Control Systems, With Steady-State Reactions Taken Into Consideration], LIAP, Interdepartmental Collection of Works, No 117, 1977.

24. Ponyrko, S.A., and Severov, L.A., "On Engineering Methods for Formulating the Equations of Motion of a Triaxial Gyrostabilizer," TRUDY LIAP, No 49, 1967.

25. Rivkin, S.S., "Statisticheskiy sintez giroskopicheskikh ustroystv" [Statistical Synthesis of Gyroscopic Devices], Leningrad, Izdatel'stvo "Sudostroyeniye", 1970.

26. Rivkin, S.S., "Direct Gyrostabilizers," in "Istoriya mekhaniki giroskopicheskikh sistem", Moscow, Izdatel'stvo "Nauka", 1975.

27. Rozenbeym, K.V., "Toward a Theory of Linear, Two-Dimensional Automatic Regulation Systems of a General Form With Modulation," AVTOMATIKA I TELEMEKHANIKA, No 5, 1970.

28. Rozenvasser, Ye.N., "Periodicheski nestatsionarnyye sistemy upravleniya" [Periodically Transient Control Systems], Moscow, Izdatel'stvo "Nauka", 1973.

29. Sveshnikov, A.G., and Tikhonov, A.N., "Teoriya funktsiy kompleksnoy peremennoy" [Theory of Functions of a Complex Variable], Moscow, Izdatel'stvo "Nauka", 1967.

30. Severov, L.A., and Dergachev, P.B., "On the Question of the Gyroscopic Stabilization of a Rotating Body," IZV. VUZOV. SER. PRIBOROSTROYENIYE, Vol 12, 1969.

31. Seyvet, P., "Dynamics of Ideal Suspensions With Respect to Bodies Rotating in Space," MEKHANIKA (Collected Translations), No 5 (105), 1967.

32. Sukhanov, B.N., "On Improving the Accuracy of a Two-Dimensional, Single-Channel Measurer of Angular Velocities," in "Prikladnaya giroskopiya", Izdatel'stvo LGU, 1974.

33. Sukhanov, B.N., and Ginzburg, R.Ye., "A Method for Improving the Resistance of a Centrifugal-Pendulum Measurer of Angular Velocity to Interference Caused by Vibration of the Base," in "Doklady nauchno-tekhnicheskogo seminara. Povedeniye giroskopa i giroskopicheskikh ustroystv v usloviyakh intensivnoy vibratsii osnovanii" [Reports From the Scientific and Technical Seminar on the Behavior of Gyroscopes and Gyroscopic Devices Under Conditions of Intense Vibration of the Base], Tomsk, Tomsk Polytechnic Institute, 1971.

34. Taft, V.A., "Osnovy spektral'noy teorii i raschet tsepey s peremennymi parametrami" [Principles of Spectral Theory and the Calculation of Circuits With Variable Parameters], Moscow, Izdatel'stvo "Nauka", 1964.

35. Taft, V.A., "Elektricheskiye tsepi s peremennymi parametrami" [Electrical Circuits With Variable Parameters], Leningrad, Izdatel'stvo "Energiya", 1968.

36. Solodovnikov, V.V., editor, "Tekhnicheskaya kibernetika. Teoriya avtomaticheskogo regulirovaniya" [Technical Cybernetics: Theory of Automatic Regulation], Moscow, Izdatel'stvo "Mashinostroyeniye", Vol 1, 1967.

37. Solodovnikov, V.V., editor, "Tekhnicheskiye kinernetika. Teoriya avtomaticheskogo regulirovaniya", Moscow, Izdatel'stvo "Mashinostroyeniye", Vol 2, 1967.

38. Turichin, A.M., "Elektricheskiye izmereniya neelektricheskikh velichin" [Electrical Measurements of Nonelectrical Values], Moscow, Izdatel'stvo "Energiya", 1967.

39. Feodos'yev, V.I., "Soprotivleniye materialov" [Resistance of Materials], Moscow, Izdatel'stvo "Nauka", 1974.

40. Fikhtengol'ts, G.M., "Kurs differentsial'nogo i integral'nogo ischisleniya" [A Course in Differential and Integral Calculus], Moscow, Izdatel'stvo "Nauka", 1967.

41. Sheldon, S.L.Ch., "Sintez optimal'nykh sistem avtomaticheskogo regulirovaniya" [Synthesis of Optimum Automatic Regulation Systems], Moscow, Izdatel'stvo "Mashinostroyeniye", 1964.

42. Craig, R.J.G., "Theory of Errors of a Multigimbal, Elastically Supported Tuned Gyroscope," JEEE TRANS. ON AEROSPACE AND ELECTRON SYSTEMS, Vol AES-8, No 3, 1972.

43. Erdley, H.F., "Vibrating Rotor Gyroscopes (Litton Systems, Inc.)," United States Patent, Class 74-5.6, No 3382726, Application 21 May 1965, Publication 14 May 1968.

44. Erdley, H.F., Lipman, J.S., and Shapiro, S., "Vibratsionnyy giroskop i inertsial'naya platforma, soderzhashchaya vibratsionnyy giroskop" [A Vibration Gyroscope and an Inertial Platform Containing a Vibration Gyroscope], Swedish Patent, Class 42 c 25/50 (GOlc 19/00), No 312446, Application 6 July 1965, Publication 14 July 1969.

45. Eklund, Harry Nils, "Angular Rate Measuring Device," United States Patent, Class 74-5.6, No 3191445, Application 29 June 1965, Publication 11 March 1968.

46. Howe, E.W., and Savet, R.N., "The Dynamically Tuned Free Rotor Gyro," CONTROL ENG., No 11, 1964.

47. Miller, B., "New Inertial Navaid Flight-Tested," AVIAT. WEEK, Vol 92, No 18, 1970.

48. Miller, B., "Inertial Navaid Features New Multisensors," AVIAT. WEEK, Vol 95, No 24, 1971.

49. Shclift, Helmut, W., "Asymmetric Gyroscope (Northrop Corp.)," United States Patent, Class 74-5.34 (GOl c 19/00), No 3804625, Application 21 February 1973, Publication 23 April 1974.

11746
CSO: 8144/0135

- END -